2012

Biochar characterization and engineering

Catherine Elizabeth Brewer
Iowa State University

Biochar characterization and engineering

by

Catherine Elizabeth Brewer

A dissertation submitted to the graduate faculty

in partial fulfillment of the requirements for the degree of

DOCTOR OF PHILOSOPHY

Co-Majors: Chemical Engineering; Biorenewable Resources and Technology

Program of Study Committee:
Robert C. Brown, Co-Major Professor
David A. Laird, Co-Major Professor
Thomas E. Loynachan
Klaus Schmidt-Rohr
Brent H. Shanks
Dennis R. Vigil

Iowa State University

Ames, Iowa

2012

DEDICATION

I dedicate this dissertation in memory of my grandfather,

GEORGE JACOB GUMM

who received his high school diploma at the age of 75
after dropping out of high school
to serve his country during World War II,

and in honor of my grandmother,

BETTY ANN HEIDEL GUMM

who gave up a full scholarship to veterinary school
to help take care of her family when her father died.

TABLE OF CONTENTS

LIST OF TABLES

LIST OF FIGURES

ACKNOWLEDGEMENTS

I would like to acknowledge funding from the ConocoPhillips Company, a National Science Foundation Graduate Research Fellowship, an Iowa State University Plant Sciences Institute Graduate Research Fellowship, an ISU Katzer Energy Graduate Research Fellowship, and an ISU College of Engineering Cowell First-Year Graduate Fellowship. This funding has allowed me the freedom to choose the topic of my research, without which I would not have been able to study biochar, and the financial independence to attend national and international conferences, and pursue professional development experiences.

I would like to thank my family for their continual patience and support, especially my husband, Brent Brewer.

I would like to thank my committee for their guidance, support and flexibility as I have sought to define my project.

I would like to acknowledge my colleagues at CSET for providing char samples and production information, analytical support and advice, and encouragement; two high school teachers, Eric Hall and Jeff Rudisill, and two undergraduates, Daniel Assmann and Hernań Treviño, who worked with me on biochar production and characterization projects; and collaborators from many departments on and off campus: David Laird, Pierce Fleming, Sam Rathke, Rivka Fidel and Natalia Rogovska (soil properties and CEC); Klaus Schmidt-Rohr, Xiaowen Fang and Yan-Yan Hu (NMR); Rachel Unger, Randy Killorn and Thomas Loynachan (agronomic studies); John McClelland and Roger Jones (FTIR); Dedrick Davis and Mustafa Ibrahim (soil physical properties); Warran Straszheim (SEM); Scott Schlorhotz and Michael Thompson (XRD); Phillip Dixon and Dennis Lock (statistics); Jeff Schroeder, Phil Schroeder, Eugene Baptist, Phillip Tate, and Gilbert Garbutt (Belize project).

CHAPTER 1. INTRODUCTION

1.1 Motivation

The motivation to study the characteristics of biochar came from two sources. The first was a session on biochar and nutrient cycling at the *2007 Growing the Bioeconomy* Conference hosted by Iowa State University. Speaking in that session were Drs. Johannes Lehmann of Cornell University and Stephen Joseph of the University of New South Wales, two of the earliest and most prominent proponents of biochar. Their talks focused on the potential of the soil-applied charcoal to address many challenges facing the world today: renewable energy, soil degradation, hunger, climate change, and waste management. Unlike many other platforms for extracting renewable energy from biomass, biochar builds up soil fertility and food availability rather than act as a competing interest. Properly understood and applied, biochar has potential for creating many different win-win-win situations with very few drawbacks.[1, 2]

The second motivating factor was that char, in one form or another, is produced as a co-product by all three biomass thermochemical processes studied at Iowa State University: slow pyrolysis/torrefaction, fast pyrolysis and gasification. As the industries around these technologies develop and scale-up, a decision must be made about how to utilize this char. Should char be burned to recover energy as process heat and power, or should another potentially higher-value application be pursued instead? If one were to use the chars as biochars, how would they compare to biochars currently being studied (mostly chars from the slow pyrolysis of wood)? How would they compare to activated carbon precursors? Would whatever value they have in carbon sequestration, nutrient cycling and soil conditioning applications outweigh other potential uses? How would they contribute to the conversion platform's overall sustainability?

A first step in answering these questions is to determine the properties of fast pyrolysis and gasification chars so that relevant comparisons can be made. Many analytical techniques are available from the charcoal fuel, activated carbon, and soil science fields that could be used for biochars; identifying techniques and procedures

that yield meaningful information is the first challenge. From there, one can gain a better understanding of how thermochemical processing conditions affect biochar properties and how these biochar properties eventually influence a biochar's effectiveness in the soil.

1.2 General Hypotheses

At the time that I began the research for this dissertation, the general consensus in the biochar community was that biochars are mostly alike, slow pyrolysis is the thermochemical process that should be used to produce biochars, and that wood would be the primary feedstock. Little information about reaction condition effects on char properties outside of fuel and activated carbon applications was available, and that information was typically for slow pyrolysis chars. For biochar purposes, the pyrolysis reaction was generally treated as a black box—the effects of biochar addition to the soil and its carbon sequestration potential were of more interest. Fast pyrolysis chars were generally avoided in biochar discussions due to assumptions that they would have low yields of recalcitrant carbon (i.e. they would contain significant amounts of under-pyrolyzed biomass) and that they might contain toxic volatile compounds from adsorbed bio-oils.

In this context, the general hypotheses guiding this research were as follows:

- Biochars produced under different pyrolysis reaction conditions will have different physical and chemical properties because different reaction conditions alter the thermodynamics and kinetics of the pyrolysis reaction.
- Biochars produced from different feedstocks have different physical and chemical properties because they contain different ratios and forms of organic biomass building blocks (cellulose, hemicellulose, lignin, extractives, etc.), each of which reacts by different pyrolysis mechanisms. Different feedstocks also have different mineral compositions that catalyze some pyrolysis reactions and dictate the mineral composition of the resulting chars.
- Biochar properties can be tailored by manipulation of reaction conditions and feedstocks.

- Fast pyrolysis and gasification chars have some properties that are favorable for soil amendment and carbon sequestration applications, and other properties that pose challenges for these applications.
- Characterization methods exist or can be developed to provide biochar property information such that biochar production parameter effects can be understood and controlled, and biochars can be differentiated from each other.

1.3 Organization of Chapters

The end of this first chapter contains a review of the most recent published literature relevant to biochar characterization and engineering.

The second chapter was originally written as a book chapter on biochar for a multi-volume online reference on renewable energy;[3] Robert Brown was a co-author and the chapter is due to be published in June 2012. The goal of the chapter was to provide background information, written in an encyclopedic style, to non-experts on the current state of biochar science and technology. The chapter covers the history of biochar and *terra preta* soils, soil organic matter and black carbon, biochar as a carbon sequestration agent, biochar production methods, biochar properties and characterization methods, scenarios where biochar could be applied, challenges that need to addressed, and future directions for biochar research.

The third chapter is the initial characterization study of biochars available from pyrolysis and gasification reactors at ISU's Center for Sustainable Environmental Technologies (CSET). The co-authors on this project were Justinus Satrio, Klaus Schmidt-Rohr, and Robert Brown; it was published in 2009.[4] The goal of this study was to identify methods that might be used for biochar characterization and provide general property information for fast pyrolysis and gasification biochars, which had received very little attention in prior biochar studies. The chapter focuses on ^{13}C solid-state nuclear magnetic resonance spectroscopy (NMR) techniques.

The fourth chapter is a study that combines biochar characterization and soil incubation techniques to determine the effects of the extent of pyrolysis on fast

pyrolysis biochars. The co-authors on this project were Yan-Yan Hu, Klaus Schmidt-Rohr, Thomas Loynachan, David Laird and Robert Brown; it was accepted for publication in 2011 for a special 2012 edition of the *Journal of Environmental Quality*.[5] The chapter explores many ways in which extent of pyrolysis might be measured and how it relates to biochar properties and interactions with a soil environment.

The fifth chapter is a collaborative study with the Agronomy department using 17 different biochars from the thermochemical processing of switchgrass, corn stover and wood feedstocks. The co-authors on this project were Rachel Unger, Klaus Schmidt-Rohr and Robert Brown; it was published in 2011.[6] The goal of the project was to narrow down a collection of available biochars to promising biochars that might be investigated further in a micro-plot field study. The study consisted of characterization of the biochars and a soil incubation study tracking soil fertility properties over an eight week period.

The sixth chapter is a manuscript for a study looking at the effects of pyrolysis temperature and the presence of oxygen in the pyrolysis atmosphere on biochar properties, specifically the carbon composition. The co-authors on this project were Eric Hall, Jeff Rudisill, Klaus Schmidt-Rohr, David Laird and Robert Brown; it is currently in preparation for publication. Biochars were synthesized from corn stover under carefully controlled slow pyrolysis conditions across a range of temperatures and two different reaction atmospheres. The goal of the study was to construct a carbon composition baseline to which other chars could be compared, including biochars made under slightly aerobic conditions.

The seventh chapter describes general conclusions from the combined biochar studies and future work to be done in the area of biochar characterization and engineering.

Finally, an appendix provides background on the theory and application of solid-state ^{13}C NMR to the characterization of biochar, specifically the data acquisition and analysis methods used in chapters 3-6.

1.4 Recent Literature Review

In the last several months, numerous new articles on biochar characterization and engineering relevant to topics in this dissertation have appeared in the literature. Many of these articles focused on the stability of biochars based on soil incubations[7-21] or the ability of biochars to adsorb or retain chemical compounds such as heavy metals,[22-29] C and N from manure effluent,[18] plant nutrients,[30-35] phenols,[36, 37] enzyme substrates,[38] organic pollutants,[39, 40] pharmaceuticals,[41] and herbicides.[42, 43] Unfortunately, only some studies utilized more than one kind of biochar and attempted to relate processing conditions to biochar properties and soil effects.

Studies involving fast pyrolysis biochars are still relatively uncommon since chars produced in fast pyrolysis are typically reserved for energy production. A group at the Technical University of Denmark has published two studies on wheat straw biochars produced on a fast pyrolysis centrifuge reactor (PCR): one showing that short-term carbon loss from the biochar labile carbon fraction decreases with pyrolysis temperature[7] and the other showing that slow pyrolysis biochars contain less labile carbon than fast pyrolysis biochars made at the same temperature.[44] One study at the Connecticut Agricultural Experiment Station showed that Dynamotive hardwood CQuest® biochar improves mycorrhizal associations and decreases diseases in asparagus.[45] A group at the University of Tennessee produced switchgrass and pine biochars on an auger fast pyrolyzer; they used principle component analysis (PCA) of Fourier transform infrared spectroscopy (FTIR), Raman spectroscopy, thermogravimetric analysis and X-ray diffraction (XRD) to distinguish between biochars from the different feedstocks and production temperatures.[46] Biochars made from rice husk and corn cob with varying residence times on an auger fast pyrolyzer at the University of Science & Technology of China were shown to be similar to or superior to surface-modified activated carbons for the adsorption of phenols (soil application was not considered).[37] Rogovska, et. al found that biochars from high temperature pyrolysis and gasification of corn stover contain compounds that inhibit corn growth in water extracts, but that these inhibiting compounds can be removed with water leaching.[47] One unusual study conducted by

the National Renewable Energy Lab (NREL) showed that peanut hull slow pyrolysis biochar mixed with peanut hull fast pyrolysis bio-oil and urea can be an effective slow-release fertilizer soil amendment.[48]

Several studies described the properties of biochars from new feedstocks, including some nontraditional feedstocks. Biochar from the slow pyrolysis of green tide filamentous algae was found to have low carbon contents, and high nitrogen and ash contents compared to biochars made from lignocellulosic feedstocks.[49] Biochar from the slow pyrolysis of a unicellular marine diatom was shown to have relatively high cation exchange capacity and N content.[50] A comparison of biochars from legume and non-legume feedstocks showed biochars from legume feedstocks to have higher liming potentials for acidic soils.[51] Biochars produced from a variety of livestock manures at two slow pyrolysis temperatures showed expected temperatures trends and high nutrient contents compared to lignocellulosic biochars.[52] Pyrolysis temperature also produced similar trends in biochars from the slow pyrolysis of wastewater sludge.[53] Poultry litter has appeared as a feedstock in several new studies and generally shows common temperature trends and a relatively high loss of feedstock N during pyrolysis.[32, 54]

One contributing factor to the increase in feedstock variety is the desire to use locally available agricultural residues. Deal, et al. compared kiln and gasification biochars made from feedstocks available near Kampala, Uganda.[55] Torres-Rojas, et al. estimated the amount of biochar that can be produced from wood and agricultural feedstocks available around farms in Western Kenya.[56] Mankasingh, et al. compared biochars made in Anila® stoves from feedstocks available in Tamil Nadu, India.[57] Streubel, et al. amended five different Washington soils with slow pyrolysis biochars made from feedstocks available in the Pacific Northwest.[58]

The use of solid-state ^{13}C nuclear magnetic resonance spectroscopy (NMR) for biochar characterization is becoming more common. A comparison of swine manure hydrothermal carbonization (HTC) char and slow pyrolysis biochar showed a much higher extent of aromatization in the slow pyrolysis biochar.[59] Continued analytical efforts to distinguish biochars in soils from other condensed carbon structures

compared the use of NMR with the carbon 1s near edge X-ray absorption fine structure spectroscopy (NEXAFS).[60]

Another analytical technique used in this dissertation that was relatively uncommon in the literature but that is beginning to appear is Fourier transform infrared spectroscopy with photoacoustic detection (FTIR-PAS). (Most FTIR of biochar is done with attenuated total reflectance (FTIR-ATR) or diffuse reflectance (DRIFT)). One recent study used FTIR-PAS to show the changes in functional groups with the increase in temperature for biochars derived from four different agricultural straws.[61]

Literature Cited

1. Laird, D. A., The charcoal vision: A win-win-win scenario for simultaneously producing bioenergy, permanently sequestering carbon, while improving soil and water quality. *Agronomy Journal* **2008,** 100, (1), 178-181.
2. Laird, D. A.; Brown, R. C.; Amonette, J. E.; Lehmann, J., Review of the pyrolysis platform for coproducing bio-oil and biochar. *Biofuels, Bioproducts & Biorefining* **2009,** 3, (5), 547-562.
3. Brewer, C. E.; Brown, R. C., Expanding the Envelope: Biochar. In *Comprehensive Renewable Energy*, Ruddy, D., Ed. Elsevier: 2012; Vol. 5.
4. Brewer, C. E.; Schmidt-Rohr, K.; Satrio, J. A.; Brown, R. C., Characterization of biochar from fast pyrolysis and gasification systems. *Environ. Prog. Sustainable Energy* **2009,** 28, (3), 386-396.
5. Brewer, C.; Hu, Y.-Y.; Schmidt-Rohr, K.; Loynachan, T. E.; Laird, D. A.; Brown, R. C., Extent of pyrolysis impacts on fast pyrolysis biochar properties. *J Environ Qual* **2012,** 41, in press.
6. Brewer, C.; Unger, R.; Schmidt-Rohr, K.; Brown, R., Criteria to select biochars for field studies based on biochar chemical properties. *Bioenergy Res.* **2011,** 4, (4), 312-323.
7. Bruun, E. W.; Hauggaard-Nielsen, H.; Ibrahim, N.; Egsgaard, H.; Ambus, P.; Jensen, P. A.; Dam-Johansen, K., Influence of fast pyrolysis temperature on biochar labile fraction and short-term carbon loss in a loamy soil. *Biomass Bioenerg.* **2011,** 35, (3), 1182-1189.
8. Cross, A.; Sohi, S. P., The priming potential of biochar products in relation to labile carbon contents and soil organic matter status. *Soil Biology and Biochemistry* **2011,** 43, (10), 2127-2134.
9. Fabbri, D.; Torri, C.; Spokas, K. A., Analytical pyrolysis of synthetic chars derived from biomass with potential agronomic application (biochar). Relationships with impacts on microbial carbon dioxide production. *Journal of Analytical and Applied Pyrolysis* **2012,** 93, (0), 77-84.

10. Jones, D. L.; Murphy, D. V.; Khalid, M.; Ahmad, W.; Edwards-Jones, G.; DeLuca, T. H., Short-term biochar-induced increase in soil CO2 release is both biotically and abiotically mediated. *Soil Biology and Biochemistry* **2011,** 43, (8), 1723-1731.
11. Kammann, C.; Ratering, S.; Eckhard, C.; Müller, C., Biochar and hydrochar effects on greenhouse gas (carbon dioxide, nitrous oxide and methane) fluxes from soils. *J Environ Qual* **2012,** 41, in press.
12. Luo, Y.; Durenkamp, M.; De Nobili, M.; Lin, Q.; Brookes, P. C., Short term soil priming effects and the mineralisation of biochar following its incorporation to soils of different pH. *Soil Biology and Biochemistry* **2011,** 43, (11), 2304-2314.
13. Mašek, O.; Brownsort, P.; Cross, A.; Sohi, S., Influence of production conditions on the yield and environmental stability of biochar. *Fuel* **2012**, in press.
14. Peng, X.; Ye, L. L.; Wang, C. H.; Zhou, H.; Sun, B., Temperature- and duration-dependent rice straw-derived biochar: Characteristics and its effects on soil properties of an Ultisol in southern China. *Soil and Tillage Research* **2011,** 112, (2), 159-166.
15. Calvelo Pereira, R.; Kaal, J.; Camps Arbestain, M.; Pardo Lorenzo, R.; Aitkenhead, W.; Hedley, M.; Macías, F.; Hindmarsh, J.; Maciá-Agulló, J. A., Contribution to characterisation of biochar to estimate the labile fraction of carbon. *Organic Geochemistry* **2011,** 42, (11), 1331-1342.
16. Qayyum, M. F.; Steffens, D.; Reisenauer, H. P.; Schubert, S., Kinetics of carbon mineralization of biochars compared with wheat straw in three soils. *J Environ Qual* **2012,** 41, in press.
17. Rogovska, N. P.; Laird, D. A.; Cruse, R. M.; Fleming, P.; Parkin, T.; Meek, D., Impact of biochar on manure carbon stabilization and greenhouse gas emissions. *Soil Sci. Soc. Am. J.* **2011,** 75, (3), 871-879.
18. Sarkhot, D. V.; Berhe, A. A.; Ghezzehei, T. A., Impact of bichar enriched with dairy manure effluent on carbon and nitrogen dynamics. *J Environ Qual* **2012,** 41, in press.
19. Yoo, G.; Kang, H., Effects of biochar addition on greenhouse gas emissions and microbial responses in a short-term laboratory experiment. *J Environ Qual* **2012,** 41, in press.
20. Zavalloni, C.; Alberti, G.; Biasiol, S.; Vedove, G. D.; Fornasier, F.; Liu, J.; Peressotti, A., Microbial mineralization of biochar and wheat straw mixture in soil: A short-term study. *Applied Soil Ecology* **2011,** 50, (0), 45-51.
21. Zimmerman, A. R.; Gao, B.; Ahn, M.-Y., Positive and negative carbon mineralization priming effects among a variety of biochar-amended soils. *Soil Biol. Biochem.* **2011,** 43, (6), 1169-1179.
22. Buss, W.; Kammann, C.; Koyro, H.-W., Biochar reduces copper toxicity in *Chenopodium quinoa* Willd. in a sandy soil. *J Environ Qual* **2012,** 41, in press.
23. Chen, X.; Chen, G.; Chen, L.; Chen, Y.; Lehmann, J.; McBride, M. B.; Hay, A. G., Adsorption of copper and zinc by biochars produced from pyrolysis of hardwood and corn straw in aqueous solution. *Bioresource Technology* **2011,** 102, (19), 8877-8884.

24. Choppala, G. K.; Bolan, N. S.; Megharaj, M.; Chen, Z.; Naidu, R., The influence of biochar and black carbon on reduction and bioavailability of chromate in soils. *J Environ Qual* **2012,** 41, in press.
25. Fellet, G.; Marchiol, L.; Delle Vedove, G.; Peressotti, A., Application of biochar on mine tailings: Effects and perspectives for land reclamation. *Chemosphere* **2011,** 83, (9), 1262-1267.
26. Inyang, M.; Gao, B.; Ding, W.; Pullammanappallil, P.; Zimmerman, A. R.; Cao, X., Enhanced lead sorption by biochar derived from anaerobically digested sugarcane bagasse. *Separation Science and Technology* **2011,** 46, (12), 1950-1956.
27. Uchimiya, M.; Wartelle, L. H.; Klasson, K. T.; Fortier, C. A.; Lima, I. M., Influence of pyrolysis temperature on biochar property and function as a heavy metal sorbent in soil. *Journal of Agricultural and Food Chemistry* **2011,** 59, (6), 2501-2510.
28. Uchimiya, M.; Chang, S.; Klasson, K. T., Screening biochars for heavy metal retention in soil: Role of oxygen functional groups. *Journal of Hazardous Materials* **2011,** 190, (1–3), 432-441.
29. Uchimiya, M.; Cantrell, K. B.; Hunt, P. G.; Novak, J. M.; Chang, S., Retention of heavy metals in a Typic Kandiudult amended with different manure-based biochars. *J Environ Qual* **2012,** 41, in press.
30. Ippolito, J. A.; Novak, J. M.; Busscher, W. J.; Ahmedna, M.; Rehrah, D.; Watts, D. W., Switchgrass biochar affects two aridisols. *J Environ Qual* **2012,** 41, in press.
31. Schnell, R. W.; Vietor, D. M.; Provin, T. L.; Munster, C. L.; Capareda, S., Capacity of biochar application to maintain energy crop productivity: soil chemistry, sorghum growth, and runoff water quality effects. *J Environ Qual* **2012,** 41, in press.
32. Schomberg, H. H.; Gaskin, J. W.; Harris, K.; Das, K. C.; Novak, J.; Busscher, W. J.; Watts, D. W.; Woodroof, R. H.; Lima, I. M.; Ahmedna, M.; Rehrah, D.; Xing, B., Influence of biochar on nitrogen fractions in a coastal plain soil. *J Environ Qual* **2012,** 41, in press.
33. Spokas, K. A.; Novak, J. M.; Venterea, R. T., Biochar's role as an alternative N-fertilizer: ammonia capture. *Plant Soil* **2011**, In Press.
34. Streubel, J. D.; Collins, H. P.; Tarara, J. M.; Cochran, R. L., Biochar produced from anaerobically digested fiber reduces phosphorus in dairy lagoons. *J Environ Qual* **2012,** 41, in press.
35. Yao, Y.; Gao, B.; Inyang, M.; Zimmerman, A. R.; Cao, X.; Pullammanappallil, P.; Yang, L., Biochar derived from anaerobically digested sugar beet tailings: Characterization and phosphate removal potential. *Bioresource Technology* **2011,** 102, (10), 6273-6278.
36. Gell, K.; van Groenigen, J.; Cayuela, M. L., Residues of bioenergy production chains as soil amendments: Immediate and temporal phytotoxicity. *Journal of Hazardous Materials* **2011,** 186, (2-3), 2017-2025.
37. Liu, W.-J.; Zeng, F.-X.; Jiang, H.; Zhang, X.-S., Preparation of high adsorption capacity bio-chars from waste biomass. *Bioresource Technology* **2011,** 102, (17), 8247-8252.

38. Bailey, V. L.; Fansler, S. J.; Smith, J. L.; Bolton Jr, H., Reconciling apparent variability in effects of biochar amendment on soil enzyme activities by assay optimization. *Soil Biology and Biochemistry* **2011,** 43, (2), 296-301.
39. Jeong, C. Y.; Wang, J. J.; Dodla, S. K.; Eberhardt, T. L.; Groom, L., Effect of biochar ammendment on tylosin adsorption-desorption and transport in two different soils. *J Environ Qual* **2012,** 41, in press.
40. Zhang, W.; Wang, L.; Sun, H., Modifications of black carbons and their influence on pyrene sorption. *Chemosphere* **2011,** 85, (8), 1306-1311.
41. Yao, Y.; Gao, B.; Chen, H.; Jiang, L.; Inyang, M.; Zimmerman, A. R.; Cao, X.; Yang, L.; Xue, Y.; Li, H., Adsorption of sulfamethoxazole on biochar and its impact on reclaimed water irrigation. *Journal of Hazardous Materials* **2012**, in press.
42. Jones, D. L.; Edwards-Jones, G.; Murphy, D. V., Biochar mediated alterations in herbicide breakdown and leaching in soil. *Soil Biology and Biochemistry* **2011,** 43, (4), 804-813.
43. Zhang, G.; Zhang, Q.; Sun, K.; Liu, X.; Zheng, W.; Zhao, Y., Sorption of simazine to corn straw biochars prepared at different pyrolytic temperatures. *Environmental Pollution* **2011,** 159, (10), 2594-2601.
44. Bruun, E. W.; Ambus, P.; Egsgaard, H.; Hauggaard-Nielsen, H., Effects of slow and fast pyrolysis biochar on soil C and N turnover dynamics. *Soil Biology and Biochemistry* **2012,** 46, 73-79.
45. Elmer, W. H.; Pignatello, J., Effect of biochar amendment on mycorrhizal associations and Fusarium crown and root rot of asparagus in replant soils. *Plant Disease* **2011**, in press.
46. Kim, P.; Johnson, A.; Edmunds, C. W.; Radosevich, M.; Vogt, F.; Rials, T. G.; Labbé, N., Surface functionality and carbon structures in lignocellulosic-derived biochars produced by fast pyrolysis. *Energy & Fuels* **2011,** 25, (10), 4693-4703.
47. Rogovska, N. P.; Laird, D. A.; Cruse, R. M.; Trabue, S.; Heaton, E., Methods for assessing biochar quality. *J. Environ. Qual.* **2012**, in press.
48. Magrini-Bair, K. A.; Czernik, S.; Pilath, H. M.; Evans, R. J.; Maness, P. C.; Leventhal, J., Biomass derived, carbon sequestering, designed fertilizers. *Annals of Environmental Science* **2009,** 3, 217-225.
49. Bird, M. I.; Wurster, C. M.; de Paula Silva, P. H.; Bass, A. M.; de Nys, R., Algal biochar--production and properties. *Bioresource Technology* **2011,** 102, 1886-1891.
50. Grierson, S.; Strezov, V.; Shah, P., Properties of oil and char derived from slow pyrolysis of Tetraselmis chui. *Bioresource Technology* **2011,** 102, (17), 8232-8240.
51. Yuan, J.-H.; Xu, R.-K.; Wang, N.; Li, J.-Y., Amendment of acid soils with crop residues and biochars. *Pedosphere* **2011,** 21, (3), 302-308.
52. Cantrell, K. B.; Hunt, P. G.; Uchimiya, M.; Novak, J. M.; Ro, K. S., Impact of pyrolysis temperature and manure source on physicochemical characteristics of biochar. *Bioresource Technology* **2012,** 107, 419-428.
53. Hossain, M. K.; Strezov, V.; Chan, K. Y.; Ziolkowski, A.; Nelson, P. F., Influence of pyrolysis temperature on production and nutrient properties of

wastewater sludge biochar. *Journal of Environmental Management* **2011,** 92, (1), 223-228.
54. Song, W.; Guo, M., Quality variations of poultry litter biochar generated at different pyrolysis temperatures. *Journal of Analytical and Applied Pyrolysis* **2012**, in press.
55. Deal, C.; Brewer, C. E.; Brown, R. C.; Okure, M. A. E.; Amoding, A., Comparison of kiln-derived and gasifier-derived biochars as soil amendments in the humid tropics. *Biomass Bioenerg.* **2012,** 37, 161-168.
56. Torres-Rojas, D.; Lehmann, J.; Hobbs, P.; Joseph, S.; Neufeldt, H., Biomass availability, energy consumption and biochar production in rural households of Western Kenya. *Biomass and Bioenergy* **2011,** 35, (8), 3537-3546.
57. Mankasingh, U.; Choi, P.-C.; Ragnarsdottir, V., Biochar application in a tropical, agricultural region: A plot scale study in Tamil Nadu, India. *Applied Geochemistry* **2011,** 26, (Supplement 1), S218-S221.
58. Streubel, J. D.; Collins, H. P.; Garcia-Perez, M.; Tarara, J.; Granatstein, D.; Kruger, C. E., Influence of contrasting biochar types on five soils at increasing rates of application. *Soil Biol. Biochem.* **2011,** 75, 1402-1413.
59. Cao, X.; Ro, K. S.; Chappell, M.; Li, Y.; Mao, J., Chemical structures of swine-manure chars produced under different carbonization conditions investigated by advanced solid-state ^{13}C nuclear magnetic resonance (NMR) spectroscopy. *Energy & Fuels* **2011,** 25, (1), 388-397.
60. Heymann, K.; Lehmann, J.; Solomon, D.; Schmidt, M. W. I.; Regier, T., C 1s K-edge near edge X-ray absorption fine structure (NEXAFS) spectroscopy for characterizing functional group chemistry of black carbon. *Organic Geochemistry* **2011,** 42, (9), 1055-1064.
61. Yuan, J.-H.; Xu, R.-K.; Zhang, H., The forms of alkalis in the biochar produced from crop residues at different temperatures. *Bioresource Technology* **2011,** 102, (3), 3488-3497.

CHAPTER 2. BACKGROUND

2.1 Introduction

Biochar is the carbonaceous solid residue obtained upon heating biomass under oxygen-deficient conditions. It has potential as a nutrient recycler, soil conditioner, income generator, waste management system, and agent for long-term, safe and economical carbon sequestration. The goal of this chapter is to introduce some of these topics and highlight future research directions.

2.2 Archeology and Soil Fertility Beginnings

Original interest in biochar did not stem from concerns over burning fossil fuels or anthropogenic global warming. Rather, research into biochar began from trying to understand the secrets of dark, permanently fertile soils in the central Amazon called *terra preta* or, more generally, Amazonian dark earths. In 1542, a Spanish explorer named Francisco de Orellana returned home from a voyage down the Rio Negro tributary of the Amazon River (near the modern-day city of Manaus, Brazil—see map in Figure 1) and described the presence of large, well-established networks of agricultural settlements and cities along the river banks. These were not the legendary city of gold he had been looking for, but he considered them worth reporting to the Spanish court nonetheless. In years to come, other gold seekers, explorers and missionaries would scour the region but would find no evidence to support Orellana's claims. There were no walled cities, no extensive farming; only solitary groups of hunter-gatherers moving from place to place.

Anthropologists studying the possibility of large, densely-populated, permanent settlements in the central Amazon also expressed doubt in Orellana's claims of advanced civilizations based on the area's infertile soils. Large permanent settlements require access to intensive and sustainable agriculture that, even today, is nearly impossible on the yellow jungle soils. These soils present several serious problems for agricultural farming: low soil organic matter content, acidic conditions, low nutrient retention, high temperatures and high rainfalls.

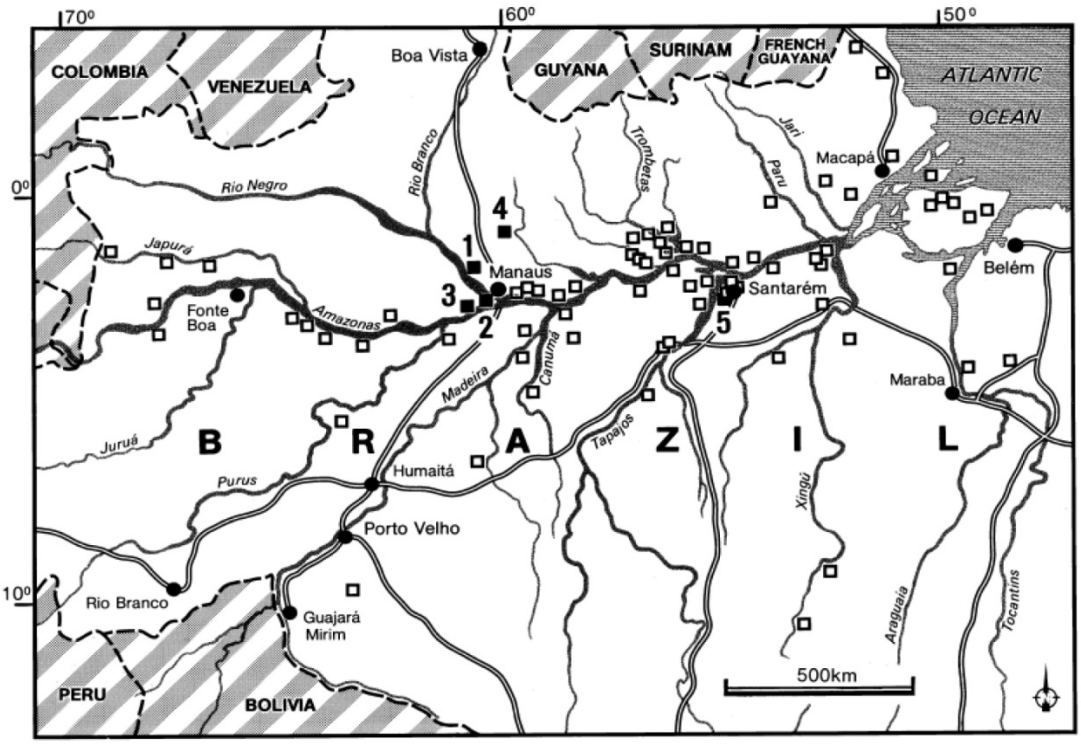

Figure 1. Map of Brazil showing some of the known (open shapes) and investigated (closed) terra preta sites along the Amazon River in Brazil. (Reprinted from Organic Geochemistry, Vol. 31, B. Glaser, E. Balashov, L. Haumaier, G. Guggenberger, W. Zech, Black carbon density fractions of anthropogenic soils of the Brazilian Amazon region, Pages 669-678, Copyright (2000), with permission of Elsevier.)

2.2.1 Soil Organic Matter

Soil organic matter (SOM) is the overall name for three groups of organic materials in soils: living biomass such as microorganisms, plant and animal residues, and humic substances, which are defined as plant or animal residues that are degraded to the point that the original biomass can no longer be identified. Humic substances are further divided into fractions based on their solubility in strong alkali and/or strong acid: humin (insoluble in base), humic acid (soluble in base but not in acid) and fulvic acid (soluble in base and acid). SOM, especially the humic fraction, gives soil a slightly darker color and is composed of approximately 50% carbon (referred to as soil organic carbon) and 5% nitrogen. SOM is also a source of slow-release macronutrients such as phosphorus and sulfur, microbial food, and micronutrients such as trace metals.

Soil organic matter is critical to several aspects of soil quality (Table 1). It promotes good soil structure by serving as the “glue” of soil aggregates, adds water retention capacity to fast-draining sandy soils, increases infiltration and drainage in clayey soils, and decreases soil bulk density, thus improving aeration and root penetration. Negatively charged functional groups on SOM’s surface substantially increase the soil’s cation exchange capacity (CEC). CEC is the ability to adhere and exchange positively charged cations such as important nutrients like potassium (K^+), calcium (Ca^{2+}), magnesium (Mg^{2+}), etc. Clays with a large degree of isomorphic substitution and SOM make up the majority of a soil’s CEC. SOM, especially the fulvic acid and humic acid fractions, can form organic complexes with otherwise insoluble trace metal micronutrients such as copper, zinc, iron and manganese, making them plant-available. The hydrophobic nature of some SOM makes it an excellent sorbent for other hydrophobic molecules such as pesticides, aromatic compounds and oily substances. The available carbon in the SOM provides energy and biomass building material for microorganisms that among other things fix nitrogen, form symbiotic relationships with plants, and cycle soil nutrients. For all of these reasons, crop residues are left in fields, and compost, peat, and manure are applied to fields and incorporated into soils. Like other organic materials, however, SOM is eventually mineralized to carbon dioxide by abiotic chemical oxidation or microbial respiration, or can be lost to erosion.

Maintaining SOM in tropical soils can be particularly difficult. High temperatures increase the rate of abiotic and biotic organic matter decomposition, meaning that added crop residues, manure and composts are mineralized to CO_2 very quickly. In addition, high rain fall increases soil erosion. The loss of SOM quickly depletes the weathered soil’s cation exchange capacity, which then allows chemical fertilizers to leach from the soil and into the water cycle. The loss of SOM and the leaching of basic cations that normally buffer soil pH cause the soil to become very acidic. As the pH decreases, the solubility of plant-toxic metals such as aluminum and cadmium increase. All of these factors make growing agricultural crops in the central Amazon very difficult. Techniques such as slash and burn improve the soil fertility for

a few crop cycles, but soon the mineral ash nutrients have leached away, the deposited carbon has been mineralized, and the farmer must allow the land a long (10-20 year) fallow period and clear a new area of land. Liming the soils can increase soil pH, and adding chemical fertilizers can improve the crop yield, but these techniques are expensive and the effects are relatively short-lived.

Table 1. Effects and benefits of soil organic matter.

Soil Organic Matter Effect on Soil	**Associated Benefit**
Increases soil aggregate stability	Improved soil structure
	Less erosion
Increases macroporosity/	Improved aeration
Decreases soil bulk density	Improved water infiltration
	Improved root penetration
Provides energy source	Increased microbial activity and diversity
	Increased nutrient cycling
Provides nutrient source	Increased N, P, S and micronutrient availability
	Increased plant productivity
Increases water-holding capacity	Increased plant-available water
	Less runoff, flooding and water pollution
Increases cation exchange capacity	Increased Ca, Mg, K and micronutrient availability
	Improved pH stability
Forms organic complexes with trace metals	Increased micronutrient availability
	Adsorption of heavy metal pollutants
Sorbs hydrophobic compounds	Immobilization of toxic organic compounds
	Less water pollution
Buffers pH	Less risk of Al and trace metal toxicity due to low pH
	Less risk of micronutrient deficiency due to high pH
	Increased microbial activity and diversity

If intensive, expensive, modern soil technology cannot achieve a sustainable crop yield in the central Amazon, anthropologists argued, how could natives grow

enough food year after year to support a large permanent population at Orellana's time 500 years ago?

The answer to that question took several decades of discovery and rediscovery to formulate into a cohesive hypothesis. Over the course of nearly a century and a half, numerous researchers in several locations would make the connection between dark soils, the abundance of ancient artifacts from previous settlements, high amounts of soil organic matter, and the possibility of sustainable agriculture on poor jungle soil; unfortunately, much of their work failed to gain the attention of the wider community and was forgotten until someone else made similar discoveries.

2.2.2 Terra Preta

From Orellana's time until the middle of the 19th century, explorers passing through the central Amazon region did not make reference to the dark soils or the soil management practices of the natives in their writings. In the 1870's, several English-speaking geologists began making comments about fertile dark soils on sites of previous native villages as they surveyed areas around "Confederado" farms. "Confederados" were landowners from the Confederate States who had moved to South America after the end of the American Civil War. In 1875, explorer James Orton commented that areas around Santarém with black soil were more fertile for growing rice than South Carolina. Briton C. Barrington Brown is believed to be the first to record the term terra preta or dark earth; he and co-author William Lidstone described the native farmers' preference for cultivating black soils at ancient village sites in Guyana and near Óbidos that had obvious "artificial" origin. In 1879, Charles Hartt and Herbert Smith, who had surveyed the lower Tapajós earlier that decade, referred to dark soil areas as "kitchen middens" due to the amount of pottery found and the assumption that the fertility was caused by high organic residue deposition. It is speculated that the displaced Confederate farmers had learned about the value of the dark soils from local farmers and had chosen the locations for their farms accordingly. Figure 2 shows sample soil profiles of terra preta soils and a typical jungle Oxisol soil. Dark soil layers can be up to several

meters thick, and cover patches from a few square meters to several square kilometers in size.

Figure 2. Examples of Amazonian Dark Earths in comparison to a typical jungle soil profile. Top left: a terra preta containing numerous artifacts at the Hatahara site. Top right: a deep terra preta. Middle left: a close-up of terra preta from the Laranjal Coast Bottom left: a soil profile from the Açutuba Coast. Bottom right: a typical jungle Oxisol soil profile. (Source: Newton Falcão, Instituto Nacional de Pesquisas da Amazônia, Manaus, Brazil.)

The next significant mention of dark earths in the Amazon came in 1903 when Friedlich Katzer published a book in Leipzig, Germany on Amazon geology.[1] Katzer, who had previously worked on naturally occurring black soils in central Europe called Chernozems, was one of the first to report extensive analytical data based on

his fieldwork in the lower Amazon, south of Santarém. He described the Amazonian dark soils as containing decomposed organic matter, mineral residues, and charred plant material. Nearly a century ahead of his time, Katzer concluded that the high organic matter content of the dark earths showed that they were different from the surrounding jungle soils, but at the same time, they were made by human activity and therefore, were also not the same as Chernozems. A phrase often quoted from his writing that summarizes his insightful observations about these dark soils is that the Amazon's "more distinguished wealth lies in its soils."

Following Katzer, a handful of other geologists, anthropologists and archeologists would also make note of the Amazonian dark earths and their apparently anthropogenic origins in the 1920s and 30s. Most notable was Curt Unkel Nimuendaju, a German-nationalized Brazilian anthropologist, who worked in the lower Tapajós and posthumously contributed significant notes and maps on the dark earths in that area. The next three decades of Amazonian dark earth research focused on formulating other, non-anthropogenic origin theories for the fertile soils. Among the theories were that terra preta came from volcanic ash, that the fertile sites were locations of former lakes and ponds that had accumulated organic matter and therefore, attracted artifact-leaving native farmers; or that the dark soils were the results of repetitive short-term settlements.

The work that really began to draw international attention to Amazonian dark earths and their potential was that of Dutch soil scientist, Wim Sombroek. In his 1966 book, *Amazon Soils*, he described and provided lab analysis results for the dark soils of the Belterra Plateau.[2] (Ironically, Belterra Plateau was the same place where rubber tree plantations were relocated in 1934 for reasons unrelated to soil fertility following the infamous Fordlandia failure). Sombroek also mapped the distribution of dark soils along the bluffs of the Tapajós River. He introduced the term terra mulata or brown soil to describe the high organic matter soils often surrounding terra preta soils and likely the sites of ancient native field agriculture. Unlike terra preta soils, which were more likely waste disposal zones, terra mulatas are slightly lighter in color, contain few artifacts, have lower concentrations of plant nutrients,

and appear to be the result of semi-intensive cultivation over long periods of time, containing material from low-temperature field burning. Figure 3 shows an example of the difference in appearance of a terra preta, a terra mulata, and an adjacent jungle soil. For the next four decades up until his death in 2003, Sombroek was responsible for enormous amounts of dark earth research and advocated the creation of terra preta nova, or new dark earth, to improve soil carbon stores and intensive agriculture.

Figure 3. Terra preta, terra mulata and the adjacent Latassol soil from a site in the central Amazon. All three soils have similar soil texture. (Source: Newton Falcão, Instituto Nacional de Pesquisas da Amazônia, Manaus, Brazil.)

"Modern" scientific study of Amazonian dark earths began in the late 1970's with publications in Japanese and German soil science journals by Renzo Kondo

(1978),[3] and Wolfgang Zech and Gerhard Bechtold (1979).[4] Since then and especially since 2000, numerous journal articles, review papers and two books have been published describing terra preta sites and soil management practices throughout South America, anthropogenic dark earths found in some central African communities, traditional Japanese horticulture practices incorporating charcoal, and improved soil fertility around former charcoal production sites throughout the world. A short study by Bruno Glaser, et al. published in *Naturwissenschaften* in 2001 is often cited as demonstrating that black carbon (BC) in soils is the key to terra preta's long organic matter residence times and continuing fertility.[5]

Several researchers have investigated the effects of charcoal addition on jungle soils, in combination with mineral fertilizers and other organic amendments, to try to identify which factors and interactions contributed to terra preta's success. In his 2006 dissertation and related publications with colleagues, Christoph Steiner described the results of several such field studies and the potential for a "slash and char" system of agriculture to replace "slash and burn."[6] In general, it was found that charcoal additions alone were not nearly as effective as combinations of charcoal and mineral fertilizer or charcoal and organic amendments (chicken manure, compost, kitchen scraps) applied to the soil. The effect of charcoal was more that it helped soils retain the added fertilizers and organic matter, so that fewer inputs needed to be added less often, even with the tropical heat and high rainfall.[7] The benefit of "slash and char" over "slash and burn" is that there is more of the beneficial carbon left (~50%) after pyrolysis than the few percent typically left after a high temperature burn that is mineralized or washed away in two or three years. Overall, the secret to sustainable agriculture in the tropics, according to field study results and supported by local wisdom passed down for generations, appeared to be a "fire and organic matter" combination.

2.3 A New Focus: Carbon Sequestration

Researchers carbon-dating charcoals found in terra preta soils found that they were hundreds to thousands of years old, meaning that carbon removed from the

atmosphere by plants long ago had been effectively sequestered as a stable solid. During a time when vast amounts of research funding is being channeled into developing carbon capture and storage (CCS) technologies, carbon stability in soil has enormous significance and has brought anthropogenic soils like terra preta into the international limelight for a new reason: a way to sequester carbon and thus combat global warming.[8]

2.3.1 The Global Carbon Cycle

The concerns about carbon dioxide emissions stem from the concern about imbalances in the global carbon cycle. This cycle consists of three main carbon locations: the atmosphere, the biosphere, and the lithosphere, also sometimes called the geosphere. In the atmosphere, carbon exists as gases (carbon dioxide, carbon monoxide, methane, etc.) as well as some fine particulates such as soot. The biosphere includes carbon held in living organisms such as plants, animals, and microorganisms. Carbon stored in the lithosphere includes fossil fuels such as crude oil, natural gas and coal, mineral formations such as carbonates, and soil and sediment carbons such as residues, organic matter, humus, and black carbon. Significant carbon is also stored in the hydrosphere, as carbon dioxide in the air is in equilibrium with carbonic acid in the world's oceans, rivers and lakes. When the carbon cycle is balanced, carbon removed from the atmosphere by photosynthesis exists in the biosphere until the organism dies, at which point the carbon is returned to the atmosphere by mineralization or stored in the lithosphere in a more stable form.

By burning fossil fuels, excessively tilling agricultural fields and cutting down forests, humans move carbon from the lithosphere and biosphere to the atmosphere faster than photosynthesis can remove it; such processes are therefore carbon positive. Figure 4 shows the major sources, sinks and fluxes of the global carbon cycle. Overall, there is a net annual increase in atmospheric carbon on the order of 5 gigatons (10^{15} grams) of carbon per year (Gt C/yr). Many of today's bioenergy systems and environmentally conscience consumer products strive to be carbon

neutral, where the rate of carbon dioxide production throughout the process is equal to the rate of carbon removal from the atmosphere.

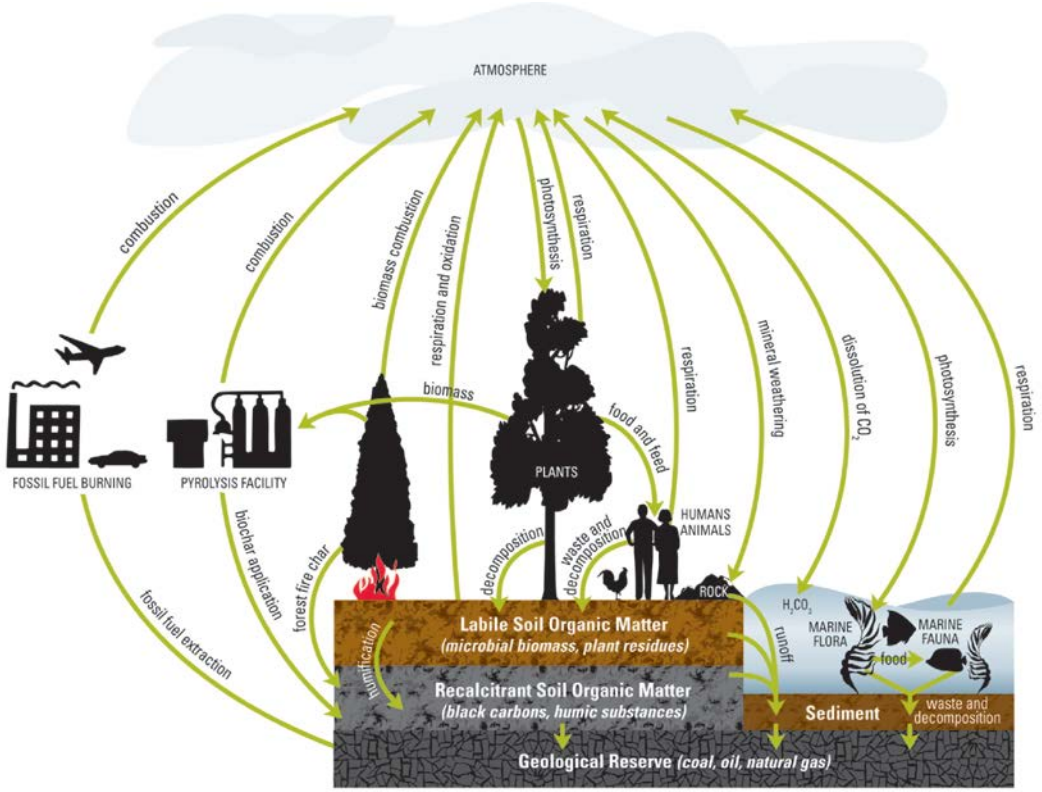

Figure 4. The global carbon cycle representing natural and anthropogenic contributions. (Source: chapter authors, graphic design by Christine Hobbs)

The carbon neutrality of a product or process is heavily dependent on where “start” and “end” are defined in the life cycle analysis and what aspects of the process are included in the accounting. In the case of fossil fuel use, carbon capture and storage technologies currently under development hope to collect, pressurize, and permanently store carbon dioxide flue gases in geological formations such as former natural gas reservoirs, deep underground saline aquifers, or active oil wells to increase the amount of recovered oil. As long as that carbon dioxide stays out of the atmosphere and no additional carbon dioxide is released in the transportation, upgrading, storage, etc. of these fuels, these processes could be considered carbon neutral. Biochar has the potential to be carbon negative, that is its production and application have the potential to turn the carbon dioxide removed from the

atmosphere by plants into a solid carbon that will stay solid (and out of the atmosphere) for a sufficiently long time. Carbon dating evidence from terra preta soils and existing studies of black carbons (BC) in the environment demonstrate how this can be possible.

2.3.2 Black Carbons

Black carbons are found nearly everywhere in the environment: terrestrial soils, sediments under bodies of water, and the atmosphere as small particulates (referred as “elemental carbon” in atmospheric sciences). BC tends to be the oldest and most stable form of organic carbon in soils, especially when soil aggregates form around BC particles and protect them from microbial and chemical oxidation. Black carbons are most frequently found in areas prone to vegetation fires such as forests and open prairies. The incredible fertility and dark color of Midwestern US soils are often attributed to thousands of years of prairie fires building up organic carbon, and especially black carbon. (The relatively young age of the soils, the organic matter from perennial grass roots and sufficient rainfall are also factors.) Even in areas with few vegetation fires, black carbon can still be deposited in soils as small particulates in the atmosphere from far away fires fall to the ground. Black carbons in river and ocean beds are deposited through erosion of soils and burial in the sediments. Overall, the long-term existence of BC in so many of the world’s soils and sediments gives credibility to the possibility of using biochar as a way to stably sequester large amounts of carbon.

As important as black carbons are in the global carbon cycle, the exact amount of carbon sequestered as BC is very difficult to quantify and has long been the subject of analytical methodology discussions. By definition, black carbon is a carbonaceous material that is pyrogenic (fire-derived) and recalcitrant (resistant to biotic or abiotic degradation). Char, the product of solid phase thermochemical reactions, and soot, the gas-phase condensation products of combustion, are both considered black carbons. The analytical difficulty is that pyrogenic carbons exhibit different degrees of recalcitrance. Table 2 lists some different types of

thermochemically produced carbons from brown-colored, barely-burned biomass to graphite-like soot, as well as their relative reactivities, formation temperatures, and representative thermochemical properties. Each of these materials has slightly different chemical and physical properties, meaning that, for a given analytical technique, some will be identified as black carbon and some will not. Adding to the confusion, there are several other carbon forms in the environment, such as coal, shale and some humic substances that are recalcitrant but are not pyrogenic. The presence of these materials in a sample can result in an overestimate of black carbon content based on false positive results. (Note: The analysis for black carbon should not be confused with analyses for humic substances. The former is based on recalcitrance, the later on solubility. In theory, black carbon in soil would be included in all three of the humic substances based on the alkali/acid separation, especially the humin fraction for the more condensed black carbons, and the humic acid fraction for the less condensed BC.)

Table 2. A black carbon continuum. (Arrangement of table based on Fig. 1 from Masiello C.A., New directions in black carbon organic geochemistry, Mar. Chem., 92, 201-213, 2004.)

Black Carbon Type	Slightly Charred Biomass	Charred Biomass	Activated Carbon	Soot	Graphitic Black Carbon
Representative Formation Process	Torrefaction	Pyrolysis/ Gasification	Gasification/ Activation	Combustion Gas-Phase Reactions	High Temperature Carbonization
Formation Temperature	200-350°C	400-800°C	800°C+	High	High
Relative Reactivity	High	←	→	Low	Very Low
Relative Size	>mm	µm-mm	µm-mm	<µm	<µm
Plant Structures	Abundant	Significant	Few	None	None

To address this black carbon quantification issue, a round-robin study was organized by Hammes, et al. in the early 2000s to compare how much “black

carbon" was in different reference materials according to methods found in the literature or methods frequently employed in a given laboratory.[9] Seventeen labs from several countries and across several disciplines (environmental science, atmospheric science, civil engineering, etc.) were sent samples of the same twelve materials: some different types of black carbon, some matrix samples like soil or air particulates containing black carbon, and some non-BC materials known to interfere in black carbon analyses.[10] Each lab analyzed the samples using the techniques they had available and shared their results with the other laboratories. The most common kind of method used was some sort of oxidation in which chemicals (acids, dichromate, hypochlorite (bleach)) and/or heat would oxidize and remove different fractions of the carbon present. Another method was a derivitization or "molecular marker" method called benzene polycarboxylic acids (BPCA); the aromatic carbons in black carbon are hydrolyzed and partially oxidized to form specific aromatic carboxylic acids that can be analyzed by gas chromatography. From the atmospheric science methodologies, a thermal/optical transmittance and reflectance (TOT/R) method was also used. Researchers involved in the study quickly learned that different methods yielded very different results and even labs using the same method could not achieve good intra-laboratory reproducibility due to small differences in method protocol.[9] These same problems encountered in BC analysis demonstrate some of the difficulty facing biochar today. Different methods were designed to provide information specific to a given kind of carbon used in a given application and this information may not be useful in a different setting. The challenge with BC is to decide which methods provide the most meaning for black carbon in global carbon accounting.

2.3.3 Carbon Sequestration Potential of Biochar

The potential of biochar as a carbon sequestration agent depends upon both the amount and the rate that carbon dioxide could be removed from the atmosphere and stored as carbonaceous solid in soils. The amount that could be removed is enormous. To reduce CO_2 levels in the atmosphere to pre-industrial levels, every

hectare of arable land (about 6% of the Earth's surface) would have to incorporate about 90 metric tons of biochar, a large but not inconceivable quantity. (For comparison, biochar for agronomic purposes is often applied at rates of 50 metric tons per hectare.)

More daunting is the time it would take to remove this excess carbon from the atmosphere. Assuming that 4 metric tons per hectare of biomass residue could be removed annually from the arable lands of the world, then it would take 93 years to return to pre-industrial levels of atmospheric carbon dioxide. Even with the most efficient and inexpensive pyrolysis process, the supply of available biomass will always be a limiting factor on the rate at which biochar can be produced and applied.

2.3.4 Half-life of Biochar in Soils

One aspect of biochar that is critical to its inclusion in future policymaking is the ability to quantify biochar's expected residence time in the soil. For example, if a given amount of biochar with certain properties is applied to soil, how much carbon will remain in 10 years? 100 years? 1000 years? How does one verify that biochar added to the soil stays there and is not lost to mineralization, erosion, etc.? How many carbon credits would biochar be worth?

To answer the first question, one must consider kinetic models. Researchers measure the rate of degradation by tracking the amount of material remaining over time. A typical decay curve is shaped like a hyperbola: the curve declines sharply early, then gradually levels off. In terms of chemical reactions, the rate of decay is very fast at the beginning, then slows until the line eventually flattens and the rate no longer changes. Nuclear scientists use these types of kinetic models on a regular basis to measure the half-life of radioactive isotopes. If it were possible to measure the "half-life" of biochar in soil and know how much carbon had been added at time zero, one could predict the amount of carbon remaining in the soil after a given amount of time. The rate of biochar mineralization (i.e. oxidation to carbon dioxide and loss from the soil) depends on how resistant the biochar is to biological digestion or abiotic (non-biological) oxidation. Fresh biochar is a mixture of more and

less resistant forms of carbon. The less resistant forms are oxidized quickly, causing a steep initial drop in mass and leaving evermore resistant forms of carbon behind. The more resistant forms of carbon break down more slowly, so that it takes longer each time per drop in mass. Eventually, the carbon forms remaining are so recalcitrant that the mass of biochar does not appear to change at all, suggesting a degradation rate of zero. In truth, the rate of degradation never actually stops (otherwise the earth would be covered in a very thick layer of char), it simply is so slow that it cannot be measured within a reasonable time scale.

The degradation of biochar in soil is different from the degradation of fresh biomass in two ways: the initial loss of carbon in the thermochemical processing and the amount of carbon remaining at the “steady-state” point. With biomass, 100% of the biomass is initially applied to soil; with char, about 50% of the carbon is removed in the pyrolysis process meaning that only about 50% of the carbon in the original biomass is actually applied to the soil. The carbon in the untreated biomass is degraded in the soil relatively rapidly by microorganisms (much of the available carbon is gone in a few weeks); by the time the rate of decay has stabilized, there is very little of the biomass carbon remaining in the soil. In contrast, the carbon in the biochar is much more resistant to decay, the rate of loss levels off much faster and more carbon remains in the soil over the long-term. Figure 5 shows what a graph of mass remaining in relation to soil residence time might look like. In general, the higher the temperature of the pyrolysis process, the less carbon there is in the biochar but the more stable that carbon is.

Several scientists have attempted to measure the residence time of biochars (and black carbons) in soils, both at ambient conditions as would occur in nature or using elevated temperatures to accelerate the process, and have encountered difficulties. First, the slow rate of oxidation pushes the limits of analytical detection. This is especially true in soil incubation situations where the signal from the degradation of microbial biomass or soil organic matter is so much larger than the signal from the biochar degradation. Isotope labeling techniques, such as creating biochars from ^{14}C-enriched biomass and applying it to unlabeled soil, show promise

in addressing this problem since the sources of evolved CO_2 can be identified and the detection limits in ^{14}C isotope analytical methods are much lower. The second problem is that measuring the degradation of biochar over a few months or years may overestimate the rate of “steady-state” degradation and thereby, underestimate the residence time of biochar in soils. One way to address this problem is to study the rate of decomposition of much older chars such as those from around old charcoal kilns which were in operation during a known time period; in this way, the measured rate of decomposition would better represent the “steady-state” rate. Unfortunately, this approach means that not much can be known about the original sample or how much carbon was initially applied. In another approach, increasing the incubation temperature accelerates chemical reactions, allowing the results from many years worth of reactions to be observed in days or weeks. These methods are only effective, however, if there is a reliable way to correlate the accelerated reaction rates with the “real-life” reaction rates. Also, elevated temperatures could potentially cause chemical reactions to occur that would not normally happen at ambient temperatures.

Based on the results of studies so far, scientists are confident that the residence time of biochars in soil is on the magnitude of hundreds, if not thousands, of years depending on the conditions under which the biochar was made and the soil environment in which it is applied. For the purposes of carbon credits and accounting, evidence that a biochar with certain properties will remain sequestered in a certain soil environment for a minimum amount of time (such as >1000 years) will probably be sufficient. As with black carbons, however, defining what these quantities are and determining exactly how to measure them will be anything but straightforward.

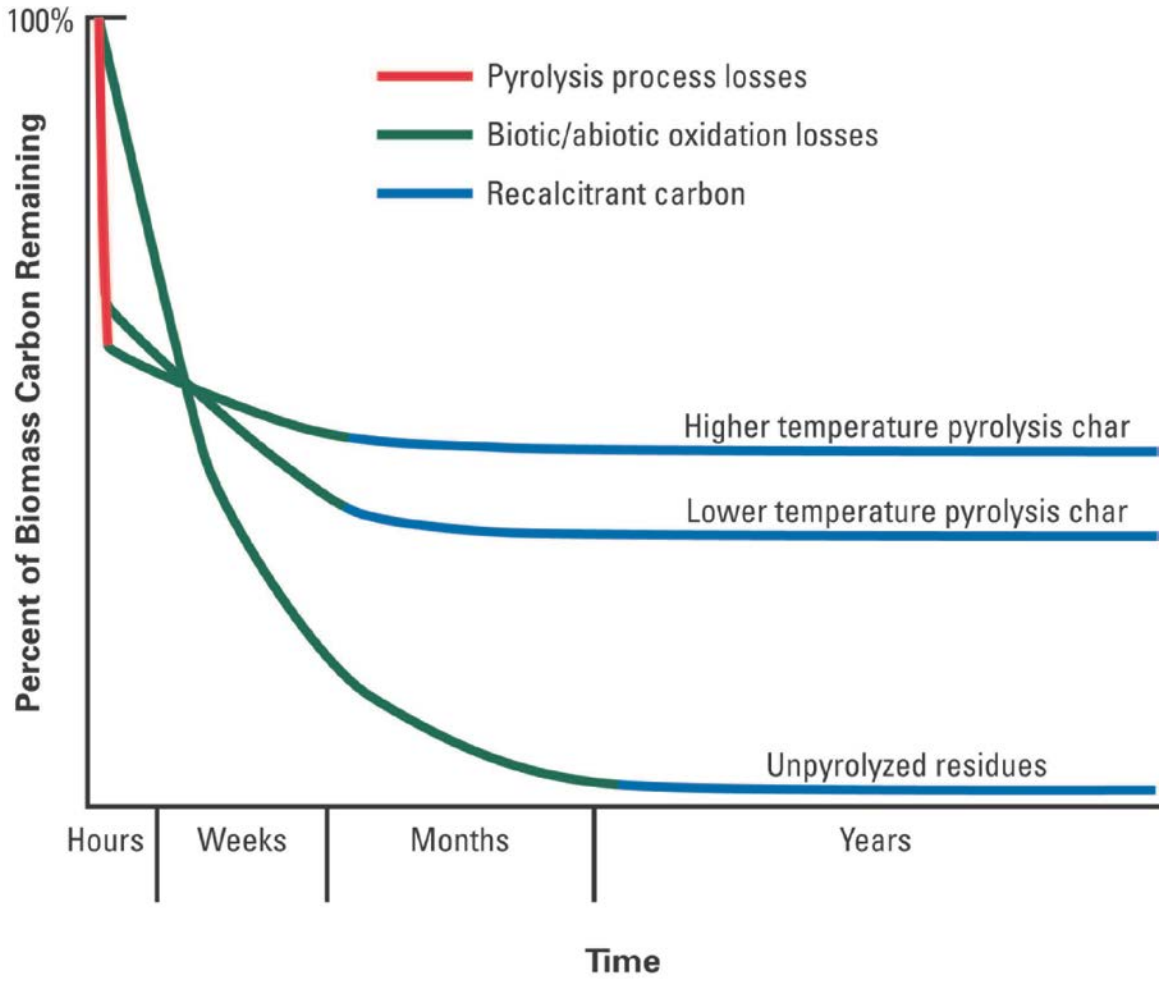

Figure 5. Schematic of the degradation kinetics of unpyrolyzed biomass feedstock, low temperature biochar and high temperature biochar in the environment.

2.3.5 Efforts to Encourage the Adoption of Biochar into Agricultural Practices

The idea of combined carbon sequestration and soil fertility improvement is understandably attracting much international attention. Several organizations have formed around the goals of promoting biochar research and implementation as part of a sustainable economy. The International Biochar Initiative (IBI), a non-profit organization formed in 2006, is by far the largest, though numerous states, countries and regions have also formed their own initiatives. Among its activities, IBI organizes regional and international conferences, coordinates communication between biochar researchers, businesses and users, and works to promote the incorporation of

biochar into legislation, such as including biochar research and development into the 2008 United States Farm Bill. More recently, IBI has been working with the United Nations Convention to Combat Desertification (UNCCD) and several member nations and parties to promote biochar as part of the mitigation strategies in post-Kyoto climate agreements under the UN Framework Convention on Climate Change (UNFCCC), including the December 2009 meeting in Copenhagen. While specific mention of biochar was not retained in the language of the negotiation document consolidated by the Ad Hoc Working Group on Long-Term Cooperative Action (AWGLCA) leading up to Copenhagen, language on mitigation options that could include biochar was retained in an appendix, suggesting biochar has the potential to be specifically identified as a strategy in future international treaties on greenhouse gas emissions and climate change.

2.4 Biochar Sources

In theory, potential biochars could come from just about any thermochemical processing of a carbonaceous material. Feedstocks could include agricultural wastes, forestry residues, used tires, old building materials, municipal solid wastes, etc. Those feedstocks and processes suitable for the sustainable production of biochar are, in reality, limited by feedstock material safety and availability, market conditions for biochar and its process co-products, local soil properties, and the combined environmental impacts. The five processes explored in this section and summarized in Table 3: slow pyrolysis, torrefaction, fast pyrolysis, flash pyrolysis and gasification, represent the processes receiving the most attention across the thermochemical platform for production of biochar, as well as heat, power, fuels and chemicals. All of these processes create some amount of three products: solid (char and/or ash), liquid (bio-oil or tar) and gas (syngas or producer gas). Depending on the product quantity and quality goals, each process uses different reaction conditions (temperature, pressure, heating rate, residence time, reactive or inert atmosphere, purge gas flow rate, etc) to optimize the production of one or more specific products.

A key to analyzing a thermochemical process is to understand what occurs during combustion, i.e. burning in the presence of sufficient or excess oxygen. Some or all of these steps occur in the other thermochemical processes, but often to a lesser extent. The first step in combustion is drying since most biomass contains at least some moisture. As water boils at a relatively low temperature, steam is the first thing to be removed. Fires are more difficult to get started than to maintain because water evaporation is an endothermic (energy-requiring) process. Energy must be added to start a fire before any energy can be extracted from the fire. The second combustion step is volatilization or pyrolysis (no oxygen needed yet). As heat breaks the chemical bonds within the biomass, smaller molecules vaporize and escape from the biomass particle. It is not until the third step: gas phase oxidation, however, that one sees a flame. As hot volatile molecules leave the biomass particle, they come in contact with oxygen and are oxidized, releasing heat and light. If there is enough oxygen present, the only products are carbon dioxide and water. If there is not enough oxygen, however, these volatiles do not burn completely and can result in heavy smoke/tar or gas-phase polymerization to soot. When all of the volatile parts of the biomass have been oxidized and removed, only a very hot, slow-burning solid shell is left to undergo the final step of combustion: solid-phase oxidation. These solid glowing “coals” are still reacting with oxygen, but because the oxygen has to diffuse to the surface of the solid rather than react with gas-phase volatiles, the process is much slower and does not give off a visible flame. Eventually, all of the carbon is oxidized to carbon dioxide and only the non-combustible mineral material, the ash, is left. The extent to which each combustion process occurs depends on the amount of energy available (i.e. the temperature), the amount of oxygen, and the residence time of the biomass particle and product fractions in the oxidizing atmosphere. In combustion chambers and boilers, for example, high temperatures and excess oxygen are used to drive all reactions to completion.

Table 3. Thermochemical processes, their representative reaction conditions, particle residence times, and primary products.

Thermochemical Process	Temperature Range (°C)	Heating Rate	Pressure	Residence Time	Primary Product
Slow Pyrolysis	350-800	Slow (<10°C/min)	Atmospheric	Hours-Days	Char
Torrefaction	200-300	Slow (<10°C/min)	Atmospheric	Minutes-Hours	Stabilized, friable biomass
Fast Pyrolysis	400-600	Very Fast (~1000°C/sec)	Vacuum-Atmospheric	Seconds	Bio-oil
Flash Pyrolysis	300-800	Fast	Elevated	Minutes	Biocarbon/ Char
Gasification	700-1500	Moderate-Very Fast	Atmospheric-Elevated	Seconds-Minutes	Syngas/ Producer gas

2.4.1 Slow Pyrolysis and Traditional Charcoal Making

Charcoal for heating and other purposes is traditionally made by slow pyrolysis: heating in the absence of oxygen to moderate or high temperatures. The process is characterized by slow heating rates and long residence times. Necessary heat to start and drive the reaction is usually provided internally by combusting a portion of the feedstock. In research and situations where greater control is needed, heat is often produced externally and transferred to the biomass by a heat carrier or through the reaction container walls (i.e. placing a sealed reaction vessel inside a furnace). The goal of slow pyrolysis is a high-carbon, energy-dense solid char product. The co-products are a watery, low molecular weight acidic liquid called pyroligneous acid or wood tar, and a low-energy, combustible gas.

Charcoal production has existed in the repertoire of human technologies for thousands of years, most likely since humans learned how to control fire. In early fire

pits, bits of charcoal would have been left over after a fire, especially if the center of larger pieces did not burn completely. Humans gradually learned that they could produce more of this black, light and friable material if they covered burning wood or debris. Some of the first techniques to produce charcoal, such as in pit kilns or mound kilns, were used up through the early 20th century and are still practiced in developing countries around the world.

To build a pit kiln, workers would dig a hole, pack it with dry material (mostly wood) leaving room at each end for an air inlet and outlet, and ignite the material on one end. Once a strong fire was going, less dense material (branches, leaves, etc.) was piled on top, followed by a layer of soil thick enough to keep out the air (~20 cm). Air would be allowed to enter on one side of the pit and exit on the other, causing the combustion region to gradually move across the pit. Workers would tend the kiln constantly over the next two or three days, opening and closing holes in the soil layer to control the amount of air. Once the carbonization process was complete, the pit would be uncovered and the newly made charcoal allowed to cool. The advantages of a pit kiln are that they are inexpensive and can be constructed just about anywhere that has a supply of biomass and workable, dry soil. On the downside, these kilns must be monitored constantly during the entire burn and even then, the operators still have limited control over the reaction conditions. The resulting yields of charcoal are generally very low (~10-30%), have wide variations in quality due to inhomogeneous conditions within the pit, and risk containing significant amounts of contaminants such as the soil used to cover the pile. Pit kilns tend to be energy inefficient and create large amounts of air pollution from the venting of the volatiles (smoke), non-condensable gases (carbon monoxide, methane, low molecular weight hydrocarbons, etc.) and particulate matter. For this reason, pit kilns are typically located outside of populated areas and charcoal makers often suffer from the health issues associated with breathing this polluted air.

Mound kilns are essentially aboveground pit kilns, using similar burn-and-cover methods and being susceptible to many of the same problems. One advantage of using a mound kiln instead of a pit kiln is that a mound kiln can be constructed in

areas where the water table is high or the soil is difficult to work. Maintaining the mound shape and preventing too much airspace requires careful stacking of the feedstock (wood). First, a large, tall piece of wood is set vertically in the center surrounded by small, easily-ignited wood pieces. Around the center post is stacked progressively shorter and smaller logs, all vertically arranged with small pieces packed in between. As with the pit kiln, the mound is then covered with a layer of branches and leaves followed by soil. The center log is removed to serve as a flue and the fire is ignited by dropping burning material into the center opening. The burn/carbonization process is controlled by opening or sealing holes in the soil layer along the bottom edges of the mound. A model of a mound kiln is shown in Figure 6.

Building kilns from brick, concrete or metal was the next step in improving charcoal making technology. Not only are these kilns more permanent in nature, they also allowed for greater heat insulation and control of conditions, thus increasing char yield, consistency and quality. Brick kilns are made of bricks sealed together with mortar or mud set on top of a brick base, are shaped like mounds or beehives, and tend to be larger than the mound kilns. One opening is used to load in wood, while another on the opposite side is used to unload the finished charcoal. Vents along the bottom of the kiln can be opened or closed depending on the color of the smoke leaving the “eye” hole in the top center of the kiln (white = drying, yellow/brown= volatilization, bluish/clear = carbonization complete). Carbonization generally takes close to a week of adding air through the vents, followed by a couple days leaving just the “eye” hole open to vent volatiles, and finally, a cooling period with the kiln completely sealed. This method allows for a slower, more even burn that means less carbon is lost during the combustion phase. Also, by using bricks instead of loose soil, the charcoal coming out is less likely to be contaminated with mineral matter.

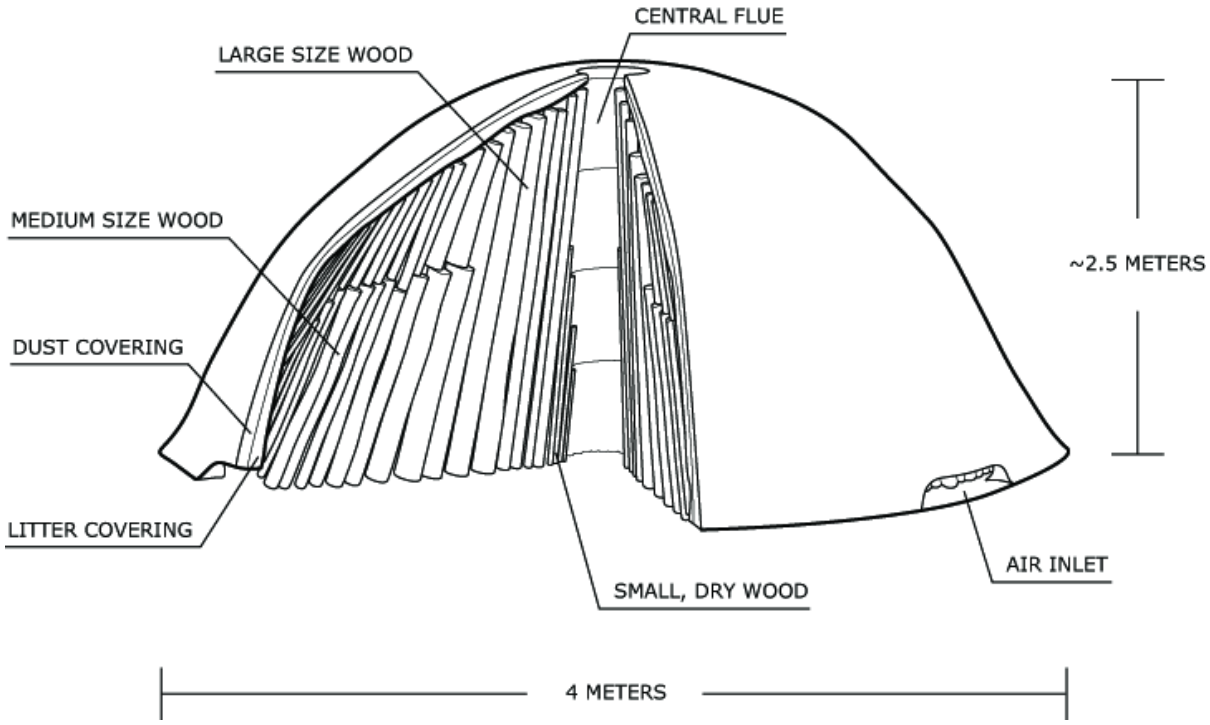

Figure 6. Example of a mound kiln. (Reproduced with permission from Fig. 8.2 in Brown RC (2009) Biochar Production Technologies in Lehmann, J., & Joseph, S. (Eds.) Biochar for Environmental Management: Science and Technology. London: Earthscan.)

Rectangular, reinforced concrete kilns with steel doors and clay pipe stacks, also called Missouri kilns, were very common in regions where a lot of charcoal was produced for the steel industry and several are still commercially operational today, especially for the production of grill charcoal briquettes. The rectangular shape and large doors made mechanized loading of feedstock and removal of finished charcoal much easier. Missouri kilns tend to be much larger than brick kilns (they produce around 13 tons of charcoal about every three weeks) yet still have good heat insulation properties. Air inlet pipes that could be easily closed and thermocouples located throughout the kiln gave operators much more control over hot and cold spots in the kiln. Since all of the emissions leave through a few pipe stacks, it is possible to collect the gases as they leave the kiln for potential recovery of liquid products or passage through an afterburner to control air pollution. With all of the additional controls, Missouri kilns can consistently achieve yields of about 33% relatively high quality charcoal.

Metal kilns can also be used; they provide the same level of control as a brick or concrete kiln but are much more easily moved. These types of kilns originated in Europe in the 1930s and are frequently found in developing countries. With steel, one can create a kiln that can be manufactured in one place and reassembled near the biomass source. One of the best known designs is that of a transportable metal kiln by Tropical Products Institute for use in rural, high-rainfall areas.

Future design of kilns for clean and efficient large scale char production will likely focus on continuous process kilns, instead of the kiln types already mentioned, which all run as batch processes. The advantage of a continuous process is increasing consistency and control as operations are run at a steady state and thus can avoid the hassles and inefficiencies inherent with repeated start-up and shut-down cycles. One common design for continuous process kiln is a rotary kiln. Feedstock in the form of ground wood or other biomass is added to the top of what looks like a winding staircase or slide. Paddles or brushes move the feedstock around in a circle, pushing it gradually down the reactor through three different zones. In the top zone, the biomass is dried by hot combustion gases from the lower zones. In the middle zone, a limited amount of outside air is added to keep a combustion front going. Below the combustion front, is the cooling zone, where the charcoal made in the combustion zone is cooled with recycled combustion gases. Charcoal exits out the bottom, while the unrecycled combustion gases containing the tars and vapors exit out the top to an afterburner. From a gas perspective, air enters in the middle zone where the oxygen all reacts with the vapors coming off the biomass, creating heat and combustion products. Then, the now-hot and oxygen-depleted air goes through the drying zone, transferring heat from the combustion to the incoming fresh biomass. Finally, the cool, oxygen-free gas is recycled to the bottom of the reactor to cool the hot charcoal or let out the top to the afterburner. An example of such a kiln is shown in Figure 7. The advantages of this system are increased control of reaction conditions and very low emissions. Operators can adjust the reaction temperature by controlling the rate of biomass being fed in the top and the rate at which air is allowed into the middle combustion zone. Since the

process is continuous, parameters can be tweaked over a long period of time until a desired steady state is reached. Recycling the spent combustion gases provides a way to cool the finished charcoal without the risk of starting a fire (from to the presence of oxygen) and without needing an external inert coolant such as nitrogen or water. Use of an afterburner means that any unburned particle matter, hydrocarbons or carbon monoxide gases can be completely oxidized before they are released to the environment. The emissions from such a kiln are thus very clean, consisting of water, carbon dioxide and almost no NO_X, SO_X, or mercury.

2.4.2 Torrefaction and Feedstock Pretreatment

Torrefaction can be thought of as low temperature (200-300°C) slow pyrolysis. One example of a torrefaction process is the roasting of coffee beans. Torrefaction removes water and some volatiles from biomass, making the biomass easier to grind, transport and store. Wet, untreated biomass presents several logistical problems. It requires a lot of energy to cut or grind because it is flexible and does not readily crumble. It has a low bulk energy density, so a large volume has to be transported to move relatively little energy. Finally, its high moisture content makes it more susceptible to microbial decay, meaning that a significant amount can be lost to fermentation during storage. By heating the biomass to 200-300°C, the moisture and some of the more readily available carbon structures can be driven off. The resulting products are much the same as those from regular slow pyrolysis except that the solid char product is browner in color than black. This brown “char” is easy to grind, has a higher energy density and is slightly hydrophobic, making it less likely to absorb water and less likely to decay in storage. While this torrefaction char may not be as suitable for direct use as a biochar, the ability to transform raw biomass into a more easily-managed feedstock that is available year round is potentially critical to the economical implementation of other thermochemical processes.

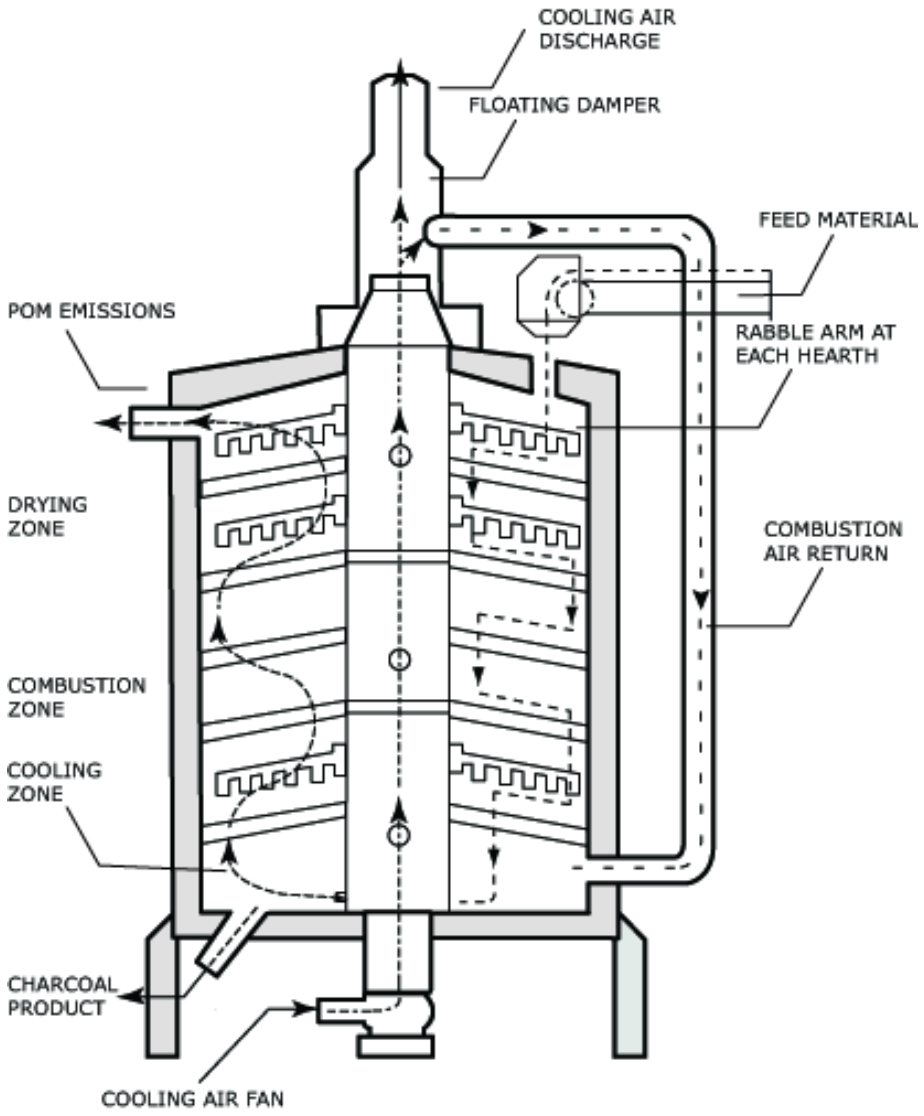

Figure 7. Example of a continuous process kiln. (Reproduced with permission from Fig. 8.7 in Brown RC (2009) Biochar Production Technologies in Lehmann, J., & Joseph, S. (Eds.) Biochar for Environmental Management: Science and Technology. London: Earthscan.)

2.4.3 Fast Pyrolysis and Bio-oil

Fast pyrolysis, like slow pyrolysis, is the heating of biomass in the absence of oxygen. Unlike slow pyrolysis, however, fast pyrolysis uses very high heating rates (~1000°C/s), short residence times and the rapid quenching of vapors to maximize the production of the liquid product, bio-oil. The theory behind fast pyrolysis design highlights the difference between a thermodynamically controlled process and a kinetically controlled process. In a thermodynamically controlled process, reactants

and products are allowed sufficient contact time to reach thermodynamic equilibrium. The final distribution of products depends on process conditions such as temperature and pressure, but not on reaction rate. In thermochemical processing, slow pyrolysis represents a thermodynamically controlled process; the amount of char or gas products varies with temperature, pressure and feedstock composition, but would be the same regardless of whether the reaction lasted for a few hours or a few days. In fast pyrolysis, a kinetically controlled reaction, the goal is to create and separate vapors as quickly as possible before they can condense and carbonize as secondary chars or crack into light molecular weight non-condensable gases. In other words, one wants to avoid thermodynamic equilibrium. This is accomplished through a high rate of heat transfer to the biomass, causing the drying and volatilization steps to occur almost instantaneously. Methods to achieve such high heat transfer rates include reducing the particle size, selecting an effective heat carrier (such as sand or steel shot), and using a fluidized bed, heated blade (ablative pyrolysis), or screw mixer (auger pyrolysis) reactor design. Once heated, the large amount of created volatile molecules and aerosols quickly expand out of the biomass particles (sometimes causing the particles to fracture apart) and are removed from the reaction zone by a vacuum (vacuum pyrolysis) or high flow rates of an inert sweep gas. Outside of the reaction zone, the hot vapors are quickly separated from the solid char (which can catalyze secondary carbonization or cracking reactions) by cyclones or other kinds of filters. Finally, the vapors and aerosols are condensed out of the gas phase by cooling, scrubbing, electrostatic precipitation, etc. while the non-condensable gases are sent on to an afterburner for energy or heat recovery. To achieve a maximum yield of oil (~70% by weight), fast pyrolysis reactors are designed to achieve a vapor residence time of no more than a few seconds and moderate temperatures (400-600°C).

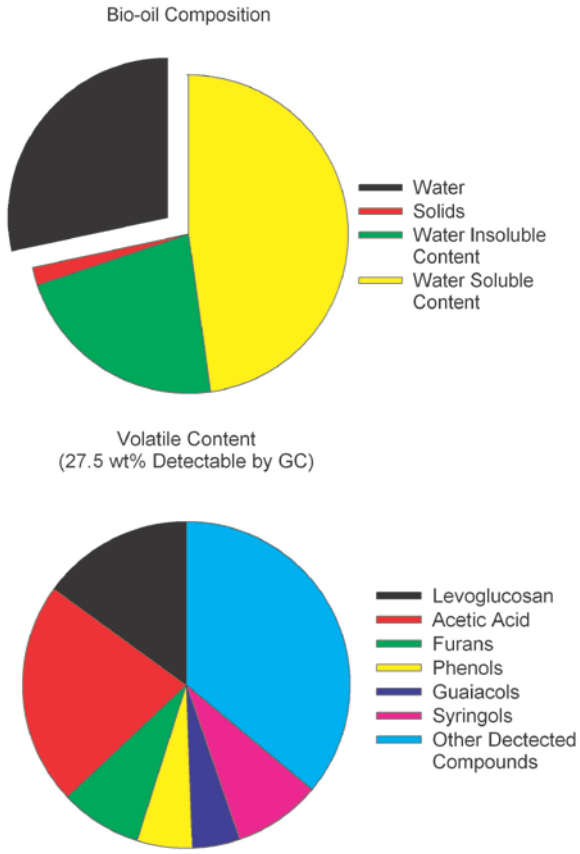

Figure 8. Composition of bio-oil from the fast pyrolysis of red oak based on solubility (above) and gas chromatography (GC) detectable volatile compounds (below). Percents are weight percent of the whole bio-oil on a wet basis. (Source: Anthony J.S. Pollard,Center for Sustainable Environmental Technologies, Iowa State University.)

Bio-oil from fast pyrolysis is a complicated mixture of water and oxygenated organic compounds including organic acids, aldehydes, alcohols, furans, pyrans, anhydrosugars and aromatic compounds (see Figure 8). Approximately 300 different compounds have been identified in bio-oil from the decomposition of hemicellulose, cellulose and lignin. As a feedstock for the production of organic chemicals and transportation fuels, bio-oil has been compared to crude petroleum in that can provide a wide variety of products but requires fractionation and upgrading. There are three key differences between crude oil and bio-oil that pose a significant problem for its direct use in existing refineries, namely water content, oxygen content and high acidity. Bio-oil is also unstable, especially when stored at high

temperatures. It tends to separate into aqueous and hydrophobic phases, and the high acidity and oxygen content catalyze polymerization reactions that dramatically increase oil viscosity. Research aimed at improving bio-oil properties has included bio-oil collection system designs that separate the oil into fractions, catalytic reforming of aqueous bio-oil to produce hydrogen, and bio-oil upgrading through hydrogenation to remove carboxylic acids and oxygen. Currently, bio-oil can used as a heavy oil replacement in commercial boilers and some steam turbines for heat and electricity, as an energy-dense, pumpable biorenewable feedstock for gasification, and as a petroleum replacement in the production of asphalt (i.e. “bio-asphalt”).

2.4.4 Flash Pyrolysis and the Effects of Pressure

Flash Pyrolysis™ is a batch pyrolysis process that uses moderate pressures (2-25 atm) to minimize reaction time and maximize biocarbon yield. The research and recently commercial technology is based on the work of Michael J. Antal Jr.’s group at the Hawaii National Energy Institute, University of Hawaii—Manoa.[11] The flash pyrolysis process uses pressure to promote volatile condensation and secondary char formation (exactly opposite of the vapor removal goals of fast pyrolysis). In this process, biomass is packed into canisters which are loaded into a high pressure chamber. Compressed air is pumped into the chamber and the combustion/pyrolysis reaction is initiated by electric heaters on the bottom of the reactor. The biomass at the bottom of the reactor begins to burn, heating the biomass above it. After about 30-45 minutes, the oxygen in the chamber has been depleted and all of the biomass has been transformed into biocarbon. Vented gases are sent to an afterburner that can potentially produce heat and/or electricity. The increased pressure shifts the thermodynamic equilibrium of the reaction to heavily favor char formation and also increases the rate of reaction, making the overall throughput rate only slightly slower than continuous fast pyrolysis process. Current marketing of the process is focused on more traditional uses of charcoal (coal replacements and activated carbons) but has strong potential in the areas of waste management (waste-to-carbon) and biochar horticulture and agriculture applications.

2.4.5 Gasification and Syngas

As the name implies, the primary product of gasification is the non-condensable gas fraction. The process is characterized by higher temperatures (750-1800°C) and the presence of some oxygen, measured in equivalence ratio or the fraction of the amount of oxygen needed for stoichiometric combustion (typically around 0.25 or 25%). The product gas, called syn gas ("synthesis gas"), or producer gas if it contains nitrogen, consists mostly of carbon monoxide (CO) and hydrogen (H_2) with smaller amounts of carbon dioxide, methane and other low molecular weight hydrocarbons. Overall, gasification is very similar to combustion, but due to the limited oxygen, it is not able to complete the gas-phase and solid-phase oxidation steps which would yield carbon dioxide (CO_2) and water (H_2O). In an ideal gasification situation, the reaction is thermodynamically controlled. The gas composition and carbon conversion can be predicted based on temperature and pressure, and the only co-product is char. In reality, there is not sufficient time for the reaction to reach equilibrium, resulting in the creation of sticky, viscous tars that can clog reactor plumbing and cause significant problems in downstream gas applications. Much research has been devoted to the development of methods to address this tar problem such as the use of steam and/or catalysts to promote tar cracking, tar filtering or scrubbing systems for downstream gas cleaning, and raising the reaction temperature and/or residence time.

There are numerous gasification reactor configurations such as bubbling fluidized beds, circulating fluidized beds (indirectly heated gasification), downdraft reactors, and updraft reactors, as well as several reaction modes. For example, a "slagging" gasifier is run at very high temperatures (>1000°C) such that the mineral components in the feedstock vitrify during the reaction and form a very stable slag. This vitrification may be advantageous in cases when toxic or heavy metal components of a feedstock need to be stabilized, such as with the gasification of some municipal wastes. Slagging reactors would not be conducive to the production of biochar or the recycling of plant nutrients. A "non-slagging" reactor (i.e. at 750-900°C) yields a small amount of high-ash char (~10 wt %) and tends to produce

more tars (up to 10 wt %). Indirectly heated gasifiers consist of two reactors with a heat carrier circulating between them: a combustion chamber where tars, chars or other carbon sources are burned to provide energy to the heat carrier, and a gasification chamber where heat from the heat carrier and some added oxygen are used to drive the gasification reactions.

The oxygen needed for the gasification can come from air (air-blown gasification) or from a mixture of steam and oxygen (steam/oxygen-blown gasification). Steam/oxygen-blown gasification has three advantages over air-blown. First, the product gas stream is not diluted with nitrogen. Second, steam can easily be separated from the gas stream by condensation. Finally, steam in the reaction can be used to accomplish an in situ water-gas-shift (WGS) reaction to increase the hydrogen content of the product gas. The WGS reaction is based on the equilibrium between water, carbon monoxide, carbon dioxide, and hydrogen:

$CO + H_2O \leftrightarrow CO_2 + H_2$

One downside of steam/oxygen-blown gasification is that it requires the use of expensive gas separation equipment to produce pure oxygen from air.

There are several uses for syngas and producer gas. The most direct use is to use it as an alternative to natural gas (i.e. methane). Prior to the widespread use of natural gas, “town gas” from the gasification of coal was commonly used in heaters, stoves and light fixtures. Syngas, which contains carbon that has already been mostly oxidized, is much less energy dense than natural gas especially where the product gases were diluted with nitrogen from air. Transportation fuels and chemicals can be synthesized from syngas. One important reaction is the production of methanol from one mole of carbon monoxide and two moles of hydrogen:

$CO + 2H_2 \leftrightarrow CH_3OH$

Hydrocarbons can even be produced from syngas through the catalytic Fisher-Tropsch process which uses low-moderate temperatures, high pressures and cobalt, iron, ruthenium or nickel transition metal catalysts to produce a distribution of alkanes and paraffin waxes. Depending on the reaction conditions, the alkanes can

range from the shorter-chain gasoline fraction to the medium-length jet fuels to the longer diesel fuels and waxes:

$(2n+1)H_2 + nCO \leftrightarrow C_nH_{(2n+2)} + nH_2O$

One challenge with the Fisher-Tropsch synthesis is that its optimal hydrogen-to-carbon monoxide ratio is around 2 while the ratio in the syngas from the gasifier is lower (generally closer to 1), meaning that significant amounts of CO must be converted to CO_2 by the WGS reaction to provide the necessary hydrogen. Another challenge to this and other catalytic processes is the coking or fouling of the catalyst. Even tiny amounts (on the parts per billion scale) of some species that foul catalysts can be enough to ruin a process. Therefore, compounds containing sulfur, nitrogen, halides: fluoride, bromide, chloride and iodide, and tars or particulate matter that can coke on catalysts must be meticulously removed from the product gas stream prior to the catalysis reactor. For this reason, the gas cleaning/conditioning segment of a gasification process is often one of the most complicated and expensive system components.

2.4.6 Biochar as a Co-Product

As seen from the five thermochemical process described above, biochar can be a primary or an auxiliary co-product. The key to designing an efficient and sustainable process for a given feedstock, region and economic environment is to consider the potential uses of every co-product. Just because a process may be optimized for a product other than biochar, does not mean that biochar cannot significantly contribute to the overall scheme. For example, a fast pyrolysis process designed for maximum high quality oil yields might still produce 10-15% weight of biochar and 15-20% combustible gases. The biochar can be applied to the soils from which the biomass was harvested to recycle plant nutrients (concentrated in the solid fraction) and sequester some carbon. The non-condensable gases can be combusted to produce process heat. One problem with traditional charcoal making technologies and a key difference in comparison with modern processes is the lack of utilization of the gas and liquid fractions, causing a low overall process efficiency

and significant pollution. Future thermochemical processes that can carefully control and take advantage of each product fraction, and possibly alternate between primary product fractions based on feedstock availability, market demand and local conditions, are the most likely to be successful.

2.5 Biochar Properties

Biochar properties are easiest to describe if char is treated as having two fractions: the “carbon” fraction and the inorganic ash fraction. The “carbon” fraction includes hydrogen, oxygen and other elements bonded to carbon and is the fraction most affected by reaction conditions. Reaction time, temperature, heating rate, etc. convert—to some degree—the mostly carbohydrate organic components into the condensed aromatic structures characteristic of char. The inorganic ash fraction is the fraction most affected by feedstock properties; the reaction conditions have some effect on the ash properties and ash-to-carbon ratio of the char, but overall, whatever mineral constituents are in the biomass become concentrated in the ash.

2.5.1 Biochar Composition

Quantifying the amount of ash and the amount of (mostly carbon) organic material is done by proximate analysis, a thermogravimetric method traditionally considered the most basic for determining char quality. According to the ASTM standard for wood charcoals (D1762-84), mass lost at 110°C is moisture, mass lost in an inert atmosphere at 950°C constitutes “volatile matter,” mass lost at 750°C in an oxic atmosphere (normally air) is “fixed carbon,” and the remainder is “ash.” This analysis and the selected temperatures were designed for chars used as combustion fuels in high temperature boilers. For such an application, moisture and ash represent fractions of the char that do not contribute to the energy content. A “good” charcoal is one that is mostly fixed carbon, with some volatiles to ease the ignition process and low moisture and ash. Use of some form of proximate analysis (temperatures and heating times vary slightly) is prevalent in biochar literature, though numerous researchers have questioned the relevance of proximate analysis

data for soil applications. For example, the connection between a char compound's "volatility" and its recalcitrance in soil is not clear. It is true that dense aromatic carbons that are recalcitrant in soil also tend to have low "volatile matter content," and that "high volatile matter" chars have appeared to cause nitrogen immobilization problems in some soil studies (**see** section 24.7.3 Potential soil/crop drawbacks) but much more work is needed to make this analysis more useful for determining char quality in relation to soil application.

The second most common analysis and one that is critical to further characterizations is the measurement of carbon, hydrogen and nitrogen content, also known as elemental or CHN analysis. In this technique, a sample (liquid or solid) is combusted at very high temperatures with excess oxygen and the produced carbon, hydrogen and nitrogen species (CO_2, H_2O and nitric oxide, NO, respectively) are trapped and quantified. Results from this analysis are typically reported in terms of percent weight of a dry sample. Elemental analysis can also include the separate trapping and measurement of sulfur (CHNS) and oxygen content (CHNOS). The total or "ultimate" analysis of a char includes information from both the elemental and the proximate analyses, in addition to the chlorine content. The composition of a given char, therefore, will often be reported as a certain amount of moisture, carbon, hydrogen, nitrogen, sulfur, chlorine and ash, with the difference in total dry weight assumed to be oxygen. The practice of determining oxygen "by difference" stems from the difficulty in obtaining a consistent direct oxygen measurement due to the decomposition of mineral oxides in the ash.

The composition of potential biochars varies greatly with feedstock and pyrolysis process. For example, biochars from the slow pyrolysis of hardwoods might have over 90% carbon with very little of anything else; on the other hand, biochars from the fast pyrolysis of switchgrass might have only 35% carbon, some oxygen and over 60% ash from the high silica content in the feedstock and the low solid carbon yield of the process. In general, the higher the temperatures and residence time, the less carbon, oxygen and hydrogen remain in the solid product. One way to represent the extent of a thermochemical reaction is through a Van Krevelen diagram which

plots the molar oxygen-to-carbon ratio (O/C) in relation to the molar hydrogen-to-carbon ratio (H/C). An example Van Krevelen plot of chars from torrefaction, slow pyrolysis, fast pyrolysis and gasification is shown in Figure 9. Lignocellulosic feedstocks, which consist mostly of carbohydrates, have O/C ratios close to 1 and H/C ratios close to 2. As these feedstocks are heated, both ratios decrease as oxygen and hydrogen are removed as CO, CO_2, H_2O and other O- and H-containing volatiles, thus “concentrating” the carbon. Later, as fresh chars oxidize in the environment and gain oxygen-containing surface functional groups, the O/C ratio increases again, fast at first, then more gradually over time until it approaches a steady state.

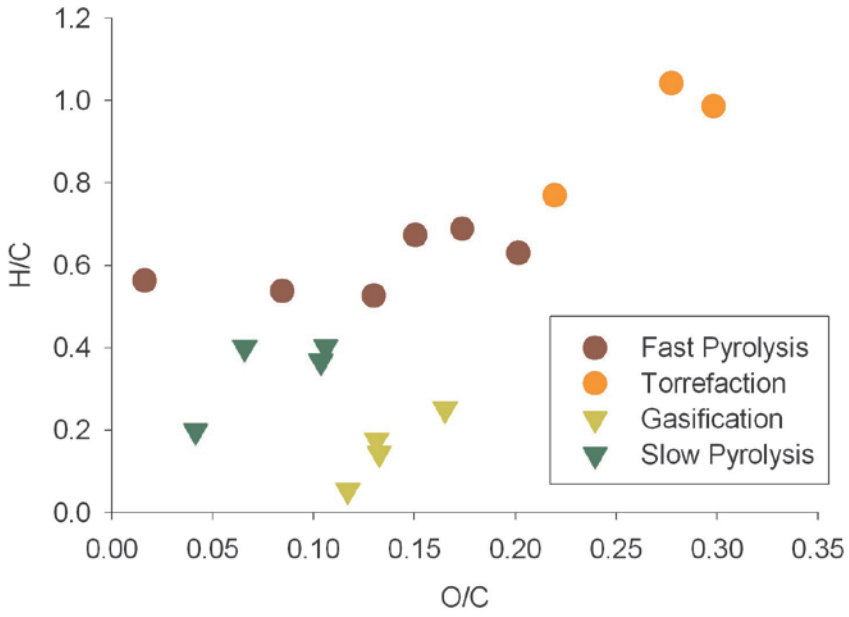

Figure 9. Van Krevelen plot of biochars from torrefaction, slow pyrolysis, fast pyrolysis and gasification. O/C and H/C ratios are molar ratios. In general, both ratios decrease with increasing reaction temperature.

The composition of the ash fraction of biochar is mostly dependent on the minerals found in the feedstock since most inorganic elements do not volatilize at typical pyrolysis temperatures. There are several ways of determining which elements are present and in what relative quantity. One of the easier techniques is X-ray fluorescence (XRF) spectroscopy. Fluorescence occurs when an atom

absorbs energy from an electromagnetic photon, raising the energy level of an electron; as the electron relaxes, it emits a lower energy electromagnetic photon. Each element has characteristic wavelength or set of wavelengths that it emits when bombarded with X-ray radiation and the intensity of the emission is relative to the amount of that element present in the sample. XRF spectroscopy uses this phenomenon to measure the amounts of nearly all the elements larger than sodium present in a sample. Data from XRF analysis is often reported as weight percents of the most common elemental oxide. For example, the instrument would measure the number of calcium atoms but the results would be report the weight percent of calcium oxide, CaO, in the sample. If samples such as char or feedstock contain the element in a different form, such as calcium hydroxide, $Ca(OH)_2$, the mass balances may not match exactly. The relative amounts of one element to another, however, will be accurately reflected. Another way in which the ash composition of a char sample might be measured is digesting or leaching the sample, then measuring the concentration of given ions in the resulting solution. For example, to determine the amount of potassium in a char sample, one might combust the sample, dissolve the resulting ash in acid, then measure the potassium concentration of the solution by atomic absorption spectroscopy (AAS) or inductively-coupled plasma atomic emission spectroscopy (ICP-AES).

The elemental composition of char closely resembles that of its feedstock. The elements found in biomass chars, therefore, include plant macro and micronutrients (in ratios similar to the plant material) such as calcium, copper, iron, potassium, magnesium, manganese, molybdenum, nickel, phosphorus, sulfur, and zinc. As plants occasionally take up other elements even though they are not essential, char can also contain sodium, chlorine, silicon and traces of others. If the feedstock sample was contaminated with soil or other chemicals, these will also appear in the ash analysis. For this reason, crop and forestry residues may contain soil minerals such as aluminum and silicon, which may affect the thermochemical process and certain analytical techniques.

2.5.2 Physical Properties

The particle size of chars produced at lower heating rates is similar to the particle size of the feedstock before pyrolysis. If the feedstock was ground to 1 mm particles, one would expect the majority of the char produced to also be in the 1 mm range. As volatile matter is slowly removed during the pyrolysis process, the char becomes more porous but still holds its overall shape and size. The fines generated during pyrolysis, such as those one would find at the bottom of charcoal kilns, are the result of the partial feedstock combustion (high-ash chars) and the generation of dust from rubbing the now-friable char particles together. At higher heating rates, the rapid escape of volatiles is believed to play an additional role in fines generation as particles fracture (explode) from the generated internal pressure. The typical pre-process grinding of feedstock to improve heat transfer for fast pyrolysis and gasification also means that chars from these processes tend to be very fine (1-100 µm). Overall, particle size decreases, so does the risk of problems from dust. The majority of char particles are larger than the PM_{10} (<10 µm) and PM_2 (<2 µm) air pollution cutoffs for particulate matter that can cause respiratory health problems; even so, measures for controlling dust and particulate matter exposure during handling are still strongly recommended. Particle size down to approximately 50 µm is most easily measured by sieve methods. Laser particle counting techniques can be useful for the smaller particles sizes. Settling techniques, such as the techniques used to classify soil texture, however, are difficult to use on chars due to their low density (char floats instead of sinks in water).

The density of char can be measured in two ways: bulk density, which includes structural and pore space volume, and particle density (also known as skeletal or true density), which includes only the volume occupied by solid molecules. Bulk density is measured by adding a known amount of sample mass into a container of known volume. Compaction has a significant effect on pore volumes, so measurement standards frequently have specific protocols for sample packing or settling. Biochar bulk density is low, around 0.2-0.5 g/cm^3 (specific gravity of 0.2-0.5), but this can vary with feedstock and process. For example, chars from high-ash

feedstocks or processes that result in low char carbon contents will have significantly higher densities due to the mineral material contribution. Particle density is measured using a pycnometer and since pore volume is no longer included, it is higher than the bulk density for a given solid. Particle density is not affected by compaction. Biochar particle density is usually between 1.5-1.7 g/cm^3 and generally increases with pyrolysis temperature as the solid carbon condenses into dense aromatic rings structures. Some high temperature chars can even have particle densities approaching that of solid graphite (2.25 g/cm^3). As with bulk density, particle density also increases with mineral ash content and can exceed 2.0 g/cm^3 for high-ash chars.

There are three kinds of porosity in biochars based on pore size. According to material scientists, pores can be divided into micropores, mesopores and macropores, which have internal diameters of <2 nm, 2-50 nm and >200nm, respectively. (Note: soil scientists may use different systems of classifications such as calling all pores with diameters <200 nm micropores.) Each size range of pores contributes to a different property of the sample. In the activated carbon industry, micropores (<2 nm) contribute the vast majority of the surface area and are considered important for adsorption applications. For soil applications, macropores in biochar affect the soil's hydrology and microbial environment. The larger the pores, the easier water, plant roots and fungal hyphae can penetrate the particle. For smaller microorganisms, pores provide shelter from larger, predatory organisms. Biochars will frequently have specific pore size distributions and arrangements due to maintenance of the plant structure. This regularly-sized and extensive porosity can be seen in the scanning electron micrographs of biochar shown in Figure 10. Pore size distribution in solid materials can be measured several ways. One method is gas sorptometry. Two examples of this method applied to chars are micropore analysis by carbon dioxide and mesopore analysis by nitrogen. Another method is mercury porosimetry, which calculates the pore size based on the pressure required to push mercury into the pore (the smaller the pore, the higher the pressure needed). Mercury porosimetry is typically used to measure pores in the macro and

mesopore range. One limitation of mercury porosimetry is that pores between particles (inter-particle porosity) and pores within particles (intra-particle porosity) are measured simultaneously. Porosity, when reported as a single sample property, is simply defined as the amount of total pore volume relative to the total bulk sample volume.

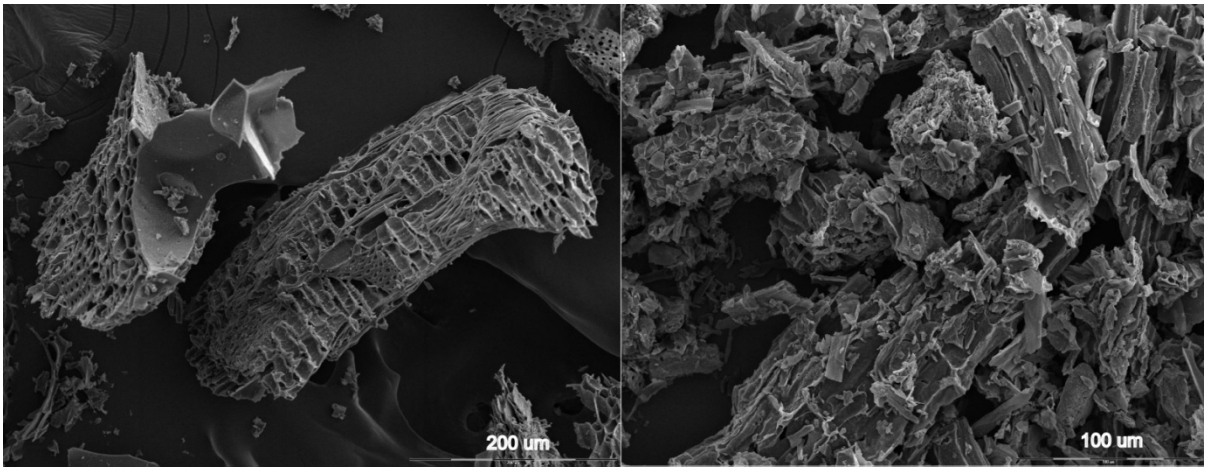

Figure 10. Scanning electron micrographs of biochar particles showing porosity. Left: Hardwood slow pyrolysis biochar from a commercial kiln. Right: Biochar from the fast pyrolysis of corn stover. (Source: David Laird, USDA ARS, National Laboratory for Agriculture and the Environment, Ames, IA. Images taken by Terry Pepper)

The surface area of biochar is another important physical property of biochar that has a significant impact on the magnitude of interactions between biochar and the soil environment; the higher its surface area, the more chemical interactions char can participate in per gram. Selecting a method for measuring biochar surface area that provides meaning for soil applications has been an area of contention. The most common type of analysis is a gas sorption isotherm measurement. Different analysis gases and isotherm temperatures can give different values of surface area. In the activated carbon field, surface area is traditionally measured by the Brunauer-Emmet-Teller (BET) nitrogen gas physisorption method at 77K over the relative pressure range P/P_0 = 0.05-0.30. BET surface areas for lower temperature biochars are often around 1 m^2/g, which is only slightly higher than that of lignocellulosic biomass and is due to the majority of pores being macropores. High BET surface

areas are the result of long residence times, higher temperatures and/or the use of activation processes such as heating with steam; all of these processes promote the formation of micropores in the carbon structure. Depending on the feedstock and pyrolysis process, some biochars can have surfaces areas in the hundreds and even thousands of meters squared per gram, potentially making them suitable for activated carbon applications. Achievable surface area does reach a maximum, however, as micropore structure eventually collapses into macropores and surface area in lost. Among other methods suggested for measuring surface area are the ethylene glycol mono-ethyl ether (EGME) specific surface area method (typically used for soils) and gas sorption methods using larger and/or more hydrophobic molecules to imitate the organic matter that would adsorb to biochar in soil. Most biochar literature reports surface area values in terms of the BET method, but more work is needed to demonstrate how this or other measurements relate to the quantity of reactive surface sites.

2.5.3 Chemical Properties

Part of the decision to use char as a charcoal or as a biochar is the char's higher heating value (HHV); the higher the energy content of the char, the higher its value as a fuel. Higher heating value is measured by bomb calorimetry and represents the energy that can be extracted from the char by combustion if all of the combustion products are allowed to cool back to 25°C. The other way of quantifying energy content, lower heating value, also measures the energy of combustion but assumes that water put into the vapor phase stays as steam. In general, HHV increases with increasing carbon and hydrogen content and decreases with increasing moisture, oxygen and ash content. As char composition varies significantly with feedstock and process, the HHV of chars also varies. Low ash slow pyrolysis chars can have higher heating values above 30 MJ/kg (higher than several coals); char co-products from fast pyrolysis and gasification processes have much lower HHV values (in the teens and lower twenties of MJ/kg).

The majority of biochar's chemical properties are related to two "carbon fraction" concepts, aromaticity and surface functionality. Aromaticity is defined as the fraction of carbons in char that participate in aromatic bonds. Lignocellulosic feedstocks, which consist of sugar polymers (all aliphatic carbons) and lignin (some aromatic rings), have relatively low aromaticity. As the pyrolysis reaction progresses, oxygen and hydrogen are removed, leaving the remaining carbons to form new aromatic carbon-carbon bonds. The "orderliness" of the aromatic structures also increases with increasing temperature, forming gradually larger sheets of interconnected aromatic rings. Eventually, the arrangement of these aromatic carbon sheets changes from random to aligned, stacked sheets resembling graphite at the highest temperatures. The degree of aromatic condensation in biochars is believed to be related to recalcitrance in the environment; carbons in dense aromatic structures are more resistant to oxidation and few microorganisms have enzymes capable of breaking down such bonds. This stability comes from the fact that electrons are shared over more than one bond in aromatic molecules. By "spreading out" electrons over the molecule, aromatic molecules can exist at lower energy (i.e. more thermodynamically favored) states than non-aromatic molecules. Such sharing of electrons is so efficient in graphite and some highly condensed chars that these materials can even conduct electricity. Most of the techniques used to measure the degree of aromatic condensation in char are the same as those used to analyze surface functionality and will be discussed later in this section. Two other techniques being explored are particle density (the closer the density is to graphite, the more aromatic the char) and electrical conductance/resistivity (the lower the resistance to electron movement, the greater the aromatic condensation).

Many chemical interactions between biochar and the environment are directly related to its surface chemistry. In lignocellulosic feedstocks, the surface functional groups present are mostly hydroxyls (-OH), carboxylic acids (COOH) and small alkyl chains such as methyl groups ($-CH_3$). With this kind of surface chemistry, feedstocks tend to be polar, hydrophilic and relatively reactive. Chars coming out of the pyrolysis reaction have very different surface chemistry. Most of the functional

groups (containing oxygen, hydrogen and nitrogen) have volatilized off, leaving aromatic carbon surfaces behind. These surfaces are reduced (i.e. the carbon is in the C^0 oxidation state), non-polar, and hydrophobic. As the surface is exposed to air over time, the carbon oxidizes, creating new oxygen-containing aromatic functional groups such as hydroxyls (-OH), carbonyls (-C=O) and carboxylic acids (-COOH), and making the surface polar again. These oxygen-containing functional groups are the same as those found on soil organic matter and are critical for biochar-soil interactions in similar ways. First, these functional groups are variable charge, meaning that they can receive or donate a proton (H^+) depending on the pH. At a higher pH, the carboxylic acids (-COOH) and some of the hydroxyls (-OH) give up protons and become negatively charged ($-COO^-$ and $-O^-$, respectively). At low pH environments, these same groups can accept a proton. In this way, the carbon fraction of the biochar acts as a weak acid and partially buffers the pH of the system. (The ash fraction of the feedstock affects pH separately and may override any effect of the carbon fraction, especially with high-ash, alkaline chars.) Second, the negatively charged surface functional groups can attract positively charged cations and thus contribute significantly to the soil's cation exchange capacity. In cases of metal toxicity due to low soil pH, biochar can help in two ways: raising the pH, which makes plant-toxic metals like aluminum (Al^{3+}) less soluble, and adsorbing the positively charged metal ions, which removes them from the solution. Finally, the hydrophobic and hydrophilic regions of the biochar surface can serve as adsorbents for non-polar and polar organic molecules in the environment. This adsorptive power can be good, such as when char adsorbs organic matter or environment contaminants. On the downside, these same surfaces might also adsorb a pesticide and reduce its effectiveness.

There are several ways to analyze the surface functionality of biochar to give information about its potential chemical interactions. In all of these methods, it is important to keep in mind that biochar surfaces are changing with exposure to the environment, especially at first. Fresh char just out of the pyrolyzer will have much

different surface characteristics than biochar that has been sitting in the open air for several weeks or that has been in the soil for several years.

Since pH affects so many physical, chemical and biological properties of soil, being able to predict the pH effects of a biochar is critical to choosing the right char for the right application. The simplest way to measure pH is to make a char and water slurry and use a standard laboratory pH meter. As with soils, pH is sometimes also measured in a solution of potassium chloride (KCl) or a buffer to quantify the exchangeable acidity (i.e. the protons on the CEC that can be readily released in the presence of other cations). Another way to measure a char's acidity is a Boehm titration. In this method, char is titrated with gradually increasing strengths of base to quantify the types of acidic functional groups present. A char's alkalinity can be measured in a similar fashion using acids of differing strengths. The total acid-neutralizing ability of a biochar is especially important for high-ash chars that can act as liming agents in soils.

Fourier transform infrared spectroscopy (FTIR) is frequently used to identify and qualitatively track changes in functional groups in biochar and soil samples. Since biochars are opaque solids, an FTIR analysis requires special sample preparation and/or detection method. Some common methods include conventional transmission FTIR using potassium bromide (KBr) pressed pellets, Diffuse Reflectance Infrared Fourier Transform (DRIFT) spectroscopy, and FTIR using a photoacoustic detector (FTIR-PAS). A sample set of FTIR-PAS feedstock and char spectra are shown in Figure 11. Important peaks in the feedstock and biochar spectra are the O-H stretch (3400 cm^{-1}), the aliphatic C-H stretch (3000-2860 cm^{-1}), the aromatic C-H stretch (3060 cm^{-1}), the carboxyl (C=O) stretch (1700 cm^{-1}) and the various aromatic ring modes at 1590 and 1515 cm^{-1}. The feedstock spectrum is dominated by the O-H stretch, aliphatic C-H stretch and carboxyl C=O stretch. As the pyrolysis reaction progresses, certain peaks (O-H stretch and carboxyl C=O stretch) disappear, the C-H peaks shift from being more aliphatic to more aromatic (and eventually disappear altogether), and peaks representing aromatic carbon compounds begin to appear. In biochar aging studies, such as those presented by Cheng, et al., FTIR spectra

can be used to demonstrate the degree of biochar oxidation (appearance of C-O and O-H peaks), albeit only qualitatively.[9]

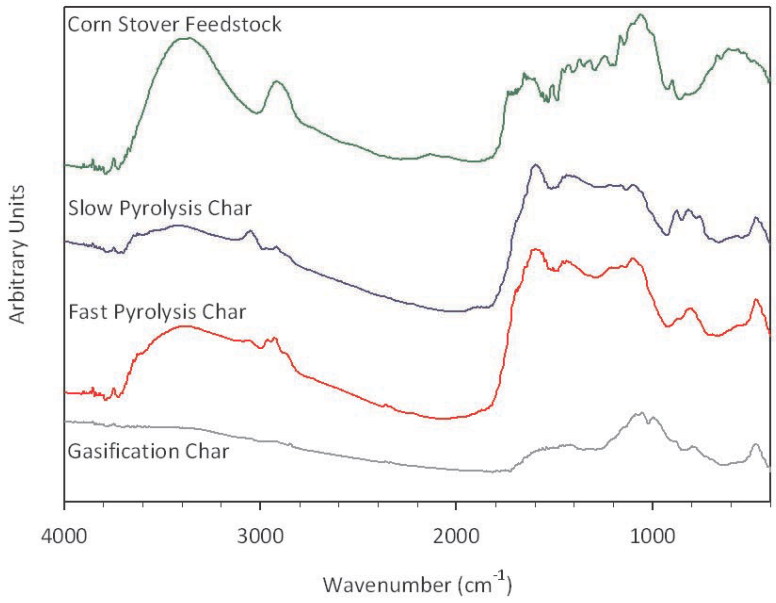

Figure 11. Fourier-transform infrared photoacoustic spectroscopy (FTIR-PAS) spectra of corn stover feedstock and biochars.

One complicated yet informative technique used to characterize the carbon fraction of biochars is ^{13}C solid-state nuclear magnetic resonance spectroscopy (NMR). NMR uses a very strong magnetic field and radio frequency (RF) pulses to study the structure of molecules using the resonance frequencies of nuclei with specific spins. For biochars, ^{13}C and ^{1}H (proton) nuclei can be used to determine the relative quantity of carbon functional groups, the approximate degree of condensation of the aromatic rings, and the overall structure of the char molecules. Figures 12 and 13 show some of the kinds of information that can be obtained using NMR techniques. In Figure 12, the ^{1}H-^{13}C cross polarization with total suppression of spinning sidebands (CP/TOSS) spectrum of a typical lignocellulosic material is compared to that of corn stover chars, including some that were only partially pyrolyzed. Unlike FTIR spectra, where pyrolyzed and partially pyrolyzed samples may be difficult to distinguish, the difference is very apparent in the NMR spectra as the aliphatic oxygen-containing functional groups in the feedstock are gradually

replaced by the dominating aromatic carbon signal of the pyrolyzed chars. In Figure 13, information from direct polarization (DP) spectral analysis, and dipolar dephasing and re-coupling experiments, have been combined to create chemical models of what “average” slow pyrolysis, fast pyrolysis and gasification char from switchgrass might look like. In spite of the chemically detailed and quantitative information that NMR can provide, its expense, complexity and analysis time requirements make it unlikely to be an “everyday” biochar characterization technique. Rather, NMR is more likely to serve as a verification tool in the development of other characterization techniques.

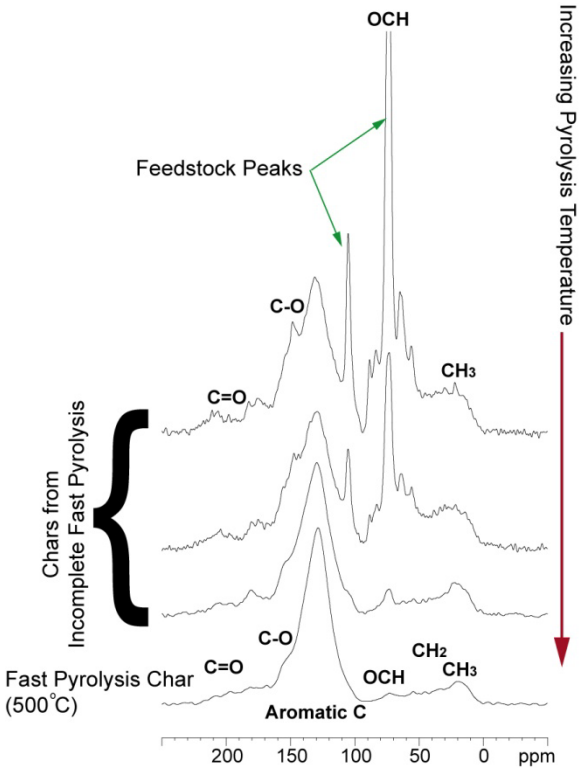

Figure 12. Cross polarization with total suppression of spinning sidebands (CP/TOSS) ^{13}C NMR spectra of incompletely and completely pyrolyzed biochars from the fast pyrolysis of corn stover. Note that as the pyrolysis temperature increases, the peaks from the lignocellulosic feedstock gradually shift to the aromatic carbon peaks characteristic of char.

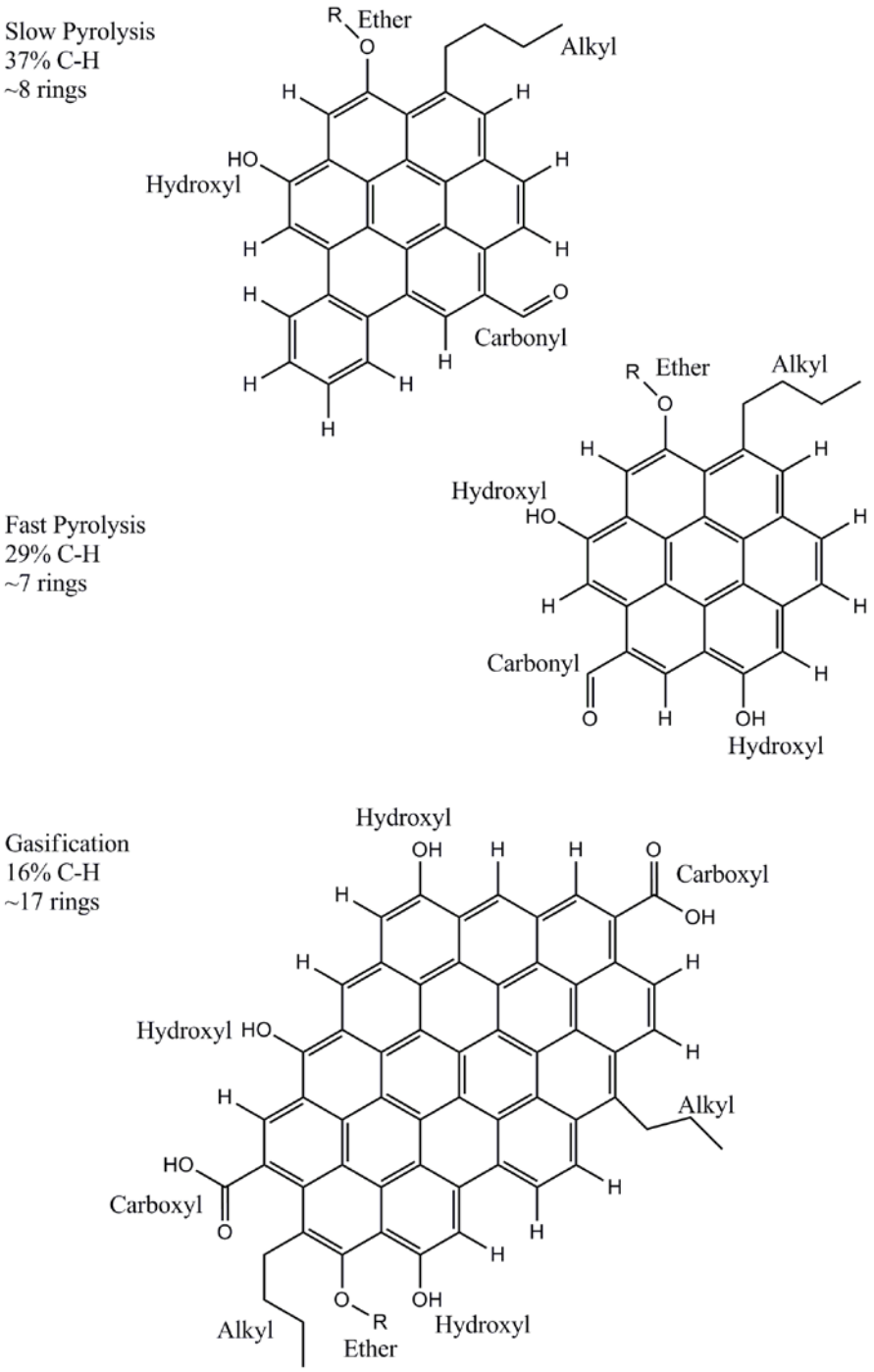

Figure 13. Model compounds of char from slow pyrolysis, fast pyrolysis and gasification of switchgrass. (Redrawn and modified from C.E. Brewer, K. Schmidt-Rohr, J.A. Satrio, R.C. Brown, Characterization of biochar from fast pyrolysis and gasification systems, Environ. Prog. Sustain. Energy, 28(3), 386-396, 2009.)

One of the several soil analysis techniques that researchers have tried to apply to biochars alone is the measurement of cation exchange capacity (CEC). Like many soil chemical analyses, CEC measurement involves mixing the solid with an extracting solution, allowing the system time to equilibrate, separating the liquid phase from the solid phase, and measuring a change in the chemical composition of the liquid. Three properties of biochar make them difficult to analyze with these kinds of methods. First, the low bulk density of biochars creates a problem for liquid-solid separation. Mineral-rich soil solids are typically removed from solution by centrifuging or settling. These separation techniques, however, are not efficient for biochars, which tend to split into three fractions upon centrifugation: some that floats, some that sinks and some that stays suspended. Filtering samples does provide a workable alternative if the filter is fine enough but can add time and difficulty to the analysis. Second, the high pH of some chars interferes with pH control during the analysis. Many soil and biochar chemical properties, such as CEC, are heavily dependent on pH and biochars that are high in ash, especially in low-solubility basic metal oxides, continuously push the pH up outside of the analysis range, even in buffered methods such as CEC by ammonium acetate. To obtain meaningful data on pH-dependent properties, these chars may need to be rinsed and the alkalinity neutralized prior to analysis. Finally, biochars can contain elements that are not in the form being tested by the analysis and therefore give erroneously high results. For example, a CEC analysis that considers all base cations extracted from a sample by ammonium acetate to be “exchangeable” would overestimate the CEC of a high-ash biochar that contained significant amounts of alkali metal oxide or hydroxide crystals. Researchers developing methods to measure such properties in biochar may need to consider rinse or digestion steps in their protocols. Overall, the use of existing soil chemistry methods to characterize the soil-relevant properties of biochar has many potential advantages, but there are key differences between biochars and soils that require consideration in method development and caution in data interpretation. In some cases, it may be necessary to obtain biochar

characteristics by comparing changes in soil properties on amended and control soils, rather than direct measurement.

Several other analytical methods have been used to investigate the chemical properties of biochars and can be found in the literature. Among these are X-ray photoelectron spectroscopy (XPS) of biochar surfaces, stable isotope analysis, water holding capacity and other adsorption measurements, stability measurements using chemical or radiation-catalyzed oxidations, and characterization of compounds obtained by leaching or pyrolyzing biochar. The challenge with any biochar chemical analysis technique is the correlation of measured biochar properties with desired soil responses such that researchers can make predictions about a biochar's performance based on its properties.

2.5.4 Biochar Engineering

The idea of biochar engineering is based on the assumption that knowledge of pyrolysis reaction conditions, biochar properties and soil responses to biochar amendments can be used to design an optimum biochar for a given region depending on its feedstock availability and soil needs. Research in this area involves a reiterative process of producing biochars under known conditions, characterizing the biochars, measuring soil responses to biochar amendments, and finally formulating biochars with favorable properties. Work similar to this has been done in the past to estimate char production conditions based on its properties. For example, spectra of char made at known pyrolysis temperatures have been used to estimate the temperature of forest fires based on the spectra of chars from the fire. As would be expected from the wide variety of feedstocks, production systems and soils, data from biochar engineering research is very location-specific. A few trends, however, have started to emerge: in general, the higher the temperature of the pyrolysis process, the less carbon in the feedstock is converted to char but that carbon is more condensed with fewer remaining functional groups. These biochars will likely cause higher pH conditions, will be more hydrophobic, and will take longer to oxidize in the soil. Biochars like this are likely to be well-matched with acidic soils in more

tropical regions that will benefit from the higher pH and whose warmer climate will speed up the otherwise slow oxidation process. For soils such as calcareous, saline soils in drier, more temperate regions, a lower temperature biochar made from low-ash feedstocks may be more beneficial. Such biochars are likely to have retained more oxygen-containing, hydrophilic and slightly acidic functional groups that will help bring the pH closer to neutral and improve water holding capacity without adding too much more mineral matter to the soil. Evidence to support or challenge these trends is expected in the near future, especially as more field trials using a wider variety of soils and biochars are conducted.

2.6 Promising Biochar Scenarios and Synergies

Biochar is unique among biorenewable resource technologies in that it provides the potential to address several problems at once: soil quality, water quality, crop yield, carbon sequestration, energy production, and greenhouse gas emissions. How to get the most out of any biochar system will require the creativity and cooperation of multiple players across agriculture, government and industry. What follows is a description of what some future biochar utilization scenarios and synergisms might look like.

2.6.1 Bio-energy and Biochar Co-production

The three products from the thermochemical processing of biomass: char, bio-oil/tar and syngas are essentially energy products, providing a way to obtain renewable energy from the sun through plant photosynthesis. One can expect, therefore, that energy production will be a key part of any biochar system, whether that energy is used immediately, such as combusting the syngas on-site for heat and electricity, or transformed into another form for later use, such as the production of liquid transportation fuels through bio-oil reforming and upgrading. Energy and biochar co-production can occur across several scales, from small on-farm gasifiers for electricity generation to city or co-op size flash pyrolyzers for waste management,

all the way up to several-hundred-ton-per-day industrial biorefineries making transportation fuels and chemicals and using biomass from two or three counties.

Consider one example of a distributed fast pyrolysis bio-oil and biochar system: farmers collect about half of their plant residues and transport them a few kilometers to the cooperative's fast pyrolyzer. The pyrolyzer turns about 60% of the biomass into bio-oil which is trucked 150 km to the bio-oil refinery. At the refinery, the aqueous fraction of the bio-oil is steam reformed into hydrogen that is used to catalytically upgrade the lignin-derived bio-oil fraction into hydrocarbons that are then sold as transportation and farm equipment fuel. 20% of the biomass fed into the co-op pyrolyzer is turned into syngas, which is combusted to heat the pyrolyzer and supply energy to the on-site biomass drying and grinding systems. The 20% remaining from the original biomass exits as a fine, medium-ash biochar that the farmers take back to the fields, where they slurry the biochar with the liquid manure that they use as a fertilizer supplement and spread this mixture on the fields.

In another scenario, a city uses a combination of a composting system and a flash pyrolyzer to manage its yard and municipal wastes. Weekly collections of grass clipping, leaves, tree and garden residues, food scraps, and non-recyclable paper and plastic wastes are delivered to the waste management site. The more nitrogen-rich wastes are composted, while the higher-carbon and less compost-friendly wastes are pyrolyzed in one-ton batches which produce biocarbon yields of about 50%. The syngas product from the process is combusted and used in a steam turbine for electricity that supplies power to the pyrolyzer, several public buildings and a few local manufacturing facilities. The biocarbon products are blended with the finished compost and used as topsoil in parks and public areas or sold to local nurseries and gardeners.

For all of the potential bio-energy and biochar scenarios, carbon market benefits from fossil fuel displacement and carbon sequestration will be critical to creating a favorable economic situation that will drive implementation. Without monetary incentives to sequester carbon, power companies utilizing biomass may not see the advantage of saving the char for soil application rather than combusting it for

substantial additional energy. Likewise, a farmer might not feel that the long-term benefits of biochar application justify the short-term time, effort and expense required to purchase/produce and apply biochar. One advantage biochar has over other carbon sequestration schemes is the ease in carbon accounting; the amount of biochar applied to a field and the carbon content of the biochar can be verified in a relatively straightforward manner. If the pyrolyzer is properly designed and operated, one can also assume that nearly all (>95%) of the carbon in the biochar will remain sequestered in the soil for millennia and the only emissions from the process are carbon-neutral carbon dioxide and water. The co-production of electricity, heat and/or fuels offers additional opportunities for carbon credits from displacing fossil fuels, especially coal and natural gas.

2.6.2 Farming Impacts

Less visible but just as important as the direct impacts of biochar carbon sequestration and energy co-production on mitigating climate change are the indirect impacts biochar application has on soil input requirements, nutrient leaching, water usage and green house gas emissions. While such benefits are expected to some extent from biochar application in nearly all soils and climates, the greatest improvements in yield and soil quality are mostly likely in regions with poor soil quality or adverse growing conditions. For example, crop yields in already fertile soils may not improve significantly with biochar application during good growing seasons; the effects of biochar might only be observed under some kind of environmental stress such as a drought, a decrease in applied nutrients, or a heavy rain storm. Either way, biochar's recalcitrance means is will be present for many growing seasons to have an impact and any decision to apply biochar should be made with the short and long-term impacts in mind.

In several studies of biochar application to soils, biochar has been shown to decrease nutrient leaching and other losses such as ammonia volatilization and denitrification, meaning that nutrient inputs are less likely to end up in the water supply or the atmosphere. The increase in CEC from the biochar application holds

more beneficial base cations such as potassium and calcium in locations that plants can us them. The change in pH, especially the neutralization of acidic soils, improves the environment for microorganisms that regulate nutrient cycling and immobilizes plant-toxic elements such as aluminum. As overall nutrient use efficiency increases, higher yields can be achieved with fewer fertilizer inputs, meaning that less energy and natural gas are needed in fertilizer production, fewer chemicals have to be mined (i.e. rock phosphate, limestone, etc.), less fertilizer and lime need to be transported to farms, and the farmer has to make fewer passes across a given field (all reducing the amount of fossil fuels being used). The avoided water contamination represents another savings in the energy and chemicals (used to treat the water), as well as prevents the negative environmental impacts of nutrient-enriched runoff such as eutrophication (i.e. the cause of hypoxic dead zones in bodies of water).

Biochar application has also been shown to improve soil's ability to retain water and make it available to plants. Two properties of biochar are believed to contribute to this ability: its pore size distribution and its surface chemistry. Pore size is critical to water availability in that it determines how tightly water is held within pores. If a pore is too big, the force of gravity will be greater than water's surface tension and water will drain out of the pore. Sandy soils, which have mostly big pore spaces, tend to have good drainage properties for this reason but can dry out easily. If a pore is too small, capillary forces holding the water inside the pore are so strong that plant roots cannot extract the water. This is why a clayey soil might contain significant amounts of water but plants may still start to wilt. The pore sizes in biochar are typically in the intermediate range where water no longer drains freely but plants can still extract it. The hydrophilic chemical functional groups on biochar surfaces may further enhance this physical water retention through hydrogen bonding and electrostatic attraction. The hydrophobic regions of biochar may also help in water retention by adsorbing other kinds of soil organic matter, which in turn may contain pores or hydrophilic surfaces that attract water. In these ways, biochar can increase soil's water use efficiency, meaning that drier areas or areas with

intermittent rainfall may benefit from biochar application through increased resistance to drought and decreased need for irrigation. Such a benefit has drawn the attention of the United Nations Convention to Combat Desertification since many regions of the world are facing increasing water shortages from population increases and changing weather patterns caused by climate change.

Carbon dioxide is only one of several greenhouse gases emitted from soils; two others of significant importance, methane and nitrous oxide (N_2O), cause even stronger heat trapping effects, having approximately 20 and 300 times the radiative forcing as carbon dioxide, respectively. These gases are generally produced by soil microorganisms under anaerobic conditions. In the case of nitrous oxide, lack of oxygen stimulates the denitrification process by which nitrate (NO_3^-) in the soil solution is used as a terminal electron receptor and reduced to nitrous oxide and nitrogen (N_2) gas. Studies of greenhouse gas emissions from biochar-amended soils have shown that biochar may decrease both methane and nitrous oxide emissions, in some cases up to 70% of the N_2O compared to the control soils. While the reasons for these observed decreases are not understood, it is believed that the decrease in soil bulk density from biochar addition may help prevent anaerobic conditions by improving air penetration into the soil. Agricultural soil management is by far the greatest source of nitrous oxide emissions in the United States (contributing about 2/3 of the total), indicating that the potential benefit of emission reductions from soil through biochar addition is very significant.

2.6.3 Site Remediation

One challenge of cleaning up areas devastated by natural disasters, such as hurricanes, or pests, such as the mountain pine beetle, is deciding what to do with all of the dead biomass. Left alone, this biomass gradually decomposes, emitting significant amounts of previously sequestered carbon dioxide, as well as methane and nitrous oxide. Pyrolyzing these residues offers several advantages. First, the high temperatures of the pyrolysis process sterilize the material, preventing the continued spread of a biological pest, including invasive plant species. Second,

some of the carbon that would have been lost to the atmosphere as carbon dioxide can be sequestered in a manner that is also beneficial to the soil environment and may help the recovery process. Finally, some energy and other co-products may be recovered from the process which could provide an economical benefit to the affected region.

Biochar's adsorptive properties, as well as its promotion of plant and microbial activity, have also attracted the attention of those interested in the remediation of soils contaminated by organic chemicals. Like activated carbons (albeit perhaps not as effective on a mass basis), biochars have been shown to adsorb a wide variety of organic compounds, especially polycyclic aromatic hydrocarbons (PAHs) and phenolic compounds. Other studies focusing on char's ability to remove metals ions from aqueous solutions have demonstrated some success. These adsorptive properties suggest that biochar may be especially beneficial in the containment step of the remediation process, perhaps not as effective as purpose-made activated carbons but potentially more cost effective. Bioremediation processes, i.e. those using microorganisms, plants, or their enzymes to decompose organic contaminants, utilize predominantly aerobic processes. Biochar applications which lower soil bulk density may improve soil aeration and thus may accelerate these processes. At the same time, biochar's strong adsorbing ability might also make the sorbed contaminants less susceptible to enzymatic attack.

24.6.4 Developing Countries

In addition to the potentially dramatic improvements in soil quality and crop yields, biochar implementation provides several other opportunities for people living in developing countries. Not least of these opportunities is improving the efficiency and safety of energy production for cooking and heating. Many households obtain their energy from open fires or crude stoves and spend significant time collecting fuel. The burning process in open fires and many of these stoves is very inefficient and results in significant air pollution which contributes to numerous health problems and premature deaths in those working around these fires. One branch of biochar

research is devoted to addressing these problems through the design of efficient stoves made from simple materials that produce heat and biochar simultaneously. Two representative designs of such stoves include the top-lit updraft (TLUD) gasifier and the Lucia Stove from WorldStove. The basic TLUD gasifier uses two air streams, a restricted one entering on the bottom of the heating chamber (the primary air) to gasify the biomass, and another going around the sides of the container (the secondary air) to supply oxygen to the top part of the stove where the flammable vapors are combusted as they exit (a schematic is shown in Figure 14).

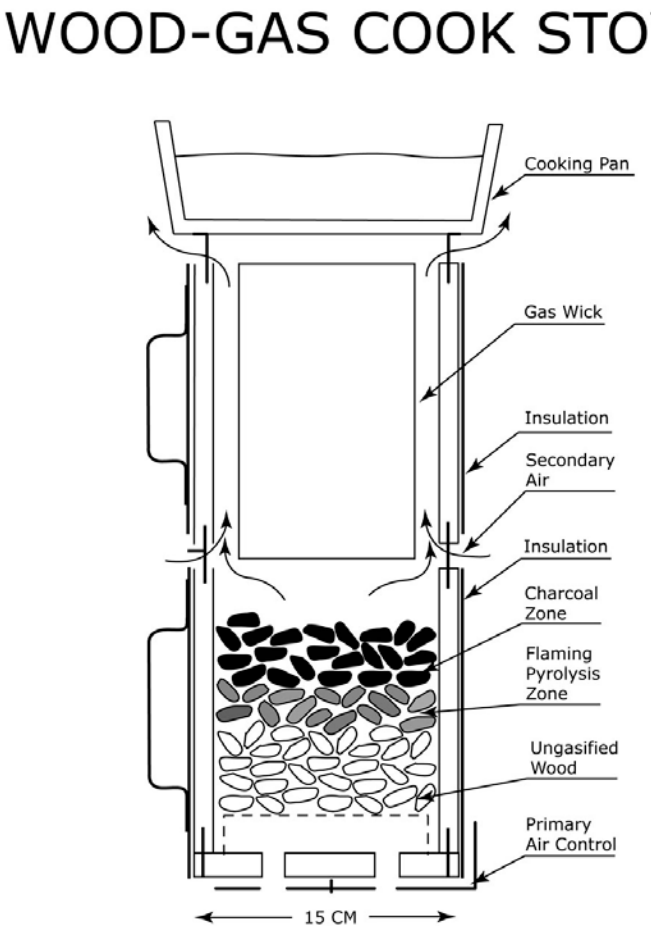

Figure 14. Schematic of a top-lit updraft (TLUD) gasifier wood cook stove. (Reproduced with permission from Fig. 8.20 in Brown RC (2009) Biochar Production Technologies in Lehmann, J., & Joseph, S. (Eds.) Biochar for Environmental Management: Science and Technology. London: Earthscan.)

The Lucia Stove also uses gasification to produce vapors that are the combusted as they exit but only uses one air stream. Once a fire has been started in the stove,

a fan is used to pull the pyrolysis vapors out the bottom of the heating chamber, up the sides between the inner and outer metal cylinders, and in towards the center at the top of the stove. New air is pulled into the stove through the flame front at the top so that there is little oxygen left in the heated gas when it reaches the biomass fuel (see Figure 15). The scale of these stoves can range from the very small single-household stoves to much larger stoves that can serve public buildings such as schools or hospitals; some run only in a batch mode while others can be refilled throughout the process. Both kinds of stoves produce a small amount of char (10-20% of the initial biomass) that remains after the gasification has stopped and that can be applied to nearby fields or gardens. Like other biochars, the amount and properties of this char depend on the feedstock and the reaction conditions such as the temperature reached inside the stove and the length of time the stove was running. hese kinds of stoves are very clean-burning (most of the emissions are carbon dioxide and water only) and they are much more efficient (some have >90% carbon conversion), producing more heat using less fuel and lower quality fuels such as crop residues. The advantages of being able to use crop residues are that less forest has to be cut down and there would be an incentive to collect and pyrolyze crop residues rather than burn them in the fields.

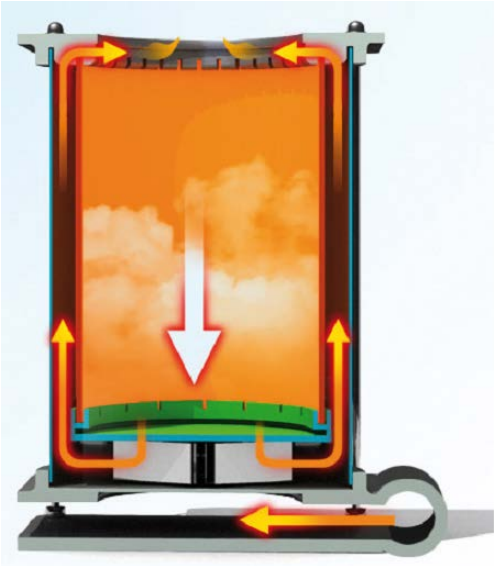

Figure 15. Diagram of gas flows in a Lucia Stove from WorldStove. (Source: Nathanial Mulcahy, WorldStove, Tortona, Italy.)

The implementation of biochar production and application systems in developing countries also creates an opportunity for income generation. This income would likely come from carbon credits for avoided emissions (from reforestation or preventing deforestation/in-field crop residue burning) and sequestering biochar. One such program existing today that could be implemented for a biochar or stove-biochar combination project is the Clean Development Mechanism (CDM) program, a program stemming from the Kyoto Protocol that allows developed nations to gain emission reduction credits by funding emission reduction projects in developing countries that would otherwise not have happened. Small biochar producers might organize larger cooperatives and sell carbon credits on the world carbon markets, in addition to selling biochar to local farmers to improve their soils. With efficient stoves, those responsible for collecting fuel and cooking (mainly women) could devote more time and resources to other income-increasing activities such as producing handicrafts to sell or furthering their educations.

One criticism of biochar is that its production might encourage deforestation. Another is that production of biochar in inefficient kilns would create air pollution, especially in developing countries where pollution is less regulated. To be sustainable (a key defining quality of biochar), biochars need to be produced from materials that would otherwise decompose (such as forestry slash, dead biomass, crop residues, urban yard wastes, etc.) and that do not compete with food production (i.e. energy crops grown on prime agricultural land). Biochar must be produced in efficient reactors that produce very few or no emissions aside from carbon dioxide and water. For many kiln designs, this can be achieved with proper heat insulation, effective inlet air control and process monitoring, and a type of afterburner system to crack tars and completely combust any remaining carbon monoxide, hydrocarbons, etc.

2.7 Challenges to Applying Biochar

2.7.1 Economics of Alternative Uses

Reaping the many potential benefits from biochar and its co-products will not happen without overcoming certain challenges. Perhaps the most daunting of these challenges is economic. To be sustainable in a market-driven society, biochar utilization (and the whole thermochemical biorenewable platform) must provide valuable benefits to consumers that can compete with multiple alternatives. As can be seen from the charcoal and activated carbon industries today, there are other and sometimes very high-value alternative uses for chars. For example, future high costs of emissions from coal-burning power plants and metal smelters may drive these industries to obtain their power and heat from charcoal instead, thus diverting chars that might have been applied to soils. Likewise, producers of certain low-ash chars may decide to make more profit by selling the chars as activated carbons for water treatment rather than to farmers or gardeners. Prior to the accumulation of much more biochar field trial data and research regarding biochar mechanisms, demonstrating the economical value of biochar soil application to consumers or making any kind of performance guarantees will be very difficult. Business plans for the large-scale production and sale of biochar, therefore, may need to focus on co-products such as heat or electricity with more developed markets until such biochar quality and performance information becomes available.

2.7.2 Handling

Biochar, like charcoal, is a flammable solid and as such, requires careful handling. According to the UN Hazardous Goods classification system (used to regulate the shipping and handling of potentially dangerous materials), chars are Class 4.2 Spontaneously Combustible Materials, meaning that they can self-heat and even ignite when exposed to air. This classification likely stems from the testing of freshly pyrolyzed materials that have not yet surface oxidized. When such chars are first exposed to the oxygen in the air, the relatively fast surface oxidations that occur release small amounts of heat that catalyze further oxidations (and more

heat), which can cause the char to ignite. Some ways to mitigate this risk include making sure that fresh, cooled biochar has been carefully and completely exposed to air prior to shipping, packing biochar in air-tight containers or under an inert gas like nitrogen to limit oxygen exposure, and/or mixing char with sufficient water to absorb any produced heat. For storage, biochars should be kept in cool, dry places--preferably in air-tight containers—away from heat and ignition sources, sparks or strong oxidizing chemicals.

The greatest health danger of biochar and the greatest challenge to field application is dust. When inhaled, small char particles can cause respiratory irritation and lung damage. Some biochars, especially those high in alkali ash content, can be irritating to the skin. For this reason, those handling biochar are recommended to use personal protective equipment such as safety glasses, dust masks, and protective clothing. In general, the finer the biochar is, the greater the risk of dust. Extra care must be taken around char dust to avoid sparks, which, under certain conditions, could pose an explosion hazard. In regards to biochar field application strategies, several engineering solutions have been suggested though many have yet to be tested. Among the proposed solutions are mixing biochars with liquids such as manure, fertilizers or water and using liquid spreading techniques, co-applying biochar with a semi-moist solid such as compost, pelletizing biochar alone or with biodegradable binders, and applying solid biochars using agricultural lime application techniques plus some kind of water spraying mechanism. One potential use for biochar that would include an application component but that has been little explored is the addition of biochar to animal feed, with subsequent soil application of the biochar-rich manure.

Methodology for the soil incorporation of biochar is another area of uncertainty, especially for reduced tillage or no-till management systems In many cases, biochar is surface applied then plowed or disked into the soil. For reduced tillage systems, it has been suggested that biochar be applied one time at a relatively high rate and tilled in, after which the field could be returned to its original tillage scheme.

2.7.3 Potential Soil/Crop Drawbacks

For most soils, the application of biochar will be beneficial for soil quality and crop yields with the worst cases scenario being no effect at all. There are three cases, however, where char may produce a negative effect. The first case involves the pH effects of biochar application, especially when very alkaline (pH values around 10), high-ash biochars are used. If adding biochar raises the soil pH too high, certain microbial populations involved in nutrient cycling and the plant-availability of certain micronutrients like iron would be adversely affected.

The second case is contamination of the soil with heavy metals or other toxins from applying biochar made from inappropriate feedstocks such as municipal wastes containing arsenic, cadmium, lead, etc. An example of this would be the pyrolysis of certain treated wood products used in fences or decks. To avoid this problem, questionable feedstocks should be tested prior to use or avoided.

The third case is nitrogen immobilization due to a high ratio of available carbon to available nitrogen in the biochar amendment. When they are actively growing (i.e. producing more biomass), microorganisms need about 1 mole of nitrogen for every 5 to 10 moles of carbon that they consume. If a source of carbon is added to the soil without sufficient nitrogen, microorganisms must scavenge nitrogen from the soil environment, which can result in little nitrogen being available for plants which can greatly limit crop growth. In general, an amendment needs to have a C:N ratio that is no higher than about 30 to avoid nitrogen immobilization (the additional C is used for maintenance respiration). Biochars, which are mostly carbon, usually have very high C:N ratios on an elemental composition basis; fortunately, nearly all of this carbon will not be available to microorganisms meaning that the effective C:N ratio is much lower. If a biochar is not pyrolyzed sufficiently, however, some of the carbon may still be bioavailable and may cause nitrogen immobilization, resulting in short-term negative effects on crop yield. Depending on magnitude of the carbon overloading, the nitrogen in the microbial biomass will eventually become plant-available again as microorganisms die off and the nitrogen is recycled, but by then (a few weeks to a few months later), the plants may not be able to recover. An example of nitrogen

immobilization is shown in Figure 16. In this study, corn stover and carbonized corn stover (i.e. corn stover biochar) were used as soil amendments in pots growing corn. Both amendments had high C:N ratios but only the corn in the pots with the highest rates of uncarbonized amendment showed signs of nitrogen immobilization (the stunted plant growth in pots with 1.0 and 2.0% by weight of corn stover added).

Figure 16. An example of nitrogen immobilization by microorganisms: the effect of soil amendment bio-available C: N ratio on corn growth in a greenhouse study. Soils used in the study were amended with either corn stover (CS), which had a high available C:N ratio, or carbonized corn stover (CCS), which had a much lower available C:N ratio due to the carbonization process, at applications rates of 0.5, 1.0 or 2.0 wt% of soil. The corn grown on soils amended with the higher amounts of corn stover (total C:N = 71) did worse than that grown on soils amended with the carbonized crop residue (total C:N = 49). (Source: Christoph Steiner, Biorefining and Carbon Cycling Center, University of Georgia, USA.)

2.8 Future Progress and Development

Future progress in biochar implementation will likely center around addressing the issue of biochar quality standards and performance expectations so that the

market for biochar can be developed. As previously mentioned, most companies selling biochar today produce energy as their primary project as they wait for agronomic research data to quantify the value of a given biochar application. As biochar quality varies significantly depending on feedstock and process conditions, the development of some kind of rating system is critical. The International Biochar Initiative currently has an interdisciplinary task force from multiple countries working to draft standards regarding production process sustainability (i.e. a biochar life cycle assessment), characterization methodology and product labeling. Once this kind of developmental framework is in place, biochar producers, consumers and policymakers will be able to make more meaningful comparisons between biochars and biochar systems that will influence decisions about what kind of biochar to make, which biochar product to buy, and which biochar systems to support in new legislation. Other critical research areas in the near future will be developing economic models to evaluate and predict the effects of biochar implementation, as well as more fundamental approaches to understand how biochar production conditions and properties are related and the mechanisms influencing biochar's effects on the soil environment.

References

1. Katzer, F., *Frundzuge der Giologie des unteren Amazonasgebietes (das Saates Para in Brasilien)*. Verlag von Max Weg: Leipzig, Germany, 1903.
2. Sombroek, W. G., *Amazon Soils: A Reconnaisance of the Soils of the Brazilian Amazon Region*. Center for Agricultural Publications and Documentation: Wageningen, The Netherlands, 1966.
3. Kondo, R., Opal phytoliths, inorganic, biogenic particles in plants and soils. *Japan Agricultural Research Quarterly* **1978,** 11, 198-203.
4. Zech, W.; Pabst, E.; Bechtold, G., Analytische Kennzeichnung von Terra Preta do Indio. *Mitteilungen der Deutschen Bodenkundlichen Gesllshaft* **1979,** 29, 709-716.
5. Glaser, B.; Haumaier, L.; Guggenberger, G.; Zech, W., The 'Terra Preta' phenomenon: a model for sustainable agriculture in the humid tropics. *Naturwissenschaften* **2001,** 88, (1), 37-41.
6. Steiner, C. Slash and Char as Alternative to Slash and Burn. Ph.D. diss, University of Beyreuth, Bayreuth, Germany, 2006.
7. Steiner, C.; Teixeira, W.; Lehmann, J.; Nehls, T.; de Macêdo, J.; Blum, W.; Zech, W., Long term effects of manure, charcoal and mineral fertilization on crop

production and fertility on a highly weathered Central Amazonian upland soil. *Plant & Soil* **2007,** 291, (1), 275-290.
8. Lehmann, J.; Gaunt, J.; Rondon, M., Bio-char sequestration in terrestrial ecosystems – a review. *Mitigation Adaptation Strategies Global Change* **2006,** 11, (2), 395-419.
9. Hammes, K.; Schmidt, M. W. I.; Smernik, R.; Currie, L. A.; Ball, W. P.; Nguyen, T. H.; Louchouran, P.; Houel, S.; Gustafsson, O.; Elmquist, M.; Cornellisen, G.; Skjemstad, J. O.; Masiello, C. A.; Song, J.; Peng, P. a.; Mitra, S.; Dunn, J. C.; Hatcher, P. G.; Hockaday, W. C.; Smith, D. M.; Hartkopf-Froder, C.; Bohmer, A.; Luer, B.; Huebert, B. J.; Amelung, W.; Brodowski, S.; Huang, L.; Zhang, W.; Gschwend, P. M.; Flores-Cervantes, D. X.; Largeau, C.; Rouzand, J.-N.; Rumpel, C.; Guggenberger, G.; Kaiser, K.; Rodionov, A.; Gonzalez-Perez, F. J.; Gonzalez-Perez, J. A.; De la Rosa, J. M.; Manning, D. A. C.; Lopez-Capel, E.; Ding, L., Comparison of quantification methods to measure fire-derived (black/elemental) carbon in soils and sediments using reference materials from soil, water, sediment and the atmosphere. *Global Biogeochemical Cycles* **2007,** 21.
10. Hammes, K.; Smernik, R. J.; Skjemstad, J. O.; Herzog, A.; Vogt, U. F.; Schmidt, M. W. I., Synthesis and characterisation of laboratory-charred grass straw (Oryza sativa) and chestnut wood (Castanea sativa) as reference materials for black carbon quantification. *Organic Geochemistry* **2006,** 37, (11), 1629-1633.
11. Antal, M. J.; Allen, S. G.; Dai, X.; Shimizu, B.; Tam, M. S.; Gronli, M., Attainment of the theoretical yield of carbon from biomass. *Ind. Eng. Chem. Res.* **2000,** 39, (11), 4024-4031.

CHAPTER 3. CHARACTERIZATION OF BIOCHAR FROM FAST PYROLYSIS AND GASIFICATION SYSTEMS

A paper published by *Environmental Progress & Sustainable Energy*

Catherine E. Brewer, Klaus Schmidt-Rohr, Justinus A. Satrio, Robert C. Brown

Abstract

Thermochemical processing of biomass produces a solid product containing char (carbon) and ash. This char can be combusted for heat and power, gasified, activated for adsorption applications, or applied to soils as a soil amendment and carbon sequestration agent. The most advantageous use of a given char depends on its physical and chemical characteristics, although the relationship of char properties to these applications is not well understood. Chars from fast pyrolysis and gasification of switchgrass and corn stover were characterized by proximate analysis, CHNS elemental analysis, Brunauer-Emmet-Teller (BET) surface area, particle density, higher heating value (HHV), scanning electron microscopy (SEM), x-ray fluorescence (XRF) ash content analysis, Fourier transform infrared spectroscopy using a photo-acoustic detector (FTIR-PAS), and quantitative ^{13}C nuclear magnetic resonance spectroscopy (NMR) using direct polarization and magic angle spinning. Chars from the same feedstocks produced under slow pyrolysis conditions, and a commercial hardwood charcoal, were also characterized. Switchgrass and corn stover chars were found to have high ash content (32-55 wt%), much of which was silica. BET surface areas were low (7-50 m^2/g) and higher heating values ranged from 13-21 kJ/kg. The aromaticities from NMR, ranging between 81 and 94%, appeared to increase with reaction time. A pronounced decrease in aromatic C-H functionality between slow pyrolysis and gasification chars was observed in NMR and FTIR-PAS spectra. NMR estimates of fused aromatic ring cluster size showed fast and slow pyrolysis chars to be similar (~7 to 8 rings per

cluster), while higher-temperature gasification char was much more condensed (~17 rings per cluster).

Keywords: switchgrass, corn stover, char quality, solid-state ^{13}C NMR

3.1 Introduction

Thermochemical processing of biomass has received significant recent attention as a platform for economically producing energy and chemicals from biorenewable resources.[1, 2] Product composition from these processes varies with reaction conditions and includes non-condensable gases (syn or producer gas), condensable vapors/liquids (bio-oil, tar), and solids (char, ash). In fast pyrolysis systems, dry biomass is heated very rapidly (up to 1000°C/sec) in the absence of oxygen and the products quickly removed and quenched to maximize production of bio-oils. Traditional charcoal-making typically employs slow pyrolysis conditions: slow heating rates (1-20°C/min) in the absence of oxygen and long char residence times (hours to days). Gasification uses higher temperatures and some oxygen (less than the stoichiometric ratio) to produce a non-condensable gas rich in hydrogen and carbon dioxide. Both fast pyrolysis and gasification yield some amount of char, typically 15-20% and 5-10% of the feedstock mass, respectively. How to best use this co-product depends on the local economic circumstances and the char properties. Combusting the char to supply process heat is common,[3, 4] while a few chars may be suitable for further activation to be used in higher-value adsorption applications.[5, 6]

Use of co-product chars as biochars, i.e. chars from biomass applied to soil as a soil amendment and/or a carbon sequestration agent, is another option.[2] While biochars have been used for millennia in some cultures' agricultural practices, current interest in biochars stems from the investigation of *terra preta* soils in the central Amazon. These dark, incredibly fertile soils have been shown to contain man-made charcoal which functions as soil organic matter.[7-9] The link between char properties and their efficacy in soils, however, is not well understood, much less how to engineer the process conditions to produce desired biochar properties. This is

especially true for chars from gasification and fast pyrolysis; most research in this area has focused on product yields and char combustion properties.[4, 10-12]

The purpose of this research was to provide a thorough characterization of chars produced under typical fast pyrolysis and gasification conditions using locally-common feedstocks: switchgrass and corn stover. This characterization serves as the initial step in an overall engineered biochar production scheme. The next steps would include soil incubation and crop growth studies using chars from these processes, the formulation of desired biochar properties based on soil tests, and finally, the engineered production of chars with these properties.

A key aspect of determining char quality for biochar (and other) applications is the ability to quantitatively characterize the forms of carbon present, as the type of carbon is believed to be related to char's reactivity and recalcitrance in soil.[8, 13-17] Concern has been expressed about "incompletely" pyrolyzed biomass as it may provide too much bio-available carbon to the soil without enough simultaneous nitrogen, resulting in nitrogen immobilization and therefore, negative short-term effects on plant yield.[15] Previous studies have used proximate analysis to differentiate between "volatile" and "fixed" carbon,[18] x-ray diffraction (XRD) to measure carbon crystallinity,[3] FTIR spectroscopy to identify char carbon functionality,[19, 20] and various solid-state ^{13}C NMR techniques such as cross-polarization / magic angle spinning (CP/MAS) to measure carbon functionality and aromaticity,[14, 19, 21-23] and other highly aromatic materials.[24, 25] The difficulty with all of these methods is the semi-quantitative nature of the information they provide. CP NMR, for example, tends to underestimate the non-protonated fraction of black carbons due to the slow transfer of hydrogen magnetization to carbons in the middle of large aromatic structures and is sensitive to signal loss by interaction with unpaired electrons, rendering up to 70% of carbon "invisible." [26, 27] The direct-polarization (DP) or Bloch-decay MAS NMR approach is superior in most respects[26, 28, 29] since it is inherently quantitative and detects most carbon.[26] Further, DP/MAS NMR can be combined with dipolar dephasing to quantify the fraction of non-protonated aromatic C.[30] This study explores the application of these quantitative

NMR techniques to study the structure of fast pyrolysis and gasification chars. The use of two complementary NMR methods for estimating the size of clusters of fused aromatic rings in chars, based on spectral analysis and ^{1}H-^{13}C dipolar distance, is also demonstrated.

3.2 Experimental

3.2.1 Char Selection

Seven representative chars were selected for this study, one from each thermochemical process for each feedstock and one commercially available wood charcoal. Switchgrass and corn stover were obtained locally (Story County, IA). Prior to thermochemical processing, feedstocks were ground in a hammer mill to pass a ¼" screen and dried to <10% moisture. Mixed hardwood charcoal was obtained from a commercial kiln (Streumph Charcoal Company, Belle, MO). This char had been used in a biochar soil column nutrient leaching study[31] and was considered a good candidate for comparison.

3.2.2 Slow Pyrolysis

Slow pyrolysis was performed by placing feedstock into a paint-can fitted with a nitrogen purge (1L/min flow rate) and thermocouple for temperature measurement. The sealed can was placed into a muffle furnace and heated at approximately 15°C/min to 500°C. Corn stover (50 g) was held at 500°C for 30 minutes; switchgrass (125 g) was held at 500°C for 2 hours. The char was then cooled under nitrogen flow and stored in sealed glass jars. Mass yield of char was 33.2% and 41.0% for corn stover and switchgrass, respectively.

3.2.3 Fast Pyrolysis

Fast pyrolysis was performed on a 5 kg/hour capacity bubbling fluidized bed reactor optimized for bio-oil production.[5] The sand bed was fluidized with nitrogen pre-heated at 500°C. Char was collected using a high-throughput cyclone catch and cooled under nitrogen before being stored in resealable plastic bags.

3.2.4 Gasification

Gasification was performed on a 3 kg/hour capacity bubbling fluidized bed reactor using an air/nitrogen fluidizing gas (0.20 equivalence ratio). For reactor set-up details, see Meehan, et al.[32] The average steady state temperature was 760°C for switchgrass and 730°C for corn stover. Char was again collected by cyclone, cooled under nitrogen, and stored in resealable plastic bags.

3.2.5 Physical Properties

BET surface area was measured by nitrogen gas sorption analysis at 77K (NOVA 4200e, Quantachrome Instruments, Boynton Beach, FL). Prior to analysis, samples were vacuum degassed at 300°C for 4-16 hours (conditions typical for carbons). Degassing time varied based on the time necessary to reach a stable surface area measurement. Particle density was measured by helium pycnometer (Pentapycnometer, Quantachrome Instruments) using degassed samples from BET analysis and long purge times (10 min) to prevent errors due to volatile content outgassing.

Char particle structure and surface topography were analyzed by scanning electron microscopy (SEM) using a Hitachi S-2460N variable pressure scanning electron microscope (VP-SEM). Samples were mounted on carbon disks. Variable pressure mode allowed for examination of insulating samples with minimal sample preparation. A residual atmosphere of 60 Pa (0.5 Torr) of helium was adequate to eliminate charging from samples while allowing reasonably high magnifications (up to 1500x).

3.2.6 Chemical Properties

Moisture, volatiles, fixed carbon and ash content were determined in triplicate by ASTM proximate analysis method for wood charcoals (ASTM D1762-84, reapproved 2007). Fused quartz crucibles were used and chars were not ground prior to analysis (most were already fine powders). Elemental analysis was performed by

LECO Corporation (St. Joseph, MI) using TRUSPEC-CHN and TRUSPEC-S analyzers (LECO). Samples (~0.1 g) with larger particles were crushed using a mortar and pestle before analysis. Oxygen content was not able to be determined consistently due to high inorganic oxygen content (in the ash) decomposing during analysis. Higher heating value (HHV) of chars was determined by oxygen bomb calorimeter (Parr Instrument Company, Moline, IL) according to Parr Sheet No. 240M, 205M and 207M.

Mineral content was measured by x-ray fluorescence spectrophotometer (PHILIPS PW2404) equipped with a rhodium target X-ray tube and a 4kW generator. Dry char (4 g) was mixed with x-ray pellet mix powder (1.5 g) and boric acid (1 g) for 2 min in a puck grinder, then pressed into a pellet under vacuum to 25 tons pressure for 15 sec. Dry feedstock was also analyzed to verify that char had not been contaminated by sand from the fluidized bed.

3.2.7 FTIR-PAS

Surface functionality was investigated by Fourier transform infrared (FTIR) spectroscopy using a Digilab FTS-7000 FTIR spectrophotometer equipped with a PAC 300 photoacoustic detector (MTEC Photoacoustics, Ames, IA). The sample chamber was purged with helium for several minutes prior to analysis to prevent the interference of water and carbon dioxide. Spectra of dried feedstock and char samples were taken at 4 cm^{-1} resolution and 1.2 kHz scanning speed for a total of 64 co-added scans.

3.2.8 Solid-state ^{13}C NMR

^{13}C NMR experiments were performed using a Bruker DSX400 spectrometer at 100 MHz (400 MHz ^{1}H frequency). Quantitative ^{13}C Direct Polarization/Magic Angle Spinning (DP/MAS) NMR experiments were performed using 4-mm sample rotors at a spinning speed of 14 kHz. The 90^{o} ^{13}C pulse-length was 4.5 μs. Sufficiently strong ^{1}H decoupling at $\gamma B_1/2\pi$ = 72 kHz with the two-pulse phase-modulated (TPPM) scheme was applied during an acquisition time of 2 ms. Recycle delays (10-40 s)

were determined by the Cross Polarization/Spin-Lattice Relaxation Time/Total Sideband Suppression (CP/T_1-TOSS) technique to make sure that all carbon sites were >95% relaxed.[33] Delays were confirmed by a series of DP experiments with increasing recycle delays. To obtain quantitative information on the non-protonated aromatic carbon fraction, DP/MAS ^{13}C NMR with recoupled dipolar dephasing was used.[30] The dipolar dephasing time was 67 μs. The total time for DP/MAS and DP/MAS with gated decoupling experiments was typically 23 h per sample.

Qualitative char composition information, in particular alkyl carbon composition, was obtained with good sensitivity by ^{13}C CP/TOSS NMR experiments with samples in 7-mm rotors at a spinning speed of 7 kHz, a CP time of 1 ms, a ^{1}H 90^{o} pulse-length of 4 μs, and a recycle delay of 0.5 s. Four-pulse TOSS was employed before detection and TPPM decoupling was applied for optimum resolution.

The size of fused aromatic rings typical of charcoal can be estimated based on recoupled ^{1}H-^{13}C dipolar dephasing.[34] In short, two ^{1}H 180^{o} pulses per rotation period prevent magic angle spinning (MAS) from averaging out weak CH dipolar couplings. Composite $90^{o}x$-$180^{o}y$-$90^{o}x$ pulses were used to reduce effects of imperfect pulse flip angles. In order to detect non-protonated carbons with good relative efficiency, DP/TOSS was used at a spinning speed of 7 kHz, in 7-mm rotors for the pyrolysis chars. All experiments on the gasification char had to be performed in 4-mm rotors, where the pronounced 400-MHz radio-frequency absorption due to sample conductivity was less severe than for the larger amount of material in the 7-mm rotor. The ^{13}C 90^{o} and 180^{o}-pulse lengths were 4.5 μs and 9 μs, respectively. The recycle delays were the same as used for DP/MAS spectra. Instead of the total aromatic signal between 107 and 142 ppm, only the signal of non-protonated C (after 40 μs of regular gated decoupling) was considered in the analysis. For reference, milled-wood lignin[35] (a better-defined sample than the commercial lignin in)[34] was run under the same conditions, with a 60 s recycle delay.

3.3 Results and Discussion

3.3.1 Physical Properties

SEM micrographs of switchgrass and the three types of switchgrass char are shown in Figure 17. Overall plant structure was visible in all of the chars. Increased porosity from volatiles escaping during thermochemical degradation can also be seen. The particle size decrease observed in the gasification and fast pyrolysis char is believed to be caused by rapid devolatilization creating very porous (macroporous) and fragmented chars.[36] In general, gasification chars are fine powders while fast pyrolysis are very fine powders.[3] Table 4 shows the particle densities and BET surface areas of the representative chars. Surface areas were very low (7-50 m^2/g) compared to commercial activated carbons and increased with process temperature and char residence time. Particle density, also known as solid or true density, increased with ash (mineral) content and process temperature. It has been suggested that particle density can be used to estimate the charring temperature. As temperature and reaction time increase, the degree of graphitization increases and char's particle density (typically 1.5-1.7 g/cm^3) approaches that of solid graphite (2.25 g/cm^3).[37] The presence of minerals, which are denser than most forms of carbon, can also cause higher apparent particle density in high-ash chars.

3.3.2 Chemical Properties

Results from proximate and elemental analysis of chars are shown in Table 4. Switchgrass and corn stover chars had high ash contents (32-55 wt %) at the expense of carbon content. For most char applications, this high ash content puts switchgrass and corn stover chars at a disadvantage compared to chars from low-ash feedstocks. Char higher heating values (Table 4) are similar to those presented by Boateng and are comparable to coals.[3] Table 5 lists the ash composition of switchgrass, corn stover and hardwood chars as determined by XRF. (Due to the nature of the samples and the calibration method, the relative concentrations of the elements are accurate, but the overall mineral content in the char is overestimated.)

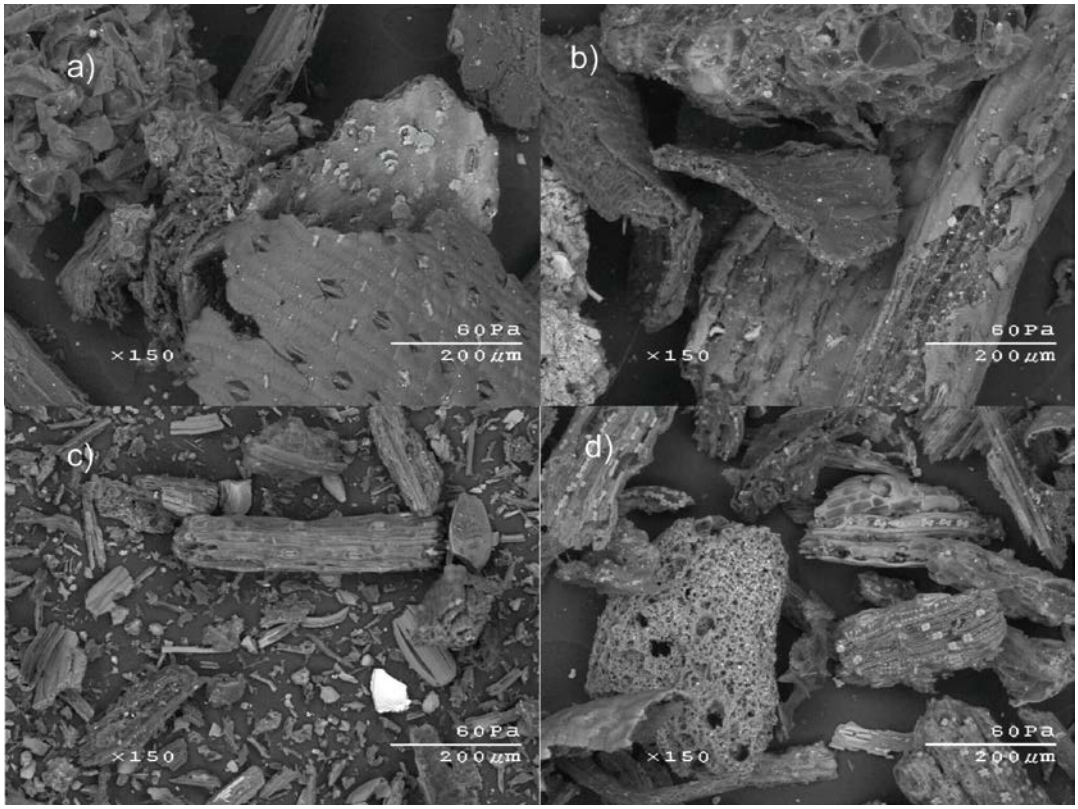

Figure 17. Scanning electron micrographs of switchgrass a) feedstock, b) slow pyrolysis char, c) fast pyrolysis char and d) gasification char.

Table 4. Composition, physical properties and higher heating value (HHV) of representative chars. Elemental composition values are reported on a dry weight basis; HHV and proximate analysis results presented on a wet basis. S.P. = slow pyrolysis, F.P. = fast pyrolysis, ND = not determined.

Char	Particle Density	BET Surface Area	Moisture	Volatiles	Fixed C	Ash	C	H	N	S	HHV (as received) (MJ/kg)
	g/cc	m^2/g	--wt %--								MJ/kg
Switchgrass S. P.	1.76	50.2	0.9	7.1	39.5	52.5	39.4	1.3	0.7	0.002	15.37
Switchgrass F. P.	1.78	21.6	2.7	16.4	26.4	54.6	38.7	2.5	0.6	0.21	16.34
Switchgrass Gasification	2.06	31.4	2.5	10.3	34.3	53.0	42.8	1.6	0.8	0.17	15.86
Corn Stover S. P.	1.54	20.9	1.8	11.1	54.7	32.4	62.8	2.9	1.3	0.05	21.60

Corn Stover F. P.	1.85	7.0	1.0	14.9	34.4	49.7	37.8	2.5	0.8	0.06	13.83
Corn Stover Gasification	1.92	23.9	1.9	5.5	38.5	54.0	38.5	1.3	0.7	0.09	15.29
Switchgrass F. P.3	ND	7.7	3.8	28.4	42.0	25.9	63	3.7	0.8	ND	19.37
Hardwood S. P.	1.60	19.7	2.6	19.7	63.8	13.9	65.3	2.6	0.6	0.05	22.64

Table 5. Ash composition of switchgrass, corn stover and hardwood char samples by X-ray fluorescence spectroscopy prepared by the pressed pellet method. All values are dry weight %. Elements are represented as their respective oxides. F.P. = fast pyrolysis.

Element	**Switchgrass F.P. Char**	**Corn Stover F.P. Char**	**Hardwood Char**
Al_2O_3	0.49	2.33	0.60
CaO	3.65	3.80	22.37
Cl	0.47	0.59	0.03
Fe_2O_3	0.76	1.87	2.36
K_2O	6.00	4.03	1.35
MgO	1.55	2.02	0.48
MnO_2	0.15	0.13	0.83
Na_2O	0.07	0.20	0.06
P_2O_5	3.86	1.19	0.20
SiO_2	43.62	29.98	5.67
SO_3	0.99	0.28	0.27
Other	0.25	0.64	0.51
Total	61.86	47.06	34.73

Corn stover and switchgrass ashes predominantly contain silica while hardwood ash contains mostly alkali metals. Biomass combustion research has shown that feedstocks containing more silica have relatively high slagging tendencies.[38] Furthermore, contamination by sand or soil during biomass collection enhances this tendency.[38] For this reason, chars from switchgrass and corn stover (collected by

farming equipment) have three inherent challenges compared to traditional charcoals for use as fuels: high overall ash content, high silica content, and contamination by soil.

3.3.3 Aromaticity from NMR

Figure 18 presents quantitative ^{13}C DP/MAS NMR spectra, of switchgrass slow pyrolysis, fast pyrolysis, and gasification chars. The corresponding quantitative spectra of non-protonated carbons and CH_3 groups, obtained after 68 μs of dipolar dephasing,[26] are also shown (thick lines). The spectra are dominated by the band of the aromatic carbons around 128 ppm, the majority of which is not protonated. Small signals of C=O and alkyl groups are also detected. These are seen more clearly in the CP/TOSS spectra of Figure 19, which overrepresent the signals of protonated C and contain no residual spinning sidebands. In addition to spectra of pyrolysis chars, the spectrum of the switchgrass feedstock is shown for reference in Figure 19c. Figure 19d shows the CP spectrum of fast pyrolysis char from corn stover. The relative fractions of eight types of functional groups obtained from the DP spectra are compiled in Table 6. The sum of the aromatic C-O, non-protonated aromatics and aromatic C-H fractions gives the total aromaticity. While the aromaticities of the different chars are similar (see first column of Table 8), the fraction of protonated aromatic carbons decreases significantly from slow pyrolysis to gasification.

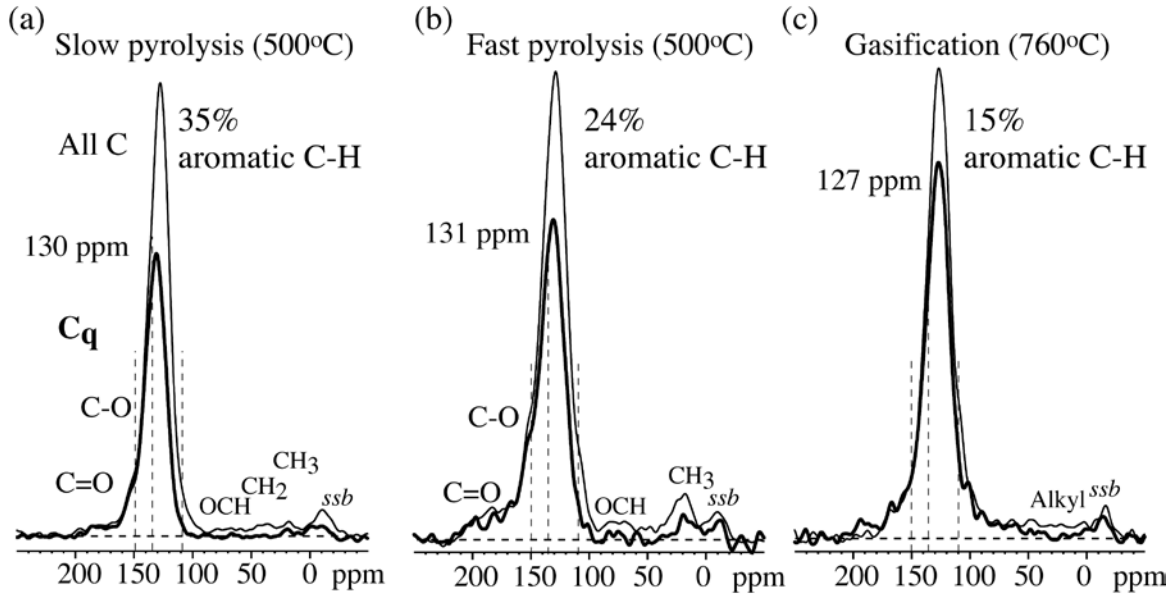

Figure 18. Quantitative ^{13}C NMR spectra, obtained with direct polarization at 14-kHz MAS, of three chars made from switchgrass: (a) Slow pyrolysis, (b) fast pyrolysis, (c) gasification char. Thin line: Spectrum of all carbons; bold line: corresponding spectrum of non-protonated C and CH_3, obtained after 68 μs of dipolar dephasing. ssb = spinning side band.

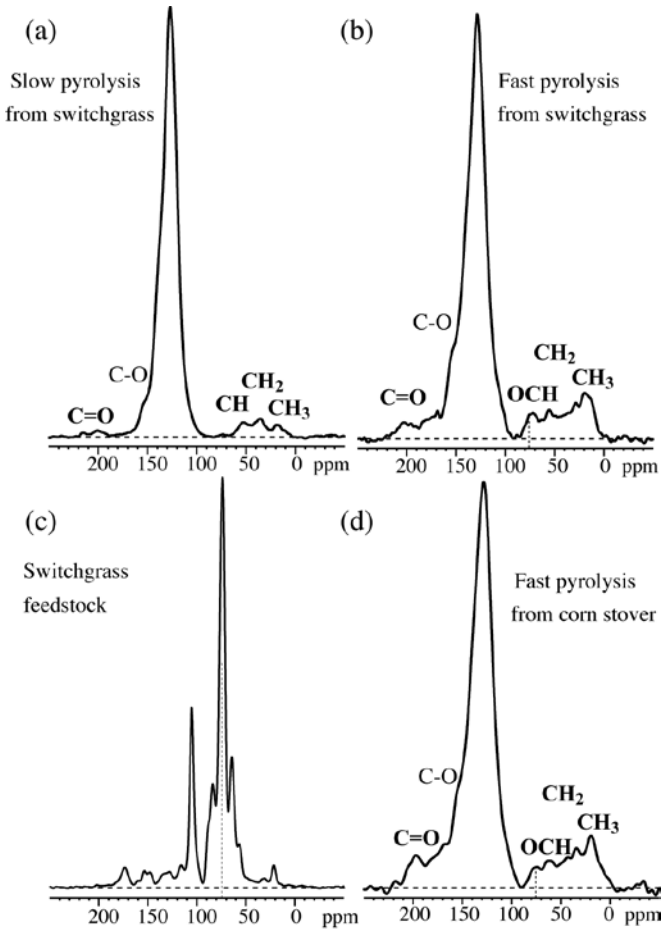

Figure 19. CP/MAS/TOSS ^{13}C NMR spectra, highlighting the signals of alkyl residues, of (a) slow pyrolysis char, (b) fast pyrolysis char from switchgrass, (c) the switchgrass feedstock for reference, and (d) fast pyrolysis char from corn stover.

From the abundance and estimated composition of the functional groups in Table 6, the elemental composition can be estimated. Since C-OH and C-O-C groups have similar resonance positions, their ratio cannot be determined; a 50:50 ratio of ethers and OH groups was assumed in the analysis. The resulting fractional oxygen contents listed in Table 6 take into account ether oxygen shared between its two bonded carbons. Since ether oxygen atoms are not protonated, the H contribution is correspondingly reduced. Table 7 compares these NMR-derived composition values with those from combustion analysis. The good agreement validates the NMR assignments. Both elemental analyses consistently show much higher oxygen

content for the fast pyrolysis char. The detailed NMR analysis, see Table 6, reveals higher fractions of all kinds of oxygen-containing moieties.

Table 6. Quantitative NMR spectral analysis of switchgrass and corn stover chars. S.P. = slow pyrolysis, F.P. = fast pyrolysis. Error margins: ± 1%.

	Carbonyls		**Aromatics**			**Alkyls**		
Moieties:	**C=O**	**COO**	**C-$O_{0.75}H_{0.5}$**	**$C_{non-pro}$**	**C-H**	**$HCO_{0.75}H_{0.5}$**	**$CH_{1.5}$**	**CH_3**
ppm:	**210-183**	**183-165**	**165-145**	**145 – 90**	**145 - 90**	**90-50**	**50-25**	**25-6**
Switchgrass S. P.	0.8.%	1.4%	6.7%	52%	35%	1.4%	1.6%	1.3%
Switchgrass F. P.	3.3%	3.2%	10.3%	49%	24%	3.6%	2.6%	4.0%
Switchgrass Gasification	2.0%	2.2%	6.4%	66%	15%	4.0%	2.0%	2.0%
Corn Stover F. P.	3.5%	4.2%	11.7%	42%	27%	3.3%	3.7%	4.8%
Corn Stover Gasification	2.5%	2.8%	8.2%	61%	18%	3.0%	2.3%	1.3%

Table 7. Elemental analysis of switchgrass and corn stover chars from NMR and combustion (in parentheses). S.P. = slow pyrolysis, F.P. = fast pyrolysis.

Char	**C (wt%)**	**H (wt%)**	**O+N (wt%)**
Switchgrass S. P.	(39.4% ± 0.4)	1.53% (*1.31* ± *0.01%*)	4.9% (*~6.3%*)
Switchgrass F. P.	(38.7 ± 0.2%)	1.63% (*2.49* ± *0.03%*)	10.1% (*~5.7%*)
Switchgrass Gasification	(42.8 ± 0.1%)	1.18% (*1.60* ± *0.02%*)	7.9% (*~3.9%*)
Corn Stover F. P.	(37.8 ± 0.6%)	1.82% (*2.48* ± *0.05%*)	11.3% (*~10.5%*)
Corn Stover Gasification	(38.5 ± 0.2%)	1.08% (*1.29* ± *0.01%*)	8.2% (*~7.2%*)

3.3.4 Degree of Aromatic Condensation from NMR

In addition to determining aromaticity, NMR can also provide an estimate of the degree of aromatic condensation. Various research groups have attempted to use NMR to quantify the fraction of bridgehead carbons (f_{bridge}) as a measure of the degree of aromatic condensation. Several groups simply assumed that all carbons resonating around 130 ppm are bridgehead C, and that aromatic C-H resonances are in a narrow band around 108 ppm;[39, 40] the clear dipolar dephasing by >20% of the 130-ppm band in the spectra in Figure 18, however, demonstrates the significant presence of C-H signal and thus shows that this assumption is false.

Table 8. Aromaticities, fractions of aromatic edge carbons, and minimum number of carbons per aromatic cluster in switchgrass and corn stover chars.

Char	Aromaticity	χ_{CH}	$\chi_{edge,min}$	$\chi_{edge,max}$	$n_{C,min}$	H_{arom}/H_{alk}
Switchgrass S. P.	94%	0.37	0.44	0.51	>23 C	4.5
Switchgrass F. P.	83%	0.29	0.41	0.61	>16 C	1.2
Switchgrass Gasification	86%	0.17	0.25	0.40	>37 C	1.4
Corn Stover F. P.	81%	0.33	0.48	0.72	>12 C	1.2
Corn Stover Gasification	87%	0.21	0.30	0.44	>31 C	2

A better approach was suggested by Solum et al., who focused on the signals of non-protonated C (selected by dipolar dephasing) and assigned those between 135 and 90 ppm to bridgehead carbons.[24, 25] Still, the spectra in Figure 18 show no indication of a minimum near 135 ppm that would indicate a spectral separation of bridgehead from other non-protonated aromatic carbons; instead, the spectra suggest that the bridgehead carbon band extends beyond 135 ppm and cannot be

reliably separated from smaller bands of other non-protonated aromatic C. Indeed, in two coals of high aromaticity, the assumptions of Solum et al. resulted in a higher fraction of alkylated aromatics than that of total alkyl carbons, which confirms that some bridgehead carbon signal was assigned incorrectly.[24] In addition, the use of cross polarization from ^{1}H is likely to result in an underrepresentation of the bridgehead carbons far from the nearest ^{1}H and must, therefore, be avoided in the study of chars.

We propose here that the degree of aromatic condensation can be estimated most reliably by combining two complementary approaches: spectral analysis and long-range H-C dipolar dephasing. From quantitative ^{13}C NMR spectra, one can estimate the fraction of carbons along the edges of the aromatic rings, $\chi_{edge} = 1 - \chi_{bridge}$, which decreases with increasing aromatic ring cluster size. The usually dominant spectral contributions to the aromatic edge carbons in chars come from aromatic C-H and aromatic C-O moieties, whose fractions $\chi_{CH} = f_{aCH}/f_{ar}$ and $\chi_{C-O} = f_{aC-O}/f_{ar}$ can be determined quite easily from the ^{13}C spectra. (f_{ar}, f_{aCH} and f_{aC-O} stand for aromatic carbon fractions: total aromatic carbon, aromatic carbon bonded to hydrogen, and aromatic carbon bonded to oxygen, respectively.) Together, they constitute the minimum aromatic edge fraction,

$$\chi_{edge,min} = \chi_{CH} + \chi_{C-O} \qquad (1)$$

Additional contributions can come from alkyl C and C=O bonded to the aromatic rings. Thus, the upper limit of the edge fraction is provided by

$$\chi_{edge,max} = \chi_{edge,min} + \chi_{alkyl} + \chi_{C=O} \qquad (2)$$

If the fraction of C=O groups exceeds that of alkyls, one can show that some of the C=O must be bonded to the aromatic rings (and thus contribute to $\chi_{edge,min}$), but this is not relevant with the samples studied here. Table 8 lists the values of $\chi_{edge,min}$ and $\chi_{edge,max}$ for the chars studied. Given the relatively small alkyl ($\chi_{alkyl} = f_{alkyl}/f_{ar}$) and

C=O fractions in chars, the range of χ_{edge} between $\chi_{edge,min}$ and $\chi_{edge,max}$ is quite limited, particularly for the slow pyrolysis sample.

The geometry of condensation, e.g. linear (primary catenation) vs. clustered (e.g. circular catenation), can be assessed based on $\chi_{edge,max}$ in linearly condensed systems, $\chi_{edge} > 0.5$, so $\chi_{edge,max} < 0.5$ excludes linear condensation. More generally, based on the equations given by Solum et al., one can show that the number of carbons, n_C, in a cluster relates to the edge fraction by

$$3/(\chi_{edge}-0.5) \geq n_C \geq 6/\chi_{edge}^2 \geq 6/\chi_{edge,max}^2 \qquad (3)$$

with the upper limit for linear and the lower for circular condensation.[24] For instance, if $\chi_{edge,max} \leq 0.4$, then there must be more than $n_C = 37$ carbons in a cluster. The last column in Table 8 lists these minimum cluster sizes.

The second approach, long-range ^1H-^{13}C dipolar dephasing, probes distances of the aromatic carbons from hydrogen at the edge of the condensed ring system in terms of the strongly distance-dependent ^1H-^{13}C dipolar couplings.[34] The larger the average ^1H-^{13}C distance, the slower the dephasing of the ^{13}C signal; thus, a slower decay indicates a larger cluster size. The slower dephasing for the gasification char compared to the pyrolysis chars (Figure 20) indicates a larger aromatic-cluster size in the former, consistent with the spectral analysis. Curves for specific sites in model compounds,[34] with two two-bond and two three-bond couplings, provide an approximate length-scale calibration (see dashed and dash-dotted lines in Figure 20).

The dephasing for the slow pyrolysis char nearly coincides with the three-bond calibration curve, indicating that the non-protonated carbons in this char are on average at a three-bond distance from the nearest ^1H. Figure 21a shows a typical fused-ring system that is compatible with the NMR data, both spectroscopic and dipolar-dephasing, for the slow pyrolysis char. Here, the number of sites (filled triangles and squares) that dephase slower than the calibration sites is similar to the number of sites (thin-line ellipses) that dephase faster. The corresponding model for

fast pyrolysis char, see Figure 21b, has a smaller C-H and larger C-O fraction, but features an only slightly smaller fused-ring system. The slower dephasing for the gasification char in Figure 20 requires a significantly larger fraction of C at a ≥3-bond distance from the nearest ^{1}H. The structure in Figure 21c contains many more slow-dephasing (filled triangles or squares) than fast-dephasing (thin-line ellipses) sites.

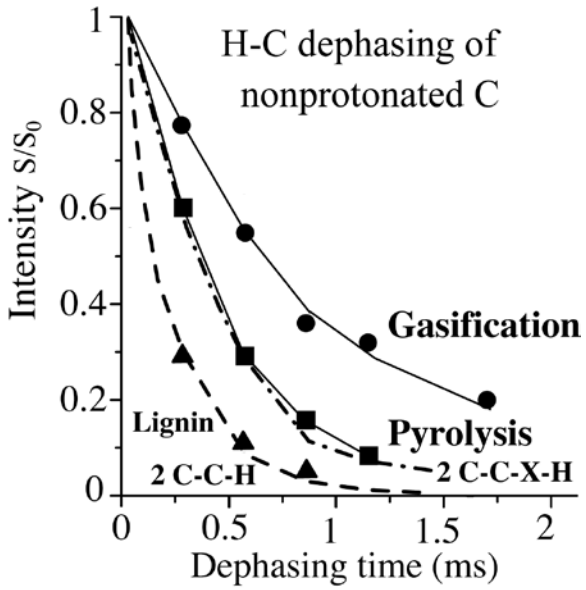

Figure 20. Plot of the area of signals of non-protonated aromatic carbons resonating between 107 and 142 ppm, under long-range ^{1}H-^{13}C dipolar dephasing. Circles: Gasification char from switchgrass. Squares: Slow and fast pyrolysis char, whose data coincide within the error margins of ±2%. Dash-dotted line: Carbons 11 and 13 of 1, 8-dihydoxy-3-methylanthraquinone, which are three bonds away from the two nearest protons. Dashed line: Carbon 1 of 3-methoxy benzamide, which is two bonds away from the two nearest protons. The new reference data for lignin (triangles) coincide with this line.

3.3.5 Comparison with Previous NMR Studies of Char

The structures with significant clustered aromatic condensation derived here from the dual NMR approach are very different from the small, linearly condensed structures proposed by Knicker for cellulose heated under oxic conditions, based on CP/NMR.[23, 41] The difference may arise primarily from differences in char production conditions, namely the presence of oxygen and the lower temperature; following the temperature-ring size relationship suggested above, a less condensed (but not necessarily linear) structure would be expected. The oxic heating conditions may

have resulted in local “hot spots,” where the temperature exceeded that of the furnace setting as some of the carbon was exothermically combusted.

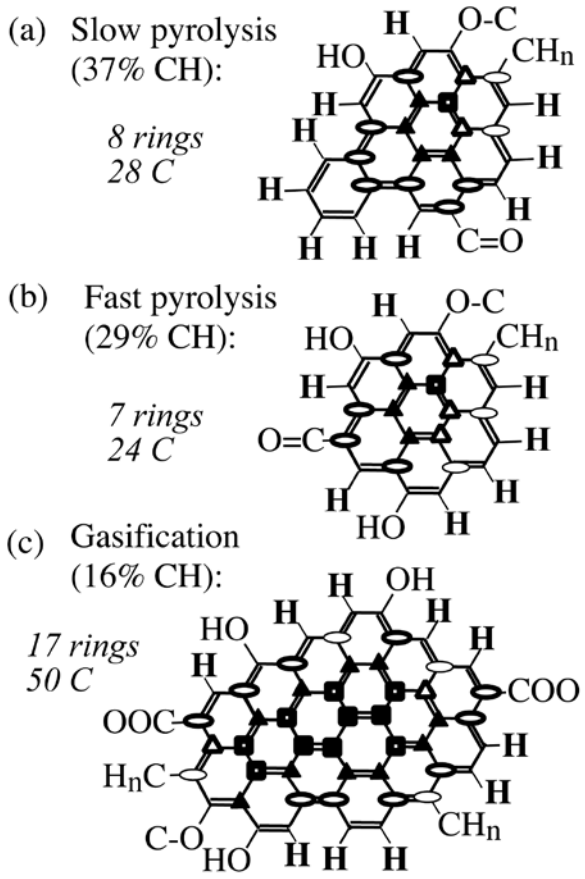

Figure 21. Typical aromatic clusters, derived from NMR, in (a) slow pyrolysis char, (b) fast pyrolysis char, and (c) gasification char from switchgrass. Symbols label the distance of carbons resonating between 107 and 142 ppm from the nearest proton(s).Thin-line ellipse: Two bonds from multiple H. Thick-line ellipse: Two bonds from one H. Open triangle: Three bonds from multiple H. Filled triangle: Three bonds from one H. Open square: Four bonds from multiple H. Filled square: Four bonds from one H, or more than four bonds from any H.

3.3.6 Form of H in Chars

Based on the quantitative NMR analysis, we can estimate the ratio of the fractions of hydrogen attached to aromatic and alkyl carbons, H_{arom}/H_{alk}. The data in Table 6 show that in spite of the high aromaticity of all chars, aromatic H is strongly dominant only in the slow pyrolysis char.

3.3.7 FTIR-PAS

FTIR-PAS is a very fast and easy method to gauge the “progress” of the pyrolysis reaction. Drying is the only sample preparation step needed to perform this analysis, which eliminates the sample handling and dilution difficulties encountered when pelletizing samples with potassium bromide.[42] The FTIR-PAS spectra in Figure 22 show the progression of switchgrass feedstock to gasification char; the spectra for corn stover (not shown) were very similar to those of switchgrass. The spectrum from commercial hardwood slow pyrolysis is also shown. The most dramatic change is the O-H stretch peak around 3400 cm^{-1}, which dominates the feedstock spectrum but is almost absent in the gasification char spectrum. Assignment of other peaks important for chars, including the aliphatic C-H stretch at 3000-2860 cm^{-1}, the aromatic C-H stretch around 3060 cm^{-1}, and the various aromatic ring modes at 1590 and 1515 cm^{-1}, can be found in a paper by Sharma, et al. on lignin chars.[20] The series of spectra in Figure 22 suggests a gradual loss of lignocellulosic functional groups, but the NMR spectra of Figure 19 show that all of the chars contain little, if any, polysaccharide residues. The relatively strong aromatic C-H stretch in slow pyrolysis char matches well with the large aromatic C-H concentration seen in the NMR spectra. It was noted that fast pyrolysis char appeared less “reacted” than the slow pyrolysis char, but again this is not supported by NMR; rather, the higher oxygen content in the fast pyrolysis char makes the distribution of functional groups more similar to those of the switchgrass feedstock.

3.3.8 Effects of Synthesis Conditions on Char Structure

NMR showed that the aromaticity of slow pyrolysis char is higher than that of fast pyrolysis or gasification chars. Tentatively, this can be attributed to the long residence time (2 h) in slow pyrolysis, compared to that of fast pyrolysis and gasification in a fluidized bed reactor(<2 s). Nevertheless, slow pyrolysis char exhibited a cluster size only slightly larger than fast pyrolysis char and much smaller than gasification char. This suggests that cluster size is controlled mostly by reaction temperature, not duration.

None of the chars contained recognizable fragments of feedstock biopolymers, showing that the reaction time was sufficient for complete conversion to char. This preempts concerns about unreacted, bio-available fractions in carbon sequestration and soil amendment applications. Elemental analysis and NMR showed consistently that fast pyrolysis char contained more oxygen in various functional groups, not just alkyl C-OH as the feedstock. The somewhat enhanced COO concentration in fast compared to slow pyrolysis char may actually result in a slightly better cation exchange capacity (CEC). In conjunction with the similar aromatic cluster size, this suggests that fast pyrolysis char should perform similarly as, if not better than, slow pyrolysis char in soil amendment applications. Gasification char, though similar to slow pyrolysis char in aromaticity, has much larger aromatic clusters, suggesting significantly different properties. The larger cluster size is proven not only by the dual NMR approach introduced here, but also by the lower ppm value of the non-protonated aromatic carbon band, which is characteristic of bridgehead carbons,[22] and by the observed radio-frequency power absorption due to conductivity of sufficiently large fused ring systems.[43]

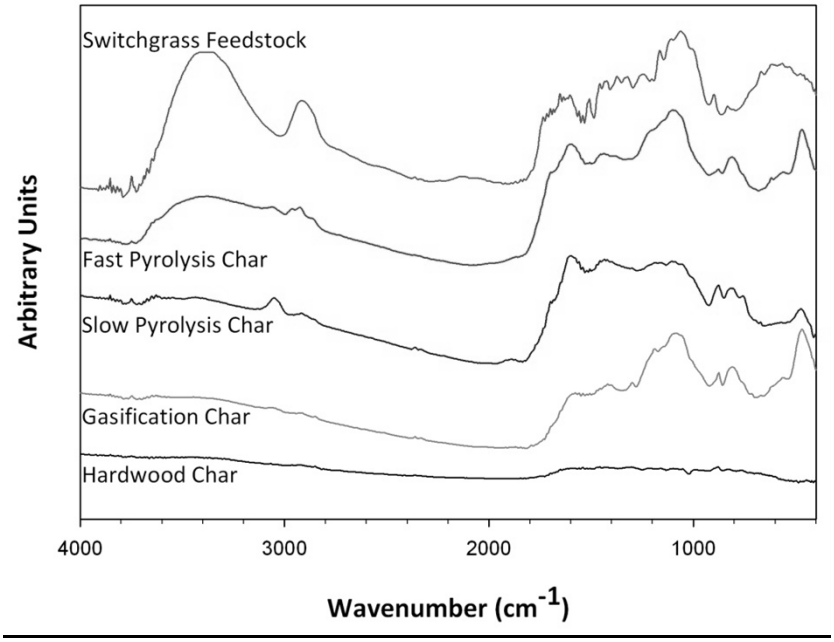

Figure 22. FTIR-PAS spectra of switchgrass, switchgrass chars and a commercial hardwood char.

3.4 Conclusions

Chars from fast pyrolysis and gasification are physically and chemically different from traditional hardwood charcoals and chars prepared from herbaceous feedstocks by slow pyrolysis. The types of carbon present appear to depend on process temperature and, to a lesser extent, reaction time. None of the chars contained a detectable amount of only partially pyrolyzed biomass.

Fast pyrolysis and gasification chars should be included in biochar trials. Their wider range of properties and reaction conditions will offer insight on how to engineer desirable biochars. The structural features of fast pyrolysis char suggest favorable properties in this application. Co-production of biochar and bioenergy may prove to be a more cost-effective and resource efficient use of biomass crops and crop residues.

Switchgrass and corn stover chars have high silica ash content and low surface area, and therefore, will present challenges to traditional char applications such as combustion or activation; the best use of switchgrass and corn stover chars may be soil application depending on the economic circumstances and the local soil properties.

Solid-state ^{13}C NMR using techniques presented here (DP/MAS, DP/MAS with dipolar dephasing, CP/TOSS, and DP/TOSS with recoupled ^{1}H-^{13}C dipolar dephasing) can provide the quantitative information needed to reliably track changes in carbon structure over reaction time and temperature, which will be meaningful to engineered char production and biochar testing.

Acknowledgements

Financial support for this research was provided by a National Science Foundation Graduate Research Fellowship and an ISU Plant Science Institute Graduate Research Fellowship (Brewer), and the ISU Bioeconomy Institute. The authors would like to thank the following for their assistance on various aspects of the analysis process: undergraduates Daniel Assmann and Hernań Treviño, CSET colleagues for providing char samples and process information, CSET staff on HHV,

Xiaowen Fang on NMR, Warren Straszheim on SEM, Scott Schlorholtz on XRF, and John McClelland and Roger Jones on FTIR-PAS. Thanks also to David Laird for his valuable comments on agronomic applications of biochar.

Literature Cited

1. Wright, M. M.; Brown, R. C., Comparative economics of biorefineries based on the biochemical and thermochemical platforms. *Biofuels, Bioproducts & Biorefining* **2007,** 1, (1), 49-56.
2. Laird, D. A., The charcoal vision: A win-win-win scenario for simultaneously producing bioenergy, permanently sequestering carbon, while improving soil and water quality. *Agronomy Journal* **2008,** 100, (1), 178-181.
3. Boateng, A. A., Characterization and thermal conversion of charcoal derived from fluidized-bed fast pyrolysis oil production of switchgrass. *Industrial & Engineering Chemistry Research* **2007,** 46, (26), 8857-8862.
4. Boateng, A. A.; Mullen, C. A.; Goldberg, N.; Hicks, K. B.; Jung, H.-J. G.; Lamb, J. F. S., Production of bio-oil from alfalfa stems by fluidized-bed fast pyrolysis. *Industrial & Engineering Chemistry Research* **2008,** 47, (12), 4115-4122.
5. Fan, M.; Marshall, W.; Daugaard, D.; Brown, R. C., Steam activation of chars produced from oat hulls and corn stover. *Bioresource Technology* **2004,** 93, (1), 103-107.
6. Azargohar, R.; Dalai, A. K., Steam and KOH activation of biochar: Experimental and modeling studies. *Microporous and Mesoporous Materials* **2008,** 110, (2-3), 413-421.
7. Lehmann, J.; Gaunt, J.; Rondon, M., Bio-char sequestration in terrestrial ecosystems – a review. *Mitigation Adaptation Strategies Global Change* **2006,** 11, (2), 395-419.
8. Glaser, B.; Lehmann, J.; Zech, W., Ameliorating physical and chemical properties of highly weathered soils in the tropics with charcoal - a review. *Biol. Fertil. Soils* **2002,** 35, (4), 219-230.
9. Glaser, B.; Haumaier, L.; Guggenberger, G.; Zech, W., The 'Terra Preta' phenomenon: a model for sustainable agriculture in the humid tropics. *Naturwissenschaften* **2001,** 88, (1), 37-41.
10. Yanik, J.; Kornmayer, C.; Saglam, M.; Yuksel, M., Fast pyrolysis of agricultural wastes: Characterization of pyrolysis products. *Fuel Processing Technology* **2007,** 88, (10), 942-947.
11. Lee, K. H.; Kang, B. S.; Park, Y. K.; Kim, J. S., Influence of reaction temperature, pretreatment, and a char removal system on the production of bio-oil from rice straw by fast pyrolysis using a fluidized bed. *Energy Fuels* **2005,** 19, (5), 2179-2184.
12. Tsai, W. T.; Lee, M. K.; Chang, Y. M., Fast pyrolysis of rice husk: Product yields and compositions. *Bioresource Technology* **2007,** 98, (1), 22-28.
13. Baldock, J. A.; Smernik, R. J., Chemical composition and bioavailability of thermally altered Pinus resinosa (Red pine) wood. *Org. Geochem.* **2002,** 33, (9), 1093-1109.

14. Novak, J. M.; Busscher, W. J.; Laird, D.; Ahmedna, M.; Watts, D. W.; Niandou, M. A. S., Impact of Biochar Amendment on Fertility of a Southeastern Coastal Plain Soil. *Soil Science* **2009,** 174, (2).
15. Joseph, S.; Peacocke, C.; Lehmann, J.; Munroe, P., Developing a Biochar Classification and Test Methods. In *Biochar for Environmental Management Science and Technology*, Lehmann, J.; Joseph, S., Eds. Earthscan: London, 2009.
16. Preston, C. M.; Schmidt, M. W. I., Black (pyrogenic) carbon: a synthesis of current knowledge and uncertainties with special consideration of boreal regions. *Biogeosciences* **2006,** 3, 397-420.
17. Schmidt, M. W. I.; Noack, A. G., Black carbon in soils and sediments: analysis, distribution, implications and current challenges. *Global Biogeochemical Cycles* **2000,** 14, 777-793.
18. Antal, M. J.; Allen, S. G.; Dai, X.; Shimizu, B.; Tam, M. S.; Gronli, M., Attainment of the theoretical yield of carbon from biomass. *Ind. Eng. Chem. Res.* **2000,** 39, (11), 4024-4031.
19. Cheng, C.-H.; Lehmann, J.; Thies, J. E.; Burton, S. D.; Engelhard, M. H., Oxidation of black carbon by biotic and abiotic processes. *Organic Geochemistry* **2006,** 37, (11), 1477-1488.
20. Sharma, R. K.; Wooten, J. B.; Baliga, V. L.; Lin, X.; Geoffrey Chan, W.; Hajaligol, M. R., Characterization of chars from pyrolysis of lignin. *Fuel* **2004,** 83, (11-12), 1469-1482.
21. Czimczik, C. I.; Preston, C. M.; Schmidt, M. W. I.; Werner, R. A.; Schulze, E.-D., Effects of charring on mass, organic carbon, and stable carbon isotope composition of wood. *Organic Geochemistry* **2002,** 33, (11), 1207-1223.
22. Knicker, H.; Totsche, K. U.; Almendros, G.; González-Vila, F. J., Condensation degree of burnt peat and plant residues and the reliability of solid-state VACP MAS 13C NMR spectra obtained from pyrogenic humic material. *Organic Geochemistry* **2005,** 36, (10), 1359-1377.
23. Knicker, H.; Hilscher, A.; González-Vila, F. J.; Almendros, G., A new conceptual model for the structural properties of char produced during vegetation fires. *Organic Geochemistry* **2008,** 39, (8), 935-939.
24. Solum, M. S.; Pugmire, R. J.; Grant, D. M., Carbon-13 solid-state NMR of Argonne-premium coals. *Energy & Fuels* **1989,** 3, (2), 187-193.
25. Kelemen, S. R.; Afeworki, M.; Gorbaty, M. L.; Sansone, M.; Kwiatek, P. J.; Walters, C. C.; Freund, H.; Siskin, M.; Bence, A. E.; Curry, D. J.; Solum, M.; Pugmire, R. J.; Vandenbroucke, M.; Leblond, M.; Behar, F., Direct Characterization of Kerogen by X-ray and Solid-State 13C Nuclear Magnetic Resonance Methods. *Energy & Fuels* **2007,** 21, (3), 1548-1561.
26. Smernik, R. J.; Oades, J. M., The use of spin counting for determining quantitation in solid state 13C NMR spectra of natural organic matter: 2. HF-treated soil fractions. *Geoderma* **2000,** 96, (3), 159-171.
27. Simpson, M. J.; Hatcher, P. G., Determination of black carbon in natural organic matter by chemical oxidation and solid-state 13C nuclear magnetic resonance spectroscopy. *Organic Geochemistry* **2004,** 35, (8), 923-935.

28. Mao, J. D.; Hu, W. G.; Schmidt-Rohr, K.; Davies, G.; Ghabbour, E. A.; Xing, B., Quantitative characterization of humic substances by solid-state carbon-13 nuclear magnetic resonance. *Soil Sci Soc Am J* **2000,** 64, (3), 873-884.
29. Hammes, K.; Smernik, R. J.; Skjemstad, J. O.; Schmidt, M. W. I., Characterisation and evaluation of reference materials for black carbon analysis using elemental composition, colour, BET surface area and 13C NMR spectroscopy. *Applied Geochemistry* **2008,** 23, (8), 2113-2122.
30. Mao, J. D.; Schmidt-Rohr, K., Accurate quantification of aromaticity and nonprotonated aromatic carbon fraction in natural organic matter by 13C solid-state nuclear magnetic resonance. *Environ. Sci. Technol.* **2004,** 38, (9), 2680-2684.
31. Laird, D.; Fleming, P.; Wang, B.; Horton, R.; Karlen, D. L., Impact of Soil Biochar Applications on Nutrient Leaching. In *2008 GSA-SSSA-ASA-CSA Joint Meeting*, Houston, TX, 2008.
32. Meehan, P. M.; Jones, S. T.; Brown, R. C., Feedstock potassium as a gasification promoter. *Submitted to Biomass and Bioenergy* **2009**.
33. Mao, J.-D.; Hu, W.-G.; Schmidt-Rohr, K.; Davies, G.; Ghabbour, E. A.; Xing, B., Quantitative characterization of humic substances by solid-state carbon-13 nuclear magnetic resonance. *Soil Science Society of American Journal* **2000,** 64, 873-884.
34. Mao, J. D.; Schmidt-Rohr, K., Recoupled long-range C-H dipolar dephasing in solid-state NMR, and its use for spectral selection of fused aromatic rings. *Journal of Magnetic Resonance* **2003,** 162, (1), 217-227.
35. Mao, J.; Holtman, K. M.; Scott, J. T.; Kadla, J. F.; Schmidt-Rohr, K., Differences between Lignin in Unprocessed Wood, Milled Wood, Mutant Wood, and Extracted Lignin Detected by 13C Solid-State NMR. *Journal of Agricultural and Food Chemistry* **2006,** 54, (26), 9677-9686.
36. Scala, F.; Chirone, R.; Salatino, P., Combustion and Attrition of Biomass Chars in a Fluidized Bed. *Energy & Fuels* **2006,** 20, (1), 91-102.
37. Downie, A.; Crosky, A.; Munroe, P., Physical Properties of Biochar. In *Biochar for Environmental Management Science and Technology*, Lehmann, J.; Joseph, S., Eds. Earthscan: London, 2009.
38. LindstroÌm, E.; OÌhman, M.; Backman, R.; BostroÌm, D., Influence of Sand Contamination on Slag Formation during Combustion of Wood Derived Fuels. *Energy & Fuels* **2008,** 22, (4), 2216-2220.
39. Mann, A. l.; Patience, R. l.; Poplett, I. J. F., Determination of molecular structure of kerogens using 13C NMR spectroscopy: I. The effects of variation in kerogen type. *Geochimica et Cosmochimica Acta* **1991,** 55, (8), 2259-2268.
40. Wei, Z.; Gao, X.; Zhang, D.; Da, J., Assessment of Thermal Evolution of Kerogen Geopolymers with Their Structural Parameters Measured by Solid-State 13C NMR Spectroscopy. *Energy & Fuels* **2005,** 19, (1), 240-250.
41. Kaal, J.; Brodowski, S.; Baldock, J. A.; Nierop, K. G. J.; Cortizas, A. M., Characterisation of aged black carbon using pyrolysis-GC/MS, thermally assisted hydrolysis and methylation (THM), direct and cross-polarisation 13C nuclear magnetic resonance (DP/CP NMR) and the benzenepolycarboxylic acid (BPCA) method. *Organic Geochemistry* **2008,** 39, (10), 1415-1426.

42. McClelland, J. F.; Jones, R. W.; Luo, S.; Seaverson, L. M., A Practical Guide to FT-IR Photoacoustic Spectroscopy. In *Practical Sampling Techniques for Infrared Analysis*, Coleman, P. B., Ed. CRC Press: Boca Raton, FL, 1993.
43. Jiang, Y. J.; Solum, M. S.; Pugmire, R. J.; Grant, D. M.; Schobert, H. H.; Pappano, P. J., A new method for measuring the graphite content of anthracite coals and soots. *Energy & Fuels* **2002,** 16, (5), 1296-1300.

CHAPTER 4. EXTENT OF PYROLYSIS IMPACTS ON FAST PYROLYSIS BIOCHAR PROPERTIES

A paper published by the *Journal of Environmental Quality*

Catherine E. Brewer, Yan-Yan Hu, Klaus Schmidt-Rohr, Thomas E. Loynachan, David A. Laird, Robert C. Brown

Abstract

A potential concern about the use of fast pyrolysis rather than slow pyrolysis biochars as soil amendments is that they may contain high levels of bioavailable C due to short particle residence times in the reactors, which could reduce the stability of biochar C and cause nutrient immobilization in soils. To investigate this concern, three corn stover fast pyrolysis biochars prepared using different reactor conditions were chemically and physically characterized to determine their extent of pyrolysis. These biochars were also incubated in soil to assess their impact on soil CO_2 emissions, nutrient availability, microorganism population growth, and water retention capacity. Elemental analysis and quantitative solid-state ^{13}C nuclear magnetic resonance spectroscopy (NMR) showed variation in O functional groups (associated primarily with carbohydrates) and aromatic C, which could be used to define extent of pyrolysis. A 24-week incubation performed using a sandy soil amended with 0.5 wt% of corn stover biochar showed a small but significant decrease in soil CO_2 emissions and a decrease in the bacteria: fungi ratios with extent of pyrolysis. Relative to the control soil, biochar-amended soils had small increases in CO_2 emissions and extractable nutrients, but similar microorganism populations, extractable NO_3 levels, and water retention capacities. Corn stover amendments, by contrast, significantly increased soil CO_2 emissions and microbial populations, and reduced extractable NO_3. These results indicate that C in fast pyrolysis biochar is stable in soil environments and will not appreciably contribute to nutrient immobilization.

Abbreviations: CP, cross polarization; DP, direct polarization; FC/V, fixed carbon to volatiles ratio; MAS, magic angle spinning; NMR, nuclear magnetic resonance spectroscopy; TGA, thermogravimetric analysis.

4.1 Introduction

Biochar is attracting considerable attention as a potential soil amendment for enhancing soil quality[1] and as a means of sequestering photosynthetically fixed C in soils for hundreds or thousands of years.[2] Most of the research on the use of biochar as a soil amendment has been conducted using biochar produced by slow pyrolysis. The economic viability of slow pyrolysis is questionable, however, because only relatively low-value heat and electrical power are potential co-products of slow pyrolysis.[3] Fast pyrolysis, by contrast, is optimized for the production of bio-oil, which can be upgraded to high-value liquid transportation fuels or processed into a variety of organic chemicals. Fast pyrolysis processes typically produce 10-30% biochars on a feedstock weight basis; these biochars contain 15 to 40% of the C and nearly all of the mineral (ash) content of the original biomass. Use of the biochar co-product of bioenergy production as a soil amendment has been proposed as a means of enhancing soil quality, sequestering C, and returning nutrients to soils, thereby making the harvesting of biomass for bioenergy production more sustainable.[4] Before fast pyrolysis biochars are applied to soils, however, more information about their properties in relation to slow pyrolysis biochars is desirable.

Biochar properties and soil responses vary considerably with biochar feedstock and processing conditions. For example, in a study of the impacts of 16 different biochars on greenhouse gas emissions from three different soils, Spokas and Reicosky[5] found that soil response was both biochar and soil-dependent, although they were not able to specifically correlate greenhouse gas flux with feedstock type, pyrolysis temperature, composition or surface area of the biochars available. Two previous studies in our lab have shown that biochars from fast pyrolysis and gasification of switchgrass (*Panicum virgatum*) and corn (*Zea mays*) stover have

very different properties compared to biochars derived from slow pyrolysis of hardwoods.[6, 7]

One biochar property of interest is C bioavailability. Biochars that contain high levels of bioavailable C could decrease crop yields due to N immobilization[8-10] and would be less effective for C sequestration.[11-13] For slow pyrolysis biochars, where variation in temperature within particles during pyrolysis is small due to the long particle residence times, the highest temperature reached during pyrolysis is believed to play a key role in the chemistry and bioavailability of biochar C.[14, 15] In a study of the bioavailability of C in red pine biochars, Baldock and Smernik (2002) found that heating the wood above 200°C in a limited oxygen environment decreased the C mineralization rate by an order of magnitude.[11] For fast pyrolysis biochars, heat transfer rates and particle residence times may be as important as peak reactor temperature. Heat transfer limitations may cause the outer part of the particles to reach a higher temperature than the core and create biochars that are fully carbonized only on the outside.[16, 17] Hence, material in the core of fast pyrolysis biochar particles may be dominated by torrified biopolymers rather than the condensed aromatic C structures believed to stabilize biochar-C against microbial degradation in soils.[13]

Information on the soil application effects and stability of fast pyrolysis biochars is currently very limited. A preliminary three year field experiment by BlueLeaf Inc. (Drummondville, Quebec, Canada) found that soybean and forage plant biomass yields were higher from a single plot amended with approximately 3.9 Mg ha^{-1} hardwood waste CQuest® fast pyrolysis biochar (Dynamotive Energy Systems Coorporation, West Lorne, Ontario, Canada) than from an adjacent unamended plot (Husk and Major, 2011, unpublished data). No indicators of N immobilization were reported. A biochar characterization and soil incubation study using wheat straw biochars made at different temperatures by a fast pyrolysis centrifuge reactor found labile carbohydrates (unreacted cellulose and hemicellulose) in the biochars made at

lower reactor temperatures.[17] Biochar C losses, as measured by soil surface CO_2 fluxes from biochar-amended soils, were relatively high (3-12%) after 115 days and were found to be inversely related to pyrolysis reactor temperature and biochar labile carbohydrate content. The authors concluded that the relative ease of degradability of the fast pyrolysis biochars compared to slow pyrolysis biochars made at similar temperatures (475-575°C) was due to the specific design of the fast pyrolyzer and the short residence times.[17]

The overall goal of this study was to fit fast pyrolysis biochars into a larger biochar property framework using *extent of pyrolysis*, analogous to the already widely used *peak reactor temperature* for slow pyrolysis biochars. The specific objectives of this study were 1) to evaluate chemical and physical properties of corn stover fast pyrolysis biochars that had been noticeably affected by reactor conditions, and 2) to quantify the impact of these biochars on CO_2 emissions, extractable soil nutrients, water retention, and microbial populations of an amended sandy soil. We hypothesized that 1) the extent of pyrolysis for fast pyrolysis biochars depends on reactor heating rate and particle residence times in addition to reactor temperature, 2) fast pyrolysis biochar with a low extent of pyrolysis (as determined by chemical properties) contain bioavailable C that will, when used as a soil amendment, increase CO_2 emissions, microorganism population growth, and N immobilization relative to biochar with a high extent of pyrolysis, and 3) amending a sandy soil with fast pyrolysis biochar will increase extractable soil nutrients and water retention capacity.

4.2 Materials and Methods

4.2.1 Biochar Production

Corn (*Zea mays*) stover was harvested locally (Story County, IA), dried to <10% moisture, and ground using a hammer mill to pass a 6 mm (¼") sieve. Three corn stover fast pyrolysis biochars were derived from this feedstock and produced on reactors at Iowa State University's Center for Sustainable Environmental

Technologies. The pyrolysis reaction parameters are listed in Table 9. The reaction temperatures refer to the reactor settings rather than the temperatures reached by the particles during pyrolysis; this is especially important for Biochars 1 and 2, which were produced under conditions that did not allow for sufficient heat transfer time on a free fall fast pyrolyzer.[18] Biochar 3 was produced in a fluidized bed fast pyrolyzer with higher heat transfer rates.[19]

Table 9. Fast pyrolysis reaction conditions and char properties of the corn stover biochars.

Biochar #	**1**	**2**	**3**
Reactor configuration	Free fall	Free fall	Fluidized bed
Reactor temperature (°C)[a]	500	600	500
Feed rate (kg/hr)	0.5	0.5	5
Feedstock particle size (µm)	500	500	6000

[a] Reactor temperature is not necessarily the temperature reached by the chars during pyrolysis; this is especially important for Biochars 1 and 2.

4.2.2 Biochar Characterization

Biochar characterization followed methods previously described.[6] Briefly, moisture, volatiles, fixed C, and ash content of the biochars were determined by a standard proximate (thermogravimetric) analysis method, ASTM D1762-84.[20] Elemental analysis was performed using TRUSPEC-CHN and TRUSPEC-S analyzers (LECO Corporation, St. Joseph, MI). Oxygen content was determined by difference. Surface area (BET) was estimated by nitrogen gas sorption analysis at 77K (NOVA 4200e, Quantachrome Instruments, Boynton Beach, FL). Particle density was measured by helium pycnometer (Pentapycnometer, Quantachrome Instruments, Boynton Beach, FL).

Solid-state ^{13}C nuclear magnetic resonance spectroscopy (NMR) experiments were performed on a Bruker DSX400 spectrometer (Bruker Biospin, Karlsruhe, Germany) at 100 MHz for ^{13}C and 400 MHz for ^{1}H. Qualitative corn stover and biochar spectra were obtained using ^{13}C cross polarization magic angle spinning with total suppression of spinning sidebands (CP/MAS/TOSS); samples were analyzed in 7-mm MAS rotors at a spinning speed of 7 kHz with 0.5 s recycle delay,

4 µs ^{1}H 90° pulse length and 1 ms CP contact time. Quantitative biochar spectra were obtained using ^{13}C direct polarization (Bloch decay) magic angle spinning (DP/MAS) NMR in 4-mm MAS rotors at a spinning speed of 14 kHz with 75 s recycle delay, 4.5 µs 90° ^{13}C pulse length, and a Hahn echo to avoid baseline distortions.[21] A spectrum with a longer recycle delay (280 s) showed no meaningful intensity increase for any of the main peaks, proving that the magnetization was fully relaxed after 75 s. To acquire the spectra of the non-protonated C fraction, DP/MAS with recoupled ^{1}H-^{13}C dipolar dephasing was used (68 µs dephasing time).[21]

4.2.3 Soil Incubation

The soil used was the A horizon of a Sparta (sandy, mixed, mesic Entic Hapludoll) loamy fine sand (87.6% sand, 8.7% silt, 3.7% clay), collected on September 10, 2009 from a hill (9-14% slope) near Ames, Iowa (41.994° N, 93.558°W). The soil was passed through a 2 mm sieve and visible root biomass was removed by hand. Soil moisture was 4 wt % on an oven dry basis; soil moisture measured by pressure plate [22] at -33 kPa soil water matric potential was 7 wt %.

Incubations were performed in glass, pint-size (0.47 L) canning jars with sealable lids. To each jar was added 100 g of 110°C dry-weight-equivalent soil, 0.5 g of oven dry (110°C) corn stover or biochar amendment (approximately 11 Mg ha^{-1}). Sterile nutrient solution (6.0 mL) containing $(NH_4)_2SO_4$ (5.5×10^{-4} mol L^{-1}) and KH_2PO_4 (5.5×10^{-5} mol L^{-1}) was also added so as to achieve a soil moisture level of 10 wt % on an oven dry basis, a maximum C:N ratio of 30:1 (assuming <40% C content in the amendments) and an N:P ratio of 10:1. The control received the nutrient solution but no amendment. There were nine replicates for each of the five treatments (Biochar 1, Biochar 2, Biochar 3, Stover and Control) and a total of 45 jars. Samples were incubated in the dark at 23°C for 24 weeks. At 8 weeks, three replicate jars from each treatment were destructively sampled for microbial population and soil property analyses; the incubation was then continued with the remaining 6 jars for each treatment. Evolved CO_2 was trapped using a vial containing 30 mL of standardized

NaOH (1 mol L^{-1}) solution in each of the sealed jars. The amount of CO_2 evolved was measured by first precipitating any dissolved CO_2 with 25 ml of $BaCl_2$ (2 mol L^{-1}), then titrating the solution to the phenolphthalein endpoint with standardized HCl (1 mol L^{-1}). Jars were left open during the titration to ensure sufficient exchange of air. Prior to resealing, a fresh aliquot of NaOH was added to the vial in each jar and the soil moisture readjusted to 10% by addition of distilled water.

4.2.4 Soil Testing

Soil pH was measured at a 1:5 soil to water ratio. Soil water retention was measured at -33 kPa and -500 kPa soil water matric potentials using the pressure plate method to estimate plant-available water. All other soil analyses were performed using standard soil methods (Bray P, ammonium acetate and Mehlich III extractable cations, total N and total C by combustion, and inorganic N by colorimetry) by the Soil and Plant Analysis Laboratory (Iowa State University, Ames, IA).

4.2.5 Enumeration of Microbial Populations

Microbial populations were estimated by a pour plate method following generally accepted recovery and enumeration practices.[23] Soil dilutions were made using sterile physiological saline solution (0.85% NaCl) and manual shaking (20 repetitions) for dispersion. Fungi were cultured at three dilutions (10^{-3}, 10^{-4} and 10^{-5}) with two replicates each on Martin's medium, a peptone dextrose agar containing rose bengal (30 mg/L) and streptomycin (30 µg/L) to limit bacterial growth.[24] Bacteria (including actinomycetes) were cultured at three dilutions (10^{-4}, 10^{-5}, 10^{-6}) with two replicates each on a tenth strength tryptic soy agar (Difco, BD, Sparks, MD). Plates containing 20-200 colonies were counted after 9 days of incubation at 23°C.

4.2.6 Statistics

The experimental set-up followed a completely randomized design. Statistical significance was determined at a 95% confidence level ($p<0.05$) using single factor ANOVA and Tukey's honest significant difference (HSD) test.

4.3 Results

4.3.1 Biochar Physical and Chemical Properties

The results of the corn stover biochar characterizations are shown in Table 10. Note the low C content and high ash content of the biochars; this is due to the high mineral (especially relatively inert silica) content of corn stover and the partitioning of most of the C from the feedstock into the liquid bio-oil fraction during fast pyrolysis. Molar H/C and O/C ratios of the amendments decreased (see Figure 23) and fixed C/volatiles ratios (see Table 10) increased in the order of Stover, Biochar 1, Biochar 2, and Biochar 3. This order was used as the amendments' relative extent of pyrolysis, from least pyrolyzed to most pyrolyzed. All BET surface areas were very low, < 9 m^2 g^{-1} (Table 10).

Table 10. Composition and physical properties of corn stover and corn stover fast pyrolysis biochars (n=3 for proximate and CHNS analyses; surface area and particle density were single measurements). Proximate analysis data reported on a wet basis; CHNOS data is on a dry basis. ND = not determined.

	Corn stover	**Biochar 1**	**Biochar 2**	**Biochar 3**
Moisture (g/kg)	37	25	18	17
Volatiles (g/kg)	726	262	171	138
Fixed carbon (g/kg)	102	249	254	252
Ash (g/kg)	135	464	557	593
Dry Ash (g/kg)	140	476	567	603
C (g/kg)	405	349	314	295
H (g/kg)	61	29	20	16
N (g/kg)	7	7	6	6
S (g/kg)	N.D.	0.6	0.3	0.2

O (g/kg by difference)	387	139	92	79
H/C molar ratio	1.81	0.99	0.77	0.63
O/C molar ratio	0.72	0.30	0.22	0.20
C/N molar ratio	68	51	54	46
Fixed carbon/volatiles	0.14	0.95	1.49	1.83
BET surface area (m^2/g)	N.D.	4.5	3.3	8.5
Particle density (g/cm^3)	N.D.	1.78	1.88	2.06

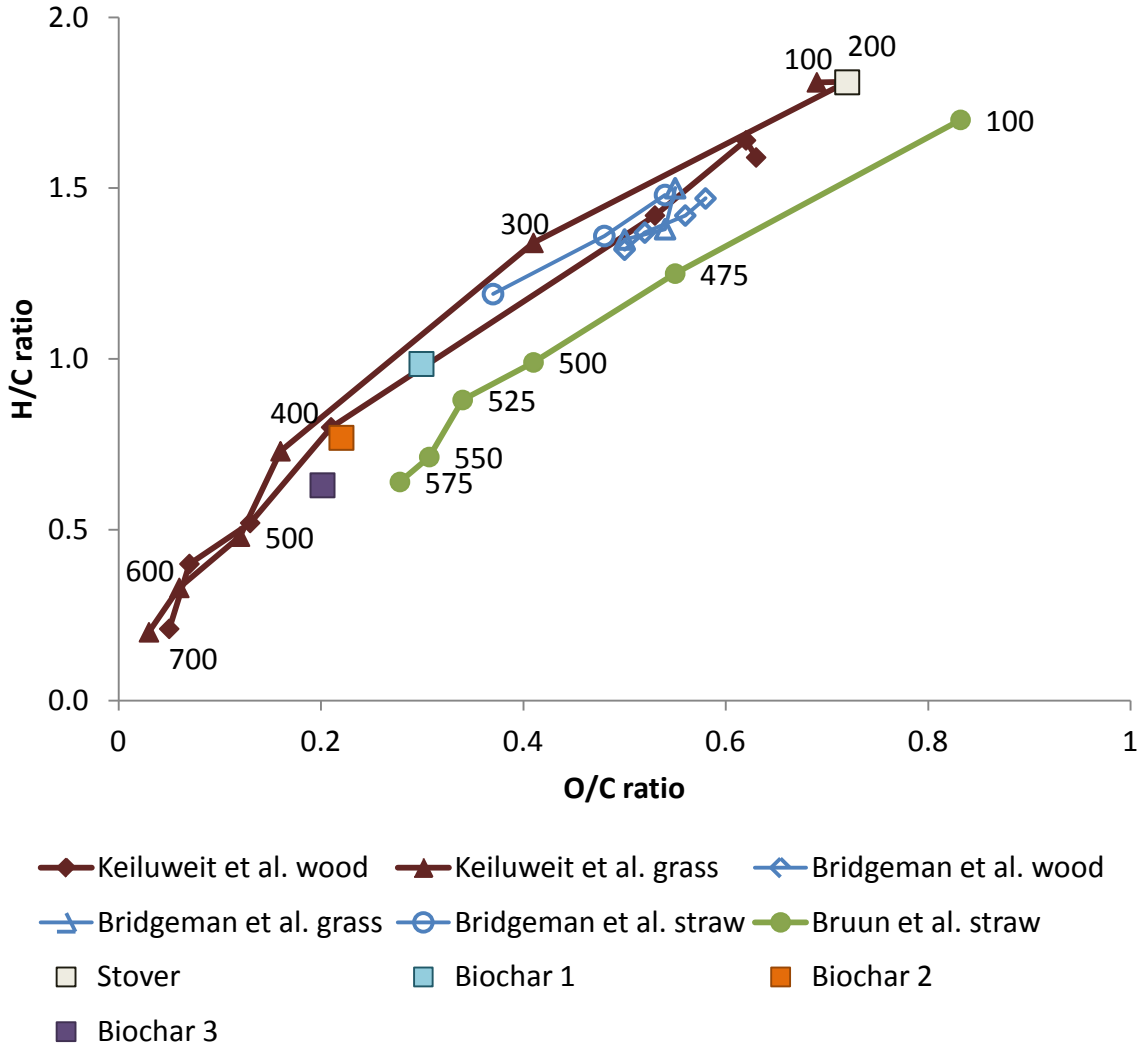

Figure 23. Van Krevelen plot of corn stover and corn stover fast pyrolysis biochars used in this study, as well as willow wood, reed canary grass and wheat straw torrefaction chars made over 230-290°C temperature range,[25] red pine chars made under limited oxygen slow

pyrolysis conditions,[11] and pine wood and fescue grass slow pyrolysis chars made at different temperatures.[15] Numbers listed are reactor temperatures (°C).

The qualitative CP/TOSS NMR spectra in Figure 24 clearly show the transition from C associated with cellulose and lignin present in the biomass to aromatic C associated with biochar as the extent of pyrolysis increases. Biochar 1 in particular has a large ~75 ppm (Hz MHz^{-1}) peak indicative of O-alkyl-C; its small width and the other sharp peaks near 106, 88, 85 and 65 ppm show that residual cellulose is present. This indicates that a part of Biochar 1, probably at the core of the particles, had not undergone sufficient thermal transformation.

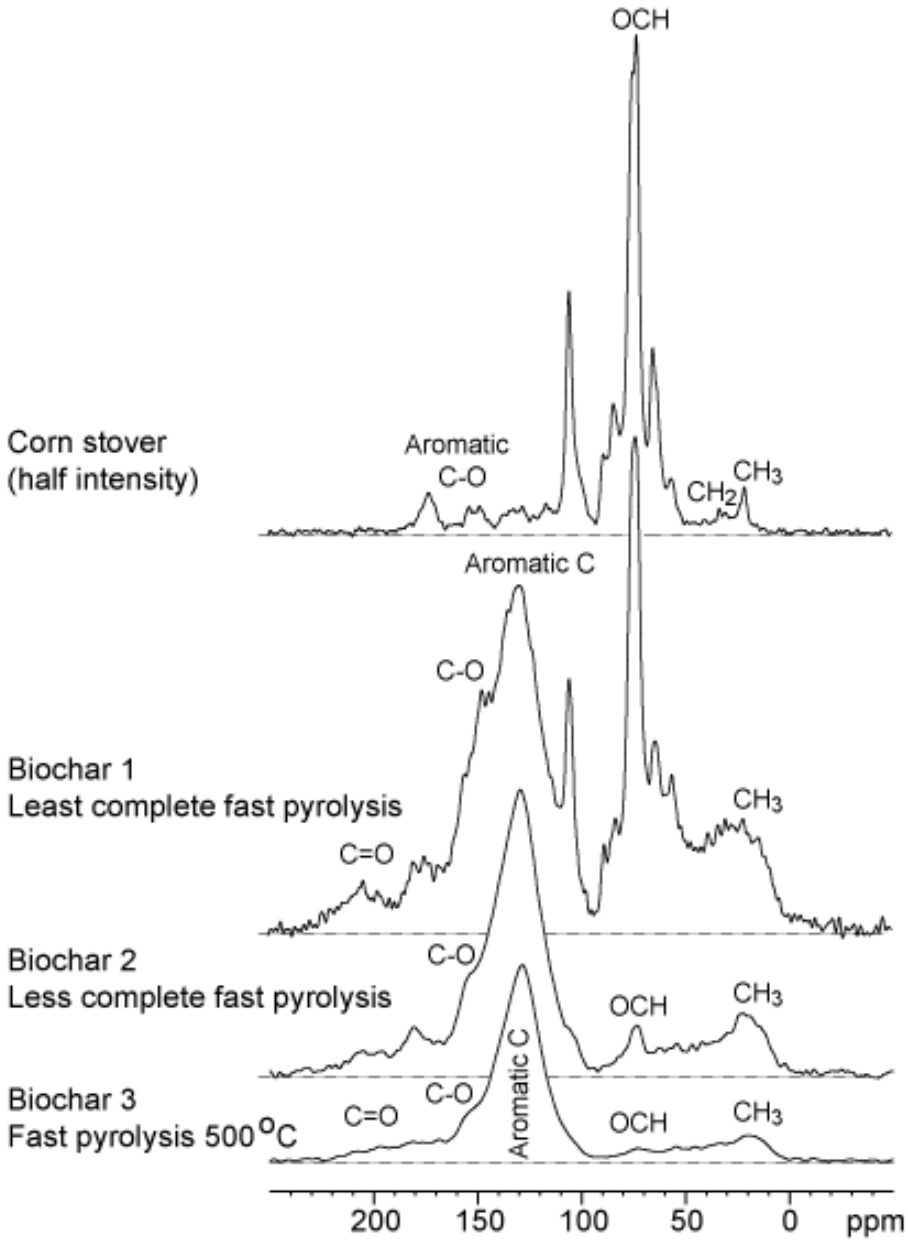

Figure 24. Qualitative carbon spectra of corn stover and corn stover biochars by solid-state ^{13}C cross polarization magic angle spinning with total suppression of spinning sidebands (CP/MAS/TOSS) nuclear magnetic resonance spectroscopy (NMR). OCH = alcohol and ether moieties.

The quantitative DP/MAS NMR spectra for all C (thick lines) and non-protonated C (thin lines) in the biochars are shown in Figure 25. All three biochars contained measurable amounts of non-protonated aromatic C as part of the overall aromatic C fraction, indicating the presence of condensed aromatic ring structures (peak at

~127 ppm in the thin-line DP/MAS with recoupled ^{1}H-^{13}C dipolar dephasing spectra). Carbon composition and aromaticity of the biochars by spectral integration are detailed in Table 11. The composition and aromaticities of the biochars were consistent with their relative extents of pyrolysis: Biochar 1 contained the most aliphatic and oxygenated C functional groups while Biochar 3 contained the most aromatic C and highest fraction of non-protonated C. The composition of Biochar 2 was intermediate.

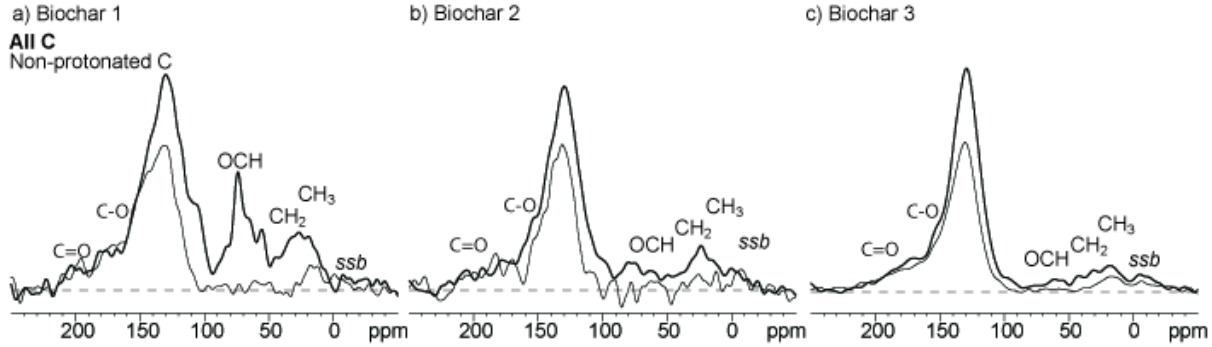

Figure 25. Quantitative solid-state ^{13}C NMR spectra of corn stover biochars, obtained with direct polarization under 14 kHz magic angle spinning (DP/MAS): a) Biochar 1 (lowest extent of pyrolysis), b) Biochar 2 (intermediate extent of pyrolysis), c) Biochar 3, fast pyrolysis at 500°C (highest extent of pyrolysis). Thick-line spectra: all C; corresponding thin-line spectra: non-protonated C and CH_3. *ssb* = spinning side band.

Table 11. Composition and aromaticity of C fraction in biochars by quantitative solid-state ^{13}C direct polarization magic angle spinning (DP/MAS) nuclear magnetic resonance spectroscopy (NMR). Values are % of total ^{13}C signal. $C_{non\text{-}pro}$ = non-protonated aromatic C. Integration included primary and secondary aromatic spinning side bands.

Moiety:	**Carbonyl**		**Aromatic**			**Alkyl**		
Range (ppm):	**C=O 210-183**	**COO 183-165**	**$CO_{0.75}H_{0.5}$ 165-145**	**$C_{non\text{-}pro}$ 145 – 90**	**C-H**	**$HCO_{0.75}H_{0.5}$ 90-50**	**$CH_{1.5}$ 50-25**	**CH_3 25-6**
Corn stover[a]	0	5	5	5	10	68	5	4
Biochar 1	4	5	11	30	18	19	7	6
Biochar 2	4	4	11	39	24	8	5	5
Biochar 3	3	5	12	44	25	3	4	4
	Aromaticity							
Corn stover[a]	20							
Biochar 1	59							
Biochar 2	74							
Biochar 3	81							

[a]Fang et al, 2010[26]

4.3.2 CO_2 Evolution from Amended Soils

The rates of CO_2 evolution (in mg CO_2-C per 100 g soil per day) from the soils are shown in Figure 26. For all treatments, the amount of microbial respiration was greatest in the first week and decreased thereafter. Evolution rate differences between all of the treatments were statistically significant in the first week. Rates of CO_2 evolution decreased with extent of pyrolysis as defined by amendment C characteristics: Stover > Biochar 1 > Biochar 2 > Biochar 3 > Control. This relationship continued in the weeks that followed (with varying degrees of statistical significance). An analytic error when measuring trapped CO_2 for Biochar 2-amended soils on day 56 resulted in that data point being excluded.

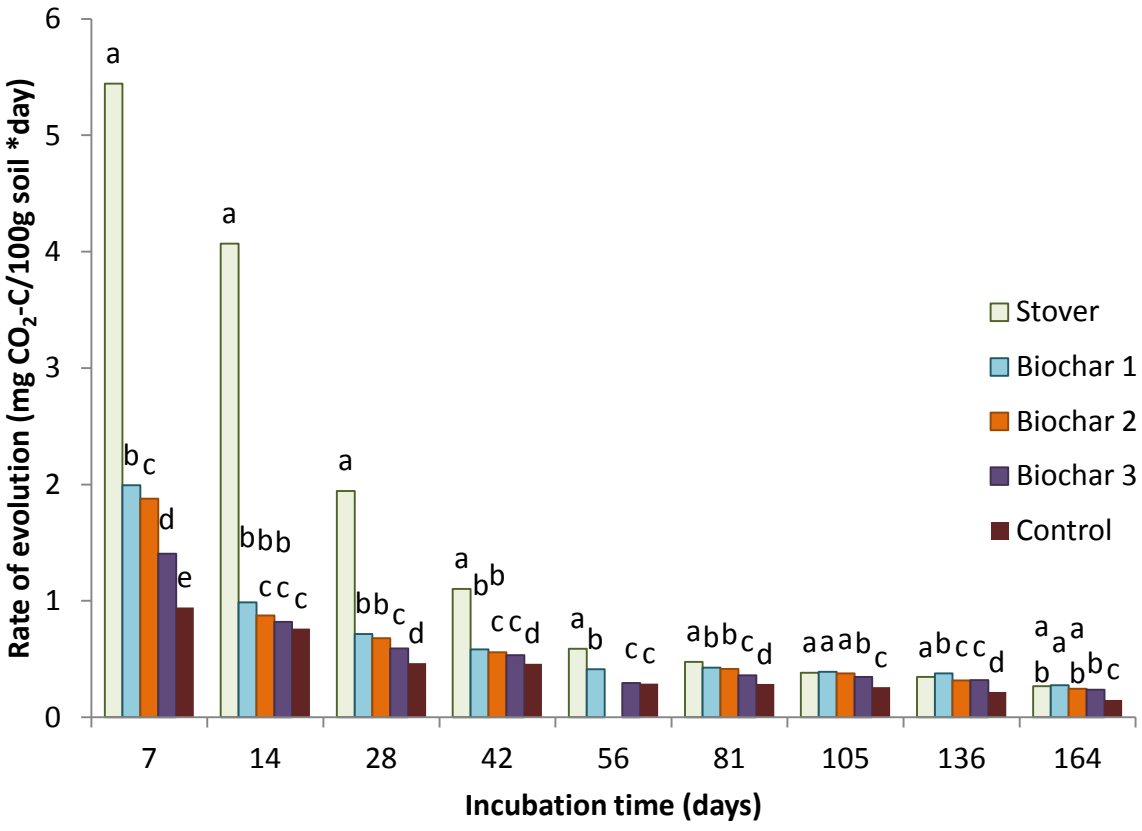

Figure 26. Rate of CO_2 evolution from control and amended soils over 24-week incubation. Rates measured on the same day that are marked with a different letter are significantly different ($p<0.05$).

4.3.3 Soil Chemical Properties

Soil chemical properties of replicates destructively sampled on day 56 are shown in Table 12. No significant differences in organic matter, total N, Na, Mg or Ca contents were observed in the amended soils. All amendments slightly increased soil pH and decreased plant-available NO_3-N and NH_4-N, though only the decreases in NO_3-N in the Stover, and the NH_4-N in the Biochar 1 and Biochar 2 were statistically significant. Bray P increased with all three biochar amendments. Available K increased significantly for all amendments but more with the biochars than with the corn stover. Finally, Mehlich III-extractable Al increased with Stover and Biochar 3, extractable Fe increased for all biochars, and extractable Mn increased for all amendments relative to the controls.

Table 12. Soil properties of corn stover and biochar-amended soils after 8 weeks of incubation. pH was measured in water (1:5 ratio). Base (K, Na, Mg, Ca) content was determined by ammonium acetate extraction; trace metal (Al, Fe, Mn) content was determined by Mehlich III extraction. Entries in a column followed by different letters are significantly different (n = 3, $p<0.05$).

Soil treatment	**Soil pH**	**Organic matter**	**Total N**	**NO_3 N**	**NH_4 N**	**Bray P**	**K**
		--g/kg--			--mg/kg--		
Control	5.9 a	17 a	1.268 a	84 a	3.7 a	37 a	96 a
Stover	6.1 bc	19 a	1.087 a	62 b	3.3 a	34 a	117 b
Biochar 1	6.1 bc	18 a	1.205 a	81 a	2.7 b	45 b	160 d
Biochar 2	6.0 ab	20 a	1.242 a	78 a	2.0 c	42 b	154 cd
Biochar 3	6.1 c	19 a	1.145 a	76 a	3.3 a	41b	140 c
	Na	**Mg**	**Ca**	**Al**	**Fe**	**Mn**	
	--mg/kg--						
Control	20 a	119 a	1146 a	178 a	58 a	36 a	
Stover	23 a	127 a	1184 a	224 ab	60 a	39 b	
Biochar 1	21 a	137 a	1162 a	209 a	70 b	40 b	
Biochar 2	21 a	132 a	1164 a	187 a	69 b	39 b	
Biochar 3	22 a	138 a	1229 a	295 b	67 b	40 b	

4.3.4 Soil Water Retention Capacity

Water retention capacities of the control and amended soils are shown in Figure 27. At the low tension (-33 kPa), none of the amendments significantly increased the soil water retention. Under drier conditions (-500 kPa tension), most of the amended soils had slightly higher soil moisture levels than the control, however, only the Stover-amended soil was significant higher than the control (8% relatively).

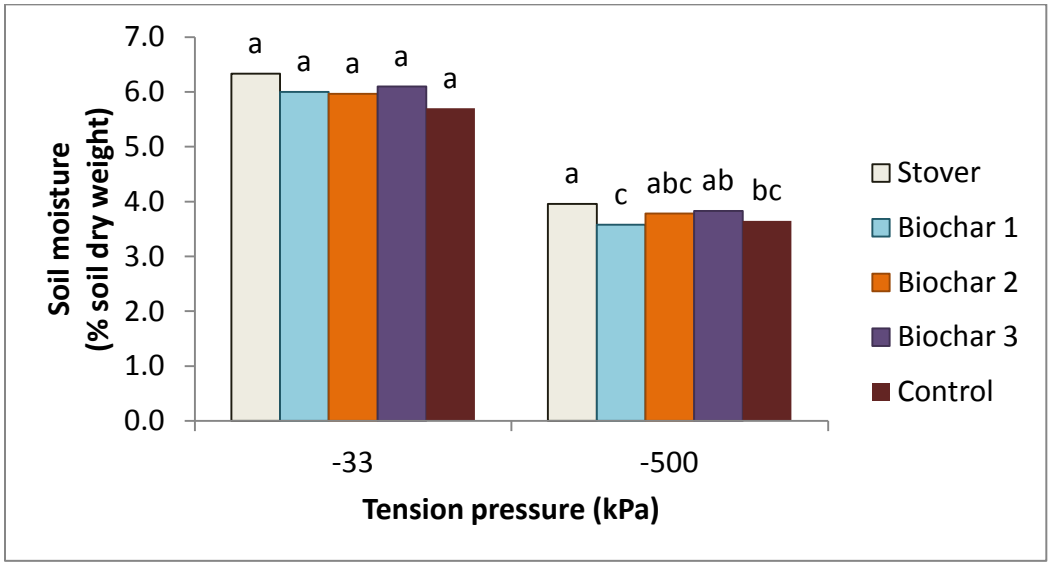

Figure 27. Soil water retention of control and amended soils measured over matric potentials representing plant-available water. Columns labeled with different letters are significantly different ($p<0.05$).

4.3.5 Enumeration of Microbial Populations

The estimates of soil microbial populations based on dilution plate counts are listed in Table 13. The soil amended with the corn stover had the highest populations of both fungi and bacteria. Fungi populations in the biochar-amended soils tended to increase with extent of pyrolysis but were not significantly different from those in the control. Populations of bacteria tended to decrease with extent of pyrolysis; however, only the population in the Biochar 3-amended soil was significantly lower from the control soil. Population ratios of bacteria to fungi were high in the control, low in the corn stover-amended soil, and decreased with extent of pyrolysis in the biochar-amended soils.

Table 13. Populations of microorganisms in control and amended soils based on pour plate counts (means ± SD, n=6). Bacteria colony counts include actinomycetes colonies. Data within a column followed by a different letter are significantly different ($p<0.05$).

Soil treatment	Fungi	Bacteria	Bacteria: fungi ratio
	colonies /g soil	colonies /g soil	colonies/colony
Control	$(6.8 \pm 1.0)*10^4$ b	$(9.9 \pm 1.9)*10^6$ b	148 ± 36 a
Stover	$(31.3 \pm 8.8)*10^4$ a	$(14.0 \pm 2.6)*10^6$ a	47 ± 16 c
Biochar 1	$(6.8 \pm 1.0)*10^4$ b	$(9.8 \pm 1.3)*10^6$ b	145 ± 30 a
Biochar 2	$(7.0 \pm 0.9)*10^4$ b	$(9.1 \pm 1.0)*10^6$ bc	130 ± 10 ab
Biochar 3	$(7.7 \pm 1.2)*10^4$ b	$(8.1 \pm 0.6)*10^6$ c	107 ± 11 b

4.4 Discussion

4.4.1 Extent of Pyrolysis and Apparent Pyrolysis Temperature

Fast pyrolysis biochars can best be compared to other biochars based on their properties and effects when amended to soils. For practical discussions, however, it may be beneficial to define apparent slow pyrolysis temperatures for fast pyrolysis biochars such that their extent of pyrolysis might be more quickly conveyed. Such apparent slow pyrolysis temperatures can be estimated for the biochars in this study using several temperature-property relationships described in the literature. McBeath and Smernik[27] related the degree of aromatic condensation with increasing pyrolysis temperatures for a set of Phalaris grass straw biochars using ^{13}C NMR spectra. The straw biochar made at 250°C has larger alkyl and oxygenated C peaks than those of Biochar 1, suggesting that Biochar 1 achieved a temperature higher than 250°C.The spectrum of the straw char made at 450°C closely resembles that of Biochar 3. Using these spectra, the temperatures reached by the biochars in this study are estimated to be between 250-450°C. A non-spectroscopic method for estimating the extent of pyrolysis compares the relative amounts of volatile and fixed C as determined by proximate or thermogravimetric analysis (TGA). Biochars with higher fixed C/volatiles (FC/V) ratios reached higher slow pyrolysis temperatures and are considered more completely pyrolyzed.[9, 28] FC/V values from pine wood and fescue grass slow pyrolysis biochars used by Keiluweit, et al.[15] range from 0.28-14.6 for slow pyrolysis reaction temperatures ranging from 100-700°C, respectively. Using the fescue grass biochar data, the analogous slow pyrolysis temperatures for Biochars 1, 2 and 3 are estimated to be 350, 375, and 400°C, respectively. Another

non-spectroscopic method for estimating the extent of pyrolysis is evaluation of biochar O/C and H/C molar ratios, most often plotted as a van Krevelen diagram. As the pyrolysis reaction progresses, the removal of H_2O, CO_2, and other small O and H-containing molecules shifts the composition of biochars towards the origin on a van Krevelen plot. Data for slow pyrolysis/torrefaction biochars produced by pyrolysis of fescue grass and pine wood[15] and reed canary grass, wheat straw and willow[25] are shown in Figure 23. Biochars 1, 2 and 3 closely follow the pattern of the Keiluweit et al.[15] data and have apparent slow pyrolysis temperatures of 350, 400, and 450°C.

A series of wheat straw fast pyrolysis biochars from Bruun et al. (2011)[17] is also plotted in Figure 23 (dry wheat straw data is represented as biochar made at a reactor temperature of 100°C). Compared to the Keiluweit et al.[15] data, the apparent slow pyrolysis temperatures for these biochars are estimated to be 300-500°C, well below the actual reactor temperatures of 475-575°C. In general, fast pyrolysis biochars' apparent slow pyrolysis temperatures will be lower than their reactor temperatures but the magnitude of this difference is dependent on the reactor's specific heat transfer rates and particle residence times.

4.4.2 C Sequestration and Soil Respiration Rates

Differences in soil CO_2 emissions between the control and amended soils are commonly used to estimate C mineralization rates and the potential of amendments to enhance soil C sequestration. With respect to biochar, such studies can provide valuable insight into biochar's relative stability but have several drawbacks. Unless isotope labeling[29] or stable C isotopic analysis (i.e. using a succession of C3-C4 plants) are used,[28, 30] it is generally not possible to distinguish CO_2 produced by the mineralization of biochar from CO_2 that comes from the mineralization of soil organic matter or organic residues in the soil. Furthermore, biochar has been reported to accelerate mineralization of soil organic matter[31] and enhance stabilization of organic residues.[28, 32] In this study, use of soil as the inoculation media meant that soil organic matter and mineral interactions were able to occur during the incubation

but also that the source of the CO_2 could not be definitively identified. Even so, the increases in CO_2 emissions for biochar-amended soils relative to the control soil were much smaller than the increase in CO_2 emissions from the stover-amended soil, suggesting that even a low extent of pyrolysis is still highly effective for stabilizing corn stover C.

4.4.3 Changes in Extractable Plant Nutrients with Soil Amendments

The harvesting of agricultural residues for bioenergy production may deplete plant nutrients from soils. During pyrolysis, nearly all of the mineral nutrients in the biomass feedstock and about half of the N and S are concentrated in the biochar fraction.[33] Use of biochar as a soil amendment returns those nutrients to the soil. Key questions, however, are whether the added nutrients are bioavailable and whether fast pyrolysis biochars bind or immobilize plant nutrients that are already in the soil. Here, extractable P, K, Fe, and Mn levels were higher for the biochar-amended soils than the control or stover-amended soils (Table 12), and no differences were observed for extractable bases (Ca, Mg, and Na). Nitrate levels were significantly lower in the stover-amended soils than any of the other soils suggesting that the stover amendments induced N immobilization. Although the control soils had the highest NO_3 levels, they were not significantly different from the NO_3 levels in any of the three biochar-amended soils. Hence, we find evidence that at least some of the nutrients added with the biochar were bioavailable and no evidence of nutrient immobilization resulting from the fast pyrolysis biochar amendments. Most biochars are mild to moderate liming agents due to ash that is admixed with the condensed C in biochars. Here the soil pH increased by only 0.2 pH units for the biochar-amended soils relative to the control soil, so effects of pH on bioavailability of nutrients would be minimal.

4.4.4 Soil Plant-Available Water Capacity

Stover amendments increase soil water retention relative to the control at -500 kPa matric potential but no effects of the biochar amendments on moisture retention

were observed at either -33 or -500 kPa tension (Figure 27). Laird et al. (2010)[33] observed that biochar additions to a typical Midwestern agricultural soil did not significantly affect water retention at -33 kPa or -1500 kPa, but significantly increased soil water retention for mid-range matric potentials (-100 and -500 kPa tension). The observed increases in soil water retention, however, were generally for soils amended with higher surface area chars and at higher rates of 10 or 20 g of biochar per kg of soil. In this study, the amount of biochar amended may not have been high enough to produce a statistically significant effect on soil water retention.

4.4.5 Enumeration of Microbial Populations

Enumeration of microorganism populations by the dilution pour plate technique is widely used, but the technique is not without disadvantages. For example, not all microorganisms can be cultured, not all organisms survive or are detached from other organisms in the dilution process, use of a pour plate is inherently aerobic and automatically excludes obligate anaerobic organisms, and having enough organisms on a plate to achieve a statistically significant count can lead to competition between colonies for energy and nutrients.[23] Furthermore, the high variability among replicate plate counts makes it difficult to detect significant differences in microbial populations. Here, the soils amended with corn stover contained significantly more organisms than the control soils while the biochar-amended soils had comparable microbial populations to those of the control soils (Table 13). We speculate that this was because corn stover supplied readily metabolized C whereas the C in the biochars was recalcitrant.

The apparent shift in microbial populations from bacteria to fungi with increasing extent of pyrolysis (see bacteria: fungi ratios in Table 13) could be the result of several factors and warrants further research. The fungi may be better adapted to survive on recalcitrant aromatic C in biochar. This possibility is supported by Warnock et al.[34] who reported increases in mycorrhizal fungi activity with the addition of biochar to soil. Shifts in soil microbial population from biochar application need to be understood as they may influence soil fertility due to changes in the

availability of nutrients, rates nutrient cycling, soil respiration, and plant health due to differences in populations of beneficial and/or pathogenic organisms.[35]

4.5 Conclusions

Determination of the extent of pyrolysis by more than reactor temperature is needed to make meaningful comparisons between fast pyrolysis and slow pyrolysis biochars derived from a given feedstock. In this study, several biochar chemical properties were observed to describe the extent of pyrolysis for three fast pyrolysis biochars that are consistent with reactor heat transfer rates, particle residence times and temperatures. Proximate analysis, elemental analysis and NMR spectroscopy showed that aromatic C content increased with extent of pyrolysis while O, H and C in functional groups associated with un-reacted biomass (alcohols, ethers, carbonyls and carboxyls) decreased. These trends in C composition were used to estimate an apparent slow pyrolysis temperature for fast pyrolysis biochars so that these biochars might more easily be compared to other biochars in the literature. CO_2 evolution rates from amended soil increased for all amendments and were inversely related to extent of pyrolysis. Rates of CO_2 evolution and microorganism population growth of the biochar-amended soils, however, were much lower than those of the stover-amended soils and addition of biochars did not significantly decrease N availability at 8 weeks. These results demonstrate that C in fast pyrolysis biochar is substantially more stable than C in fresh biomass and that any nutrient immobilization resulting from the use of fast pyrolysis biochars should be minimal. Finally, amending a sandy soil with fast pyrolysis biochar under the conditions used in this study does increase the availability of some soil nutrients, including K and P, but does not affect soil water holding capacity. Overall, the properties of fast pyrolysis biochars reaching a certain extent of pyrolysis show that, from a C stability perspective, these biochars should be safe for soil application, even if their short-term positive impacts on soil may be limited.

Acknowledgements

Funding for this research was provided by a National Science Foundation Graduate Research Fellowship (Brewer). The authors would like to acknowledge the following scientists for their assistance: the students and staff at the Center for Sustainable Environmental Technologies for supplying the biochars and reaction condition information, and for performing CHNS analyses; Dedrick Davis for performing pressure plate soil moisture measurements; and Mostafa Ibrahim for measuring soil texture. The authors would also like to thank anonymous reviewers for their helpful feedback.

Literature Cited

1. Glaser, B.; Lehmann, J.; Zech, W., Ameliorating physical and chemical properties of highly weathered soils in the tropics with charcoal - a review. *Biol. Fertil. Soils* **2002,** 35, (4), 219-230.
2. Woolf, D.; Amonette, J. E.; Street-Perrot, F. A.; Lehmann, J.; Joseph, S., Sustainable biochar to mitigate global climate change. *Nat. Comm.* **2010,** 1, 56.
3. Brown, T. R.; Wright, M. M.; Brown, R. C., Estimating profitability of two biochar production scenarios: slow pyrolysis vs fast pyrolysis. *Biofuel. Bioprod. Bior.* **2011,** 5, (1), 54-68.
4. Laird, D. A., The charcoal vision: A win-win-win scenario for simultaneously producing bioenergy, permanently sequestering carbon, while improving soil and water quality. *Agronomy Journal* **2008,** 100, (1), 178-181.
5. Spokas, K. A.; Reicosky, D. C., Impacts of sixteen different biochars on soil greenhouse gas production. *Ann. Environ. Sci.* **2009,** 3, 179-193.
6. Brewer, C. E.; Schmidt-Rohr, K.; Satrio, J. A.; Brown, R. C., Characterization of biochar from fast pyrolysis and gasification systems. *Environ. Prog. Sustainable Energy* **2009,** 28, (3), 386-396.
7. Brewer, C.; Unger, R.; Schmidt-Rohr, K.; Brown, R., Criteria to select biochars for field studies based on biochar chemical properties. *Bioenergy Res.* **2011,** 4, (4), 312-323.
8. Novak, J. M.; Busscher, W. J.; Watts, D. W.; Laird, D. A.; Ahmedna, M. A.; Niandou, M. A. S., Short-term CO_2 mineralization after additions of biochar and switchgrass to a Typic Kandiudult. *Geoderma* **2010,** 154, (3-4), 281-288.
9. Deenik, J. L.; McClellan, T.; Goro, U.; Antal, M. J.; Campbell, S., Charcoal volatile matter content influences plant growth and soil nitrogen transformations. *Soil Sci. Soc. Am. J.* **2010,** 74, (4), 1259-1270.

10. Gundale, M.; DeLuca, T., Charcoal effects on soil solution chemistry and growth of *Koeleria macrantha* in the ponderosa pine/Douglas-fir ecosystem. *Biol. Fertil. Soils* **2007,** 43, (3), 303-311.
11. Baldock, J. A.; Smernik, R. J., Chemical composition and bioavailability of thermally altered Pinus resinosa (Red pine) wood. *Org. Geochem.* **2002,** 33, (9), 1093-1109.
12. Joseph, S.; Peacocke, C.; Lehmann, J.; Munroe, P., Developing a Biochar Classification and Test Methods. In *Biochar for Environmental Management Science and Technology*, Lehmann, J.; Joseph, S., Eds. Earthscan: London, 2009.
13. Lehmann, J.; Czimczik, C. I.; Laird, D. A.; Sohi, S., Stability of Biochar in the Soil. In *Biochar for Environmental Management Science and Technology*, Lehmann, J.; Joseph, S., Eds. Earthscan: London, 2009.
14. Zimmerman, A. R., Abiotic and microbial oxidation of laboratory-produced black carbon (biochar). *Environ. Sci. Technol.* **2010,** 44, (4), 1295-1301.
15. Keiluweit, M.; Nico, P. S.; Johnson, M. G.; Kleber, M., Dynamic molecular structure of plant biomass-derived black carbon (biochar). *Environ. Sci. Technol.* **2010,** 44, (4), 1247-1253.
16. Di Blasi, C., Modeling intra- and extra-particle processes of wood fast pyrolysis. *AIChE J.* **2002,** 48, (10), 2386-2397.
17. Bruun, E. W.; Hauggaard-Nielsen, H.; Ibrahim, N.; Egsgaard, H.; Ambus, P.; Jensen, P. A.; Dam-Johansen, K., Influence of fast pyrolysis temperature on biochar labile fraction and short-term carbon loss in a loamy soil. *Biomass Bioenerg.* **2011,** 35, (3), 1182-1189.
18. Ellens, C. J. Design, optimization and evaluation of a free-fall biomass fast pyrolysis reactor and its products. M.S. thesis, Iowa State University, Ames, IA, 2009.
19. Pollard, A. J. S. Comparison of bio-oil produced in a fractionated bio-oil collection system. M.S. thesis, Iowa State University, Ames, IA, 2009.
20. *ASTM D1762-84 Standard Test Method for Chemical Analysis of Wood Charcoal*; ASTM International: West Conshohocken, PA, 2007; p 2.
21. Mao, J. D.; Schmidt-Rohr, K., Accurate quantification of aromaticity and nonprotonated aromatic carbon fraction in natural organic matter by 13C solid-state nuclear magnetic resonance. *Environ. Sci. Technol.* **2004,** 38, (9), 2680-2684.
22. Richards, L. A.; Ogata, G., Psychrometric measurements of soil samples equilibrated on pressure membranes. *Soil Sci. Soc. Am. J.* **1961,** 25, (6), 456-459.
23. Zuberer, D. A., Recovery and Enumeration of Viable Bacteria. In *Methods of Soil Analysis Part 2, Microbiological and Biochemical Properties*, Weaver, R. W.; Angle, S.; Bottomley, P.; Bezdicek, D.; Smith, S.; Tabatabai, A.; Wollum, A., Eds. Soil Science Society of America: Madison, WI, 1994; pp 119-142.
24. Johnson, L. F.; Curl, E. A.; Bond, J. H.; Fribourg, H. A., *Methods for Studying Soil Microfauna-Plant Disease Relationships*. Burgress: Minneapolis, MN, 1959.
25. Bridgeman, T. G.; Jones, J. M.; Shield, I.; Williams, P. T., Torrefaction of reed canary grass, wheat straw and willow to enhance solid fuel qualities and combustion properties. *Fuel* **2008,** 87, (6), 844-856.

26. Fang, X.; Chua, T.; Schmidt-Rohr, K.; Thompson, M. L., Quantitative ^{13}C NMR of whole and fractionated Iowa Mollisols for assessment of organic matter composition. *Geochim. Cosmochim. Acta* **2010,** 74, (2), 584-598.
27. McBeath, A. V.; Smernik, R. J., Variation in the degree of aromatic condensation of chars. *Org. Geochem.* **2009,** 40, (12), 1161-1168.
28. Zimmerman, A. R.; Gao, B.; Ahn, M.-Y., Positive and negative carbon mineralization priming effects among a variety of biochar-amended soils. *Soil Biol. Biochem.* **2011,** 43, (6), 1169-1179.
29. Kuzyakov, Y.; Subbotina, I.; Chen, H.; Bogomolova, I.; Xu, X., Black carbon decomposition and incorporation into soil microbial biomass estimated by ^{14}C labeling. *Soil Biol. Biochem.* **2009,** 41, (2), 210-219.
30. Smith, J. L.; Collins, H. P.; Bailey, V. L., The effect of young biochar on soil respiration. *Soil Biol. Biochem.* **2010,** 42, (12), 2345-2347.
31. Wardle, D. A.; Nilsson, M.-C.; Zackrisson, O., Fire-derived charcoal causes loss of forest humus. *Science* **2008,** 320, (5876), 629-629.
32. Rogovska, N. P.; Laird, D. A.; Cruse, R. M.; Fleming, P.; Parkin, T.; Meek, D., Impact of biochar on manure carbon stabilization and greenhouse gas emissions. *Soil Sci. Soc. Am. J.* **2011,** 75, (3), 871-879.
33. Laird, D. A.; Fleming, P.; Davis, D. D.; Horton, R.; Wang, B.; Karlen, D. L., Impact of biochar amendments on the quality of a typical Midwestern agricultural soil. *Geoderma* **2010,** 158, (3-4), 443-449.
34. Warnock, D.; Lehmann, J.; Kuyper, T.; Rillig, M., Mycorrhizal responses to biochar in soil – concepts and mechanisms. *Plant Soil* **2007,** 300, (1), 9-20.
35. Khodadad, C. L. M.; Zimmerman, A. R.; Green, S. J.; Uthandi, S.; Foster, J. S., Taxa-specific changes in soil microbial community composition induced by pyrogenic carbon amendments. *Soil Biol. Biochem.* **2011,** 43, (2), 385-392.

CHAPTER 5. CRITERIA TO SELECT BIOCHARS FOR FIELD STUDIES BASED ON BIOCHAR CHEMICAL PROPERTIES

A paper published by *BioEnergy Research*

Catherine E. Brewer, Rachel Unger, Klaus Schmidt-Rohr, Robert C. Brown

Abstract

One factor limiting the understanding and evaluation of biochar for soil amendment and carbon sequestration applications is the scarcity of long-term, large-scale field studies. Limited land, time and material resources require that biochars for field trials be carefully selected. In this study, 17 biochars from the fast pyrolysis, slow pyrolysis and gasification of corn stover, switchgrass and wood were thoroughly characterized and subjected to an 8-week soil incubation as a way to select the most promising biochars for a field trial. The methods used to characterize the biochars included proximate analysis, CHNS elemental analysis, BET surface area, photo-acoustic Fourier transform infrared spectroscopy (FTIR-PAS), and quantitative ^{13}C solid-state nuclear magnetic resonance (NMR) spectroscopy. The soil incubation study was used to relate biochar properties to three soil responses: pH, cation exchange capacity (CEC), and water leachate electrical conductivity (EC). Characterization results suggest that biochars made in a kiln process where some oxygen was present in the reaction atmosphere have properties intermediate between slow pyrolysis and gasification and therefore, should be grouped separately. A close correlation was observed between aromaticity determined by NMR and fixed carbon fraction determined by proximate analysis, suggesting that the simpler, less expensive proximate analysis method can be used to gain aromaticity information. Of the 17 biochars originally assessed, four biochars were ultimately selected for their potential to improve soil properties and to provide soil data to refine the selection scheme: corn stover low-temperature fast pyrolysis (highest amended-soil CEC, information on high volatile matter/O:C ratio biochar), switchgrass O_2/steam gasification (relatively high BET surface area, and amended-soil pH, EC and

CEC), switchgrass slow pyrolysis (higher amended-soil pH and EC), and hardwood kiln carbonization (information on slow pyrolysis, gasification and kiln-produced differences).

Keywords
biochar, cation exchange capacity, gasification, nuclear magnetic resonance spectroscopy, pyrolysis

Abbreviations

BET	Brunauer-Emmett-Teller (surface area)
CEC	cation exchange capacity
CP	cross polarization
DP	direct polarization
EC	electrical conductivity
FTIR-PAS	Fourier transform infrared spectroscopy with photoacoustic detection
ICP-AES	inductively coupled plasmas atomic emission spectroscopy
MAS	magic angle spinning
NMR	nuclear magnetic resonance spectroscopy

5.1 Introduction

Biochar has been demonstrated to be a potentially beneficial soil amendment[1-5] and a carbon sequestration agent. [6-10] The scarcity of data from long-term or large-scale biochar application field trials in temperate climates, however, currently limits the ability of scientists and policymakers to evaluate this potential.[11-15] Biochars can be produced from a variety of cellulose-containing feedstocks such as biomass[16-18] and municipal wastes,[19, 20] and by a variety of processes yielding bioenergy and chemical co-products such as bio-oil and syngas.[21, 22] Biochar properties, therefore, can vary widely. As soil amendments, differences in biochar properties are expected to lead to differences in soil and crop responses.[23] To conduct field trials, large amounts of biochar (on the Mg scale) must be produced to achieve reasonable plot sizes, adequate replications, and realistic biochar application rates. Each biochar being tested should be as homogeneous as possible: produced from the same feedstock and under well-

controlled, consistent reaction conditions. To keep field trial resource requirements practical, the careful selection of biochars to be tested is critical. Biochar characterization is essential to improve the understanding of biochar production-property relationships and to allow for meaningful pre-application biochar quality comparisons.[3, 24-28] Likewise, evaluation of feedstock availability, local energy needs, and demand for thermochemical co-products is important for selection of a biochar production process. The development of biochar screening methods that require relatively little time and provide as much location-specific information as possible is also desirable.[29-31]

In this study, 17 biochars from the slow pyrolysis, fast pyrolysis and gasification of corn stover, switchgrass and wood were available to be produced at Iowa State University or purchased at a 10-50 kg scale. The goal of this study was to narrow down the available biochars to the four or five most likely to give positive, measurable, and informative results under local soil conditions. The criteria used included basic biochar characteristics such as volatiles content (related to probability of short-term N immobilization[32]) and total carbon content (related to potential carbon sequestration[26]), carbon composition and aromaticity from advanced characterization techniques such as nuclear magnetic resonance spectroscopy (NMR),[25] and responses of three soil properties after a short incubation. The soil properties to be measured were selected based on responses observed in previous biochar studies: soil pH,[3, 33-37] cation exchange capacity (CEC),[1, 4, 36, 37] and electrical conductivity (EC).[33, 36, 38] A short, semi-quantitative measurement of exchangeable/extractable cations in the biochars was also used to identify the primary components responsible for increases in EC. A secondary goal of this study was to identify patterns in biochar properties that might simplify biochar evaluation and selection.

5.2 Materials and Methods

5.2.1 Biochar Production

Of the 17 biochars used in this study, 14 were produced using reactors at the Center for Sustainable Environmental Technologies (CSET) at Iowa State University (Ames, IA). Reaction conditions are summarized in Table 14. Switchgrass and corn stover were

obtained locally (Story County, IA). Red oak chips were obtained from Glen Oak Lumber and Milling (Montello, WI). Prior to thermochemical processing, feedstocks were ground in a hammer mill to pass a ¼" (6 mm) screen and dried to <10% moisture.

Table 14. Feedstocks and process used to produce biochars used in this study. *Reactor wall temperature

Biochar #	Feedstock	Process	Temperature (°C)
1	Corn stover	Fluidized bed fast pyrolysis	500
2	Corn stover	Freefall fast pyrolysis	600*
3	Corn stover	Freefall fast pyrolysis	550*
4	Corn stover	Freefall fast pyrolysis	500*
5	Corn stover	Air-blown gasification	732
6	Corn stover	Slow pyrolysis	500
7	Switchgrass	Fluidized bed fast pyrolysis	450
8	Switchgrass	Fluidized bed fast pyrolysis	500
9	Switchgrass	Fluidized bed fast pyrolysis	550
10	Switchgrass	O_2/steam gasification	824
11	Switchgrass	O_2/steam gasification	775
12	Switchgrass	O_2/steam gasification	796
13	Switchgrass	Slow pyrolysis	500
14	Red oak	Fluidized bed fast pyrolysis	500
15	Mixed hardwood	Kiln slow pyrolysis	~400
16	Wood waste	Air-blown gasification	~800
17	Eastern hemlock	Auger fast pyrolysis	550

Biochars 1-6, 7-13, and 14-17 were produced from corn stover, switchgrass and hardwoods, respectively. Fast pyrolysis biochars (Biochars 1, 7-9 and 14) were produced on a 5 kg h^{-1} capacity bubbling fluidized bed reactor optimized for bio-oil production. The sand bed was fluidized with pre-heated nitrogen and the biochar was collected using a high-throughput cyclone catch. Torrified/low-temperature fast pyrolysis corn stover samples (Biochars 2-4) were produced on a freefall fast pyrolyzer run under conditions that did not allow sufficient particle residence time, resulting in dark brown to almost black, friable particles. Temperatures listed for these biochars refer to reactor wall temperatures. (Biochars 1, 2 and 4 had been used in a previous study on extent of

pyrolysis.[39]) Gasification biochars were produced on a 3 kg h^{-1} capacity bubbling fluidized bed reactor under air-blown (Biochar 5) or steam/oxygen-blown conditions (Biochars 10-12). For air-blown gasification, the equivalence ratio was approximately 0.20; steam/oxygen-blown reactions were run under 40, 50 and 60% oxygen fluidizing gas compositions. Biochar was again collected by cyclone catches. Slow pyrolysis biochars (Biochar 6 and Biochar 13) were produced in a paint-can fitted with a nitrogen purge (1 L min^{-1} flow rate) and thermocouple for temperature measurement. The sealed can was placed into a muffle furnace and heated at approximately 15°C min^{-1}; hold time at the set temperature was 30-60 minutes.

The three remaining biochars were commercial samples. Biochar 15, a mixed hardwood charcoal, was obtained from a commercial kiln (Struemph Charcoal Company, Belle, MO); samples of this biochar had been used in two previous studies.[25, 40] Biochar 16 was waste wood biochar from an air-blown, fluidized bed commercial gasifier (Chippewa Valley Ethanol Company, Benson, MN) designed by Frontline Bioenergy, LLC (Ames, IA). Biochar 17 was produced from Eastern hemlock in a commercial auger fast pyrolyzer (Advanced Biorefinery, Inc, Ottowa, Ontario).

5.2.2 Biochar Characterization

Biochar characterization followed methods previously described.[25] Briefly, moisture, volatiles, fixed carbon and ash content of the biochars were determined according to ASTM D1762-84. Elemental analysis was performed using TRUSPEC-CHN and TRUSPEC-S analyzers (LECO Corporation, St. Joseph, MI). Oxygen content was determined by difference. Brunauer-Emmett-Teller (BET) surface area was measured by nitrogen gas sorption analysis at 77K (NOVA 4200e, Quantachrome Instruments, Boynton Beach, FL). Fourier transform infrared (FTIR) spectroscopy was performed using a Digilab FTS-7000 FTIR spectrophotometer equipped with a PAC 300 photoacoustic detector (MTEC Photoacoustics, Ames, IA). Spectra were taken at 4 cm^{-1} resolution and 1.2 kHz scanning speed for a total of 64 co-added scans.

Solid-state ^{13}C nuclear magnetic resonance spectroscopy (NMR) experiments were performed on a Bruker DSX400 spectrometer (Bruker Biospin, Karlsruhe, Germany) at 100 MHz for ^{13}C and 400 MHz for ^{1}H. Quantitative biochar spectra were obtained using

^{13}C direct polarization magic angle spinning (DP/MAS) NMR in 4-mm MAS rotors at a spinning speed of 14 kHz and under high-power ($|\gamma B1|/2\pi$ = 70 kHz) TPPM ^{1}H decoupling. To reduce power absorption due to sample conductivity, the gasification biochars were diluted with an equal volume fraction of laponite clay. Sparking observed in undiluted Biochar 15 was eliminated using the same approach. A glass insert (5 mm thick) was placed at the bottom of each rotor to constrain the sample to the space within the radio-frequency coil, and the sample mass was recorded for quantification of ^{13}C observability. A 180° pulse of 9 µs duration was used to generate a Hahn echo before detection[41] and thus avoid baseline distortions associated with detection directly after the 90^{o} excitation pulse. Based on T_1 measurements after cross polarization,[42] recycle delays of ≥ 3 T_1 of the slowest-relaxing signals, between 13 s and 75 s, were used in the direct-polarization experiments. For several samples, we checked that a spectrum with doubled recycle delay showed no significant intensity increase for any of the main peaks, confirming that the magnetization was fully relaxed. High carbon observabilities in ^{13}C spin counting experiments, [43] based on the mass of carbon in the sample, calculated from the sample mass and the carbon mass fraction, with polystyrene and alanine as reference materials, confirmed essentially complete relaxation. The ^{13}C chemical shifts were referenced to tetramethylsilane using the COO^{-} resonance of glycine at 176.49 ppm as a secondary reference. To acquire the quantitative spectra of the non-protonated carbon fraction, DP/MAS with recoupled ^{1}H-^{13}C dipolar dephasing was used (68 µs dephasing time).[41] DP/MAS NMR measuring times per sample ranged between 1 and 2 days. Semi-quantitative biochar spectra were obtained using ^{13}C cross polarization magic angle spinning with total suppression of spinning sidebands (CP/MAS/TOSS); for maximum sensitivity, samples were analyzed in 7-mm MAS rotors at a spinning speed of 7 kHz with 0.5 s recycle delay, 4 µs ^{1}H 90° pulse length, and 1 µs CP contact time.

Extractable/exchangeable cations in the biochars were measured by extracting one sample of each biochar with 0.5 M ammonium acetate solution adjusted to pH = 7.0.[44] Biochar (1.5 g) and extraction solution (15 ml) were shaken for 30 minutes in 35 ml Nalgene centrifuge tubes, centrifuged at 66 Hz for 10 minutes, and decanted for a total of three extractions. The decanted solution was filtered through 1 µm syringe filters

(Whatman Anatop 25) to remove particulate and analyzed for Ba, Ca, Fe, K, Mg, Mn, Na and Sr by inductively-coupled plasma atomic emission spectroscopy (ICP-AES) (Thermo Jarell Ash ICAP 61E, Franklin, MA).

5.2.3 Soil Incubation

A sample of Nicollet soil (fine-loamy, mixed, superactive, mesic Aquic Hapludoll) was collected after harvest in 2006 from the top 25 cm at Iowa State University's Curtiss Agronomy Farm located in Ames, IA (42.001° N, 93.661°W). The field-moist soil was stored at 4°C prior to use. Soil water holding capacity was measured by pressure plate at -33 kPa soil water matric potential. For each soil treatment, 1.5 kg of soil and 19.2 g of biochar were weighed into a bucket and then mixed by rotating the bucket. 50 g of the soil/char mixture was weighed into a French square bottle such that each would contain approximately 50 g of soil and 0.8 g of biochar (equivalent to a biochar application rate of 36 Mg ha^{-1}). A urea (46-0-0) solution was added to each bottle and mixed by hand to bring the soil to its water holding capacity and nitrogen application equivalent to 224 kg N ha^{-1}. Each combination of soil, biochar, and urea was replicated four times, along with a single no-urea control for each biochar, a single soil-only control, and a single soil-plus-urea control for a total of 87 bottles. Bottles were covered with parafilm, with a small perforation to maintain aeration, and incubated on the bench-top at room temperature (23°C) for 8 weeks. Bottles were weighed periodically and distilled water added to maintain soil moisture. After incubation, the soil samples were dried and ground for analysis.

5.2.4 Soil Testing

Soil (3 g) and deionized water (15 mL) were added to a pre-weighed centrifuge tube, shaken for 30 minutes, and the pH of biochar-amended soil suspensions was measured using an Accumet AB15 pH meter (Fisher Scientific, Pittsburgh, PA). Samples were centrifuged (AccuSpin 1, Fisher Scientific, Pittsburgh, PA) at 66 Hz for 10 min and the electrical conductivity of the decanted supernatant measured by an Orion 3 Star bench-top conductivity meter (Thermo Fisher Scientific, Waltham, MA). To prepare the soil samples for CEC analysis, rinses (3-5) with 15 mL aliquots of DI water were repeated

until the electrical conductivity of the supernatant decreased to approximately 30 µS cm^{-1}, indicating most of the soluble salts had been removed. CEC was measured using a modified ammonium acetate compulsory displacement method.[45] Rinsed soil samples were saturated with Na cations three times by addition of 10 mL of 0.5M sodium acetate (pH = 7.0), shaken for 5 minutes, and centrifuged at 66 Hz for 10 min, discarding the supernatant each time. Excess sodium cations were removed by addition of 10 mL of 1:1 (v/v) solution of ethanol and water, shaken for 15 minutes, and centrifuged at 66 Hz for 10 min. Rinsing was repeated twice more using 200-proof ethanol after which samples were allowed to dry overnight. Na cations were displaced with three aliquots (10.00 mL) of 0.5M ammonium acetate (pH = 7.0), shaken for 5 min, and centrifuged at 66 Hz for 10 min. The supernatant was decanted, filtered through a 0.45 µm, surfactant-free cellulose acetate (SFCA) membrane syringe filter (Corning, Corning, NY), and the Na concentration determined by ICP-AES.

5.2.5 Statistics

Determining statistical differences between treatments for biochar-amended soil pH, EC and CEC was done at a 95% confidence level ($p<0.05$) using single factor ANOVA and Tukey's honest significant difference test.

5.3 Results

5.3.1 Biochar Composition and Physical Properties

Biochar surface area, proximate analysis and elemental composition results are listed in Table 15 and show considerable variation between biochars based on feedstock and reaction conditions. For switchgrass and corn stover biochars, ash contents were high (44-73 wt%) and carbon contents were low (22-43%). For wood biochars, ash contents were relatively low (4-23%) and carbon contents high (62-79%). Biochars from fast pyrolysis were generally higher in volatiles (12-30%) and lower in fixed carbon (25-65%) compared to biochars from slow pyrolysis and gasification, indicating a lower degree of carbonization. All BET surface areas were low (3.3-61.6 m^2 g^{-1}) and generally increased with reaction residence time (fast pyrolysis < slow pyrolysis) and temperature (pyrolysis < gasification).

Table 15. Composition and surface area of biochars. Elemental composition values are reported on a dry weight basis; proximate analysis results reported on a wet basis. Oxygen content determined by difference. BET SA = Brunauer-Emmett-Teller surface area.

Biochar #	Moisture	Volatiles	Fixed C	Ash	C	H	N	S	O	BET SA
				--wt %--						$m^2 g^{-1}$
1	1.7	13.8	25.2	59.3	29.5	1.6	0.6	0.02	7.9	8.5
2	1.8	17.1	25.4	55.7	31.4	2.0	0.6	0.03	9.2	3.3
3	1.6	29.7	24.7	44.0	37.5	3.3	0.6	0.04	13.9	3.7
4	2.5	26.2	24.9	46.4	34.9	2.9	0.7	0.06	13.9	4.5
5	1.0	5.1	20.3	73.6	21.8	0.1	0.4	0.02	3.4	14.3
6	0.7	6.7	31.3	61.3	33.4	1.1	0.8	0.01	2.9	24.8
7	2.6	16.4	31.4	49.6	37.5	2.2	0.5	0.16	8.9	15.6
8	2.4	11.6	31.5	54.5	40.7	1.9	0.5	0.13	1.0	16.8
9	2.9	13.6	34.4	49.0	42.2	1.9	0.5	0.17	4.9	26.2
10	1.7	7.5	22.5	68.3	25.4	0.4	0.3	0.04	4.5	46.1
11	1.5	7.1	24.5	66.9	26.7	0.3	0.3	0.03	4.7	20.2
12	2.1	11.9	21.8	64.2	27.5	0.6	0.3	0.04	6.1	61.6
13	0.9	7.1	39.5	52.5	39.4	1.3	0.7	0.00	5.6	50.2
14	2.2	18.1	56.2	23.4	62.0	2.7	0.6	0.02	10.8	3.8
15	3.6	16.8	72.9	6.7	79.2	2.4	0.5	0.01	11.0	8.1
16	4.0	7.2	72.2	16.7	76.6	1.3	0.5	0.01	4.2	5.8
17	3.7	27.1	64.9	4.3	75.7	4.2	0.3	0.01	15.2	5.8

5.3.2 FTIR Properties

FTIR spectra of corn stover, wood and switchgrass biochars are shown in Figures 28, 29 and 30, respectively. With all three kinds of feedstock, clear distinctions can be made between slow pyrolysis, fast pyrolysis and gasification biochar spectra. Fast pyrolysis biochar spectra show the highest amount of oxygen-containing functional groups, especially the O-H stretch around 3400 cm^{-1} and the carboxylic C stretch around 1700 cm^{-1}.[25, 28] Slow pyrolysis biochar spectra indicate significantly fewer oxygen-containing functional groups and a stronger aromatic C-H stretch signal at 3050 cm^{-1}. The exception is the Biochar 15 spectrum, which contains almost no peaks and is more similar to gasification biochar spectra.

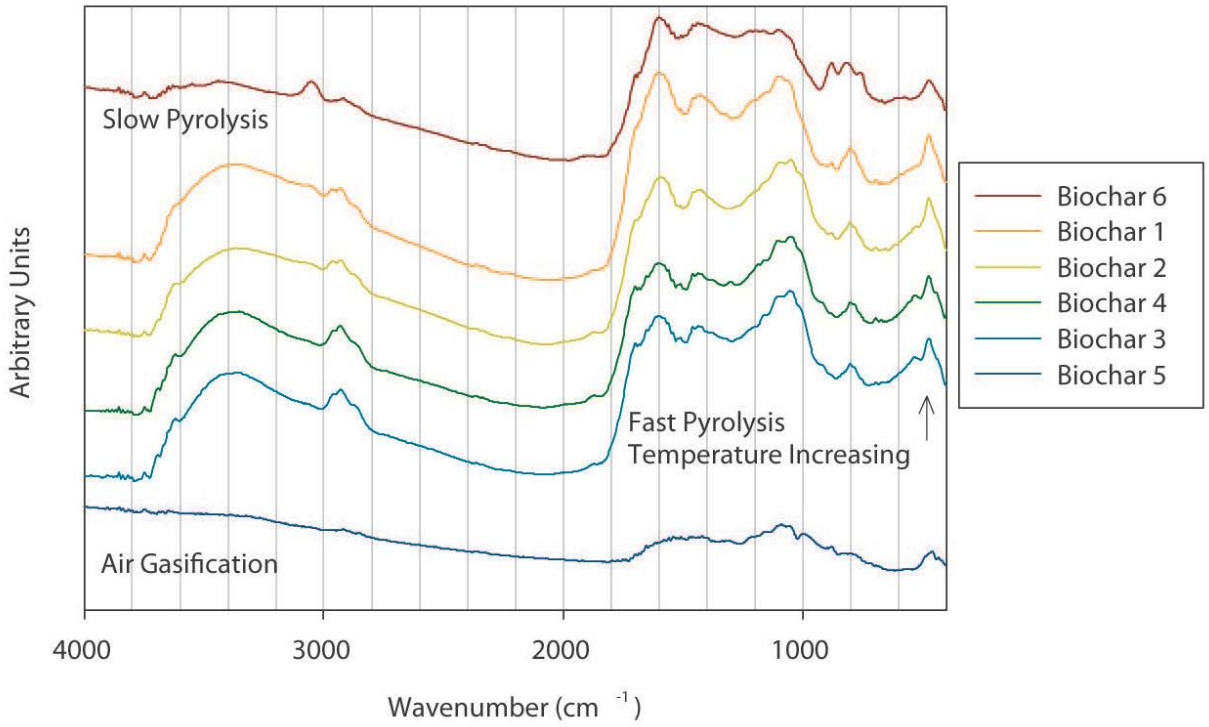

Figure 28. FTIR spectra of corn stover biochars from slow pyrolysis, fast pyrolysis and air-blown gasification.

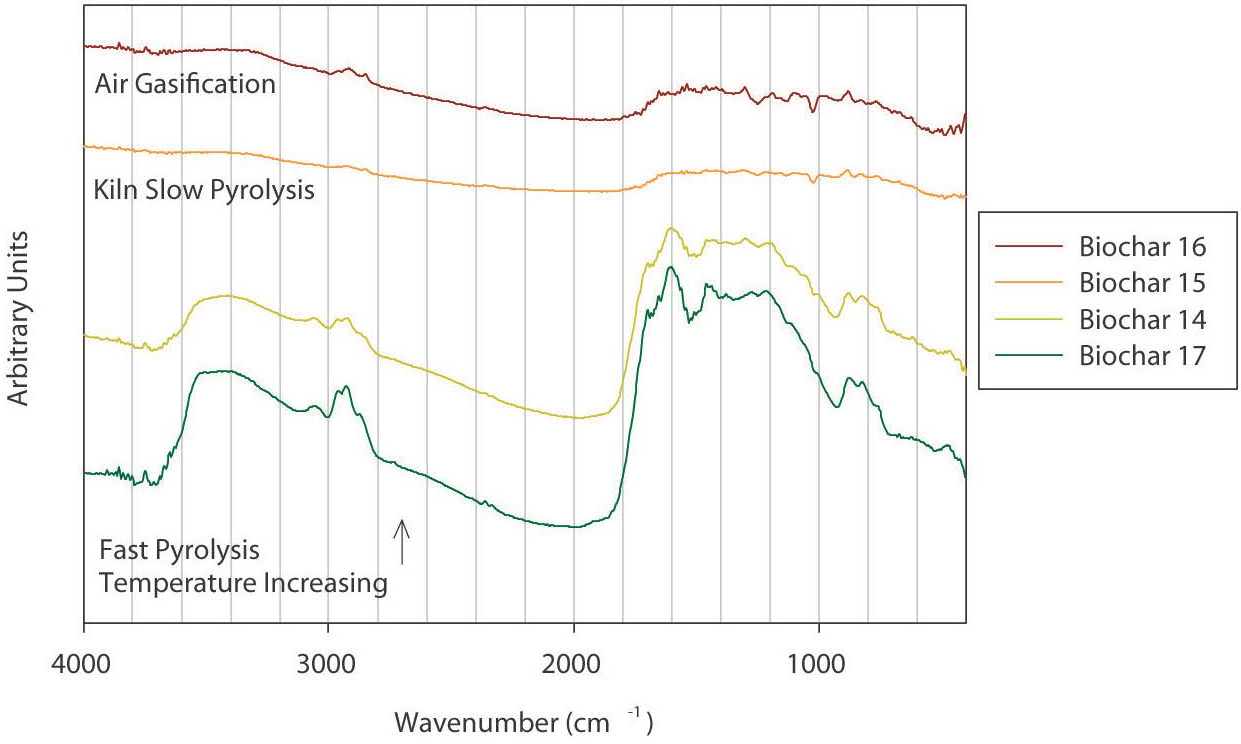

Figure 29. FTIR spectra of wood biochars from a commercial kiln slow pyrolysis process, fast pyrolysis and air-blown gasification.

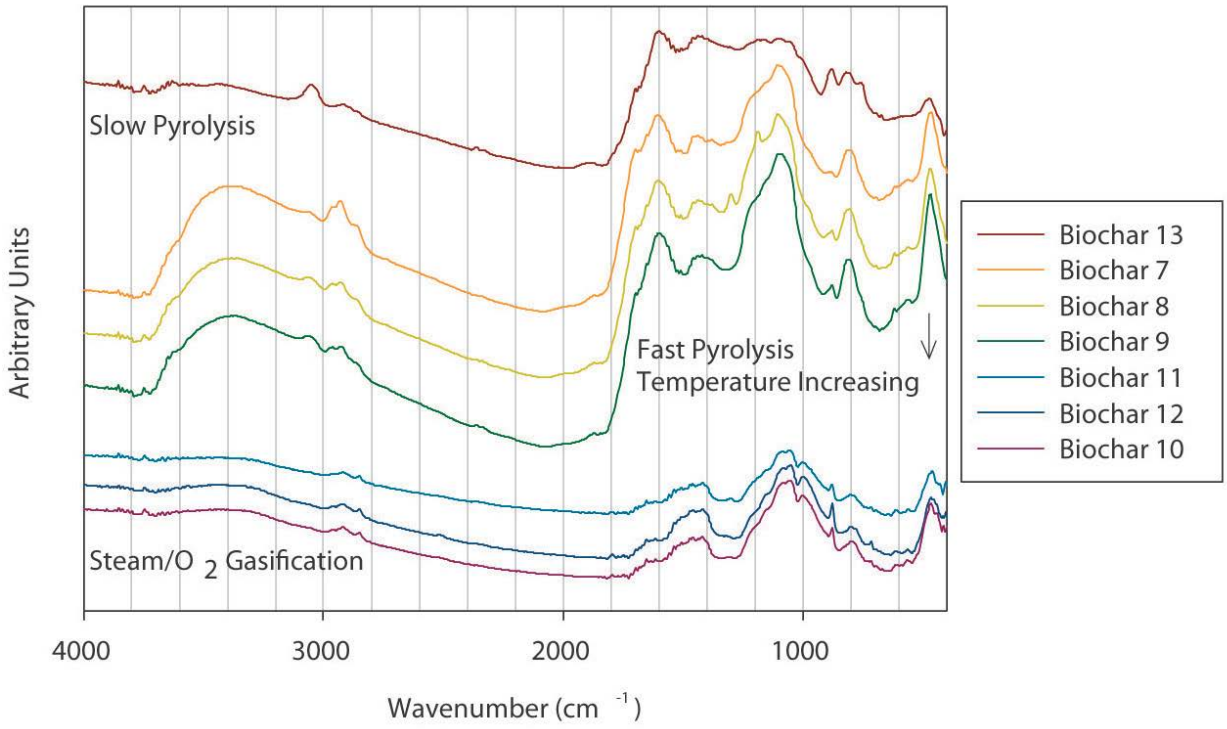

Figure 30. FTIR spectra of switchgrass biochars from slow pyrolysis, fast pyrolysis and O_2/steam-blown gasification.

5.3.3 NMR Spectra and Composition

Quantitative direct-polarization ^{13}C NMR spectra of wood, slow pyrolysis, fast pyrolysis and gasification biochars are shown in Figures 31, 32, 33, and 34, respectively. Selective spectra of non-protonated carbons (and CH_3 groups) are also shown (thin lines), providing information on the fractions of non-protonated (inner) and protonated (edge) aromatic carbons. The composition information obtained from these spectra is summarized in Table 16 and the properties of the aromatic clusters are compiled in Tables 17 and 18 as described in our previous paper.[25]

Carbon observabilities from spin counting[43] are also listed in Table 17. High values near 100% were obtained for slow pyrolysis biochars (Biochars 13 and 6) and for low-temperature fast pyrolysis biochars (Biochars 2-4), showing that all the carbons were observed fully. These samples behaved normally, absorbing little radio-frequency power. By contrast, the fast pyrolysis biochars exhibited some and the gasification biochars exhibited pronounced broadening of the electronic resonances of the NMR probe head, which resulted in a lower electronic quality factor and therefore reduced

signal intensity. In other words, NMR detector efficiency was reduced when these samples were measured, resulting in artificially lowered observability values. Preliminary calibration experiments indicated that the observabilities for fast pyrolysis biochars and wood biochar (Biochar 15) should be corrected by +5%, and those of gasification biochars (Biochars 5 and 11) by +12%, resulting in good observability values. For an unknown reason, the observability of Biochar 8 was unusually low, but this did not seem to result in significant spectral distortions, as indicated by the similar spectral intensity distribution for the closely related Biochar 9, which had good observability. It should be noted that as long as the observability of all types of carbons is similarly reduced, the spectra are not distorted.

All biochar NMR spectra were dominated by a peak of aromatic carbons, the majority of which were not protonated. The aromatic C-H fraction was largest for slow-pyrolysis chars (~30%) and intermediate for fast-pyrolysis and wood chars (~23%), while gasification biochars showed by far the smallest fraction (~10%) of aromatic C-H groups. C-H was the dominant form of carbon at the edges of the aromatic rings in slow-pyrolysis biochars, see Tables 16 and 18. The spectra in Figures 33 and 35 indicate only moderate structural changes between switchgrass pyrolysis at 500 and 550^{o}C; in particular, the fraction of aromatic C-H groups does not decrease significantly (see Tables 16 and 17).

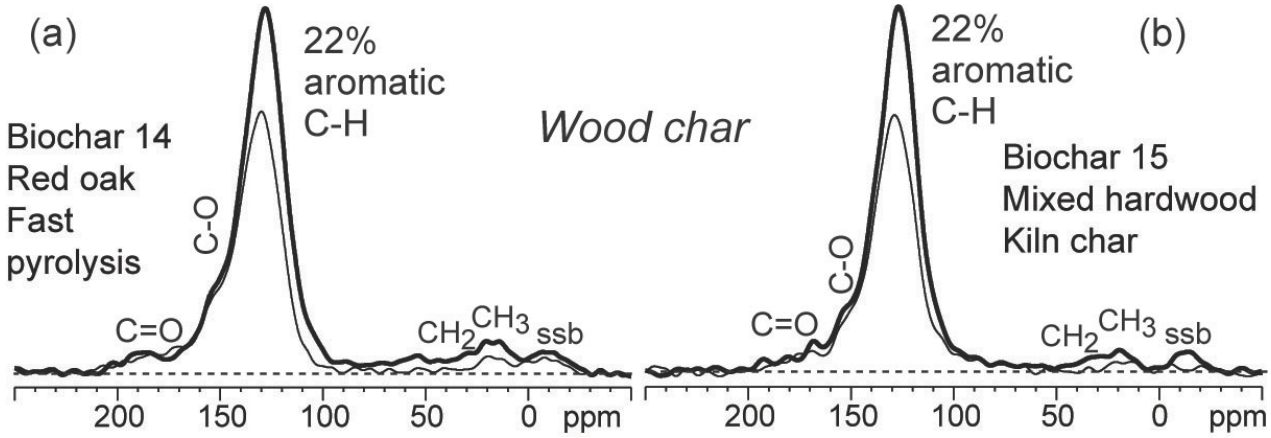

Figure 31. Quantitative ^{13}C direct polarization (DP/MAS) and direct polarization with dipolar decoupling (DP/GADE) spectra of wood biochars at a magic angle spinning (MAS) frequency of 14 kHz. (a) Red oak fast pyrolysis biochar produced at 500°C. (b) Mixed hardwood kiln biochar from a commercial process. Thick line = all carbons, thin line = non-protonated carbons and methyl groups.

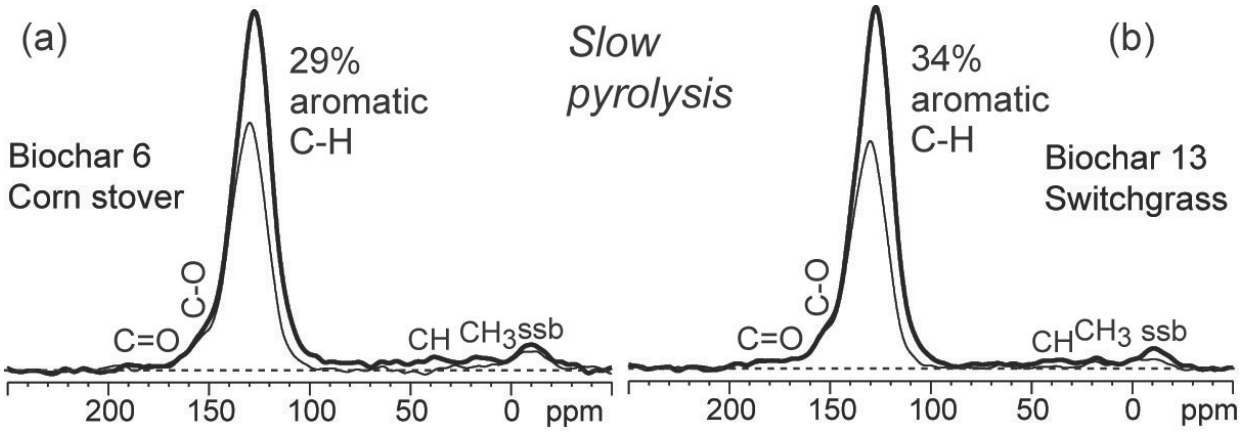

Figure 32. Quantitative ^{13}C direct polarization (DP/MAS) and direct polarization with dipolar decoupling (DP/GADE) spectra of slow pyrolysis biochars at a magic angle spinning (MAS) frequency of 14 kHz. (a) Corn stover and (b) switchgrass slow pyrolysis biochar produced at 500°C. Thick line = all carbons, thin line = non-protonated carbons and methyl groups.

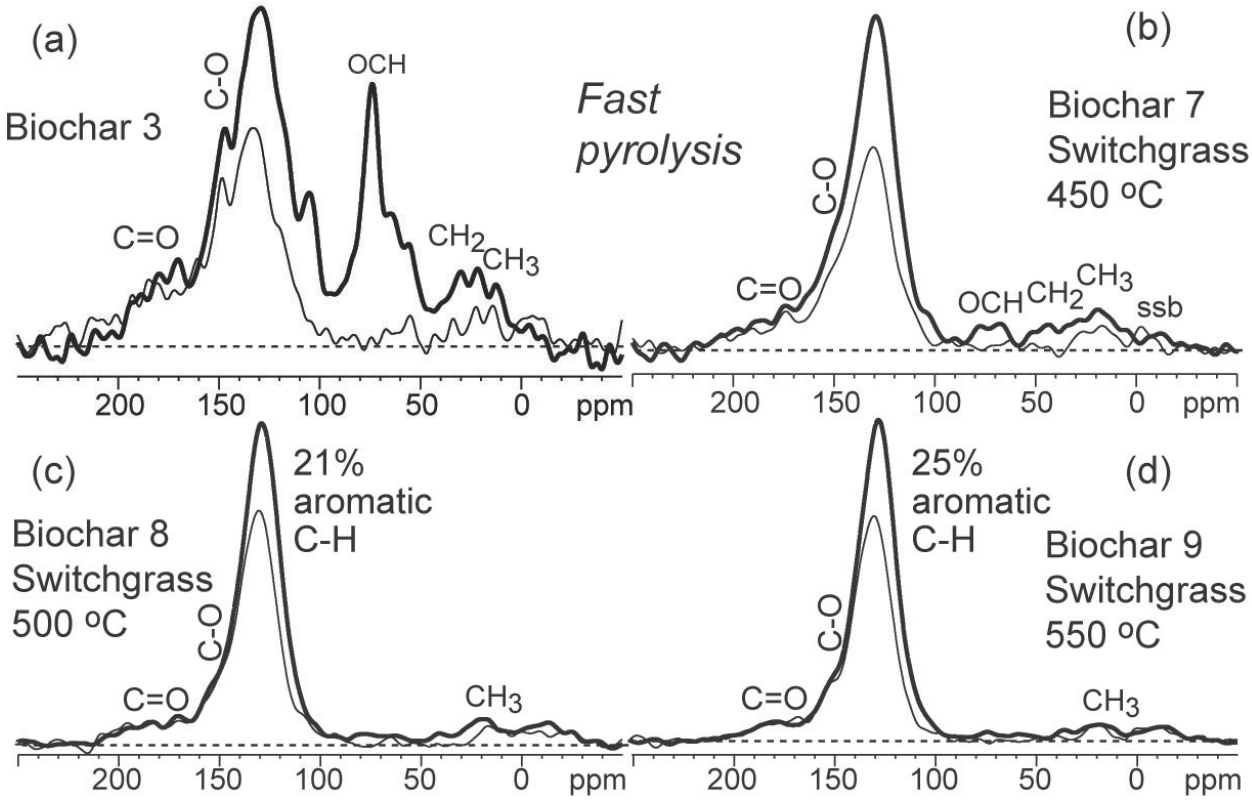

Figure 33. Quantitative ^{13}C direct polarization (DP/MAS) and direct polarization with dipolar decoupling (DP/GADE) spectra of fast pyrolysis biochars at a magic angle spinning (MAS) frequency of 14 kHz. (a) Corn stover fast pyrolysis biochar produced at 550°C reactor wall temperature. (b-d) Switchgrass fast pyrolysis biochars produced at 450, 500 and 550°C. Thick line = all carbons, thin line = non-protonated carbons and methyl groups.

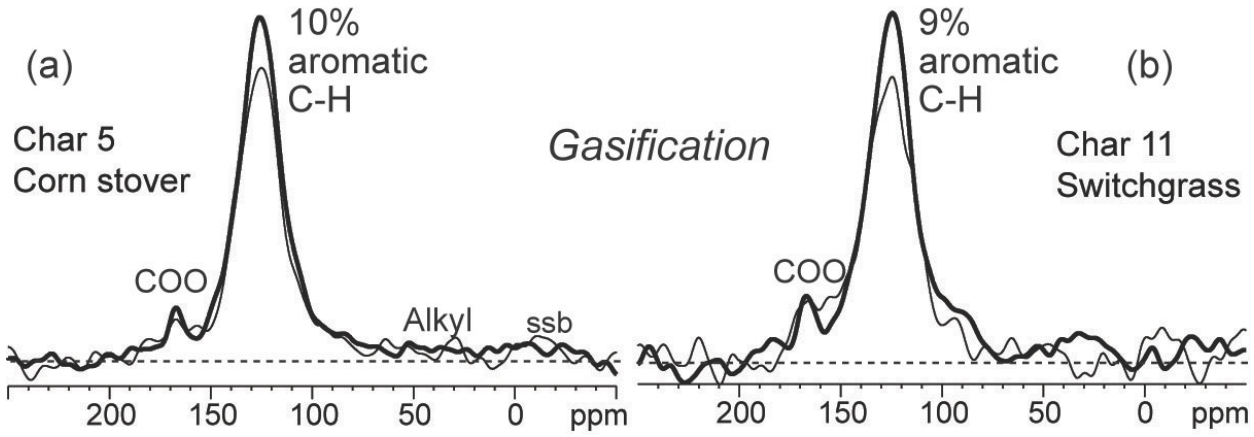

Figure 34. Quantitative ^{13}C direct polarization (DP/MAS) and direct polarization with dipolar decoupling (DP/GADE) spectra of gasification biochars at a magic angle spinning (MAS) frequency of 14 kHz. (a) Corn stover gasification biochar produced at 732°C. (b) Switchgrass gasification biochar produced at 775°C. Thick line = all carbons, thin line = non-protonated carbons and methyl groups.

Cross polarization ^{13}C NMR spectra, which enhance the signals of protonated carbons, in particular the alkyl residues, are displayed for a series of fast-pyrolysis switchgrass biochars in Figure 35; they closely matched the corresponding spectra of a different group of fast pyrolysis switchgrass biochar in our previous work.[25]

Table 16. Quantitative NMR spectral analysis of corn stover, switchgrass and red oak fast pyrolysis and slow pyrolysis chars from DP/MAS and DP/MAS/GADE spectra. All values are % of total ^{13}C signal. $CO_{0.75}H_{0.5}$ moieties assume a 1:1 ratio of alcohols and ethers. $CH_{1.5}$ moieties assume a 1:1 ratio of CH_2 and CH groups. $C_{non\text{-}pro}$, non-protonated aromatic carbon. Error margins: ± 2%.

Biochar #	**Carbonyls**		**Aromatics**			**Alkyls**		
Moieties:	**C=O**	**COO**	**$CO_{0.75}H_{0.5}$**	**$C_{non\text{-}pro}$**	**C-H**	**$HCO_{0.75}H_{0.5}$**	**$CH_{1.5}$**	**CH_3**
ppm:	**210-183**	**183-165**	**165-145**	**145-70**	**145-90**	**90-50**	**50-25**	**25-6**
1	3	5	12	44	26	2	4	4
2	4	4	11	39	25	7	5	5
3	4	6	11	27	23	21	6	5
4	4	5	11	30	21	17	7	6
5	2	4	6	69	10	4	4	2
6	1	1	7	56	29	3	2	2
7	4	5	13	45	21	5	4	4
8	3	4	10	55	21	2	2	3
9	2	3	9	53	25	3	2	3
11	2	5	7	68	9	4	4	2
13	1	1	7	53	34	1	2	1
14	2	2	11	52	22	3	3	4
15	2	3	9	57	22	2	2	3

Table 17. NMR C observabilities, aromaticities calculated on molar and mass bases, fractions of aromatic edge carbons, χ_{edge}, and minimum number of carbons per aromatic cluster, $n_{C,min} = 6/\chi_{edge,max}^2$ in biochars.

Biochar #	Observable C (%)	Aromaticity (molar %)	Aromaticity (mass %)	$\chi_{edge,min}$	$\chi_{edge,max}$	$n_{C,min}$
1	86	81	69	0.46	0.70	12
2	92	75	64	0.48	0.81	9
3	93	60	46	0.56	1.23	4
4	114	62	50	0.52	1.13	5
5	80	85	73	0.19	0.37	44
6	80	92	87	0.39	0.47	27
7	79	78	67	0.43	0.70	12
8	64	87	76	0.36	0.52	22
9	93	87	78	0.39	0.54	21
11	83	84	72	0.19	0.39	39
13	116	94	89	0.44	0.51	23
14	74	85	77	0.39	0.56	19
15	75	88	78	0.35	0.49	25

Table 18. NMR C functionality fractions ($\chi_{funcitonality}$), fractions of aromatic edge carbons (χ_{edge}) and minimum number of carbons per aromatic cluster ($n_{C,min} = 6/\chi_{edge,max}^2$), and relative aromatic-to-alkyl proton ratio (H_{arom}/H_{alk}) in biochars.

Biochar #	χ_{C-H}	χ_{C-O}	$\chi_{edge,min}$	χ_{alkyl}	$\chi_{C=O}$	$\chi_{edge,max}$	$n_{C,min}$	H_{arom}/H_{alk}
1	0.32	0.14	0.46	0.12	0.11	0.70	12	1.2
2	0.33	0.15	0.48	0.22	0.11	0.81	9	0.8
3	0.38	0.18	0.56	0.52	0.16	1.23	4	0.4
4	0.34	0.18	0.52	0.47	0.14	1.13	5	0.4
5	0.12	0.07	0.19	0.11	0.07	0.37	44	0.7
6	0.31	0.08	0.39	0.08	0.01	0.47	27	2.2
7	0.27	0.16	0.43	0.17	0.11	0.70	12	0.8
8	0.24	0.12	0.36	0.08	0.07	0.52	22	1.4
9	0.29	0.11	0.39	0.08	0.06	0.54	21	1.7
11	0.11	0.09	0.19	0.12	0.08	0.39	39	0.6
13	0.37	0.07	0.44	0.05	0.02	0.51	23	4.0
14	0.26	0.12	0.39	0.11	0.06	0.56	19	1.1
15	0.25	0.10	0.35	0.08	0.06	0.49	25	1.6

As in FTIR, fast pyrolysis biochars showed the largest signals of oxygen-containing groups, among which aromatic C-O (phenolic and aromatic ether moieties) and carbonyl (C=O) groups were the most prominent (see Figures 33 and 35). No distinct COO peaks were seen near 170 ppm for pyrolysis biochars, while the gasification biochars showed relatively sharp COO signals. Biochar 3 showed the most oxygen-containing functional groups, with sharp peaks characteristic of the sugar rings in the

cellulose of the feedstock, indicating incomplete pyrolysis as discussed in a previous paper.[39]

The analysis of the edge fractions in Tables 17 and 18 showed large minimum cluster sizes (>39 carbons) for the gasification biochars, consistent with the result in our previous paper.[25] Fast pyrolysis biochars had minimum cluster sizes of >21 C, slightly smaller than those of slow pyrolysis biochars.

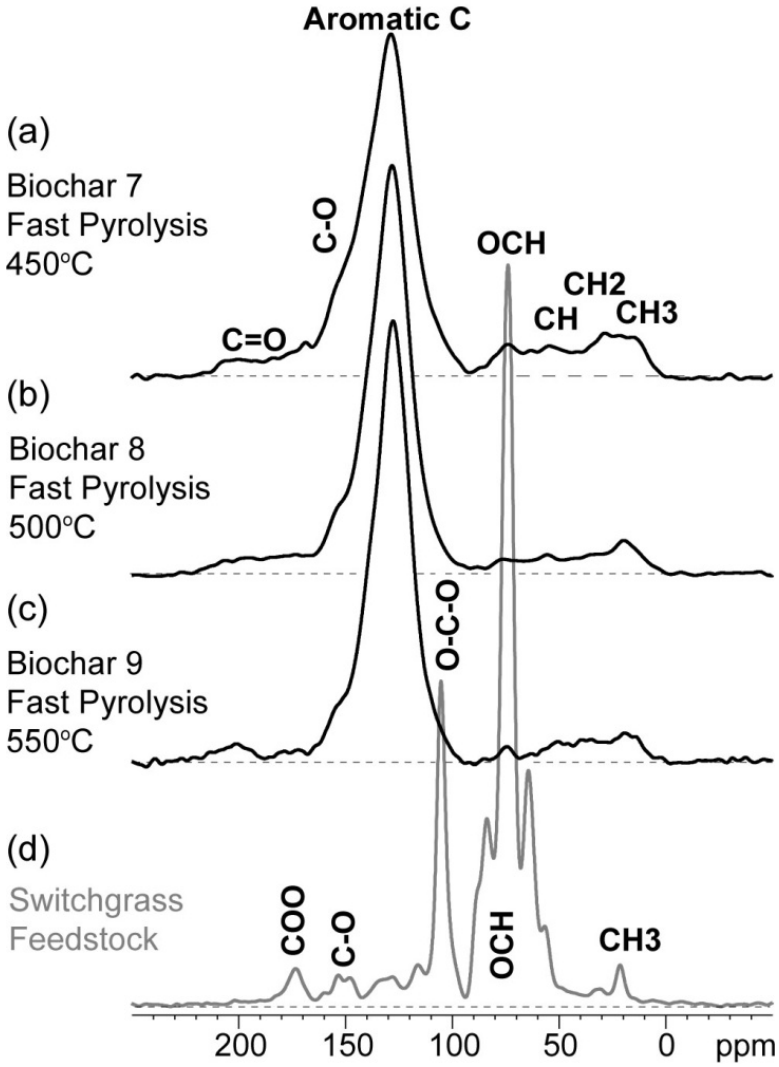

Figure 35. Semi-quantitative ^{13}C NMR with ^{1}H-^{13}C cross polarization and total suppression of spinning sidebands (CP/TOSS) at 7 kHz MAS, of switchgrass and switchgrass biochars. (a-c) Switchgrass fast pyrolysis biochars produced at 450, 500, and 550°C. (d) Fresh switchgrass feedstock.

5.3.4 Biochar Extractable Cations

The extractable cations from the biochars consisted of mostly Ca, K, and Mg, with lesser amounts of Na, Mn, Ba, Fe, and Sr (see Table 19). Relative total amounts of cations in biochars followed the general pattern of switchgrass gasification biochars > corn stover and switchgrass fast pyrolysis biochars > corn stover gasification biochar > slow pyrolysis and wood-derived biochars. A reddish-brown color was observed only in the extract solutions from the fast pyrolysis biochars that remained after filtration, indicating the presence of dissolved species, most likely dissolved organic compounds.

Table 19. Concentrations of extractable/exchangeable cations (in units of meq 100g soil^{-1}) present in biochar measured by extracting one sample of each biochar (1.5 g) with 0.5 M ammonium acetate solution (15 ml) adjusted to pH = 7.0 [44]. Filtered solutions were analyzed by inductively-coupled plasma atomic emission spectroscopy (ICP-AES). Analysis of Biochar 13 was repeated to qualitatively evaluate repeatability. BDL = below detection limits.

Biochar #	Ba	Ca	Fe	K	Mg	Mn	Na	Sr
1	0.03	31	0.01	25	21	0.11	0.6	0.04
2	0.03	29	0.04	42	22	0.10	0.2	0.03
3	0.03	28	0.06	40	24	0.09	0.4	0.02
4	0.02	28	0.09	44	25	0.10	0.4	0.02
5	0.01	44	BDL	18	12	0.07	0.7	0.01
6	0.01	12	0.01	9	5	0.08	0.3	0.01
7	0.03	20	0.01	41	17	0.35	0.3	0.05
8	0.03	20	0.01	35	14	0.30	0.3	0.04
9	0.03	22	BDL	45	17	0.29	0.3	0.05
10	0.06	43	BDL	71	29	0.12	2.8	0.06
11	0.05	72	BDL	59	26	0.11	2.3	0.05
12	0.02	89	BDL	53	12	0.01	2.3	0.04
13 (1)	0.01	8	BDL	9	2	0.05	0.3	0.01
13 (2)	0.02	11	0.01	14	3	0.08	0.3	0.01
14	0.03	15	BDL	8	2	0.06	1.0	0.02
15	0.12	42	BDL	4	1	0.33	0.3	0.08
16	0.05	32	BDL	6	4	0.27	1.4	0.04
17	0.02	6	0.01	4	1	0.05	1.5	0.01

5.3.5 Soil pH, EC and CEC effects

Table 20 shows the soil pH of the biochar amended soils after 8 weeks of incubation. Values were in the neutral range (pH =6.0-7.2) and were highest for gasification biochars (pH = 6.6-7.2), followed by slow pyrolysis biochars (pH = 6.3-7.0). Soils amended with biochar and urea tended to have lower pH after 8 weeks than soils amended with only biochar, mostly likely due to nitrification of the urea. Table 20 shows the electrical conductivity (EC) of the first water rinse leachate from the biochar amended soils. EC is an indicator of the amounts of soluble ions in the soil. Soils amended with switchgrass gasification biochars had the highest EC (406-539 µS cm^{-1}), followed by switchgrass and corn stover fast pyrolysis biochar-amended soils (141-361 µS cm^{-1}); soils amended with wood-derived biochars had the lowest EC values (143-283 µS cm^{-1}), reflecting the extractable cation concentrations measured in the biochars. Soils amended with urea tended to have higher EC than unamended soils. Table 20 shows the cation exchange capacity (CEC) of the biochar-amended soils. The CEC of the unamended soil was relatively high (26 meq 100 g $soil^{-1}$). There was only slight variation between the biochar amendments (soil CEC = 23.7-26.5 meq 100 g $soil^{-1}$) and no distinguishable correlations between biochar feedstock or process conditions and resulting soil CEC.

5.4 Discussion

5.4.1 Biochar Selection for Nicolett Soil

The criteria used to selection biochars for a field study are dependent on the soil being amended and the goals of applying the biochar. A desirable biochar for the Nicolett soil was defined here as one that would bring the soil pH closer to neutral, increase the soil CEC and return nutrients that were removed during biomass harvest, without exceeding a biochar volatile matter content of 20%[32] and an O:C ratio of 0.2.[26] All of the biochars that exceeded one or both of the volatile matter content or O:C ratio numbers (Biochars 2, 3, 4, 7 and 17) had experienced the shortest reactor residence times. Soils amended with Biochars 3 and 17, however, did have the highest CEC values, mirroring results seen in another study on low temperature biochars.[46] Biochar 3

was ultimately selected because it would provide an opportunity to collect more data on high volatile matter/high O:C ratio biochar amendment effects.

Table 20. Soil pH at a 1:5 soil: water ratio, electrical conductivity of water leachate, and cation exchange capacity of soils amended with biochars, with and without urea amendment. Within a column, data from soils amended with biochar and urea labeled with different letters are significantly different at the $p<0.05$ level (n=4). Data from unamended and no-urea soil controls (n=1) were not included in the statistical analysis.

Soil + biochar #	**pH (1:5)**		**Electrical conductivity (µS cm^{-1})**		**Cation exchange capacity (meq 100 g soil^{-1})**	
	With urea	No urea control	With urea	No urea control	With urea	No urea control
1	6.15 h	6.5	357 d	191	25.2 cde	25.8
2	6.35 ef	6.7	310 f	154	25.6 bcd	26.0
3	6.30 f	6.6	290 g	141	26.5 a	27.8
4	6.43 de	6.5	289 g	155	25.5 bcd	27.1
5	6.68 c	6.9	293 fg	335	25.6 bcd	26.7
6	6.25 g	6.5	270 hi	194	25.0 de	27.3
7	5.98 i	6.2	297 fg	274	26.2 ab	27.9
8	6.20 g	6.6	335 e	195	25.5 bcd	25.7
9	6.40 e	6.7	361 d	191	25.6 bcd	27.5
10	6.93 b	6.9	539 a	406	26.2 ab	26.8
11	7.03 a	7.0	518 b	467	25.1 cde	25.3
12	7.00 ab	7.2	464 c	416	24.6 e	26.7
13	6.50 c	7.0	230 kl	163	26.0 ab	27.9
14	6.35 ef	6.3	257 ij	237	25.8 abc	26.4
15	6.75 c	6.5	245 jk	151	23.7 f	25.4
16	6.68 c	6.6	223 l	143	25.0 de	24.6
17	6.20 gh	6.2	283 gh	145	26.4 a	26.2
No biochar control	6.1	6.1	172	281	26.3	26.1

Amendment with all three biochars from switchgrass gasification (Biochars 10, 11 and 12) resulted in large increases in soil pH and EC relative to the other biochars. From this set, Biochar 10 was selected since it also had a relatively high CEC and surface area, two traits in addition to nutrient content that had shown positive results in

another study using gasification biochar.[47] The final two biochars selected were Biochars 13 and 15: both had positive effects on soil pH and their selection would allow for a field comparison to be made between slow pyrolysis (Biochar 13), gasification (Biochar 10), and kiln carbonization (Biochar 15) biochars.

5.4.2 Unique Nature of Kiln-Produced Biochars

At first glance, Biochar 15's properties and NMR spectrum suggest that it is similar to slow pyrolysis biochars. Biochar 15's FTIR spectrum and sparking observed during NMR analysis, on the other hand, suggest that it is more similar to gasification biochars. We propose that the presence of oxygen used to drive the heat-generating combustion processes in commercial kilns creates unique biochars whose properties represent a combination of slow pyrolysis and gasification biochar properties. For example, Biochar 15 is similar to the slow pyrolysis biochars made at similar temperatures (Biochars 6 and 13) in its aromaticity and minimum number of carbons in aromatic ring clusters derived from the NMR spectra. Biochar 15 is similar to the gasification chars made in a similar reaction atmosphere (Biochars 5 and 11) in the lack of O-H and C-H stretches in the FTIR spectra, C-O functional groups by NMR, and amended soil pH. Future characterization work needs to focus on differentiating between the effects of oxygen in the reaction atmosphere and the effects of residence time on the degree of carbonization. Biochar made in kilns will likely be the most available in large quantities at this stage of the biochar industry's development due to the maturity of kiln technology.[48] Biochars from these processes, however, should be considered separately from slow pyrolysis or gasification biochars because their process temperatures will be similar to slow pyrolysis, reaction atmosphere oxygen contents will be similar to gasification, and their residence times will vary. We propose the following six-process classification grouping for biochar-producing processes based solely on their resulting biochar properties and carbon chemistry: torrefaction, slow pyrolysis, fast pyrolysis, flash pyrolysis, kiln carbonization and gasification. The characteristic reaction conditions for each process are outlined in Table 21. This grouping aims to account for effects of temperature, which has been found to be critical in relation to biochar properties,[49, 50] residence time, and oxygen content. This proposed grouping is

complementary to current schemes to differentiate thermochemical processes[51] and to classify biochars.[52]

Table 21. Proposed classification scheme for thermochemical processes based on their reaction conditions that affect the chemical properties of the biochars produced.

Thermochemical process	**Reaction temperatures**	**O_2 in reaction atmosphere**	**Heating rate**	**Residence time**	**Reaction pressure**
Torrefaction	Low	None or some	Slow	Long	Atmospheric
Slow pyrolysis	Moderate	None	Slow	Long	Atmospheric
Fast pyrolysis	Moderate	None	Very fast	Very short	Atmospheric
Flash pyrolysis	Moderate	Some	Fast	Short	Elevated
Kiln carbonization or "low-temp gasification"	Moderate	Some	Slow to moderate	Long	Atmospheric
Gasification	High	Some	Moderate to fast	Short	Atmospheric or elevated

5.4.3 Aromaticity and Fixed Carbon Fraction Correlation

Biochar's degree of aromaticity is believed to strongly influence its chemical stability.[53] Unfortunately, aromaticity is frequently measured by NMR, which requires sophisticated equipment and significant time. If aromaticity is to be used as a biochar assessment, a less expensive and more rapid measurement technique is desirable. Here, aromaticity from NMR analysis was plotted against the fixed carbon fraction (fixed carbon / (volatiles + fixed carbon)) obtained from proximate analysis, shown as unfilled shapes in Figure 36. A better correlation was obtained when biochar aromaticity was recalculated on a mass basis, shown as filled shapes in Figure 36 and tabulated in Table 17. This was done by multiplying the carbon fractions from NMR analysis (see Table 16) by the relative mass each carbon fraction would have if the O and H were included. For example, the non-protonated fraction is multiplied by 1 because it contains only C, while the C=O fraction is multiplied by a mass weighting factor of 2.3 to account for the added mass of one O ((12 g mol^{-1} C + 16 g mol^{-1} O) / 12 g mol^{-1} C = 2.3). Biochar 1, therefore, would have a ^{13}C molar basis aromaticity of 81% and a mass basis aromaticity of 69% (see Table 17). Using this mass-based method, an almost direct correlation can be seen between NMR aromaticity and proximate analysis fixed carbon

fraction (also mass based). This correlation provides evidence that fixed carbon can serve as a proxy for aromaticity when NMR analysis is not available. Grouping the biochars by the amount of oxygen present in the reaction atmosphere, the data from this study also shows a stronger correlation for the slow and fast pyrolysis biochars (no oxygen) than the correlation for the gasification and kiln carbonization biochars (some oxygen) (see Figure 36). A direct correlation would yield a trend line of y = 100*x. Trend lines for the pyrolysis biochars (n = 10) were y = 87*x + 21 (R^2 = 0.967) for the molar basis aromaticity and y = 108*x - 2 (R^2 = 0.990) for the mass basis aromaticity. Trend lines for the gasification/kiln biochars (n = 3) were y = 97*x + 8 (R^2=0.823) for the molar basis aromaticity and y = 163*x - 55 (R^2 = 0.824) for the mass basis aromaticity.

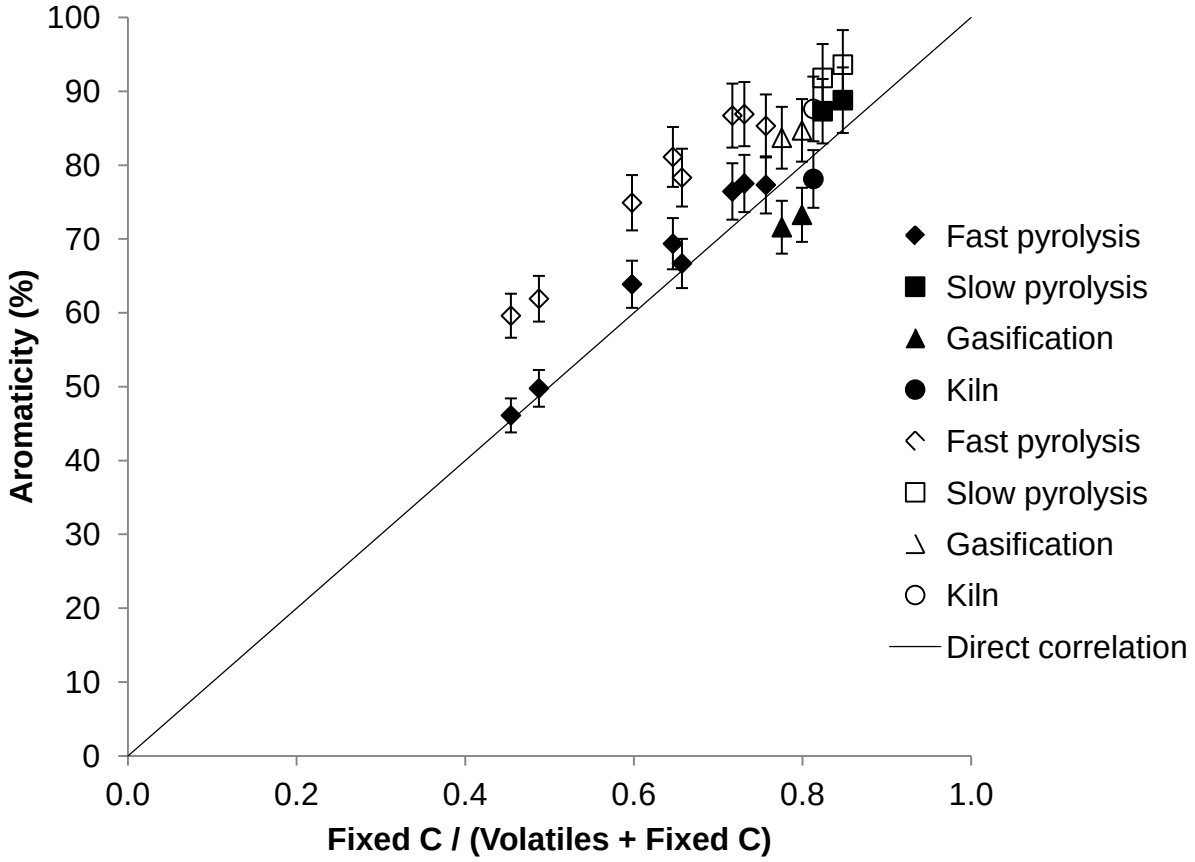

Figure 36. Biochar aromaticity from quantitative NMR analysis as a function of fixed carbon fraction from proximate analysis. Unfilled shapes represent aromaticity calculated on a molar basis and filled shapes represent aromaticity calculated on a mass basis. The reaction atmosphere for gasification and kiln carbonization contained some oxygen, while slow and fast pyrolysis occurred in an inert atmosphere.

5.4.4 Concerns about Gasification Chars

In terms of carbon stability indicators (O:C ratio, volatile matter content), soil pH, and soil EC, biochars from gasification biochars appeared favorable in this study. Some concern has been expressed, however, about biochars made at high temperatures, especially those derived from higher-ash feedstocks like switchgrass and corn stover. The high ash content of these biochars means that the biochars contain less carbon by weight and would be eligible for fewer carbon sequestration credits. The ash does contain plant nutrients (K, Ca, Mg and some micronutrients) and would exhibit a pH greater than neutral, which are generally positive traits but could be detrimental if applied in high concentrations or on an alkaline/calcareous soil.[54] In one germination study with corn seeds, the presence of growth-inhibiting organic compounds was observed in water extracts of gasification biochars; detectable amounts of polyaromatic hydrocarbons (PAH) were also observed.[55] The growth-inhibiting effects were no longer observed after the gasification biochars were further leached, suggesting the growth-inhibition may be a short-term effect. Research on a wider variety of gasification biochars is needed to determine which biochars are likely to cause negative effects and whether these effects are short-term or long-term.

5.4.5 Limitations of This Study

Two major limitations of this study are the short soil incubation period and the small number and scope of soil indicators used. Biochar has been shown to oxidize and undergo other aging reactions over time.[28, 56] Characterization of biochar before soil application, therefore, only gives that biochar's initial condition and not enough is understood about how biochar interacts with the soil environment to predict its later chemical properties. Likewise, soil pH, CEC and EC of biochar-amended soils are expected to change over time as biochar ages, ions in soil are leached or taken up by plants, nutrients are cycled and soil minerals weather. This study also made no attempt to track changes in soil physical properties such as bulk density or water retention capacity, or other plant nutrients such as available N and P, which can be the limiting factor to plant growth in some soil systems.

5.5 Conclusions

Biochar properties and their effects on soil vary widely with biochar feedstock and processing conditions. Biochar characterization and short-term soil incubations can provide some insight into the short-term effects of applying biochar that can be used to narrow down a pool of potential biochars. The characterizations and soil indicators used in this study identified four biochars that would likely show at least some positive effects when applied to a Nicolett soil and provide data to refine later selection criteria. Ideally, selection criteria would include a way to group biochars with like chemical properties through knowledge of their production processes. To that end, a six reaction grouping scheme (torrefaction, slow pyrolysis, fast pyrolysis, flash pyrolysis, kiln carbonization and gasification) was proposed to differentiate between slow pyrolysis and kiln-produced biochars, which were shown here to have very different properties that are believed to depend on the presence of oxygen in the reaction atmosphere.

Acknowledgements

Financial support for this research was provided by a National Science Foundation Graduate Research Fellowship (Brewer). The authors would like to thank the following for their assistance on various aspects of the analysis process: CSET colleagues for providing biochar samples and process information, CSET staff and undergraduates on CHNS, John McClelland and Roger Jones on FTIR-PAS, Yan-Yan Hu on NMR, Maggie Lampo, Bernardo Thompson, and Mike Cruse on setting up the soil incubation and preparing samples, Dedrick Davis on water holding capacity, and Pierce Fleming and David Laird on CEC.

Literature Cited

1. Glaser, B.; Lehmann, J.; Zech, W., Ameliorating physical and chemical properties of highly weathered soils in the tropics with charcoal - a review. *Biol. Fertil. Soils* **2002,** 35, (4), 219-230.
2. Laird, D. A., The charcoal vision: A win-win-win scenario for simultaneously producing bioenergy, permanently sequestering carbon, while improving soil and water quality. *Agronomy Journal* **2008,** 100, (1), 178-181.
3. Novak, J. M.; Busscher, W. J.; Laird, D. L.; Ahmedna, M.; Watts, D. W.; Niandou, M. A. S., Impact of biochar amendment on fertility of a Southeastern Coastal Plain soil. *Soil Science* **2009,** 174, (2), 105-112.

4. Liang, B.; Lehmann, J.; Solomon, D.; Kinyangi, J.; Grossman, J.; O'Neill, B.; Skjemstad, J. O.; Thies, J.; Luizao, F. J.; Petersen, J.; Neves, E. G., Black carbon increases cation exchange capacity in soils. *Soil Sci. Soc. Am. J.* **2006,** 70, (5), 1719-1730.
5. Oguntunde, P. G.; Fosu, M.; Ajayi, A. E.; van de Giesen, N., Effects of charcoal production on maize yield, chemical properties and texture of soil. *Biology & Fertility of Soils* **2004,** 39, 295-299.
6. Lehmann, J., Bio-energy in the black. *Front. Ecol. Environ.* **2007,** 5, (7), 381-387.
7. Gaunt, J. L.; Lehmann, J., Energy balance and emissions associated with biochar sequestration and pyrolysis bioenergy production. *Environmental Science & Technology* **2008,** 42, (11), 4152-4158.
8. Cheng, C.-H.; Lehmann, J.; Thies, J. E.; Burton, S. D., Stability of black carbon in soils across a climatic gradient. *Journal of Geophysical Research* **2008,** 113, (G2), G02027.
9. Woolf, D.; Amonette, J. E.; Street-Perrot, F. A.; Lehmann, J.; Joseph, S., Sustainable biochar to mitigate global climate change. *Nat. Comm.* **2010,** 1, 56.
10. Okimori, Y.; Ogawa, M.; Takahashi, F., Potential of CO_2 emission reductions by carbonizing biomass waste from industrial tree plantation in South Sumatra, Indonesia. *Mitigation and Adaptation Strategies for Global Change* **2003,** 8, (3), 261-280.
11. Reijnders, L., Are forestation, bio-char and landfilled biomass adequate offsets for the climate effects of burning fossil fuels? *Energy Policy* **2010,** 37, (8), 2839-2841.
12. Roberts, K. G.; Gloy, B. A.; Joseph, S.; Scott, N. R.; Lehmann, J., Life cycle assessment of biochar systems: estimating the energetic, economic, and climate change potential. *Environmental Science & Technology* **2010,** 44, (2), 827-833.
13. Bracmort, K. S., Biochar: Examination of an Emerging Concept to Mitigate Climate Change. In Congressional Research Service: Washington, D.C., 2009.
14. Pratt, K.; Moran, D., Evaluating the cost-effectiveness of global biochar mitigation potential. *Biomass and Bioenergy* **2010,** 34, (8), 1149-1158.
15. Sohi, S.; Lopez-Capel, E.; Krull, E.; Bol, R. *Biochar, climate change and soil: a review to guide future research*; CSIRO: Glen Osmond, Australia, 2009.
16. Özçimen, D.; Ersoy-Meriçboyu, A., Characterization of biochar and bio-oil samples obtained from carbonization of various biomass materials. *Renewable Energy* **2010,** 35, (6), 1319-1324.
17. Spokas, K. A.; Reicosky, D. C., Impacts of sixteen different biochars on soil greenhouse gas production. *Ann. Environ. Sci.* **2009,** 3, 179-193.
18. Lima, I. M.; Boateng, A. A.; Klasson, K. T., Physicochemical and adsorptive properties of fast-pyrolysis bio-chars and their steam activated counterparts. *Journal of Chemical Technology & Biotechnology* **2010,** 85, 1515-1521.
19. Phan, A. N.; Ryu, C.; Sharifi, V. N.; Swithenbank, J., Characterisation of slow pyrolysis products from segregated wastes for energy production. *Journal of Analytical and Applied Pyrolysis* **2008,** 81, (1), 65-71.
20. Ryu, C.; Sharifi, V. N.; Swithenbank, J., Waste pyrolysis and generation of storable char. *International Journal of Energy Research* **2007,** 31, (2), 177-191.
21. Antal, M. J.; Mochidzuki, K.; Paredes, L. S., Flash carbonization of biomass. *Ind. Eng. Chem. Res.* **2003,** 42, (16), 3690-3699.

22. Bridgwater, A. V.; Peacocke, G. V. C., Fast pyrolysis processes for biomass. *Renewable and Sustainable Energy Reviews* **2000,** 4, (1), 1-73.
23. Sohi, S. P.; Krull, E.; Lopez-Capel, E.; Bol, R.; Donald, L. S., A review of biochar and its use and function in soil. *Advances in Agronomy* **2010,** 105, 47-82.
24. Bourke, J.; Manley-Harris, M.; Fushimi, C.; Dowaki, K.; Nunoura, T.; Antal, M. J., Do all carbonized charcoals have the same chemical structure? 2. A model of the chemical structure of carbonized charcoal. *Industrial & Engineering Chemistry Research* **2007,** 46, (18), 5954-5967.
25. Brewer, C. E.; Schmidt-Rohr, K.; Satrio, J. A.; Brown, R. C., Characterization of biochar from fast pyrolysis and gasification systems. *Environ. Prog. Sustainable Energy* **2009,** 28, (3), 386-396.
26. Spokas, K. A., Review of the stability of biochar in soils: predictability of O:C molar ratios. *Carbon Management* **2010,** 1, (2), 289-303.
27. Laird, D. A.; Brown, R. C.; Amonette, J. E.; Lehmann, J., Review of the pyrolysis platform for coproducing bio-oil and biochar. *Biofuels, Bioproducts & Biorefining* **2009,** 3, (5), 547-562.
28. Cheng, C.-H.; Lehmann, J.; Thies, J. E.; Burton, S. D.; Engelhard, M. H., Oxidation of black carbon by biotic and abiotic processes. *Organic Geochemistry* **2006,** 37, (11), 1477-1488.
29. Joseph, S.; Camps-Arberstain, M.; Blackwell, R.; Zwioloski, A.; Major, J., Characterization to commercialization: what the consumer needs to know. In *3rd International Biochar Initiative Conference*, Rio de Janeiro, Brazil, 2010.
30. Cross, A.; Sohi, S.; Borlinghaus, M., The development of a toolkit for rapid assessment and prediction of biochar stability and agronomic utility. In *3rd International Biochar Initiative Conference*, Rio de Janeiro, Brazil, 2010.
31. Hayes, M.; Byrne, C.; Kwapinski, W.; Wolfram, P.; Melligan, F.; Novotny, E.; Leahy, J. J., Development of a biochar classificaiton system based on its effect on plant growth. In *3rd International Biochar Initiative Conference*, Rio de Janeiro, Brazil, 2010.
32. Deenik, J. L.; McClellan, T.; Goro, U.; Antal, M. J.; Campbell, S., Charcoal volatile matter content influences plant growth and soil nitrogen transformations. *Soil Sci. Soc. Am. J.* **2010,** 74, (4), 1259-1270.
33. Liesch, A. M.; Weyers, S. L.; Gaskin, J. W.; Das, K. C., Impact of two different biochars on earthworm growth and survival. *Annals of Environmental Science* **2010,** 4, 1-9.
34. Zhang, A.; Cui, L.; Pan, G.; Li, L.; Hussain, Q.; Zhang, X.; Zheng, J.; Crowley, D., Effect of biochar amendment on yield and methane and nitrous oxide emissions from a rice paddy from Tai Lake plain, China. *Agriculture, Ecosystems & Environment* **2010,** 139, (4), 469-475.
35. Yuan, J. H.; Xu, R. K., The amelioration effects of low temperature biochar generated from nine crop residues on an acidic Ultisol. *Soil Use and Management* **2010**, doi: 10.1111/j.1475-2743.2010.00317.x.
36. Chan, K. Y.; Van Zwieten, L.; Meszaros, I.; Downie, A.; Joseph, S., Using poultry litter biochars as soil amendments. *Australian Journal of Soil Research* **2008,** 46, 437-444.
37. Laird, D. A.; Fleming, P. D., Impact of biochar amendments on the quality of a typical Midwestern agricultural soil. *Geoderma* **2010,** 158, 443-449.

38. Brockhoff, S. B.; Christians, N. E.; Killorn, R. J.; Horton, R.; Davis, D. D., Physical and mineral-nutrition properties of sand-based turfgrass root zones amended with biochar. *Agronomy Journal* **2010,** 102, (6), 1627-1631.
39. Brewer, C.; Hu, Y.-Y.; Schmidt-Rohr, K.; Loynachan, T. E.; Laird, D. A.; Brown, R. C., Extent of pyrolysis impacts on fast pyrolysis biochar properties. *J Environ Qual* **2012,** 41, in press.
40. Laird, D. A.; Fleming, P. D.; Karlen, D. L.; Wang, B.; Horton, R., Biochar impact on nutrient leaching from a Midwestern agricultural soil *Geoderma* **2010,** 158, 436-442.
41. Mao, J. D.; Schmidt-Rohr, K., Accurate quantification of aromaticity and nonprotonated aromatic carbon fraction in natural organic matter by 13C solid-state nuclear magnetic resonance. *Environ. Sci. Technol.* **2004,** 38, (9), 2680-2684.
42. Mao, J. D.; Hu, W. G.; Schmidt-Rohr, K.; Davies, G.; Ghabbour, E. A.; Xing, B., Quantitative characterization of humic substances by solid-state carbon-13 nuclear magnetic resonance. *Soil Sci Soc Am J* **2000,** 64, (3), 873-884.
43. Smernik, R. J.; Oades, J. M., The use of spin counting for determining quantitation in solid state 13C NMR spectra of natural organic matter: 2. HF-treated soil fractions. *Geoderma* **2000,** 96, (3), 159-171.
44. Suarez, D., Properties of Alkaline-Earth Metals. In *Methods of Soil Analysis. Part 3. Chemical Methods*, Sparks, D. L., Ed. Soil Science Society of America: Madison, WI, 1996; pp 583-584.
45. Sumner, M. E.; Miller, W. P., Cation exchange capacity and exchange coefficients. In *Methods of Soil Analysis Part 3: Chemical Methods*, 3rd ed.; Sparks, D. L., Ed. Soil Science Society of America: Madison, WI, 1996; pp 1201-1229.
46. Gaskin, J. W.; Steiner, C.; Harris, K.; Das, K. C.; Bibens, B., Effect of low-temperature pyrolysis conditions on biochar for agricultural use. *Transactions of the ASABE* **2008,** 51, (6), 2061-2069.
47. Borchard, N.; Siemens, J.; Moeller, A.; Ladd, B. M.; Amelung, W.; Utermann, J., Effects on soil properties and biomass by biochar from slow pyrolysis, fast pyrolysis and gasification. In *ASA, CSSA, SSSA 2010 International Annual Meeting*, Long Beach, CA, 2010.
48. Antal, M. J.; Gronli, M., The art, science, and technology of charcoal production. *Ind. Eng. Chem. Res.* **2003,** 42, (8), 1619-1640.
49. Keiluweit, M.; Nico, P. S.; Johnson, M. G.; Kleber, M., Dynamic molecular structure of plant biomass-derived black carbon (biochar). *Environ. Sci. Technol.* **2010,** 44, (4), 1247-1253.
50. Zimmerman, A. R., Abiotic and microbial oxidation of laboratory-produced black carbon (biochar). *Environ. Sci. Technol.* **2010,** 44, (4), 1295-1301.
51. Bridgwater, A. V., IEA Bioenergy 27th update. *Biomass Bioenerg.* **2007,** 31, (4), VII-XVIII.
52. Joseph, S.; Peacocke, C.; Lehmann, J.; Munroe, P., Developing a Biochar Classification and Test Methods. In *Biochar for Environmental Management Science and Technology*, Lehmann, J.; Joseph, S., Eds. Earthscan: London, 2009.
53. Krull, E. S.; Baldock, J. A.; Skjemstad, J. O.; Smernik, R. J., Characteristics of Biochar: Organo-chemical Properties. In *Biochar for Environmental Management Science and Technology*, Lehmann, J.; Joseph, S., Eds. Earthscan: London, 2009.

54. Mozaffari, M.; Russelle, M. P.; Rosen, C. J.; Nater, E. A., Nutrient supply and neutralizing value of alfalfa stem gasification ash. *Soil Science Society of America Journal* **2002,** 66, (1), 171-178.
55. Rogovska, N. P.; Laird, D. A.; Cruse, R. M.; Trabue, S.; Heaton, E., Methods for assessing biochar quality. *J. Environ. Qual.* **2012**, in press.
56. Cheng, C.-H.; Lehmann, J.; Engelhard, M. H., Natural oxidation of black carbon in soils: Changes in molecular form and surface charge along a climosequence. *Geochimica et Cosmochimica Acta* **2008,** 72, (6), 1598-1610.

CHAPTER 6. TEMPERATURE AND REACTION ATMOSPHERE OXYGEN EFFECTS ON BIOCHAR PROPERTIES

Abstract

Biochar properties can vary widely depending on feedstock and processing conditions, which can make meaningful comparisons between biochars difficult. Biochar characterization methods can provide some useful metrics for comparisons such as van Krevelen diagrams, fixed carbon fractions, and aromatic ring cluster size estimates. One key parameter known to influence biochar properties is the highest treatment temperature (HTT) reached during the reaction; clear trends can be observed in the characteristics of slow pyrolysis biochars over the 200-800°C HTT range. These trends, however, do not hold for biochars made under slightly oxic conditions, such as in gasification and (internally heated) kiln carbonization processes. In this study, corn stover slow pyrolysis biochars were produced under both inert nitrogen and 5% oxygen atmospheres over a 200-800°C HTT range. The biochars were characterized by proximate analysis, CHN elemental analysis and solid-state ^{13}C nuclear magnetic resonance spectroscopy (NMR) to understand the combined effects of HTT and oxygen on biochar properties. The goal of the study is to determine if the presence of oxygen in the reaction atmosphere at a given HTT would be beneficial for the creation of oxygenated functional groups on biochar surfaces similar to biochars that have “aged” in the soil environment.

6.1 Introduction

Biochar, the carbonaceous solid product of biomass thermochemical processing, is a potentially beneficial soil amendment[1, 2] and carbon sequestration agent.[3-6] Biochar’s effectiveness in each application will be dependent on its properties; studies have shown that these properties vary widely with feedstock, reaction conditions, and post-production treatments.[7] One reaction condition that significantly affects biochar properties is the maximum temperature reached during pyrolysis, referred to as the highest treatment temperature (HTT). Among the properties

affected by HTT are biochar yield, carbon content, ash content, elemental ratios, fixed and labile carbon fractions, carbon surface functionality, pH, cation exchange capacity, surface area, aromaticity, polycyclic aromatic hydrocarbon (PAH) content, extractable humic and fulvic acids, and electrical conductivity.[8-24] For slow pyrolysis biochar created under a carefully controlled inert atmosphere, clear trends can be observed in biochar properties over the 200-800°C HTT range.[10, 13, 21, 22] When the reaction atmosphere contains some oxygen, however, biochar properties have been observed to deviate from these trends. For example, red pine biochars produced in open crucibles in a semi-sealed furnace had relatively low O:C and H:C elemental ratios compared to other biochars made at similar temperatures under a nitrogen environment.[19] A mixed hardwood biochar produced in a commercial, internally-heated kiln at 400°C exhibited little H-C or O-C functionality by infrared spectroscopy (FTIR), similar to biochars produced by gasification at much higher temperatures.[11, 25] One goal of this study was to elucidate the effects of oxygen in the reaction environment on biochar properties in comparison to the effects of HTT so that atmospheric oxygen and temperature can be considered separately when selecting production conditions.

Biochar properties are dynamic in the soil environment. Several studies have shown the gradual formation of oxygen-containing functional groups on biochar surfaces over time in soils; these O-containing functional groups are believed to contribute to increased biochar-soil interactions, especially biochar cation exchange capacity (CEC).[26-28] Likewise, biochars made at lower temperatures that retained more O-containing acid functional groups were shown to have higher CECs than biochars made at higher temperatures.[29] For this reason, it may be desirable to produce biochars with a greater number of O-containing functional groups directly from the reactor rather than wait for these functional groups to develop over time. A second goal of this study was to determine if oxygen in the reaction environment would lead to such an increase in O-containing functional groups.

6.2. Materials and Methods

6.2.1 Feedstock

Corn stover (*Zea mays* L.) was obtained from the Iowa State University BioCentury Research Farm (Boone, IA) and dried to <10% moisture. Corn stover was ground using a Retsch SM200 cutting mill (Newton, PA) and sieved to a 212-500 µm particle size using a Ro-Tap Model B sieve shaker (W.S. Tyler, Mentor, OH).

6.2.2 Biochar Production

Corn stover slow pyrolysis biochars were produced at seven levels of HTT: 200, 300, 400, 500, 600, 700 and 800°C, and under two reaction gas compositions: nitrogen and a 5% oxygen/ 95% nitrogen mixture, for a total of 14 biochars. Biochars are identified here using their HTTs followed by N_2 or O_2 to indicate the reaction gas. (For example, 300 O_2 represents biochar made at 300°C under the O_2/N_2 gas mix atmosphere.)

Biochars were produced in a stainless steel box reactor (24 cm x 14 cm x 15 cm). Corn stover (75 g) was spread in the bottom of the reactor, creating a layer approximately 1 cm thick. A stainless steel lid was placed snuggly on top; the lid contained two 7 mm diameter perforations to allow a thermocouple wire and purge gas tubing to be inserted, as well as six smaller (0.8 mm diameter) perforations to allow volatiles to escape during pyrolysis. The box reactor was placed in a programmable Thermo Scientific Lindberg/Blue M Moldatherm box furnace (Fisher Scientific, Pittsburgh, PA). A thermocouple wire was inserted into the corn stover layer just above the bottom of the reactor and biomass temperatures were recorded every minute during the reaction using an EX540 multimeter (Extech Instruments, Nashua, NH). A gas purge line was also inserted into the corn stover layer to ensure positive gas pressure in the reactor throughout the reaction.

Prior to heating, the reactor was purged for 15 min with the reaction gas at a rate of 1.5 L min^{-1}. The following heating program was then used: heat from 20°C to HTT-50°C over 50 min, hold at HTT-50°C for 70 min, heat from HTT-50°C to HTT over 30 min, and hold at HTT for 90 min. (The hold time at HTT-50°C was used to

prevent the furnace from overshooting the desired HTT.) Once the heating program was complete, the furnace was turned off and the purge gas switched to nitrogen at a flow rate of 500 ml min^{-1}; the biochar sample was allowed to cool overnight under nitrogen, then removed from the reactor and stored in sealed containers.

6.2.3 Biochar Characterization

Biochars were characterized using proximate analysis, elemental analysis and solid-state ^{13}C nuclear magnetic resonance spectroscopy (NMR). Moisture, volatiles, fixed C, and ash contents of the biochars were determined on a TGA 1000 (Navas Instruments, Conway, SC) based on the ASTM D1762-84 proximate analysis method.[30] Samples were heated under nitrogen to constant weight at 105°C for moisture, ramped up to 950°C (32 °C min^{-1}) and held for 6 min under nitrogen for volatiles, then, after cooling the furnace to 600°C under nitrogen, ramped up to 750°C (16 °C min^{-1}) in air to constant weight for ash. Elemental analysis was performed using a TRUSPEC-CHN analyzer (LECO Corporation, St. Joseph, MI). Oxygen content was determined by difference. Solid-state ^{13}C nuclear magnetic resonance spectroscopy (NMR) experiments were performed on a Bruker DSX400 spectrometer (Bruker Biospin, Karlsruhe, Germany) at 100 MHz for ^{13}C and 400 MHz for ^{1}H. Qualitative biochar spectra and T_1 relaxation time estimates were obtained using ^{13}C cross polarization magic angle spinning with total suppression of spinning sidebands (CP/MAS/TOSS); samples were analyzed in 4-mm MAS rotors at a spinning speed of 7 kHz with 0.5 s recycle delay, 4 µs ^{1}H 90° pulse length and 1 ms CP contact time. A ^{13}C chemical shift anisotropy (CSA) filter was used to separate the signals of the anomeric/alkyl carbons from those of the aromatic carbons for the 300 N_2 and 300 O_2 biochars.[31] The ^{1}H 90° pulse length was 4 µs, the contact time was 1 ms, and the CSA filter time was 70 µs. Quantitative biochar spectra were obtained using ^{13}C direct polarization (Bloch decay) magic angle spinning (DP/MAS) NMR in 4-mm MAS rotors at a spinning speed of 14 kHz with 75 s recycle delay, 4.5 µs 90° ^{13}C pulse length, and a Hahn echo to avoid baseline distortions.[32] The ^{13}C chemical shifts were referenced to tetramethylsilane using the

COO^- resonance of glycine at 176.49 ppm as a secondary reference. To acquire the spectra of the non-protonated C fraction, DP/MAS with recoupled ^1H-^{13}C dipolar dephasing (DP/GADE) was used (68 µs dephasing time).[32]

6.3 Results

Biochar yields and proximate analysis results are shown in Table 22. As expected, biochar yields decreased between 200 and 500°C, then leveled off slightly at the higher temperatures. Yields for the O_2 biochars were lower than those for the N_2 biochars made at the same temperature, with differences of 30-92 g kg^{-1}. Volatiles decreased, and fixed C and ash generally increased with increased HTT. The dry, ash-free fixed C fraction of the biochars, which has been used as a proxy for aromaticity and extent of pyrolysis,[11] is shown in Figure 37 as a function of HTT. The fixed C fraction of the N_2 biochars increased, especially between 200-500°C, then leveled off with increasing HTT; the fixed C fraction of the O_2 biochars followed this same general pattern, with the exception of biochar 500 O_2. The reason for this deviation is unknown.

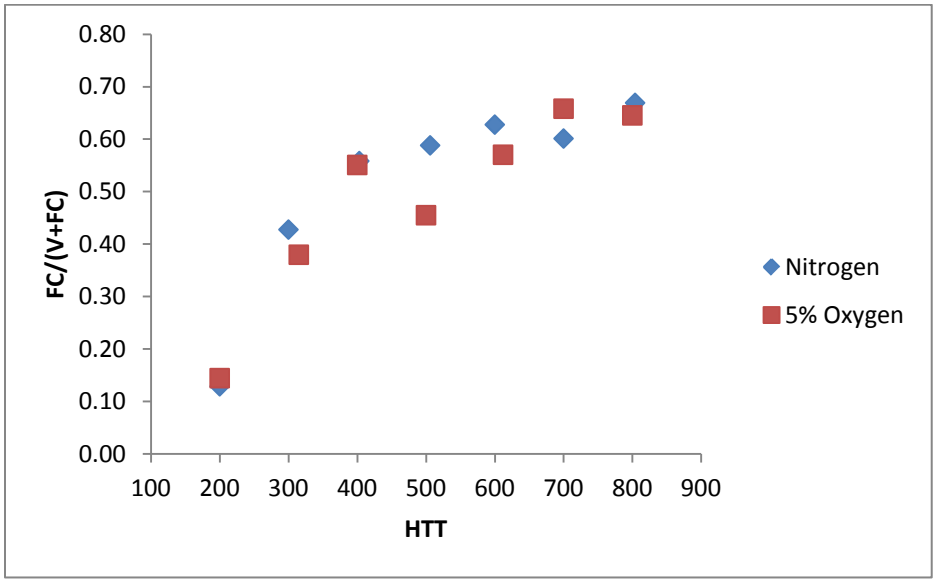

Figure 37. Biochar fixed carbon (FC/(V+FC)) fraction on a dry, ash free basis compared to highest heating temperature (HTT) reached during the slow pyrolysis production process.

Table 22. Yields and proximate analysis results for corn stover slow pyrolysis biochars. Yield and moisture reported on a wet basis; volatiles, fixed carbon and ash reported on a dry basis.

Biochar	Yield (g kg^{-1})	Moisture (g kg^{-1})	Volatiles (g kg^{-1})	Fixed C (g kg^{-1})	Ash (g kg^{-1})
200 N_2	878	19	837	124	39
300 N_2	413	12	526	393	81
400 N_2	305	13	392	496	112
500 N_2	268	34	359	513	127
600 N_2	255	29	324	548	128
700 N_2	253	18	324	489	187
800 N_2	246	24	284	576	140
200 O_2	848	10	819	139	42
300 O_2	364	18	546	334	120
400 O_2	239	11	384	471	145
500 O_2	176	25	419	350	231
600 O_2	180	82	343	456	201
700 O_2	189	24	280	539	181
800 O_2	165	25	281	512	207

Results from the elemental analysis of the biochars are shown in Table 23. In general, carbon content increased, and hydrogen and oxygen content decreased with increasing HTT; nitrogen content remained relatively stable. A van Krevelen diagram of the data, which can also be used to represent extent of pyrolysis,[33, 34] is shown in Figure 38. Data points for the N_2 biochars generally moved towards the origin with increasing HTT. The progression for the O_2 biochars was less clear, especially for the 500 O_2 biochar; O/C ratios were similar or slightly higher and H/C ratios were lower for O_2 biochars than for N_2 biochars.

Table 23. Elemental analysis results for corn stover slow pyrolysis biochars. Values reported on a dry basis. Oxygen content determined by difference (O = total – ash – C – H – N).

Biochar	C ($g\ kg^{-1}$)	H ($g\ kg^{-1}$)	N ($g\ kg^{-1}$)	O ($g\ kg^{-1}$)
300 N_2	631	48	7	233
400 N_2	686	38	7	157
500 N_2	711	30	7	125
600 N_2	752	22	6	92
700 N_2	728	9	10	66
800 N_2	767	10	7	76
300 O_2	608	33	13	227
400 O_2	655	32	13	155
500 O_2	652	24	7	87
600 O_2	664	16	6	113
700 O_2	719	9	8	83
800 O_2	694	5	9	85

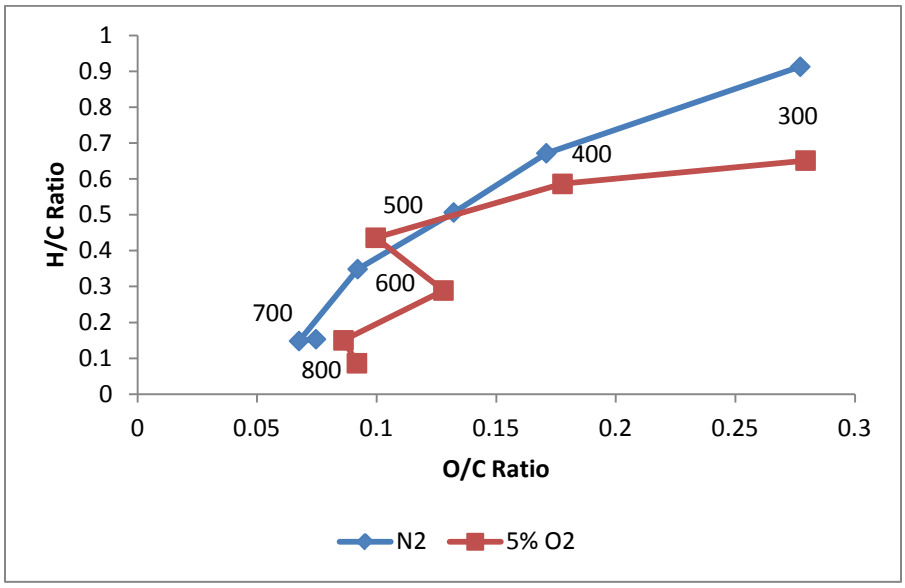

Figure 38. Van Krevelen plot for corn stover slow pyrolysis biochars made under nitrogen (N2) and 5% oxygen (O2) reaction environments. Numbers indicate HTTs in °C.

Quantitative DP/MAS spectra of the N_2 and O_2 biochars are shown in Figure 39; selective spectra of non-protonated carbons (and CH_3 groups) are also shown (thin lines). Data analysis results from the spectra are shown in Tables 24, 25 and 26. Data analysis followed methods described in a previous paper.[25] The horizontal

dashed lines in the 300°C and 400°C biochar spectra indicate the relative amounts of alkyl carbons between the N_2 and O_2 samples.

Spectra from the 200 N_2 and 200 O_2 biochars are very similar to those shown elsewhere for lignocellulosic feedstocks; almost no signal for non-protonated carbons is visible (thin-line spectra).[11, 33] For biochars made at HTTs of 400°C and higher, the NMR spectra were dominated by a peak of aromatic carbons, the majority of which were not protonated. The spectra indicate only moderate structural changes between biochars made at HTTs of 500 and 600°C for both series of biochars. The spectra for the 300°C biochars were intermediate between the characteristic "feedstock" spectra and the characteristic "biochar" spectra. A clear difference, however, can be seen between the 300 N_2 and the 300 O_2 biochar spectra with the 300 O_2 spectrum exhibiting a much greater apparent extent of pyrolysis.

Table 24. Quantitative NMR spectral analysis of corn stover slow pyrolysis biochars from DP/MAS and DP/MAS/GADE spectra. All values are % of total ^{13}C signal. $CO_{0.75}H_{0.5}$ moieties assume a 1:1 ratio of alcohols and ethers. $CH_{1.5}$ moieties assume a 1:1 ratio of CH_2 and CH groups. $C_{non\text{-}pro}$, non-protonated aromatic carbon.

Biochar	**Carbonyls**		**Aromatics**			**Alkyls**		
Moieties:	**C=O**	**COO**	**$CO_{0.75}H_{0.5}$**	**$C_{non\text{-}pro}$**	**C-H**	**$HCO_{0.75}H_{0.5}$**	**$CH_{1.5}$**	**CH_3**
ppm:	**210-183**	**183-165**	**165-145**	**145-70**	**145-90**	**90-50**	**50-25**	**25-6**
200 N_2	0.4	3.4	5.0	4.2	18.5	60.2	5.0	3.6
300 N_2	2.1	4.3	10.3	25.5	19.5	13.6	14.5	9.9
400 N_2	1.8	2.8	12.5	43.2	26.0	3.8	5.1	4.9
500 N_2	1.9	2.3	7.5	59.9	24.4	1.7	1.3	1.1
600 N_2	1.1	1.7	5.6	64.8	21.0	4.1	1.3	0.5
200 O_2	1.0	5.4	6.1	5.7	18.7	55.5	4.2	3.5
300 O_2	3.4	5.3	13.0	35.8	22.6	5.6	7.3	6.6
400 O_2	1.2	2.8	11.4	47.6	25.3	3.3	3.9	4.4
500 O_2	1.7	2.8	8.4	56.8	27.3	1.9	1.2	0.7
600 O_2	1.8	3.2	6.9	54.7	29.1	3.6	1.0	0.2

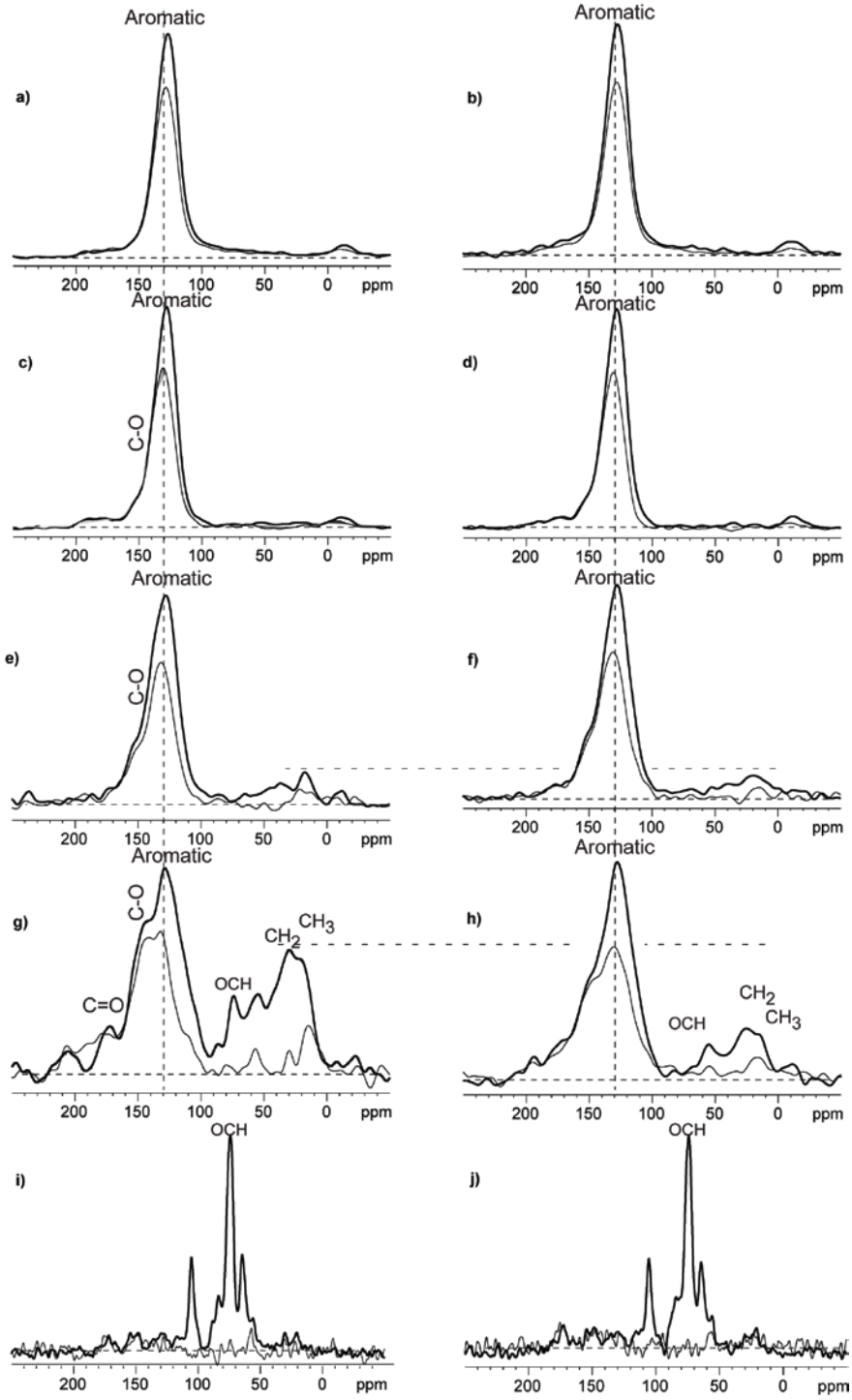

Figure 39. Quantitative ^{13}C direct polarization (DP/MAS) and direct polarization with dipolar decoupling (DP/GADE) spectra of corn stover slow pyrolysis biochars at a magic angle spinning (MAS) frequency of 14 kHz: a) 600 N_2, b) 600 O_2, c) 500 N_2, d) 500 O_2, e) 400 N_2, f) 400 O_2, g) 300 N_2, h) 300 O_2, i) 200 N_2, and j) 200 O_2. Thick line = all carbons, thin line = non-protonated carbons and methyl groups.

Table 25. NMR C functionality fractions ($\chi_{funcitonality}$), fractions of aromatic edge carbons (χ_{edge}) and minimum number of carbons per aromatic cluster ($n_{C,min} = 6/ \chi_{edge,max}^2$), and relative aromatic-to-alkyl proton ratio (H_{arom}/H_{alk}) in corn stover slow pyrolysis biochars.

Biochar	χ_{C-H}	χ_{C-O}	$\chi_{edge,min}$	χ_{alkyl}	$\chi_{C=O}$	$\chi_{edge,max}$	$n_{C,min}$	H_{arom}/H_{alk}
200 N_2	0.67	0.18	0.85	2.48	0.14	3.47	0	0.2
300 N_2	0.35	0.19	0.54	0.69	0.12	1.34	3	0.3
400 N_2	0.32	0.15	0.47	0.17	0.06	0.70	12	0.9
500 N_2	0.27	0.08	0.35	0.04	0.05	0.44	31	3.1
600 N_2	0.23	0.06	0.29	0.06	0.03	0.39	40	2.2
200 O_2	0.61	0.20	0.81	2.07	0.21	3.10	1	0.2
300 O_2	0.32	0.18	0.50	0.27	0.12	0.89	8	0.6
400 O_2	0.30	0.14	0.44	0.14	0.05	0.62	16	1.1
500 O_2	0.30	0.09	0.39	0.04	0.05	0.48	27	4.0
600 O_2	0.32	0.08	0.40	0.05	0.06	0.50	24	3.9

Semi-quantitative CP/MAS/TOSS NMR spectra for the 300, 400 and 500°C biochars, as well as the alkyl carbon spectra obtained using a CSA filter for the 300°C biochars, are shown in Figure 40. As with the DP/MAS spectra, the 400 and 500°C biochar spectra are dominated by the aromatic carbon peak, with very little remaining alkyl carbon. The peaks corresponding to contributions from the cellulose and hemicellulose fractions of the biomass (labeled OCH) can be more easily distinguished in the CP/MAS spectrum of the 300°C biochars and are consistent with the alkyl carbon spectra. The horizontal dashed lines in the 300°C and 400°C biochar spectra indicate the relative amount of alkyl carbons between the N_2 and O_2 samples.

Table 26 shows the aromaticity of the biochars calculated from the DP/MAS spectra, and an estimate of the T_1 times based on fitting a curve ($y = a*\ln(x) + b$) to data points obtained from measuring the signal remaining in the 160-110 ppm range of the CP/MAS/TOSS spectra at different CP times relative to the signal of the spectrum with a very short (1 ms) CP time. Aromaticities of the biochars generally increased over the 200-500°C range and were higher for O_2 biochars than the N_2 biochars. T_1 times reached a maximum for the 400°C biochars, but otherwise generally decreased with increased HTT and were shorter for O_2 biochars.

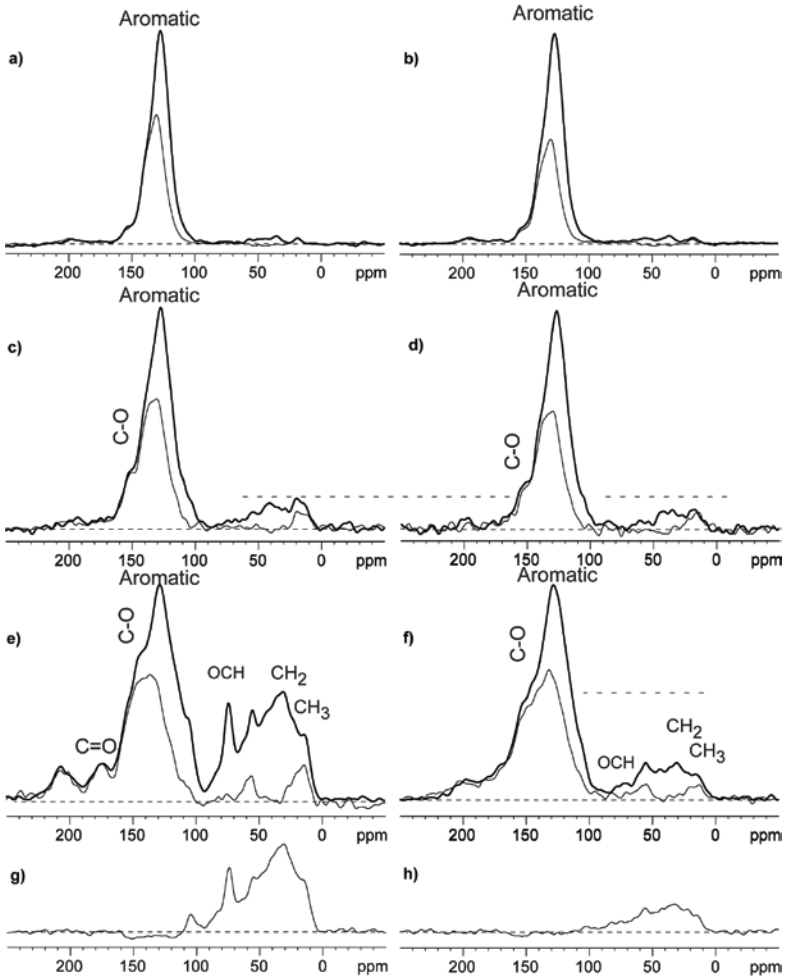

Figure 40. Semi-quantitative ^{13}C NMR with ^{1}H-^{13}C cross polarization and total suppression of spinning sidebands (CP/TOSS) at 7 kHz MAS, of corn stover slow pyrolysis biochars: a) 500 N_2, b) 500 O_2, c) 400 N_2, d) 400 O_2, e) 300 N_2, f) 300 O_2, g) 300 N_2 alkyl carbons using CSA filter and h) 300 O_2 alkyl carbons using CSA filter. Thick line = all carbons, thin line = non-protonated carbons and methyl groups (obtained using dipolar decoupling (CP/GADE)).

Table 26. Aromaticity based on quantitative DP/MAS NMR analysis and estimated T_1 relaxation times based on CP/MAS NMR analysis of corn stover slow pyrolysis biochars.

Biochar	Aromaticity (%)	T_1 (s)
200 N_2	27.7	
300 N_2	55.3	40.8
400 N_2	81.7	47.2
500 N_2	91.8	5.1
600 N_2	91.4	1.5
200 O_2	30.5	
300 O_2	71.4	20.4
400 O_2	84.3	33.5
500 O_2	92.5	5.1
600 O_2	90.7	2.2

6.4 Discussion

6.4.1 Effects of HTT and Atmospheric Oxygen Content

Trends in the N_2 biochar properties with increased HTT were consistent with those observed in other studies: decreased biochar yields, volatiles content, O/C and H/C ratios and the number of functional groups, and increased aromaticity, fixed carbon and ash content. The overall effect of the addition of 5% oxygen to the reaction atmosphere seems to be an increase in “apparent HTT” since increased atmospheric oxygen content resulted in decreased biochar yields, H/C ratios and the number of functional groups, and increased aromaticity and ash content. This increase in apparent HTT is most clear for the 300 and 400°C biochars. On the other hand, volatiles content increased and fixed carbon content decreased (on a dry, ash-free basis) with increased atmospheric oxygen for five of the seven HTTs, which would suggest a lower extent of pyrolysis. Very little information on the effects of pyrolysis reaction atmosphere oxygen is available in the literature. Spokas, et al. found that the presence of oxygen reduced sorbed volatile organic compounds on the surfaces of biochars, but otherwise did not comment on the properties of the biochars.[35]

In regards to O-containing functionality in the biochars, O/C ratios were approximately the same or increased slightly with increased atmospheric oxygen content. From the NMR data, alkyl alcohol and ether functionalities ($HCO_{0.75}H_{0.5}$) slightly decreased, aromatic alcohol and ether functionalities ($CO_{0.75}H_{0.5}$) and carbonyl (C=O) functionalities showed no apparent trend, and carboxyl (COO) functionalities slightly increased with increased atmospheric oxygen content. This COO group increase is important since an increase in total biochar acidity and overall O/C ratio has been shown to improve the ability of biochars to stabilize heavy metal cations in soil,[36] and may indicate that biochars made under slightly oxic conditions may have improved O-functional group-related soil interaction capabilities. In practical terms, however, this increase in O/C ratio and O-functional group content is small compared to the amount reported from oxidation in the soil environment.[26, 27]

Addition of oxygen to the pyrolysis atmosphere may improve biochar's hydrophilicity and therefore, its ability to increase soil water retention. Kinney, et al found that a decrease in H/C ratio was closely related to increased biochar hydrophilicity[37] and the H/C ratio decreased in biochars with increased atmospheric oxygen content at all HTTs in this study.

6.4.2 Mass Transfer Limited Combustion Reactions

For biochars produced under the 5% oxygen gas mixture, a light-gray top layer was observed when the cooled biochar was removed from the reactor. The biochar under this thin gray layer was black. We hypothesize that the oxygen in the reaction gas reacted quickly with the top layer of biomass to create combustion processes rather than diffuse through the biomass to evenly oxidize the surfaces. This may lead to different biochar properties in the gray layer than in the bulk layer and would be worth additional investigation assuming the layers could be effectively separated, perhaps with a taller narrower biomass loading to create a thicker gray layer. No effort to distinguish the layers in the analyses was made for this study.

6.4.3 Effect of Biomass Voidage on Oxygen Content in Pyrolysis Reactor

Biomass feedstock generally has a low bulk density. The oxygen in the air-filled voids within and between biomass particles is fed into a pyrolysis reactor along with the biomass and may influence the pyrolysis reaction. If air contains 20 molar % of oxygen and a biomass feedstock has a voidage of 40% (i.e. 60% of the volume filled by the bulk biomass is solids), a substantial amount (8% of the biomass volume) of oxygen could enter the reactor. Researchers attempting to carefully control pyrolysis conditions may need to account for biomass voidage oxygen or to purge biomass samples before feeding them into the reactor.

6.4.4. Pyrolysis Atmosphere Oxygen Content and Biochar Standardization

Studies have shown HTT to be a powerful predictor of biochar properties and HTT is relatively easy to measure compared to other pyrolysis reaction parameters.

For those reasons, HTT will likely be very useful for biochar standards development. HTT may provide a method to make comparisons across biochars made from the same feedstock but under vastly different reaction conditions. This study suggests that biochars made in processes that have some oxygen in the pyrolysis reaction environment, such as internally heated kiln carbonization, may be comparable to biochars made under inert slow pyrolysis conditions—just at higher apparent HTTs. The same apparent HTT principle may be applicable to biochars produced with higher heating rates, such as in fast pyrolysis, or under increased pressures.

6.5 Conclusions

Corn stover slow pyrolysis biochar produced at different HTTs showed similar trends in biochar properties as reported by other biochar studies investigating the effects of temperature. Addition of oxygen to the reaction environment appears to result in biochars with properties that one would expect from biochars made at higher temperatures; this pattern was especially apparent for biochars made at 300 and 400°C.

Addition of oxygen to the pyrolysis reaction atmosphere only very slightly increases the O/C ratio and the presence of O-containing surface functional groups in biochars. Given the importance of oxygen to drive some biochar production processes and the influence O-containing surface functional groups have been shown to have on biochar-soil interactions, the effect of oxygen in the pyrolysis reaction atmosphere on biochar properties warrants additional investigation.

Acknowledgements

Funding for this research was provided by a National Science Foundation (NSF) Research Experience for Teachers (Hall and Rudisill), hosted by the NSF Engineering Research Center for Biorenewable Chemicals (CBiRC), and an NSF Graduate Research Fellowship (Brewer). The authors would like to acknowledge Samuel Rathke for his assistance with the slow pyrolysis reactor and colleagues at

the Center for Sustainable Environmental Technologies (CSET) for their assistance with the proximate and elemental analyses.

References

1. Glaser, B.; Lehmann, J.; Zech, W., Ameliorating physical and chemical properties of highly weathered soils in the tropics with charcoal - a review. *Biol. Fertil. Soils* **2002,** 35, (4), 219-230.
2. Laird, D. A., The charcoal vision: A win-win-win scenario for simultaneously producing bioenergy, permanently sequestering carbon, while improving soil and water quality. *Agronomy Journal* **2008,** 100, (1), 178-181.
3. Lehmann, J., Bio-energy in the black. *Front. Ecol. Environ.* **2007,** 5, (7), 381-387.
4. Gaunt, J. L.; Lehmann, J., Energy balance and emissions associated with biochar sequestration and pyrolysis bioenergy production. *Environmental Science & Technology* **2008,** 42, (11), 4152-4158.
5. Woolf, D.; Amonette, J. E.; Street-Perrot, F. A.; Lehmann, J.; Joseph, S., Sustainable biochar to mitigate global climate change. *Nat. Comm.* **2010,** 1, 56.
6. Hammond, J.; Shackley, S.; Sohi, S.; Brownsort, P., Prospective life cycle carbon abatement for pyrolysis biochar systems in the UK. *Energy Policy* **2011,** 39, (5), 2646-2655.
7. Spokas, K. A.; Cantrell, K. B.; Novak, J. M.; Archer, D. W.; Ippolito, J. A.; Collins, H. P.; Boateng, A. A.; Lima, I. M.; Lamb, M. C.; McAloon, A. J.; Lentz, R. D.; Nichols, K. A., Biochar: a synthesis of its agronomic impact beyond carbon sequestration. *J Environ Qual* **2012,** 41, in press.
8. Kloss, S.; Zehetner, F.; Dellantonio, A.; Hamid, R.; Ottner, F.; Liedtke, V.; Schwanninger, M.; Gerzabek, M. H.; Soja, G., Characterization of slow pyrolysis biochars: effects of feedstocks and pyrolysis temperature on biochar properties. *J Environ Qual* **2012,** 41, in press.
9. Uchimiya, M.; Wartelle, L. H.; Klasson, K. T.; Fortier, C. A.; Lima, I. M., Influence of pyrolysis temperature on biochar property and function as a heavy metal sorbent in soil. *Journal of Agricultural and Food Chemistry* **2011,** 59, (6), 2501-2510.
10. Keiluweit, M.; Nico, P. S.; Johnson, M. G.; Kleber, M., Dynamic molecular structure of plant biomass-derived black carbon (biochar). *Environ. Sci. Technol.* **2010,** 44, (4), 1247-1253.
11. Brewer, C.; Unger, R.; Schmidt-Rohr, K.; Brown, R., Criteria to select biochars for field studies based on biochar chemical properties. *Bioenergy Res.* **2011,** 4, (4), 312-323.
12. Bruun, E. W.; Hauggaard-Nielsen, H.; Ibrahim, N.; Egsgaard, H.; Ambus, P.; Jensen, P. A.; Dam-Johansen, K., Influence of fast pyrolysis temperature on biochar labile fraction and short-term carbon loss in a loamy soil. *Biomass Bioenerg.* **2011,** 35, (3), 1182-1189.
13. Zimmerman, A. R., Abiotic and microbial oxidation of laboratory-produced black carbon (biochar). *Environ. Sci. Technol.* **2010,** 44, (4), 1295-1301.

14. Spokas, K. A., Review of the stability of biochar in soils: predictability of O:C molar ratios. *Carbon Management* **2010,** 1, (2), 289-303.
15. Kuzyakov, Y.; Subbotina, I.; Chen, H.; Bogomolova, I.; Xu, X., Black carbon decomposition and incorporation into soil microbial biomass estimated by ^{14}C labeling. *Soil Biol. Biochem.* **2009,** 41, (2), 210-219.
16. Knicker, H.; Totsche, K. U.; Almendros, G.; González-Vila, F. J., Condensation degree of burnt peat and plant residues and the reliability of solid-state VACP MAS 13C NMR spectra obtained from pyrogenic humic material. *Organic Geochemistry* **2005,** 36, (10), 1359-1377.
17. Deenik, J. L.; McClellan, T.; Goro, U.; Antal, M. J.; Campbell, S., Charcoal volatile matter content influences plant growth and soil nitrogen transformations. *Soil Sci. Soc. Am. J.* **2010,** 74, (4), 1259-1270.
18. Daud, W. M. A. W.; Ali, W. S. W.; Sulaiman, M. Z., Effect of carbonization temperature on the yield and porosity of char produced from palm shell. *Journal of Chemical Technology & Biotechnology* **2001,** 76, (12), 1281-1285.
19. Baldock, J. A.; Smernik, R. J., Chemical composition and bioavailability of thermally altered Pinus resinosa (Red pine) wood. *Org. Geochem.* **2002,** 33, (9), 1093-1109.
20. McBeath, A. V.; Smernik, R. J.; Schneider, M. P. W.; Schmidt, M. W. I.; Plant, E. L., Determination of the aromaticity and the degree of aromatic condensation of a thermosequence of wood charcoal using NMR. *Organic Geochemistry* **2011,** 42, (10), 1194-1202.
21. Trompowsky, P. M.; Benites, V. d. M.; Madari, B. E.; Pimenta, A. S.; Hockaday, W. C.; Hatcher, P. G., Characterization of humic like substances obtained by chemical oxidation of eucalyptus charcoal. *Organic Geochemistry* **2005,** 36, (11), 1480-1489.
22. Krull, E. S.; Baldock, J. A.; Skjemstad, J. O.; Smernik, R. J., Characteristics of Biochar: Organo-chemical Properties. In *Biochar for Environmental Management Science and Technology*, Lehmann, J.; Joseph, S., Eds. Earthscan: London, 2009.
23. Makoto, K.; Choi, D.; Hashidoko, Y.; Koike, T., The growth of *Larix gmelinii* seedlings as affected by charcoal produced at two different temperatures. *Biology and Fertility of Soils* **2011,** 47, (4), 467-472.
24. Peng, X.; Ye, L. L.; Wang, C. H.; Zhou, H.; Sun, B., Temperature- and duration-dependent rice straw-derived biochar: Characteristics and its effects on soil properties of an Ultisol in southern China. *Soil and Tillage Research* **2011,** 112, (2), 159-166.
25. Brewer, C. E.; Schmidt-Rohr, K.; Satrio, J. A.; Brown, R. C., Characterization of biochar from fast pyrolysis and gasification systems. *Environ. Prog. Sustainable Energy* **2009,** 28, (3), 386-396.
26. Cheng, C.-H.; Lehmann, J.; Thies, J. E.; Burton, S. D.; Engelhard, M. H., Oxidation of black carbon by biotic and abiotic processes. *Organic Geochemistry* **2006,** 37, (11), 1477-1488.
27. Cheng, C.-H.; Lehmann, J.; Engelhard, M. H., Natural oxidation of black carbon in soils: Changes in molecular form and surface charge along a climosequence. *Geochimica et Cosmochimica Acta* **2008,** 72, (6), 1598-1610.

28. Liang, B.; Lehmann, J.; Solomon, D.; Kinyangi, J.; Grossman, J.; O'Neill, B.; Skjemstad, J. O.; Thies, J.; Luizao, F. J.; Petersen, J.; Neves, E. G., Black carbon increases cation exchange capacity in soils. *Soil Sci. Soc. Am. J.* **2006,** 70, (5), 1719-1730.
29. Mukherjee, A.; Zimmerman, A. R.; Harris, W., Surface chemistry variations among a series of laboratory-produced biochars. *Geoderma* **2011,** 163, (3–4), 247-255.
30. *ASTM D1762-84 Standard Test Method for Chemical Analysis of Wood Charcoal*; ASTM International: West Conshohocken, PA, 2007; p 2.
31. Mao, J.-D.; Schmidt-Rohr, K., Separation of aromatic-carbon ^{13}C NMR signals from di-oxygenated alkyl bands by a chemical-shift-anisotropy filter. *Solid State NMR* **2004,** 26, 36-45.
32. Mao, J. D.; Schmidt-Rohr, K., Accurate quantification of aromaticity and nonprotonated aromatic carbon fraction in natural organic matter by 13C solid-state nuclear magnetic resonance. *Environ. Sci. Technol.* **2004,** 38, (9), 2680-2684.
33. Brewer, C.; Hu, Y.-Y.; Schmidt-Rohr, K.; Loynachan, T. E.; Laird, D. A.; Brown, R. C., Extent of pyrolysis impacts on fast pyrolysis biochar properties. *J Environ Qual* **2012,** 41, in press.
34. Schimmelpfennig, S.; Glaser, B., One step forward toward characterization: some important material properties to distinguish biochars. *J Environ Qual* **2012,** 41, in press.
35. Spokas, K. A.; Novak, J. M.; Stewart, C. E.; Cantrell, K. B.; Uchimiya, M.; DuSaire, M. G.; Ro, K. S., Qualitative analysis of volatile organic compounds on biochar. *Chemosphere* **2011**, (0).
36. Uchimiya, M.; Chang, S.; Klasson, K. T., Screening biochars for heavy metal retention in soil: Role of oxygen functional groups. *Journal of Hazardous Materials* **2011,** 190, (1–3), 432-441.
37. Kinney, T. J.; Masiello, C. A.; Dugan, B.; Hockaday, W. C.; Dean, M. R.; Zygourakis, K.; Barnes, R. T., Hydrologic properties of biochars produced at different temperatures. *Biomass and Bioenergy* **2012**, in press.

CHAPTER 7. CONCLUSIONS AND FUTURE WORK

7.1 Importance of Biochar Characterization

Biochars have great potential to improve soils and sequester carbon. Biochar characterization research has shown that biochar properties and their effectiveness in different applications can vary widely. Several recent biochar research reviews have identified the ability to understand feedstock and production condition relations to biochar properties and their effects as a key knowledge gap and research need.[1-3] Indeed, one of the most pressing challenges faced by the fledging biochar industry is the inability to define and measure biochar quality. The International Biochar Initiative (IBI), which will likely be a primary certification entity, and other organizations have identified the development of biochar quality and characterization standards as a key priority.[4]

7.2 General Conclusions

The results in this dissertation demonstrate that biochars from corn stover and switchgrass will present some challenges compared to biochars produced from wood, namely in their high ash content and lower surface area. These two feedstocks, however, represent the advantages offered by herbaceous energy crops and crop residues in their greater availability and lower cost. Biochars from such feedstocks need to be included in biochar research.

Likewise, biochars produced as co-products of gasification and fast pyrolysis can make valuable contributions to biochar implementation. Gasification biochars will present challenges due to their low carbon contents, high ash contents, low chemical reactivity, and potential to contain higher levels of polycyclic aromatic hydrocarbons (PAHs) and plant-growth inhibiting compounds. In spite of these challenges, biochars from gasification should not be overlooked, especially in situations when gasification technology is the most appropriate for regional energy needs. Biochars from fast pyrolysis have even higher potential: their properties are similar to biochars produced by slow pyrolysis and the bio-oil co-product from their

production may provide enough economic incentive to warrant commercial scale implementation. Concerns about unconverted biomass, high volatiles contents, and low carbon stability of fast pyrolysis biochars can be mitigated through proper design and control of fast pyrolysis reactors.

Many of the characterization methods for biochars can be borrowed from the fields of fuel charcoal, activated carbon and soil science. Research presented in this dissertation has shown how advanced ^{13}C solid state nuclear magnetic resonance spectroscopy (NMR) techniques can provide quantitative chemical composition information not available through other characterization methods. This information can be used to better understand biochar production and soil aging mechanisms and, combined with information from complementary characterization methods, to make comparisons between biochars.

7.3 Future Work

Because biochar properties are related to processing conditions and processing conditions can be controlled, there is a huge potential for biochar engineering (so-called designer biochars[5]). Future work in the area of biochar characterization will likely focus on identifying what makes a quality biochar for a specific application, and from there, how one might produce such a biochar. Research for this dissertation has focused on how best to use biochars produced from feedstocks and by processes dictated by local availability (namely those available from research at Iowa State University). Such “forward” or process-driven biochar engineering will be important as biochar research expands to new regions with new feedstocks and new pyrolysis technologies. Continued efforts in this area will likely involve work to place new biochars within a biochar standardization framework, as well as to improve the practical utility and effectiveness of standardized biochar characterization methods.

Another kind of biochar engineering that I would like to pursue in my future research is “backward” or end use-driven biochar engineering. The goal of this kind of biochar engineering is to create a biochar to solve a specific soil amendment or carbon sequestration challenge. For example, a higher-temperature slow pyrolysis

biochar might be produced to sequester the maximum amount of carbon; in this case, the achievable carbon yield and stability would outweigh the need to improve soil fertility. Such design principles could be used to create biochars that were optimized for cation exchange capacity, liming potential, microbial activity, mycorrhizal inoculation rates, heavy metal mitigation, etc.

One specific challenge I would like to address with end use-driven biochar engineering is soil plant-available water content in areas prone to intense precipitation events followed by dry periods. This challenge is already a prominent issue for agriculture and range management in several regions of the U.S. and around the world, and is expected to become especially critical as precipitation patterns are affected by climate change.[6] The goal of this research would be to understand the effects of biochar pore structure, bulk chemistry and surface chemistry on biochar's ability to improve soil water penetration during heavy precipitation events while increasing plant-available water retention in the root zone during dry periods. Several studies have shown increased water holding capacity in soils amended with biochars[7-9] and some literature is available on biochar pore structure and hydrophobicity relationships to processing conditions.[10, 11] Much more work is needed in this promising area.

References

1. Kookana, R. S.; Sarmah, A. K.; Van Zwieten, L.; Krull, E.; Singh, B., Chapter Three - Biochar Application to Soil: Agronomic and Environmental Benefits and Unintended Consequences. In *Advances in Agronomy*, Donald, L. S., Ed. Academic Press: 2011; Vol. Volume 112, pp 103-143.
2. Spokas, K. A.; Cantrell, K. B.; Novak, J. M.; Archer, D. W.; Ippolito, J. A.; Collins, H. P.; Boateng, A. A.; Lima, I. M.; Lamb, M. C.; McAloon, A. J.; Lentz, R. D.; Nichols, K. A., Biochar: a synthesis of its agronomic impact beyond carbon sequestration. *J Environ Qual* **2012,** 41, in press.
3. Lehmann, J.; Rillig, M. C.; Thies, J.; Masiello, C. A.; Hockaday, W. C.; Crowley, D., Biochar effects on soil biota - A review. *Soil Biology and Biochemistry* **2011,** 43, (9), 1812-1836.
4. *Guidelines for Specifications of Biochars for Use in Soils*; IBI-STD-0; International Biochar Initiative: www.biochar-international.org, 10 January, 2012; p 37.

5. Novak, J. M.; Lima, I. M.; Xing, B.; Gaskin, J. W.; Steiner, C.; Das, K. C.; Ahmedna, M.; Rehrah, D.; Watts, D. W.; Busscher, W. J.; Schomberg, H. H., Characterization of designer biochar produced at different temperatures and their effects on a loamy soil. *Ann. Environ. Sci.* **2009,** 3, 195-206.
6. Calizolaio, V. *Securing Water Resources for Water Scarce Ecosystems*; United Nations Convention to Combat Desertification: 2008; p 23.
7. Laird, D. A.; Fleming, P.; Davis, D. D.; Horton, R.; Wang, B.; Karlen, D. L., Impact of biochar amendments on the quality of a typical Midwestern agricultural soil. *Geoderma* **2010,** 158, (3-4), 443-449.
8. Van Zwieten, L.; Kimber, S.; Morris, S.; Chan, K.; Downie, A.; Rust, J.; Joseph, S.; Cowie, A., Effects of biochar from slow pyrolysis of papermill waste on agronomic performance and soil fertility. *Plant and Soil* **2010,** 327, (1), 235-246.
9. Novak, J. M.; Busscher, W. J.; Laird, D. L.; Ahmedna, M.; Watts, D. W.; Niandou, M. A. S., Impact of biochar amendment on fertility of a Southeastern Coastal Plain soil. *Soil Science* **2009,** 174, (2), 105-112.
10. Sun, H.; Hockaday, W. C.; Masiello, C. A.; Zygourakis, K., Multiple controls on the chemical and physical structure of biochars. *Industrial & Engineering Chemistry Research* **2012**, in press.
11. Kinney, T. J.; Masiello, C. A.; Dugan, B.; Hockaday, W. C.; Dean, M. R.; Zygourakis, K.; Barnes, R. T., Hydrologic properties of biochars produced at different temperatures. *Biomass and Bioenergy* **2012**, in press.

Appendix. Explanation of NMR Analysis Methods

A.1 Introduction

Nuclear magnetic resonance spectroscopy (NMR) uses a very strong magnetic field and radio frequency (RF) pulses to study the structure of molecules through the resonance frequencies of specific nuclei within the molecule. In order to characterize biochars, several solid-state techniques utilizing ^{13}C and ^{1}H nuclei can be used to determine the relative quantity of carbon functional groups, the approximate degree of condensation of the aromatic rings, and the overall structure of the char molecules. The following describes some of the theory of solid-state NMR and how biochars are characterized at Iowa State University. Theory information is summarized from a variety of secondary references.[1-4]

A.2 Theory

The net magnetization (**M**) of a sample is the sum of the magnetic moments of the individual nuclei in the sample molecules. Magnetic moments can be thought of as vectors, and are the products of the magnetogyric ratio (a constant different for each type of nucleus), γ, and the angular momentum, **L**, such that

$$\mathbf{M} = \gamma \mathbf{L}$$

Within a magnetic field, **B**, a torque ($\mathbf{T} = -\mathbf{M} \times \mathbf{B}$) is exerted on the magnetic moments such that:

$$d\mathbf{M}/dt = -\gamma \mathbf{M} \times \mathbf{B}$$

The uniform magnetic field applied by the superconducting magnets in an NMR experiment is typically referred to as B_0. The applied field causes the nuclei to *precess* (wobble like a spinning top) about the field at a given *Larmor frequency*:

$$\omega_0 = -\gamma B_0$$

This Larmor frequency is the fundamental frequency at which an NMR experiment is run and varies with the nuclei and the strength of the magnetic field. For example, the instrument used to characterize biochars at ISU is a Bruker DSX 400, allowing ^{1}H experiments to be performed at 400 MHz and ^{13}C experiments at 100MHz. The key concept to NMR's usefulness is that nuclei are also influenced by neighboring nuclei and their electron clouds, each of which exerts its own small magnetic field. The resulting "combined magnetic field" precession frequency of a given nuclei, ω_L, is then:

$$\omega_L = -\gamma B_{total}$$

where $B_{total} = B_0 + B_{local}$; B_{local} is the sum of the local magnetic fields. Nuclei in different environments will, therefore, precess around the strong B_0 field at slightly different frequencies, thus resulting in a detectable spectrum. The distance on the x-axis between different signals in the spectrum is called the chemical shift and it is measured in dimensionless "units" of ppm of ω_0. (The differences between nuclei frequencies are generally on the order of Hz, where the Larmor frequency is on the order of MHz, thus ppm.) As a dimensionless scale, chemical shift is measured against a reference material, typically tetramethylsilane (TMS) for ^{1}H and ^{13}C. For ^{13}C on this instrument, the chemical shift spectrum is calibrated using a carbon peak at 176.49 ppm from 25% ^{13}C-labeled glycine as a secondary reference.

A.2.1 Solution vs. Solid-State NMR

Characterizing materials in the solid state requires the use of specialized techniques to overcome several challenges. In liquid or "solution" NMR, liquid samples or samples dissolved in a liquid solvent tend to give very sharp, high resolution spectra. Three magnetic field inter-nuclear interactions in the solid-state

make high resolution NMR spectra difficult: heteronuclear dipolar couplings, homonuclear dipolar couplings and chemical shift anisotropy (CSA).

Dipolar couplings are when the magnetic fields of nuclei affect the frequency, ω_L, of other nuclei; the nuclei involved can be the same (homonuclear) or different (heteronuclear). Since dipolar coupling is a through-space interaction (and not just across chemical bonds), the numbers of possible nucleus-nucleus and nucleus-static field orientations are immense, causing the spectral peaks to broaden and overlap substantially.

Chemical shift anisotropy also causes spectral peaks to broaden and overlap but due to a different interaction. Circulating electron clouds around the nucleus create small anisotropic magnetic fields, i.e. not the same in all directions (imagine an ellipsoid). If a nucleus and its electron cloud are oriented toward the B_0 field differently than other nuclei, it will have a different resonance frequency, even if the other nuclei are the same type and in the same type of molecule. In solution NMR, molecules can move into all possible orientations and can re-orient before dipolar couplings have a chance to develop; thus, line-broadening by dipolar couplings and CSA is not so significant.

One solid-state NMR technique that helps solve both these problems is *magic angle spinning* (MAS). “Magic angle” refers to 54.74°; this angle is significant because when the angle between a dipolar coupling vector and the B_0 is equal to 54.74°, the net dipolar coupling effect is zero. Spinning a powder sample rapidly can also “average out” a sample’s CSA. Making use of these two facts, samples for solid-state analysis are commonly packed into cylindrical rotors that, buoyed by an air stream, are spun at several kHz at an angle of 54.74° relative to the instrument’s static B_0 field.

A.2.2 Direct Polarization (DP) vs. Cross Polarization (CP)

Analyzing carbonaceous solid samples to acquire a ^{13}C spectrum also requires the use of special techniques to overcome unique challenges. Carbon-13 is a relatively rare isotope of carbon, accounting for only 1.1% of all C (the rest are

carbon-12, which does not have nuclear spin). This means the carbon nuclei that can be detected in a sample are already dilute. On top of that, ^{13}C has a small γ value (i.e. it is a relatively weak nuclear magnet), ^{13}C requires relatively long relaxation times between spectral scans, and ^{13}C gives low signal intensity. Acquiring carbon spectra with high signal-to-noise ratios through direct polarization (DP) techniques is, therefore, relatively time-consuming.

Instead of polarizing the carbon nuclei directly, a technique called ^{1}H-^{13}C cross polarization (CP) is used to greatly reduce the analysis time while still acquiring qualitative/semi-quantitative high-resolution spectra that are suitable for many applications. In this technique, protons (^{1}H nuclei) are polarized and this polarization is transferred to the nearby carbon nuclei by RF irradiation for a certain cross polarization time (on the order of 1 millisecond). A pulse sequence for dipolar decoupling is then applied to the protons, and the carbon spectrum is detected. By polarizing the protons instead of the carbons directly, CP techniques take advantage of ^{1}H's much greater abundance, higher γ value, and much faster relaxation time (~45 times faster); this allows many more scans (for better signal-to-noise ratio) to be taken in a given length of time. The drawback to CP techniques for studying chars is that it cannot be considered quantitative since the polarization transfer is not the same for every carbon, especially those on the inside of large aromatic clusters and far from protons.

A.2.3 Total Suppression of Spinning Sidebands (TOSS)

Magic angle spinning (MAS), while generally effective, does not completely remove CSA effects. If the CSA broadening is comparable to the spinning frequency, peaks with smaller intensity known as spinning sidebands (ssb) appear in the spectra at frequencies to the right and left of the "main" spectrum that correspond to integer multiples of the MAS frequency. These sidebands can become a problem if they occur within the chemical shift range of other carbon signals and interfere with identifying the "real" peaks. The higher the MAS frequency, the farther "away" from the main signal these sidebands appear. Unfortunately, it is not always

practical to just spin the sample faster. To compensate, a pulse technique called total suppression of spinning sidebands (TOSS) can be applied to mostly eliminate these sidebands from the spectrum. CP spectra of biochars are typically taken at an MAS frequency of near 7 kHz, making the use of TOSS desirable.

A.2.4 “Gated Decoupling” (GADE) and “Gated Re-coupling” (GARE)

Dipolar coupling is not always undesirable and, in some techniques, can be used to give additional information about a sample. For example, to differentiate between protonated and non-protonated carbons, an additional series of pulses can be applied to the sample that essentially turns the ^{1}H-^{13}C dipolar decoupling on and off such that the signals from protonated carbons disappear from the spectra, leaving only the non-protonated carbon signals. This pulse technique is called dipolar dephasing, but is referred to in this set of experiments as “gated decoupling” (GADE). In some cases, even longer dipolar dephasing is desirable, such as when one wants to estimate the distance between carbons and their nearest proton neighbors. This is the case with char, since the size of aromatic ring clusters can be estimated by how long it takes the protons to dephase the signal of a carbon over long (several bond) distances. Unfortunately, one purpose of MAS is to minimize protons’ dephasing ability. In a “gate re-coupling” (GARE) experiment, a series of pulses is used to interfere with the effects of MAS and thus allow the dephasing time of aromatic carbons to be measured.

A.3 Spectral Analysis and Data Interpretation for Biochar Characterization

Data from NMR comes in the form of spectra acquired under different magnetic fields and RF pulse sequences, the raw wave data having been transformed using Fourier transform. Some qualitative data can be interpreted directly from the spectra, specifically the relative presence or lack of functional groups at their characteristic locations. The most useful and quantitative information, however, comes from the integration and comparison of specific spectral peaks. Data acquisition, spectrum viewing and integration are all done at ISU on the XWIN-NMR 3.5 software; plots for

presentation are made through XWIN-PLOT 3.5 software and formatted using Adobe Illustrator.

A.3.1 Spectral Interpretation and Integration

The location of characteristic functional group peaks on ^{13}C spectra are generally the same for ^{1}H-^{13}C cross polarization (CP) and ^{13}C direct polarization (DP); the key difference in char spectra is that the aromatic C peak (~130 ppm) dominates—relative to the alkyl (~0-90 ppm) and carbonyl (~210-145 ppm) groups—in the DP spectrum more than in the CP spectrum. CP spectra are specifically used for showing alkyl and carbonyl groups. Peak integration to gain quantitative information is done using the DP and DP/GADE spectra. Since NMR signals are additive, these two spectra need to have been acquired with the same number of scans, or each integration multiplied by a ratio to account for the signal intensity difference. Below is a sample DP (thin line: all C) and DP/GADE (thick line: non-protonated C only) composite spectrum for corn stover fast pyrolysis char, which shows the basic functional group regions and the lower frequency aromatic C spinning sideband (ssb).

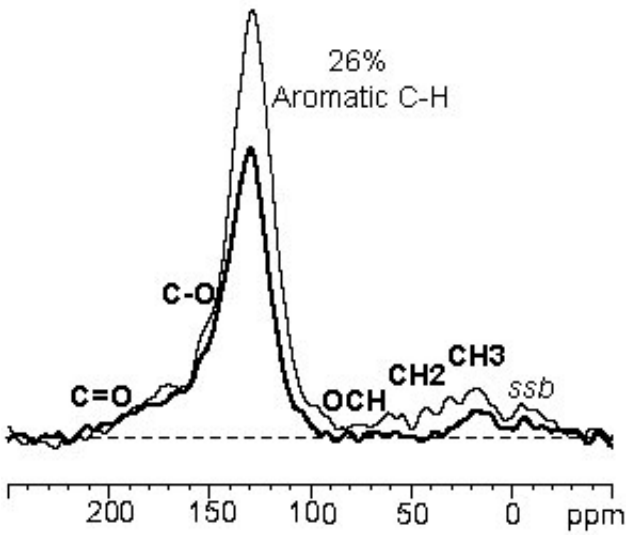

Figure 41. ^{13}C direct polarization (DP)(thin line) and DP with gated decoupling (DP/GADE) (thick line) spectra of corn stover fast pyrolysis char at a magic angle spinning (MAS) frequency of 14 kHz.[5]

To compute the relative amount of each carbon moiety present, one must first set the integral for the total carbon signal. The aromatic carbon peak has two spinning sidebands, one visible just to the right of 0 ppm, the other between ~290-250 ppm. These sidebands are significant enough that they need to be included in both the total carbon signal and the total aromatic carbon signal. In a char DP spectrum, the total carbon signal, therefore, is set as the sum of areas 287.7-250.0 ppm and 210.7-(-50.2) ppm, normalized to the value of 1.000. Next, individual moiety peaks are integrated based on the ppm locations listed in Table 27 below. The aromatic carbon integration requires three steps. First, the total aromatic carbon, $C_{aro\text{-}total}$, is determined by integrating over the main DP spectrum peak (145.5-90.3 ppm) plus both spinning sidebands (287.7-250.0 ppm and 6.2-(-50.2) ppm). Next, non-protonated aromatic carbon, $C_{non\text{-}pro}$, is determined by integrating over the same three ranges in the DP/GADE spectrum. The protonated aromatic carbon, C-H, is determined by the difference of these sums:

$$C\text{-}H = C_{aro\text{-}total} - C_{non\text{-}pro}$$

Since the signals of ethers and alcohols within the aromatic and alkyl ranges overlap, a 50/50 split is assumed and is expressed in the molecular “formulas” for those moieties. The same is the case with the alkanes (CH_2) and alkenes (CH).[6]

Table 27. Quantitative NMR spectral analysis of corn stover fast pyrolysis char from DP/MAS and DP/MAS/GADE spectra.[5] All values are % of total ^{13}C signal. $CO_{0.75}H_{0.5}$ moieties assume a 1:1 ratio of alcohols and ethers. $CH_{1.5}$ moieties assume a 1:1 ratio of alkanes and alkenes. $C_{non\text{-}pro}$, non-protonated aromatic carbon.

Char ID	**Carbonyls**		**Aromatics**			**Alkyls**		
Moieties:	**C=O**	**COO**	**$CO_{0.75}H_{0.5}$**	**$C_{non\text{-}pro}$**	**C-H**	**$HCO_{0.75}H_{0.5}$**	**$CH_{1.5}$**	**CH_3**
ppm:	**210-183**	**183-165**	**165-145**	**145 - 90**		**90-50**	**50-25**	**25-6**
1	3.3	5.7	11.5	43.0	26.1	2.5	3.8	4.1

A.3.2 Calculating Aromaticity and Edge Carbons

Several peak comparisons are used in the analysis of char to determine its aromaticity, to estimate the number of carbons in the aromatic clusters (i.e. the

degree of carbonization), and to provide information about the types of hydrogen in the sample. Table 28 below shows an example of the values that would be calculated to do this.[6]

Table 28. Aromaticities, fractions of aromatic edge carbons, and minimum number of carbons per aromatic cluster in corn stover fast pyrolysis char.[5]

Char ID	Aromaticity (%)	χ_{CH}	χ_{C-O}	$\chi_{edge,min}$	χ_{alkyl}	$\chi_{C=O}$	$\chi_{edge,max}$	nC_{min}	H_{arom}/H_{alk}
1	81	0.32	0.14	0.47	0.13	0.11	0.71	12	1.2

The aromaticity of the char is defined as the sum of relative signal intensities of the moieties under the aromatic umbrella, namely the $CO_{0.75}H_{0.5}$, $C_{non\text{-}pro}$, and C-H (Table 27). The fractions, χ, are defined as the ratio of a given moiety, f_x, to total aromatic carbon, f_{ar}. For example, χ_{CH} is the ratio of aromatic protonated carbons, f_{aCH}, to total aromatic carbon, f_{ar}. The fraction of aromatic carbons that are edge carbons is assumed to be at least the sum of the aromatic C-H and C-O moieties:

$$\chi_{edge,\,min} = \chi_{CH} + \chi_{C-O}$$

The maximum fraction of edge carbons is assumed to include the alkyl and carbonyl moieties:

$$\chi_{edge,\,max} = \chi_{edge,min} + \chi_{alkyl} + \chi_{C=O}$$

The minimum number of carbons in the aromatic cluster is determined by the number of carbons needed to satisfy the edge carbon fraction requirements. The lower the edge fraction, the larger the cluster needs to be, and vice versa. nC_{min} was calculated using a relationship described in a Solum, et al paper[7]:

$$nC \geq 6/\ \chi_{edge,\,max}^{2}$$

The ratio of aromatic protons to alkyl protons is calculated by adding up the

number of hydrogen moles present in the aromatic moieties * the amount of those moieties and dividing by the number of hydrogen moles present in the alkyl moieties * the amount of those moieties:

$$H_{arom}/H_{alk} = (1*\text{aromatic C-H}) / (3*CH_3 + 1.5*CH_{1.5} + 1.5*HCO_{0.75}H_{0.5})$$

References

1. Schmidt-Rohr, K.; Spiess, H. W., *Multidimensional Solid-State NMR and Polymers*. Academic Press: San Diego, 1994.
2. Duer, M. J., *Introduction to Solid-State NMR Spectroscopy*. Blackwell: Malden, MA, 2004.
3. Laws, D. D.; Bitter, H.-M. L.; Jerschow, A., Solid-state NMR spectroscopic methods in chemistry. *Angewandte Chemie International Edition* **2002,** 41, (17), 3096-3129.
4. Derome, A. E., *Modern NMR Techniques for Chemistry Research*. Pergamon Press: New York, 1987.
5. Brewer, C.; Unger, R.; Schmidt-Rohr, K.; Brown, R., Criteria to select biochars for field studies based on biochar chemical properties. *Bioenergy Res.* **2011,** 4, (4), 312-323.
6. Brewer, C. E.; Schmidt-Rohr, K.; Satrio, J. A.; Brown, R. C., Characterization of biochar from fast pyrolysis and gasification systems. *Environ. Prog. Sustainable Energy* **2009,** 28, (3), 386-396.
7. Solum, M. S.; Pugmire, R. J.; Grant, D. M., Carbon-13 solid-state NMR of Argonne-premium coals. *Energy & Fuels* **1989,** 3, (2), 187-193.